



ANTICANCER EFFECTS OF *MORINGA OLEIFERA* LAM. LEAF EXTRACTS ON THE HUMAN

BREAST CANCER CELLS



PRAPAKORN WISITPONGPUN

A Thesis Submitted to the Graduate School of Naresuan University

in Partial Fulfillment of the Requirements

for the Doctor of Philosophy in Biomedical Sciences

2022

Copyright by Naresuan University

ANTICANCER EFFECTS OF *MORINGA OLEIFERA* LAM. LEAF EXTRACTS ON THE HUMAN  
BREAST CANCER CELLS



A Thesis Submitted to the Graduate School of Naresuan University  
in Partial Fulfillment of the Requirements  
for the Doctor of Philosophy in Biomedical Sciences

2022

Copyright by Naresuan University

Thesis entitled "Anticancer effects of *Moringa oleifera* Lam. leaf extracts on the human breast cancer cells"

By PRAPAKORN WISITPONGPUN

has been approved by the Graduate School as partial fulfillment of the requirements

for the Doctor of Philosophy in Biomedical Sciences of Naresuan University

**Oral Defense Committee**

..... Chair  
 (Professor Paul James Brindley, Ph.D.)

..... Advisor  
 (Associate Professor Kanchana Usuwanthim, Ph.D.)

..... Co Advisor  
 (Associate Professor Dr. Sutatip Pongcharoen, Ph.D.)

..... Co Advisor  
 (Assistant Professor Nungruthai Suphrom, Ph.D.)

..... Co Advisor  
 ( Napaporn Apiratmateekul, Ph.D.)

..... Internal Examiner  
 (Assistant Professor Pachuen Potup, Ph.D.)

..... External Examiner  
 ( Wannaporn Ittiprasert, Ph.D.)

**Approved**

.....  
 ( )

Dean of the Graduate School



<b>Title</b>	ANTICANCER EFFECTS OF <i>MORINGA OLEIFERA</i> LAM. LEAF EXTRACTS ON THE HUMAN BREAST CANCER CELLS
<b>Author</b>	PRAPAKORN WISITPONGPUN
<b>Advisor</b>	Associate Professor Kanchana Usuwanthim, Ph.D.
<b>Co-Advisor</b>	Associate Professor Dr. Sutatip Pongcharoen, Ph.D. Assistant Professor Nungruthai Suphrom, Ph.D. Napaporn Apiratmateekul, Ph.D.
<b>Academic Paper</b>	Ph.D. Dissertation in Biomedical Sciences, Naresuan University, 2022
<b>Keywords</b>	MDA-MB-231 cells, TNBC, oleamide, MDMs, Polarization, Inflammasome, TAMs, macrophage, moringa

### ABSTRACT

*Moringa oleifera* Lam. (MO) is a medicinal plant distributed in many tropical and subtropical countries as well as Thailand. MO has a variety of bioactive compounds that exerts multiple biological activities, including anti-cancer and immunomodulatory activity. The present study aims to identify the potential anti-cancer compounds from the MO leaf against MDA-MB-231 breast cancer cells and to explore the regulatory effect of this bioactive compound on the progression of human macrophage polarization. MO leaf was subjected to extraction, fractionations, and screening of anticancer effect using multi-bioassay guided. The most promising fraction was selected for sub-fractionation and identification of bioactive compounds using LC-ESI-QTOF-MS/MS. There were 10 candidate compounds tentatively identified, and oleamide exhibited the strongest anti-cancer activity by inducing cell cycle arrest and triggering apoptosis through suppression of Bcl-2 and activation of caspase 3. Moreover, how oleamide influences macrophage polarization was explored using *in vitro* culture of primary human monocyte-derived macrophages (MDMs) model. Results showed that oleamide promoted naïve macrophages (M0) toward the M1 phenotype by upregulating M1-associated genes, along with downregulation of M2-associated genes (*Arg-1*, *CD206*, *CCL22*). Oleamide was found

to promote the production of IL-1 $\beta$  by activating the NLRP3 inflammasome. Finally, the effect of oleamide on the reprogramming of Tumor-Associated Macrophages (TAMs) was investigated using the Transwell co-culture model. Results demonstrated that oleamide enhances the switching of tumor-promoting M2-like into the tumoricidal M1-like TAM phenotype with increasing HLA-DR gene expression and IL-1 $\beta$  production. In conclusion, oleamide could be a potential anticancer agent and immunomodulating agent.



## ACKNOWLEDGEMENTS

Firstly, I would like to express my sincere gratitude to my advisor Assoc. Prof. Kanchana Usuwanthima for the continuous support of my Ph.D. study and related research, for her patience, motivation, and immense knowledge. Her guidance helped me in all the time of research and writing of this thesis. I could not have imagined having a better advisor and mentor for my Ph.D. study.

I would like to thank my thesis chairman: Prof. Paul James Brindley. My thesis external and internal examiners: Dr. Wannaporn Ittiprasert and Asst. Prof. Pachuen Potup. Also my thesis committee: Assoc. Prof. Dr. Sutatip Pongcharoen, Asst. Prof. Nungruthai Suphrom, and Dr. Napaporn Apiratmateekul - Not only for their time and extreme patience but also for their intellectual contributions to my development as a Ph.D.

I would like to acknowledge the Royal Golden Jubilee Ph.D. Program (Grant No. PhD/0002/2559), Thailand Science Research and Innovation, and Naresuan University (Grant No. R2564B002) for funding. Also the Blood Bank Unit of Naresuan University Hospital, Thailand for providing blood samples.

Many thanks to my lab members for the stimulating discussions, for all the help and support, and for all the fun we have had in the last five years.

Last but not the least, I would like to thank my family: my parents and my brothers. Also my boyfriend for supporting me spiritually throughout this thesis and my life in general.

PRAPAKORN WISITPONGPUN

## TABLE OF CONTENTS

	<b>Page</b>
ABSTRACT .....	C
ACKNOWLEDGEMENTS .....	E
TABLE OF CONTENTS .....	F
List of tables .....	O
List of figures.....	P
CHAPTER 1 INTRODUCTION .....	0
1. Background and Significance of the Study.....	0
2. Purposes of the Study.....	4
3. Statement of the Problems .....	4
4. Scope of the Study.....	5
5. Key Words.....	5
6. Hypotheses of the Study.....	6
CHAPTER 2 REVIEW OF LITERATURE .....	7
1. Cancer .....	7
1.1. The development of cancer .....	7
1.2. Types of cancer .....	9
2. Breast cancer .....	9
2.1. Type of breast cancer.....	11
2.1.1. Carcinoma in situ (CIS).....	11
2.1.2. Invasive Breast Cancers.....	12
2.2. Molecular subtypes of breast cancer.....	13

2.2.1. Luminal A (HR+/HER2-) (71%).....	13
2.2.2. Luminal B (HR+/HER2+) (12%).....	13
2.2.3. HER2-enriched (HR-/HER2+) (5%).....	13
2.2.4. Triple-negative (HR-/HER2-) (15-20%).....	13
3. Triple-negative breast cancer (TNBC).....	14
3.1. Potential risk factors .....	14
3.1.1. Non-modifiable risk factors .....	14
3.1.2. Modifiable risk factors .....	1
3.2. Signaling pathway involved in TNBC .....	2
3.2.1. Wnt/ $\beta$ -catenin pathway .....	2
3.2.2. TGF- $\beta$ signaling pathway .....	3
3.2.3. Signalling pathway of CSPG4 protein .....	3
3.2.4. Hedgehog signalling pathway .....	3
3.2.5. PI3K/AKT/mTOR pathway .....	3
3.2.6. Epidermal growth factor receptor .....	4
4. <i>Moringa oleifera</i> Lam.....	4
4.1. Nutritive properties of MO.....	5
4.2. Phytochemical composition of MO .....	7
4.3. Phytochemistry of MO.....	8
4.4. Anti-cancer activities of MO.....	11
4.5. Immunomodulatory Effects of MO.....	16
5. Methods Used for Extraction, Separation, and Characterization of Bioactive Compounds from Plant Extracts.....	19
5.1. Extractions.....	19

5.1.1. Maceration.....	19
5.1.2. Percolation .....	19
5.1.3. Serial exhaustive extraction .....	20
5.1.4. Supercritical fluid extraction (SFE).....	20
5.1.5. Microwave-assisted extraction.....	20
5.1.6. Ultrasound-assisted extraction.....	21
5.2. Separation methods .....	21
5.2.1. Thin-layer chromatography (TLC).....	21
5.2.2. Column chromatography (CC).....	22
5.3. Identification and characterization.....	23
5.3.1. High-performance liquid chromatography (HPLC).....	23
5.3.2. UV-Visible Spectroscopy.....	23
5.3.3. Infrared Spectroscopy (IR). .....	24
5.3.4. Nuclear Magnetic Resonance Spectroscopy (NMR).....	25
5.3.5. Mass Spectrometry for chemical compounds identification. ....	25
6. Oleamide .....	26
6.1. Structure.....	26
6.2. Biosynthesis of oleamide.....	27
6.3. Biological activity of oleamide.....	29
7. Introduction to the Immune System.....	29
7.1. Innate and adaptive immunity .....	30
7.2. Components of innate immunity.....	32
7.2.1. Epithelial barriers.....	32
7.2.2. Phagocytes: Neutrophils and monocytes/macrophages.....	32

7.2.3. Neutrophils.....	32
7.2.4. Monocytes/Macrophages.....	32
7.2.5. Dendritic cells.....	33
7.2.6. Mast cells.....	33
7.2.7. Innate lymphoid cells.....	33
7.2.8. Natural killer cells.....	33
7.2.9. Complement system.....	33
7.2.10. Cytokines of innate immunity.....	34
7.3. Components of adaptive immunity.....	34
7.3.1. Humoral immunity.....	34
7.3.2. Cell-mediated immunity.....	34
8. Macrophages.....	35
8.1. Development of monocytes and macrophages.....	36
8.2. Macrophage polarization.....	37
8.2.1. M1 macrophage.....	38
8.2.2. M2 macrophage.....	38
8.3. Macrophage-NLRP3 inflammasome.....	40
8.3.1. Priming the NLRP3 inflammasome (Signal 1). .....	41
8.3.2. Activating the NLRP3 inflammasome (Signal 2).....	41
9. Tumor-associated macrophages (TAMs).....	42
9.1. Origins of TAMs.....	43
9.2. Types of TAMs.....	43
9.2.1. M1-like TAMs.....	43
9.2.2. M2-like TAMs.....	44

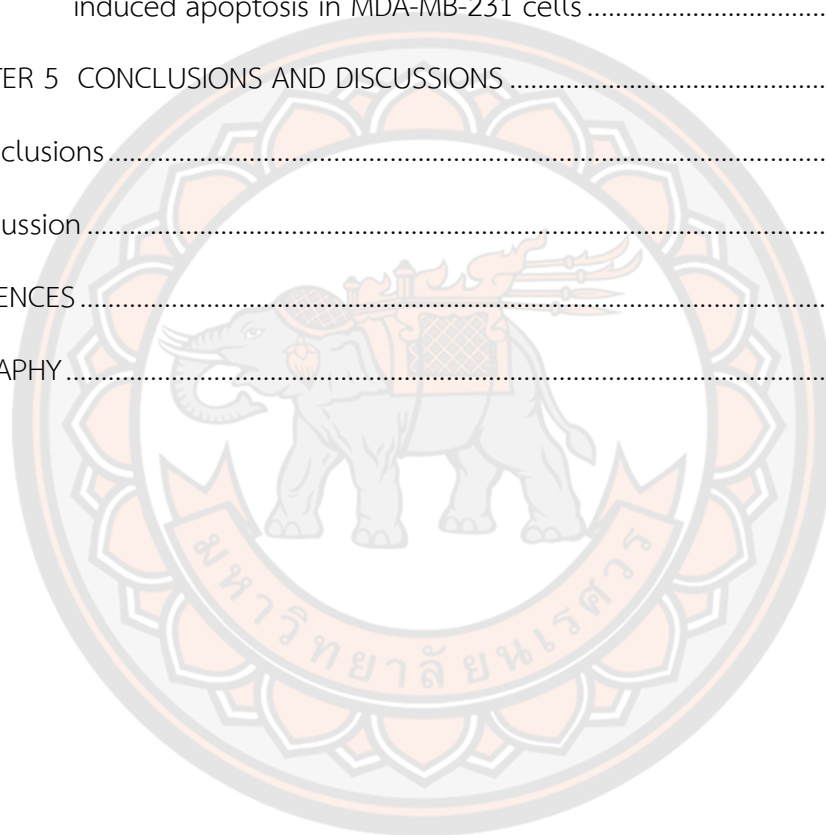
9.3. Targeting TAMs for Cancer Treatment .....	45
9.3.1. Limiting monocyte recruitment.....	45
9.3.2. Targeting TAMs activation.....	46
9.3.3. Reprogramming TAMs into anti-tumor activity.....	46
9.3.4. Targeting immune inhibitory molecules on TAMs .....	46
10. Basic methods in cellular and molecular biology .....	47
10.1. Cell culture.....	47
10.3. MTT assay.....	47
10.4. Density gradient centrifugation technique .....	48
10.5. Colony formation/clonogenic assay .....	48
10.6. Apoptosis analysis .....	49
I. Apoptosis by Annexin V/ 7-AAD staining .....	50
II. Cell apoptosis by TUNEL assay .....	51
III. Cell apoptosis by mitochondrial membrane potential assay.....	52
IV. Apoptosis-associated caspase activation assays.....	53
10.7. Cell cycle analysis.....	54
10.8. <i>In vitro</i> scratch assay.....	55
10.9. Hoechst 33342 nuclear staining dye .....	56
10.10. Reverse transcription quantitative real-time PCR (RT-qPCR).....	56
10.11. Western blot analysis.....	57
10.12. Flow cytometry .....	58
10.13. Enzyme-linked immunosorbent assay (ELISA).....	59
10.14. LDH assay.....	60
10.15. Scanning electron microscope (SEM).....	60

CHAPTER 3 RESEARCH METHODOLOGY.....	62
Population and sample .....	62
Research Instruments.....	62
Research methodology.....	65
Part 1: <i>In vitro</i> bioassay-guided identification of bioactive compound from <i>Moringa oleifera</i> Lam. Leaf against the MDA-MB-231 breast cancer cells line.....	66
1. Cell culture.....	67
2. Collection of plant materials.....	67
3. Preparation of MOL extract.....	67
4. Fractionation of crude MOL extract and active fraction .....	68
5. At-line- Liquid chromatography-electrospray ionization-quadrupole time-of-flight-mass spectrometry (LC-ESI-QTOF-MS/MS) analysis.....	69
6. Identification of active compounds.....	69
7. Cell viability assay .....	70
8. Colony formation assay .....	70
9. Apoptosis and cell cycle analysis .....	70
10. Cell migration assay .....	71
11. Hoechst staining.....	72
12. Real-Time Quantitative Reverse Transcription PCR (RT-qPCR).....	72
13. Western blot analysis .....	73
14. Isolation of human MDMs.....	74
15. Statistical analysis.....	74
Part 2: The regulatory effect of the bioactive compound on the polarization of primary Human Monocyte-Derived Macrophages (MDMs). .....	75
1. Isolation of human MDMs.....	76

2.	Preparation of heat-inactivated single donor human serum .....	76
3.	MDMs culture and polarization .....	76
4.	THP-1 cell culture and differentiation .....	78
5.	Inflammasome activation .....	78
6.	Cell viability assay .....	78
7.	Flow cytometry.....	79
8.	Real-Time Quantitative Reverse Transcription PCR (RT-qPCR).....	79
9.	Scanning electron microscope (SEM).....	80
10.	Enzyme-linked immunosorbent assay (ELISA).....	81
11.	Lactate dehydrogenase (LDH) assay.....	82
12.	Western blot analysis .....	82
13.	Statistical analysis.....	83
Part 3:	The reprogramming of TAMs with a bioactive compound (oleamide).....	83
1.	Cell Culture.....	84
2.	Harvesting tumor-conditioned media .....	84
3.	Isolation of human MDMs.....	85
4.	Preparation of heat-inactivated single donor human serum .....	85
5.	Generation of TAMs .....	86
6.	RT-qPCR analysis.....	86
7.	Cell viability assay .....	87
8.	Apoptosis analysis .....	88
9.	ELISA assay.....	88
10.	Statistical analysis.....	88
CHAPTER 4	RESULTS.....	89

Part 1: <i>In vitro</i> bioassay-guided identification of bioactive compound from MOL against the MDA-MB-231 breast cancer cells line.....	89
1.1 Certification of analysis (COA) MOL dried powder.....	89
1.2 The yield of crude MOL by sequential extraction.....	89
1.3 Screening for cytotoxic effects of crude hexane, EtOAc, and EtOH extracts of MOL on breast cancer cells and normal cells. ....	91
1.4 Anti-cancer activity of EtOAc extract of MOL and its derived fractions on MDA-MB-231 cells.....	92
1.5 The fractions on. 6-7 induced apoptosis and cell cycle arrest on the MDA-MB-231 cells line. ....	94
1.6 Sub-fractionation of fraction no. 7 and identification of compounds using the Liquid chromatography-electrospray ionization-quadrupole time-of-flight-mass spectrometry (LC-ESI-QTOF-MS/MS).....	98
1.7 The role of three-identified compounds, 7-octenoic acid, oleamide, and 1-Phenyl-2-pentanol on MDA-MB-231 cells apoptosis and cell cycle progression.....	102
1.8 Bioactive compounds suppressed MDA-MB-231 cell migration and induced apoptosis in different cancer cell lines.....	106
Part 2: The regulatory effect of oleamide on the polarization of primary human MDMs.....	109
2.1 Culture, purity, and differentiation of primary human MDMs at days 0-6. ....	109
2.2 Generation of <i>in vitro</i> culture and polarization of MDMs.....	111
2.3 Oleamide mediated M1 macrophage polarization and IL-1 $\beta$ production. ....	114
2.4 Oleamide-induced IL-1 $\beta$ production in LPS-primed MDMs involves activation of the NLRP3-inflammasome pathway.....	118
2.4 Oleamide mediated IL-1 $\beta$ production by regulating NLRP3-inflammasome in LPS-primed MDMs.....	120

Part 3: The reprogramming of TAMs with a bioactive compound (oleamide).....	122
3.1 <i>In vitro</i> generation of primary monocyte-derived TAMs by transwell co-culture model .....	122
3.2 Oleamide induced reprogramming of M2-like TAMs toward M1-like TAM phenotypes.....	125
3.3 Conditioned medium of oleamide-treated TAMs inhibited cell viability and induced apoptosis in MDA-MB-231 cells .....	127
CHAPTER 5 CONCLUSIONS AND DISCUSSIONS .....	129
Conclusions .....	129
Discussion .....	132
REFERENCES .....	142
BIOGRAPHY .....	163



## List of tables

	Page
Table 1: The nutrient compositions of leaves, leaves powder, seeds, and pods. (All values are in 100 g per plant material) (83).....	6
Table 2 Phytoconstituents of <i>Moringa oleifera</i> (25-28).....	10
Table 3 Major bioactive compound in different body parts of <i>M. oleifera</i> (84). ....	11
Table 4 Anti-cancer activities of different extracts of <i>M. oleifera</i> .....	12
Table 5 Importance of the immune system in health and disease (125).....	30
Table 6 Macrophage differentiation, characteristics, and functions (134, 135).....	40
Table 7 Primer sequences for RT-qPCR assay of the first part.....	73
Table 8 Primer sequences for RT-qPCR assay of the second part.....	80
Table 9 Primer sequences for RT-qPCR assay of the third part.....	87
Table 10 Certification of analysis of <i>Moringa oleifera</i> leaf dried powder from Khaolaor Laboratories Co. Ltd.....	90
Table 11 The yield of crude MOL extract by sequential extraction.....	90
Table 12 The yield of sub-fractions no.7.1 – 7.8 from active fraction no.7 of MOL extract.....	99
Table 13: Tentative identification of bioactive compounds identified in sub-fraction 7.7 of MOL extract by LC-ESI-QTOF-MS. ....	100

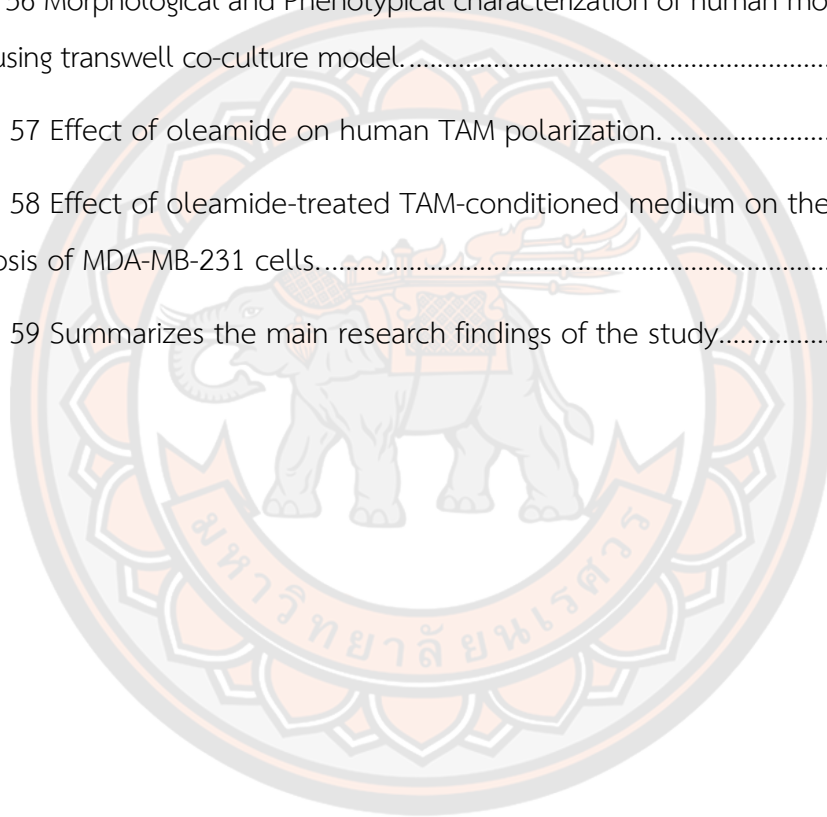
## List of figures

	<b>Page</b>
Figure 1 Development and progression of cancer. ....	8
Figure 2 Anatomy of the female breast. ....	10
Figure 3 Incidence, Prevalence, and Mortality of cancers in Thailand 2012 (59). ....	10
Figure 4 Leading sites of new cancer cases and deaths - 2018 Estimates.....	11
Figure 5 Moringa oleifera plant. (a) leaves, (b) seeds, (c) flowers, (d) barks, and (e) pods (25, 27, 28). ....	5
Figure 6 Graphical representation of the use of Moringa oleifera tree.....	9
Figure 7 Illustration of immunomodulatory potential of M. oleifera after interaction/trigger of several molecular and cellular events.....	18
Figure 8 Thin-layer chromatography (TLC) and Visualization of a TLC plate.....	22
Figure 9 The principle of UV/Visible spectroscopy. ....	24
Figure 10 Structures of the prototype long-chain primary and secondary fatty acid amide classes of lipid messengers.....	26
Figure 11 The synthetic pathway for oleamide. ....	28
Figure 12 Principal mechanisms of innate and adaptive immunity.....	31
Figure 13 Types of adaptive immunity. In humoral immunity, B lymphocytes secrete antibodies that eliminate extracellular microbes. ....	35
Figure 14 Maturation of mononuclear phagocytes. ....	37
Figure 15 A Two-Signal Model for NLRP3 Inflammasome Activation. ....	42
Figure 16 Overview of the factors regulating TAMs functions and the targets of TAMs for cancer treatment (16).....	45
Figure 17 The principle of MTT assay. ....	48

Figure 18 A summary process of the clonogenic assay. ....	49
Figure 19 Summary model of Annexin V/7-AAD staining apoptosis assay. ....	51
Figure 20 The principle of TUNEL assay. ....	52
Figure 21 The JC-1 Mitochondrial Membrane Potential Assay. ....	53
Figure 22 The cell cycle assay uses the nuclear stain DAPI to measure DNA content.....	54
Figure 23 Graphical summarizing the workflow of the in vitro wound-healing assay.....	55
Figure 24 A real-time PCR assay using SYBR Green dye.....	57
Figure 25 General process of western blot analysis. ....	58
Figure 26 The basic setup of an ELISA assay.....	59
Figure 27 Schematic representation of the principle of the LDH release assay (169). ....	60
Figure 28 Overview of the research methodology.....	65
Figure 29 Schematic models of the in vitro bioassay-guided identification of bioactive compound from MOL against the MDA-MB-231 breast cancer cells line.....	66
Figure 30 Schematic model of the regulator effect of the oleamide on macrophage polarization and inflammasome activation. ....	75
Figure 31 Scheme of primary human monocyte-derived macrophages (MDMs) culture and polarization. ....	77
Figure 32 Schematic models of the oleamide-induced reprogramming of TAMs and its anticancer effect against MDA-MB-231 cells.....	84
Figure 33 Cytotoxicity of Cytotoxicity of crude hexane, EtOAc, and EtOH extracts of MOL on the viability of MDA-MB-231 cells and primary human MDMs.....	92
Figure 34 Cell viability of MDA-MB-231 cells after treatments with EtOAc extract and its derived fractions. ....	93
Figure 35 Effect of EtOAc extract and its derived fractions on the clonogenic growth of MDA-MB-231 cells.....	94

Figure 36 Effect of crude EtOAc extract and its derived fractions on the MDA-MB-231 cell apoptosis.....	96
Figure 37 Effect of MOL extract and its derived fractions on the distribution of MDA-MB-231 cells in the cell cycle.....	97
Figure 38 Expression of apoptosis-related genes and proteins in MDA-MB-231 cells after treatment with fraction no.7 of MOL extract.....	98
Figure 39 Cell viability of MDA-MB-231 cells after treatment with sub-fractions no.7.1-7.8. ....	99
Figure 40 Cytotoxic effect and LC-ESI-QTOF-MS/MS analysis of eluted compounds from sub-fraction no. 7.7.....	101
Figure 41 Cytotoxicity of oleamide, 1-phenyl-2-pentanol, and 7-octenoic acid on MDA-MB-231 cells.....	102
Figure 42 Effect of oleamide, 1-phenyl-2-pentanol, and 7-octenoic acid on MDA-MB-231 cells apoptosis.....	104
Figure 43 Effect of oleamide, 1-phenyl-2-pentanol, and 7-octenoic acid on cell cycle progression of MDA-MB-231 cells.....	105
Figure 44 Effect of 7-octenoic acid, oleamide, and 1-phenyl-2-pentanol on the migration of MDA-MB-231 cells.....	107
Figure 45 Effect of oleamide on the apoptosis and cell cycle regulation of other cancer cell lines.....	108
Figure 46 Purity of human MDMs at days 0, 3, and 6 by flow cytometry.....	109
Figure 47 Flow cytometry analysis of CD14 and CD16 expression on human MDMs. ...	110
Figure 48 Morphology and phenotypical characterization of human MDMs (Days 0-6).....	112
Figure 49 Morphology and phenotypical analysis of macrophage polarization. ....	113
Figure 50 Morphology of polarized M0, M1, and M2 macrophages plus oleamide.....	114
Figure 51 Flow cytometry analysis of surface expressions.....	115

Figure 52 Oleamide mediated M1 macrophage polarization.....	117
Figure 53 Oleamide mediated inflammasome activation, and IL-1 $\beta$ and IL-18 production in LPS-primed MDMs.....	119
Figure 54 Oleamide promoted NLRP3 inflammasome activation in LPS-primed MDMs.....	121
Figure 55 Schematic diagram of <i>in vitro</i> generation of human monocyte-derived TAMs using the transwell co-culture model.....	122
Figure 56 Morphological and Phenotypical characterization of human monocyte-derived TAMs using transwell co-culture model.....	124
Figure 57 Effect of oleamide on human TAM polarization. ....	126
Figure 58 Effect of oleamide-treated TAM-conditioned medium on the viability and apoptosis of MDA-MB-231 cells.....	128
Figure 59 Summarizes the main research findings of the study.....	131



## CHAPTER 1

### INTRODUCTION

#### 1. Background and Significance of the Study

Breast cancer is the most frequently diagnosed cancer in women and is one of the leading causes of cancer death for women (1, 2). Worldwide, over 1.3 million cases of invasive breast cancer are diagnosed and more than 450,000 women die from breast cancer annually (1, 2). Breast cancer is a heterogeneous disease with distinct pathological entities and therefore, needs diverse therapeutic interventions. Approximately 15–20% of invasive breast cancers are triple-negative breast cancer (TNBC) which is defined as the absence of estrogen receptor, progesterone receptor, and the human epidermal growth factor receptor 2 (HER2) receptor (3). TNBC is a more aggressive subtype of breast cancer that is associated with poor prognosis and high rates of proliferation and metastases (4, 5). Unfortunately, due to the aggressive features and lack of targeted therapies, conventional chemotherapy and radiotherapy remain the preferred standard option for TNBC patients (6). Recently, signaling pathways and receptor-specific targets have been reported to be effective and approved for the treatment of TNBC under specific clinical conditions (6-8). However, some TNBC patients showed no response, which is related to the heterogeneity of TNBC (6, 7). Therefore, it is an urgent need for new drugs and therapies to improve the therapeutic effect of TNBC.

The immune system is actively involved in the development and progression of many solid tumors, including TNBC (9, 10). Accumulating evidence highlights that the response to antitumor therapy and overall survival of breast cancer patients is subject to host immunity (11). Macrophages are a heterogeneous population of the innate immune system that is involved in several processes of health and disease, including cancer (12-14). The heterogeneity of macrophages is commonly referred to as polarization, a process by which macrophages display different functional phenotypes in response to specific microenvironmental stimuli and signals (15).

Macrophage polarization is conventionally divided into two major phenotypes: classically activated macrophages (M1) and alternatively activated macrophages (M2) (12-14). M1 macrophage polarization is derived by exposure to factors such as GM-CSF, IFN- $\gamma$ , lipopolysaccharide (LPS), or other pathogen-associated molecular patterns (PAMPs) (12-15). M1 macrophages, also known as pro-inflammatory macrophages, are characterized by secreting pro-inflammatory cytokines such as TNF- $\alpha$ , IL1- $\beta$ , and IL12, and a high level of reactive oxygen species (ROS) and nitric oxide (NO) (12-15). These functions are critical in the response to bacterial and viral infection and have the potential to participate in anti-tumor immunity (12-15).

By contrast, M2 macrophage polarization is derived by exposure to M-CSF, IL-4, IL-10, IL-13, TGF- $\beta$ , glucocorticoids, or immune complexes (12-15). M2 macrophages, commonly known as anti-inflammatory macrophages, are characterized by secreting anti-inflammatory cytokines, and expressing multiple receptors expressed such as the mannose receptor (MRC1), scavenging receptor CD163, dectin-1, and DC-SIGN (12-15). M2 macrophages play a crucial role in immunoregulation, wound healing, and tissue regeneration (12-15). Certain subsets of M2 macrophages also play a critical role in promoting tumor progression (12-15).

Tumor-associated macrophages (TAMs) refer to the tumor-infiltrating macrophage, derived from the circulating blood monocytes that are recruited into the tumor microenvironment (TME) and differentiated into macrophages in response to stimuli (16, 17). TAMs play an important role in promoting tumor growth, invasion, and metastasis (16, 17). TAMs are also divided into two typical phenotypes as mentioned above: classically activated M1 and alternatively activated M2 phenotypes (16, 17). Polarization of TAMs toward M1/M2-like phenotypes can be manipulated by biomolecules derived from the TME and cancer cells (16, 17). Generally, TAMs often refer to a tumor-promoting M2-like phenotype rather than the antitumor M1 phenotype (18-20). *Accumulating evidence has suggested* that the low M1/M2 ratio is associated with tumor progression and poor prognosis while a high M1/M2 ratio tends to be correlated with positive outcomes (18-20). In TNBC patients also found that high infiltrating M2-like TAMs are associated with a higher risk of tumor metastasis (21). Therefore, finding the molecules that switch M2-like TAMs into

antitumor M1 phenotype has become one of the TAM-centered strategies for the treatment of TNBC.

*Moringa oleifera* Lam. (MO) is a highly valued medicinal plant native to India and now distributed widely across the Middle East, Africa, and Asia, including Thailand. It belongs to the family Moringaceae and is commonly referred to as the Drumstick tree (22-24). All parts of the MO possess medicinal properties, especially leaves that have the highest nutritional value (25). MO leaves (MOL) contain high levels of vitamins C and A, potassium, calcium, iron, and proteins (26). Besides, MO leaf is a good source of flavonoids, phytol, isothiocyanates, beta-carotene, lycopene, vitamin E, and amino acids (25, 27, 28). The *in vitro* and *in vivo* studies have demonstrated that MOL extract has multiple biological activities and therapeutic effects, including cardioprotective (29), hypocholesterolemic (30), neuroprotective (31), anti-inflammatory (32), antioxidant (33-35), anti-hypertensive (36, 37), antidiabetic (38, 39), antibacterial (40, 41), immunomodulatory (42, 43), and anticancer properties (44-46).

Regarding the anticancer properties, MOL extracts have been reported to disturb the growth of many cancer cells through different signalling pathways. For example, hot aqueous MOL extract was found to induce apoptosis in human lung cancer A549 cells by affecting mitochondrial viability in a ROS-dependent manner (45). A study on human cervical cancer HeLa cells found that methanolic MOL extract induced cell apoptosis by promoting DNA fragmentation (47). Hot aqueous MOL extract can cause G2/M phase cell cycle arrest in murine B16F10 melanoma cells by increasing p53, p21, and p27 protein expression (46). Moreover, oral administration of cold aqueous MOL extracts induced apoptosis of human hepatocellular carcinoma HepG2 cells by affecting the apoptosis-related proteins Bcl-2 and caspase-3 (48). In human breast cancer, most studies have been performed in the MCF-7 cell line, a hormone receptor-positive breast cancer model (48, 49). Only one study has investigated the effect of MOL on the TNBC cell line, MDA-MB-231, and it was found that ethanolic MOL extract arrested the cell cycle at the G2/M phase and effectively induced apoptosis (48). However, the underlying mechanism

and the bioactive compounds involved in the anticancer effect on TNBC have not yet been fully elucidated.

Concurrently, modulation of the immune system is a promising strategy for the treatment of breast cancer (50). Regarding to this strategy, MOL extract was reported to suppress the expression of inflammatory mediators in (51, 52). The administration of methanolic MOL extract was found to induce neutrophil adhesion in Wistar albino rats (53). In addition, the low dose of aqueous MOL extract was found to increase the number of CD4+ and CD8+ cells, while the high dose increases the B220+ cells (54). However, no studies have evaluated the effect of the MOL bioactive compound on the human M1/M2 polarization and the reprogramming to TAMs.

Taken together, the present study aims to investigate the *in vitro* anticancer effect of MOL extract against MDA-MB-231 cells using bioassay-guided fractionation, and identification of the potential bioactive compounds responsible for the observed effects. The most effective compound is subjected to further study that aim to explore the immunoregulatory effects of the bioactive compound on the progression of M1/M2 macrophage using *in vitro* culture of primary human monocyte-derived macrophages (MDMs) as a model. Cellular and molecular mechanisms underlying the MDMs polarization are also investigated. Finally, to evaluate the effect of the bioactive compound on primary human monocyte-derived TAM polarization using the Transwell co-culture model.

## 2. Purposes of the Study

1. To conduct the *in vitro* bioassay-guided fractionations and identifications of the potential anti-cancer compounds from the *Moringa oleifera* leaf (MOL) extract against TNBC cell lines, MDA-MB-231.
2. To explore the molecular mechanism underlying the anticancer effect of MOL extract and bioactive compound against the MDA-MB-231 cell line.
3. To select the most effective anti-cancer compound as a candidate for further study, focusing on the immunomodulatory activity.
4. To further investigate the regulatory effects of the bioactive compound on the progression of M1/M2 macrophage polarization.
5. To further evaluate the regulatory effects of the bioactive compound on the reprogramming of TAMs.

## 3. Statement of the Problems

Breast cancer is the most frequently found in women worldwide. TNBC is a more aggressive subtype of breast cancer and lacks targeted therapies. There is an intended interest in finding novel drugs or therapeutic strategies for the treatment of TNBC patients. TAMs are a major component of immune cell infiltration of the tumor microenvironment (TME). TAMs often refer to tumor-promoting M2-like phenotype, which plays an important role growth and development of TNBC. In this scenario, the switch of M2-like TAMs into antitumor M1 phenotype is a promising strategy for cancer immunotherapy. *Moringa oleifera* is a highly valued medicinal plant with various potential health benefits, such as anti-inflammatory, antioxidant, anticancer properties, and immunomodulatory. However, the bioactive compounds involved and the molecular mechanism underlying the anticancer effect and macrophage polarization have not yet been fully elucidated.

#### 4. Scope of the Study

MOL are subjected to sequential extraction and fractionation. Crude MOL extract and its derived fractions are screened for anti-cancer activity against the MDA-MB-231 cell line using multiple *in vitro* bioassays guided. The active fraction is selected for further separation into sub-fractions, which are next screened for anti-cancer activity. The strongest sub-fraction is selected for compound identification using the liquid chromatography coupled with electrospray ionization-quadrupole-time of flight-mass spectrometry (LC-ESI-QTOF-MS/MS). The anti-cancer activity of the identified compounds is confirmed in the MDA-MB-231 cell line and other types of cancer cell lines.

The most effective compound is subjected to further investigation that focused on the human macrophage polarization and NLRP3-inflammasome activation. The *in vitro* culture of primary human monocyte-derived macrophages (MDMs) is used as a model of study. The effect of the bioactive compound on MDMs polarization are investigated based on morphology and phenotypic characteristic. The model of NLRP3 inflammasome activation is conducted by LPS- stimulation, followed by ATP or bioactive compound. The molecular mechanism is mainly characterized based on the expression of signaling proteins.

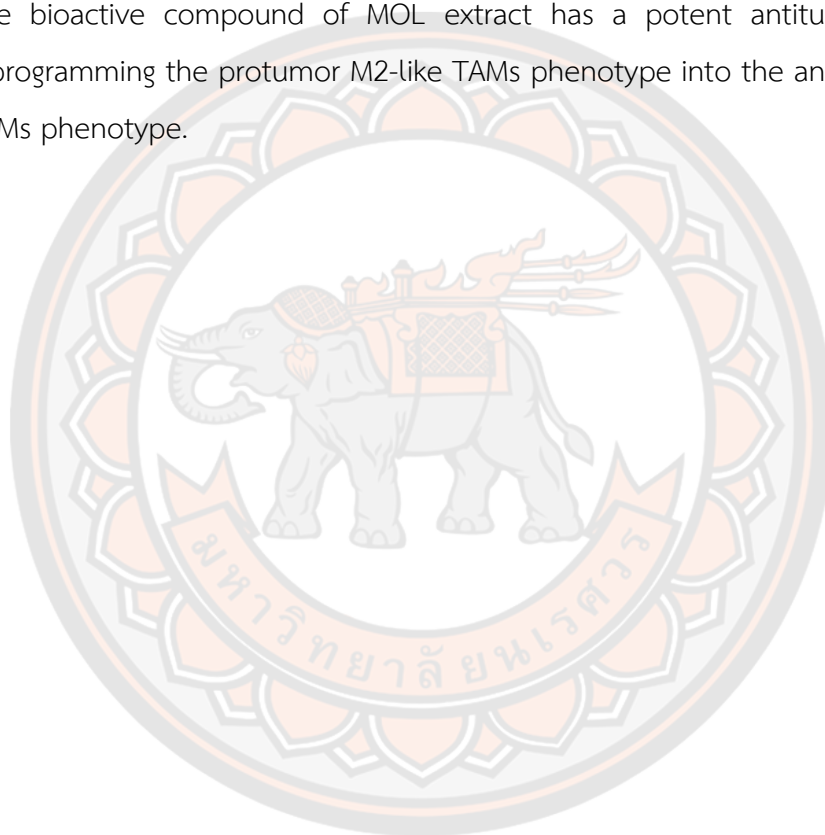
Next, human monocyte-derived TAMs are generated using transwell co-culture of human MDMs with an MDA-MB-231 cell line. This model was used to study the regulatory effect of the bioactive compound on the reprogramming of TAMs. The conditioned medium of TAMs is used to determine the anti-cancer activity against the MDA-MB-231 cell line.

#### 5. Key Words

*Moringa oleifera*, MDA-MB-231 cells, Triple-negative breast cancer, TNBC, oleamide, MDMs, Macrophage, Polarization, Oleamide, Inflammasome, NLRP3, Tumor-associated macrophages, TAMs

## 6. Hypotheses of the Study

1. The MOL extract, active fraction, and bioactive compounds have the potential to suppress growth and induce apoptosis of MDA-MB-231 cells by interfering with the intrinsic pathway at the mitochondrial level.
2. The bioactive compound of MOL extracts can promote M1 macrophage polarization and IL-1 $\beta$  production by activating the NLRP3 inflammasome in primary MDMs.
3. The bioactive compound of MOL extract has a potent antitumor effect via reprogramming the protumor M2-like TAMs phenotype into the antitumor M1-like TAMs phenotype.



## CHAPTER 2

### REVIEW OF LITERATURE

#### 1. Cancer

According to the American Cancer Society, cancer is defined as a group of diseases characterized by uncontrolled growth and the spread of abnormal cells (55). One defining feature of cancer is the rapid creation of abnormal cells that grow beyond their usual boundaries, and which can then invade adjoining parts of the body and spread to other organs; the latter process is referred to as metastasis (55).

##### 1.1. The development of cancer

The development of cancer is a multistep process involving successive genetic and epigenetic alterations that allow cells to escape homeostatic controls that ordinarily suppress inappropriate proliferation and inhibit the survival of aberrantly proliferating cells outside their normal niches. One of the fundamental features of cancer is tumor clonality, which is the development of tumors from single cells that begin to proliferate abnormally. The first step in the process, tumor initiation, is thought to be the result of a genetic alteration leading to abnormal proliferation of a “single-cell”. Cell proliferation then leads to the outgrowth of a single cell into multiple cells or tumor cells. The tumor progression continues as additional mutations occur within cells of the tumor population. Some of these mutations confer a selective advantage to the cell, such as more rapid growth, and the descendants of a cell bearing such a mutation will consequently become dominant within the tumor population. The process is called clonal selection since a new clone of tumor cells has evolved based on its increased growth rate or other properties (such as survival, invasion, or metastasis) that confer a selective advantage. The clonal selection continues

throughout tumor development, so tumors continuously become more rapid-growing and increasingly malignant, which can invade and spread to surrounding tissue or spread to tissues or organs, nearby or distant as shown in **Figure 1** (56).

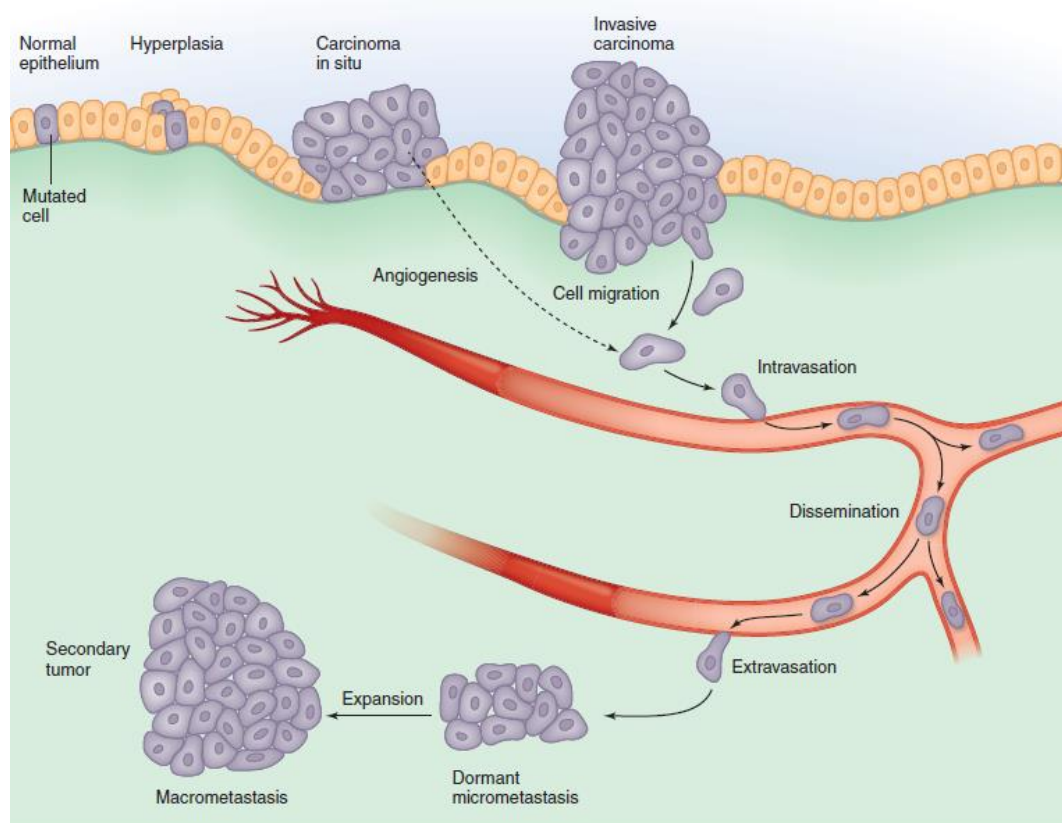


**Figure 1** Development and progression of cancer.

A single initially altered cell gives rise to a proliferative cell population (hyperplasias), which progresses to a mass of cells with abnormal morphology, cytological appearance, and cellular organization (carcinoma *in situ*). The carcinoma then increasing size and develop into malignant carcinoma or invasive malignant that is capable of invading the underlying connective tissue and penetrating blood and lymphatic vessels, thereby spreading throughout the body (56, 57).

## 1.2. Types of cancer

According to the type of origin of tumor cells, there are divided into 5 major types: 1) carcinoma - this type of cancer affects organs and glands, such as the lungs, breasts, pancreas, and skin. Carcinoma is the most common type of cancer, 2) sarcoma - this cancer affects soft or connective tissues, such as muscle, fat, bone, cartilage, or blood vessels, 3) melanoma - sometimes cancer can develop in the cells that pigment your skin. These cancers are called melanoma, 4) lymphoma - this cancer affects your lymphocytes or white blood cells, 5) leukemia - this type of cancer affects blood (58).

## 2. Breast cancer

According to the Centers for disease control and prevention (CDC), breast cancer is a disease in which cells in the breast grow out of control. Breast cancers can start from different parts of the breast but mostly begin in the ducts that carry milk to the nipple (ductal cancers). Some start in the glands that make breast milk (lobular cancers) (**Figure 2**) (2). Approximately 60% of the cancer burden in Thailand is due to five types of cancers: breast, cervix, colorectal, liver, and lung cancers (**Figure 3**). Breast, cervix, colorectal, liver, and lung cancers combined had the highest age-standardized rates in 2012 and accounted for more than half of the incidence, prevalence, and mortality in Thailand (59). In the US in 2018, there will be an estimated 266,120 new cases of invasive breast cancer diagnosed in women (**Figure 4**); 2,550 cases diagnosed in men; and an additional 63,960 cases of *in situ* breast lesions diagnosed in women. An estimated 41,400 breast cancer deaths (40,920 women, 480 men) will occur in 2018 (2).

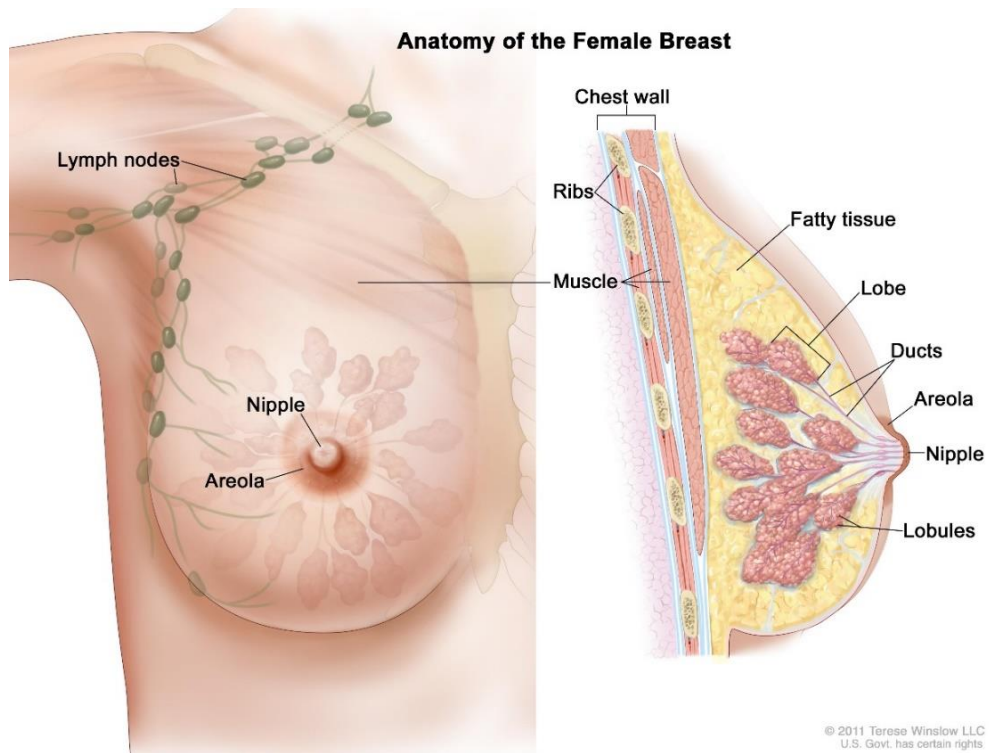


Figure 2 Anatomy of the female breast.

The nipple and areola are shown on the outside of the breast. The lymph nodes, lobes, lobules, ducts, and other parts of the inside of the breast are also shown (2).

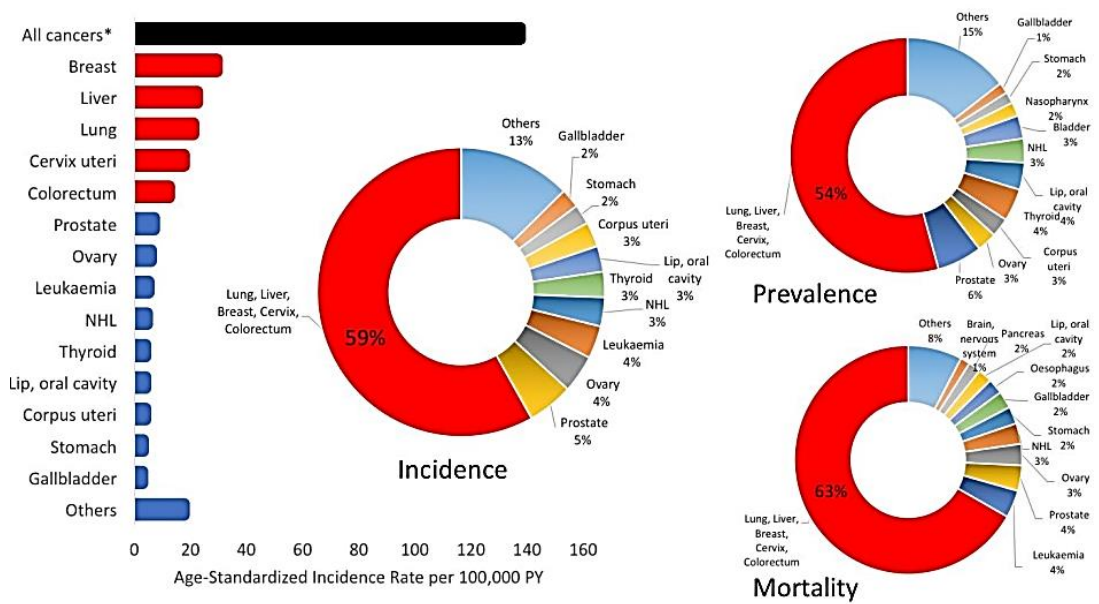


Figure 3 Incidence, Prevalence, and Mortality of cancers in Thailand 2012 (59).

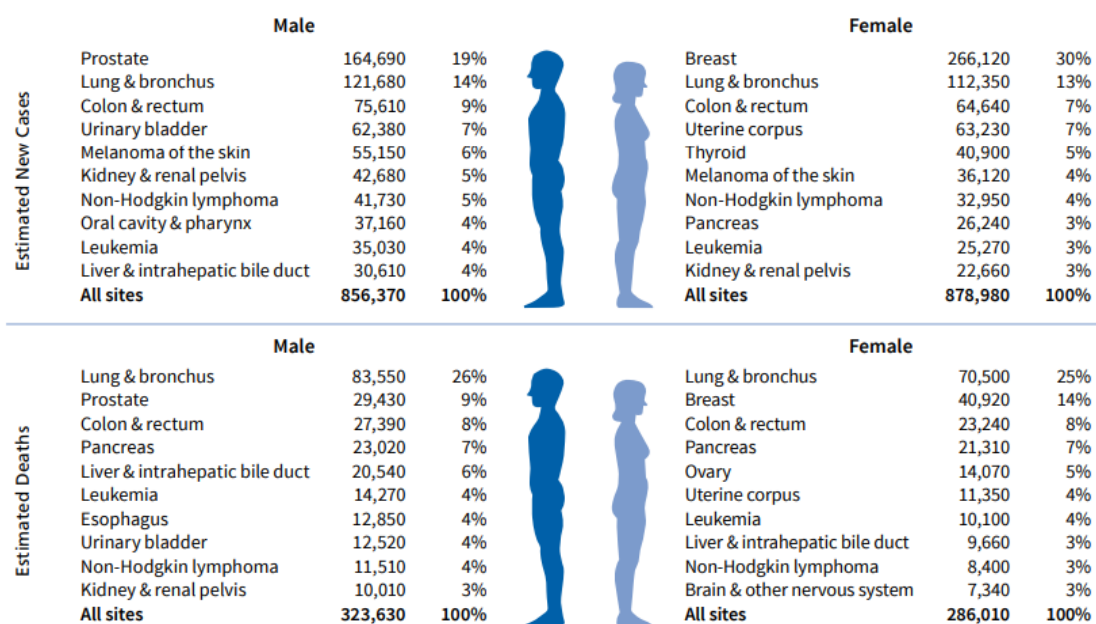


Figure 4 Leading sites of new cancer cases and deaths - 2018 Estimates.

Estimates are rounded to the nearest 10, and cases exclude basal cell and squamous cell skin cancers and in situ carcinoma except for urinary bladder. The ranking is based on modelled projections and may differ from the most recent observed data (2).

### 2.1. Type of breast cancer

Breast cancer is classified by whether cancer started in the ducts or lobules, whether the cells have "invaded" through the duct or lobule, and the way the cancer cells look under a microscope. Breast cancers are broadly grouped into those that are still in the breast lobules or ducts (referred to as "noninvasive" or "carcinoma *in situ*") and those that have spread beyond the walls of the ducts or lobules (referred to as "invasive"). It is not unusual for a single breast tumor to have combinations of these types, and to have a mixture of invasive and non-invasive cancer (60, 61).

#### 2.1.1. Carcinoma *in situ* (CIS)

CIS is early cancer, and it is still confined to the ducts or lobules where it started. It has not spread into surrounding fatty tissues in the breast or to other organs in the body. There are 2 types of breast carcinoma in situ

- Lobular carcinoma *in situ* (LCIS), also called lobular neoplasia. It begins in the lobules but has not grown through the lobule walls. However, women with this condition do run a higher risk of developing invasive cancer.
- Ductal carcinoma *in situ* (DCIS). This is the most common type of noninvasive breast cancer. In DCIS, cancer cells inside the ducts do not spread through the walls of the ducts into the fatty tissue of the breast. DCIS is treated with surgery and sometimes radiation, which are usually curative. If not treated, DCIS may grow and become invasive cancer.

#### 2.1.2. Invasive Breast Cancers.

Invasive cancer describes those cancers that have started to grow and have spread beyond the ducts or lobules. There are many kinds of invasive cancer, but the most common is called invasive ductal carcinoma and invasive lobular carcinoma.

- Invasive (infiltrating) ductal carcinoma (IDC). Cancer starts in a milk passage, or duct, of the breast, but then the cancer cells break through the wall of the duct and spread into the fatty tissue. Cancer cells can then spread into lymphatic channels or blood vessels of the breast and to other parts of the body. This is the most common type of breast cancer. About 80% of all breast cancers are invasive ductal carcinoma.
- Invasive lobular carcinoma (ILC). Invasive lobular carcinoma (ILC) starts in the milk-producing glands (lobules). Like IDC, it can spread (metastasize) to other parts of the body. About 10% to 15% of invasive breast cancers are ILC.
- Special types of invasive breast cancer. They are much less common than the breast cancers listed named above and each typically makes up fewer than 5% of all breast cancers. These

are often named after features seen when they are viewed under the microscope, such as Mixed carcinoma (which has features of both invasive ductal and lobular), Adenoid carcinoma, Low-grade adenosquamous carcinoma, Medullary carcinoma, Papillary carcinoma, and Tubular carcinoma (60, 61).

## 2.2. Molecular subtypes of breast cancer

The immunohistochemical staining was used to classify the molecular subtypes of breast cancer into four major subtypes: Luminal A, Luminal B, HER2-enriched, and triple-negative breast cancers (62).

### 2.2.1. Luminal A (HR+/HER2-) (71%).

These cancers tend to be slow-growing and less aggressive than other subtypes. Luminal A tumors are associated with the most favorable prognosis, particularly in the short term, in part because they are more responsive to anti-hormone therapy (62).

### 2.2.2. Luminal B (HR+/HER2+) (12%).

Like luminal A cancers, luminal B cancers are ER+ and/or PR+ and are further defined by being highly positive for Ki67 (an indicator of a large proportion of actively dividing cells) or HER2. Luminal B breast cancers tend to be a higher grade and are associated with poorer survival than luminal A cancers (62).

### 2.2.3. HER2-enriched (HR-/HER2+) (5%).

HER2-enriched cancers tend to grow and spread more aggressively than other subtypes and are associated with poorer short-term prognosis compared to HR+ breast cancers. However, the recent widespread use of targeted therapies for HER2+ cancers has improved outcomes for these patients (62).

### 2.2.4. Triple-negative (HR-/HER2-) (15-20%).

So-called because they are estrogen receptor (ER)-, progesterone receptor (PR)-, and HER2-, these cancers are twice as common in black women as white women in the US and are also more common in

premenopausal women and those with a BRCA1 gene mutation.<sup>14</sup> The majority (about 75%) of triple-negative breast cancers fall into the basal-like subtype defined by gene expression profiling. Triple-negative breast cancers have a poorer short-term prognosis than other subtypes, in part because there are currently no targeted therapies for these tumors (62).

### 3. Triple-negative breast cancer (TNBC)

TNBCs are regarded as aggressive types of breast cancer and constitute 15–20% of all breast cancers and are naturally recurrent. TNBCs are defined by the absence of progesterone and estrogen receptors as well as human growth factor receptor 2 expressions (4). There are four transcriptional subtypes of TNBCs: two basal subtypes, which are grouped as BL1 and BL2, a mesenchymal subtype M, and a luminal androgen receptor subtype (63). Further, TNBC can be categorized into six different subgroups based on their molecular heterogeneity: immunomodulatory, luminal androgen receptor expression, mesenchymal stem-like, mesenchymal-like, basal-like, and unstable (63). The clinical behavior of TNBCs is relatively aggressive compared to that of other subtypes of breast cancer. Additionally, these cancers have characteristic metastatic patterns and poor prognosis (63).

#### 3.1. Potential risk factors

The potential risk factors of TNBC can be divided into non-modifiable and modifiable risk factors (63).

##### 3.1.1. Non-modifiable risk factors

- Age: Approximately 80% of breast cancers (including TNBCs) are >50 years old (64). The cancer risk increases with age as follows: 1.5% risk at the age of 40 years, 3% at age 50, and more than 4% at age 70 years (64).
- Sex: Due to different-sex hormonal stimulation, the female sex is considered at a higher risk for TNBC compared to the male sex.

Females have breast cells that are very susceptible to estrogen and progesterone hormones, as well as imbalances (65).

- Genetic mutations: Mutations in genes such as BRCA1 and BRCA2 were found to be strongly associated with TNBC (66).
- Race/Ethnicity: The incidence of TNBC remains high among white non-Hispanic women (67). In addition, the mortality rate is significantly higher among black women, and black women are considered to have the lowest survival rates for malignancy (63).
- Genetic history: This is one of the major risk factors associated with breast cancer (like TNBC). Approximately 13–19% of diagnosed breast cancer patients report a first-degree breast cancer relative (63).
- History of radiation therapy: A history of radiotherapy can lead to the development of secondary tumors. This is mainly dependent on the patient's state and age (63).
- History of breast diseases: The initial symptoms of cancer are cancerous lesions in the breast. Regarding the family history of the disease, the other risk factors associated with breast cancer are *in-situ* carcinoma, atypical hyperplasia, proliferative lesions, and non-proliferative lesions (63).

### 3.1.2. Modifiable risk factors

- Drugs: Diethylstilbestrol is a major cause of breast cancer during pregnancy (68). Diethylstilbestrol intake and consumption by pregnant women not only causes breast cancer in the mother but also the child (69). This relationship is observed with diethylstilbestrol uptake even without the expression of estrogen and progesterone receptors (70).
- Body mass index: According to several epidemiological studies, obesity is a potential risk factor for breast cancer. Epidemiologically,

estrogen receptor-positive breast cancer develops in obese women in the postmenopausal period (71).

- Alcohol intake: Various studies reported alcohol consumption is a major cause of cancer in the gastrointestinal tract, along with breast cancer (72). Alcohols are the major causative agents of estrogen-positive breast cancers (72).
- Insufficient vitamin: Supplements are anti-cancer elements that can prevent breast malignancies. Research is underway to evaluate the risk of cancer with the consumption of vitamins, particularly vitamin B, C, and E folic acids and multivitamins (63).
- Exposure to chemicals and drugs: Females who have been exposed to dreadful carcinogenic chemicals are at higher risk of breast cancer and epigenetic alterations and mutations. Exposure and duration of exposure contribute to an increased risk of breast cancer mutagenesis (73).
- Smoking: Tobacco causes mutations in oncogenes and p53 suppressor genes. Active smoking and passive smokers are at a risk of cancer. Smoking during pregnancy and chain smokers are at potential risk of malignancies (63).

### 3.2. Signaling pathway involved in TNBC

#### 3.2.1. Wnt/ $\beta$ -catenin pathway

The Wnt/ $\beta$ -catenin pathway controls the maintenance of somatic stem cells in many tissues and organs and is implicated in pancreatic carcinogenesis by regulating cell cycle progression, apoptosis, epithelial-mesenchymal transition (EMT), angiogenesis, stemness, tumor immune microenvironment, etc. (74). Different Wnt ligands, such as WNT3A, WNT11, and WNT5A, are reported to be pertinent in cancer migration and invasion (75). In particular, the FZD6 receptor is associated with increased malignant cell motility in TNBC (63). The wnt/ $\beta$ -catenin signaling pathway is activated in

epithelial ovarian cancer and targets genes that regulate cell proliferation and apoptosis thereby mediating cancer initiation and progression (63).

### 3.2.2. TGF- $\beta$ signaling pathway

TGF-beta signaling is considered one of the main pathways associated with EMT and breast cancer metastasis (76). *In vivo* analysis, inhibition of TGF- $\beta$  leads results in multiplication and growth of tumor cells. The frequent overexpression of TGF- $\beta$  in the TNBC tumor microenvironment, particularly in stromal, tumor-associated immune cells, and tumor cells (63, 76). Thus, inhibition of TGF- $\beta$  plays a significant therapeutic role in patients with metastasis.

### 3.2.3. Signalling pathway of CSPG4 protein

The CSPG4 protein (non-glia antigen) is expressed as a cell surface proteoglycan by basal breast carcinoma cells. Therapeutically, CSPG4 inhibition allows for efficient management of breast cancer (77). Monoclonal antibodies can block the CSPG4 protein, which hinders survival signalling pathways in tumor cells (78).

### 3.2.4. Hedgehog signalling pathway

The Hedgehog signalling pathway is involved in cancer cell invasion, metastasis, drug resistance, and tumor recurrence. Overexpression of this pathway results in poor prediction of breast cancer mortality, especially in TNBC patients (63, 76).

### 3.2.5. PI3K/AKT/mTOR pathway

The PI3K/Akt/mTOR signalling pathway is a frequently altered oncogenic pathway in many cancers, including TNBC (63). Rapamycin and paclitaxel drugs are used to inhibit the PI3K/AKT/mTOR pathway and hence play a significant role in TNBC treatment. Furthermore, mTOR antibodies are considered more effective than mTOR inhibitors alone (79). In TNBC patients, ipatasertip (an AKT inhibitor) can promote progression-free survival by

inactivating the PI3K/AKT pathway. Despite these efforts on PI3K/AKT/mTOR pathway inhibitors, the synthesis of novel inhibitors is needed to block the PI3K/Akt/mTOR pathway and act as therapeutic agents against TNBC (80).

#### 3.2.6. Epidermal growth factor receptor

The epidermal growth factor family of receptor tyrosine kinases (ErbBs) plays essential roles in regulating cell proliferation, survival, differentiation, and migration (81). The epidermal growth factor receptor is reported in 89% of TNBC and is considered an attractive therapeutic target, particularly in BL2 subtype tumors (63). The expression of this gene results in primary tumorigenesis and metastasis. Several EGFR inhibitors, such as lapatinib and erlotinib, are currently being tested against TNBC, in addition to cetuximab and panitumumab (monoclonal antibodies) (63).

#### 4. *Moringa oleifera* Lam.

*Moringa oleifera* (MO), also known as horseradish tree, drumstick tree, or Miracle tree. This plant was originally found in India (22) and is now distributed mainly in the Middle East, African and Asian countries including Thailand (23, 24). Taxonomically, MO is assigned to the family Moringaceae of the sole genus *Moringa*. The genus “*Moringa*” is estimated to have 13 species, including *M. arborea*, *M. rivae*, *M. borziana*, *M. pygmaea*, *M. longituba*, *M. stenopetala*, *M. ruspoliana*, *M. ovalifolia*, *M. drouhardii*, *M. hildebrandi*, *M. peregrine*, *M. concanensis*, and *M. oleifera*. However, MO is the most cultivated (25). MO is a fast-growing soft wood tree that can reach 12 m in height and has drought resistance properties therefore can be grown in tropical, subtropical, and arid regions of the world. The three require temperature around 25–35°C, sandy or loamy soil with pH between 4.5 and 8, and a net rainfall of 250–3000 mm (22, 82)



Figure 5 *Moringa oleifera* plant. (a) leaves, (b) seeds, (c) flowers, (d) barks, and (e) pods (25, 27, 28).

#### 4.1. Nutritive properties of MO

Every part of MO is a storehouse of important nutrients. Recently reports of the nutrient composition analysis in MO trees have established that leaves, seeds, and stems are rich in protein, essential amino acids, minerals, vitamins, and other bioactive compounds (**Table 1**). The MO leaves are the most used part of the plant. There are rich in minerals like calcium, potassium, zinc, magnesium, iron, and copper. Vitamins like  $\beta$ -carotene of vitamin A, vitamin B (folic acid, pyridoxine, and nicotinic acid), vitamin C, D, and E. The amount of vitamins A, B, C, and E in the MO leaf is reported to be high and can be used to combat malnutrition, especially among infants and nursing mothers (25, 27, 28).

Other parts of the MO plant such as roots, stems, flowers, and fruits have been reported to have rich proximate, fatty acids, minerals, and vitamins profile. Research shows that immature pods contain around 46.78%

fiber and around 20.66% protein content. Pods have 30% of amino acid content, the leaves have 44% and flowers have 31%. The immature pods and flowers showed similar amounts of palmitic, linolenic, linoleic and oleic acids. Moreover, MO has been found to contain a relatively low amount of antinutrients such as phytates, saponins, tannins, and oxalates. These antinutrients are not necessarily toxic but may interfere with digestion and absorption of other nutrients. Therefore, MO appears nutritionally safer and healthier than the above-mentioned common vegetables (25, 27, 28).

*Table 1: The nutrient compositions of leaves, leaves powder, seeds, and pods. (All values are in 100 g per plant material) (83).*

Nutrients	Fresh Leaves	Dry leaves	Leaves powder	Seed	Pods
Calories (cal)	92	329	205	-	26
Protein (g)	6.7	29.4	27.1	35.97 ± 0.19	2.5
Fat (g)	1.7	5.2	2.3	38.67 ± 0.03	0.1
Carbohydrate (g)	12.5	41.2	38.2	8.67 ± 0.12	3.7
Fiber (g)	0.9	12.5	19.2	2.87 ± 0.03	4.8
Vitamin B1 (mg)	0.06	2.02	2.64	0.05	0.05
Vitamin B2 (mg)	0.05	21.3	20.5	0.06	0.07
Vitamin B3 (mg)	0.8	7.6	8.2	0.2	0.2
Vitamin C (mg)	220	15.8	17.3	4.5 ± 0.17	120
Vitamin E (mg)	448	10.8	113	751.67 ± 4.41	-
Calcium (mg)	440	2185	2003	45	30
Magnesium (mg)	42	448	368	635 ± 8.66	24
Phosphorus (mg)	70	252	204	75	110
Potassium (mg)	259	1236	1324	-	259
Copper (mg)	0.07	0.49	0.57	5.20 ± 0.15	3.1
Iron (mg)	0.85	25.6	28.2	-	5.3
Sulphur (mg)	-	-	870	0.05	137

#### 4.2. Phytochemical composition of MO

The MO plant has important functional properties. It contains a huge array of bioactive compounds which are commonly referred to as phytochemicals. Different parts of the MO tree have been established as good sources of carotenoids, flavonoids, polyphenol, phenolic acids, alkaloids, glucosinolates, isothiocyanates, tannins, saponins and oxalates, phytates, and vitamins. Additionally, the pharmacological activities of MO (leaf, stem, seed, and root) extracts have been well described in many studies with health benefits (25, 27, 28).

For amounts of different bioactive compounds found in MO among glucosinolates, 4-O-( $\alpha$ -L-rhamnopyranosyloxy)-benzylglucosinolate (glucomoringin) is the most predominant in the stem, leaves, flowers, pods, and seeds of MO. The highest content of glucosinolate is found in the leaves and seeds. The enzymatic catabolism of glucosinolates by the endogenous plant enzyme myrosinase produces isothiocyanates, nitriles, and thiocarbamates that are known for strong hypotensive (blood pressure lowering) and spasmolytic (muscle relaxant) effects. Among flavonoids, flavonol glycosides (glucosides, rutosides, and malonyl glucosides) of quercetin > kaempferol > isorhamnetin are predominantly found in various parts of the tree, except in the roots and seeds (25, 27, 28).

### 4.3. Phytochemistry of MO

The MO plant has important functional properties. It contains a huge array of bioactive compounds which are commonly referred to as phytochemicals (25-28). The stem of the tree contains the main alkaloids moringin and moringenine along with  $\beta$ -sitosterol and 4-hydroxymellein while the flowers are a rich source of amino acids, flavonoids, kaempferitrin and isoquercetin (25-28). The roots are a good source of anthonine and spirochin which are known to possess bactericidal activity. The trees also are regarded as a storehouse for vitamins and minerals, along with phytochemicals such as glucosinolates and phenols (25-28). The seed kernels of the tree are excellent sources of 4-( $\alpha$ -L-rhamnopyranosyloxy)-benzylglucosinolate. The roots contain both benzyl glucosinolate and 4-( $\alpha$ -L-rhamnopyranosyloxy)-benzylglucosinolate the latter existing in the leaves along with glucosinolates in the isomeric form (25-28). Quercetin-3-O-glucoside and quercetin-3-O-(6"-malonyl-glucoside) are other constituents present in the leaves. In the bark, the only detectable chemical was 4-( $\alpha$ -L-rhamnopyranosyloxy)-benzylglucosinolate (25-28). The fruit extract of MO showed three phenolic glycosides namely 4- [(2' - O -acetyl- $\alpha$ -L-rhamnosyloxy) benzyl] isothiocyanate, 4-[(3'-O-acetyl- $\alpha$ -L-rhamnosyloxy) benzyl] isothiocyanate and S-methyl Nthiocarbamate (25-28).

The isothiocyanates in *Moringa oleifera* have structural similarities with other isothiocyanates (ITCs) like sulforaphane largely present in vegetables like broccoli and phenethyl isothiocyanate from watercress (25-28). Interestingly, the presence of the sugar moiety in the ITCs in Moringa makes them more stable than the ITCs from other plant sources. These ITCs have the potential to regulate various signal transduction pathways by either inhibiting the NF- $\kappa$ B pro-survival pathway or activating the master regulator Nrf2 (25-28).

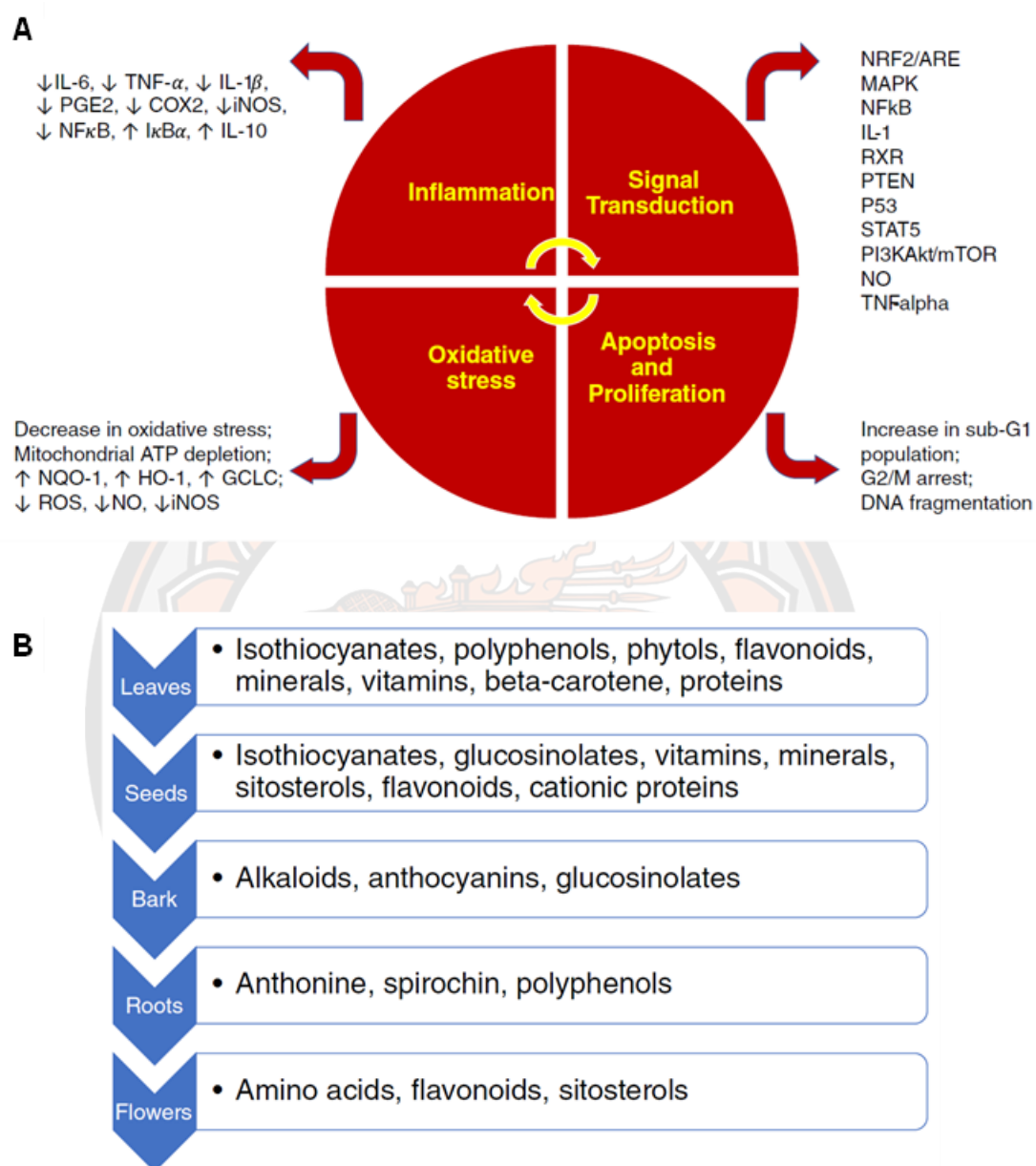


Figure 6 Graphical representation of the use of *Moringa oleifera* tree.

(A) Biomarker modulation studies on Moringa include inflammation, oxidative stress, apoptosis and proliferation, and signal transduction. (B) Moringa tree components and classes of compounds naturally occurring in them (26).

Table 2 Phytoconstituents of *Moringa oleifera* (25-28).

Plant parts	Extraction solvents	Phytoconstituents
Leaves	Aqueous and alcoholic	Niazirin and Niazirin – nitrile glycosides, 4-(4'-O-acetylalpha-L-rhamnosyloxy) benzyl isothiocyanate, Niaziminin A, and Niaziminin B, three mustard oil glycosides, niaziminin, a thiocarbamate, 4-(alpha-1-rhamnopyranosyloxy)-benzylglucosinolate, quercetin - 3-O-glucoside and quercetin-3-O-(6'-(Malonyl-glucoside)), Niazimicin, Pyrrole alkaloid (pyrrolemarumine-4''-O- $\alpha$ -L-rhamnopyranoside) and 40-hydroxyphenylethanamide ( marumoside A and B), alpha and gamma-tocopherol
Seeds	Aqueous and Hydroalcoholic	Methionine, cysteine, benzylglucosinolate, 4-(alpha-L-rhamnopyranosyloxy) benzylglucosinolate, Moringine, niazimicin niazirin
Pods	Hydro-alcoholic	Isothiocyanate, nitrites, thiocarbamates, O-ethyl-4-(alpha-L-rhamnosyloxy) benzyl carbamate, O-(1heptenyloxy) propyl undecanoate, methyl-p-hydroxybenzoate, beta-sitosterol
Bark	Alcoholic	4-(alpha-L- rhamnopyranosyloxy), benzylgiucosinolate
Flowers	Hydro-alcoholic	D-glucose, quercetin, isoquercetin, kaemopherol, kaempferitin and ascorbic acid, protein, D-mannose.
Root	Alcoholic	Moringine, moringinine, spirachin, 1,3-dibenzyl urea, alpha- phellandrene, p-cymene, Deoxy-niazimicine, 4-(alpha-L-rhamnopyranosyloxy), benzylglucosinolate.
Stem	Aqueous and Hydroalcoholic	4-hydroxyl mellein, vanillin, octacosonoic acid, $\beta$ -sitosterone and beta- sitosterol

Table 3 Major bioactive compound in different body parts of *M. oleifera* (84).

Plant parts	Bioactive compounds
Seed	glycosidic benzylamines; niazimicin; isothiocyanates; phenolics; glucosinolates
Leaf	phytol; flavonoids; phenolics; -carotene; lycopene; vicenin-2; quinic acid; octadecanoic acid; hexadecanoic acid (palmitic acid); - tocopherol (vitamin-E); G-sitosterol
Flower	$\beta$ -sitosterol; flavonoids; anthocyanin
Root	nasimizinol; oleic acid; N-benzyl-N-(7-cyanato heptanamide; N-benzyl-N-(1-chlorononyl) amide; bis [3-benzyl prop-2-ene]-1-one; N, N-dibenzyl-2-ene pent-1,5-diamide
Shell	3,5,6-trihydroxy-2-(2,3,4,5,6-pentahydroxyphenyl)-4H-chromen-4-one;-sitosterol-3-O-glucoside; 2,3,4-trihydroxybenzaldehyde; stigmasterol
Bark	epiglobulol; flavonoids; anthocyanin

#### 4.4. Anti-cancer activities of MO

MO can be used as an anticancer agent as it is natural, reliable, and safe, at established concentrations. Studies have shown that MO can be used as an anti-neoproliferative agent, thereby inhibiting the growth of cancer cells. Soluble and solvent extracts of leaves have been proven effective as anticancer agents. Furthermore, research papers suggest that the anti-proliferative effect of cancer may be due to its ability to induce reactive oxygen species in cancer cells. Research showed that the reactive oxygen species induced in the cells lead to apoptosis. This is further proved by the up regulation of caspase 3 and caspase 9, which are part of the apoptotic pathway. Moreover, the ROS production by moringa is specific and targets only cancer cells, making it an ideal anticancer agent (26, 84).

Table 4 Anti-cancer activities of different extracts of *M. oleifera*.

Plant part	Extraction solvent	Targeted biomarker	Cancer type	Ref.
Leaves	Ethanol	Reduction (about 70–90%) in colony formation. Induced cell apoptosis. Arrest the cell cycle at the G2/M phase.	Human breast cancer MDA-MB-231 cells	(85)
	Water	Increase ROS with a decrease in GSH levels in cancer cells. Reduced Nrf2 expression. Induced pro-apoptotic action by increasing DNA fragmentation, p53, caspase-9, caspase-3/7, Smac/DIABLO, and PARP-1 cleaved.	Human lung cancer A549 cells	(86)
	Cold water	Induced apoptosis, inhibited tumor cell growth, and lowered the level of internal ROS in cancer cells, suggesting that the treatment with MOL reduced cancer cell proliferation and invasion.	Human lung cancer A549 cells	(87)
	Hot water	Decrease in mitochondrial membrane potential and ATP levels, followed by an increase in ROS, caspase, proapoptotic proteins (p53, SMAC/Diablo, AIF), and PARP-1 cleavage. This resulted in decreased GSH levels and a decrease in viability	Human lung cancer A549 cells	(88)

Table 4 Anti-cancer activities of different extracts of *M. oleifera* (con.)

Plant part	Extraction solvent	Targeted biomarker	Cancer type	Ref.
Leaves	Hot water	MOL inhibited cancer cell growth by inducing cell cycle arrest at sub-G1 and reduced the expression of p65, p-ikb $\alpha$ , and ikb $\alpha$ proteins.	Human pancreatic cancer cell lines (Panc-1 and COLO357)	(89)
	Hot water	MOL increased lipid peroxidation and DNA fragmentation in SNO cells. Induced apoptosis by the increase in PS, caspase-9, and caspase-3/7, Smac/DIABLO, cleavage of PARP-1 and decreased ATP levels.	Human esophageal cancer SNO cells	(90)
	Hot water	MOL showed a dose-dependent inhibition of cell proliferation of KB cells. Induction of apoptosis, morphological changes, DNA fragmentation, and induced ROS production	Human tumor (KB) cells line	(91)
	Hot water	Decreased the activity of harmful fecal enzymes as well tumors incidence in male CD1-mice.	<i>In vivo</i> AOM/DSS-induced colorectal carcinogenesis model	(92)

Table 4 Anti-cancer activities of different extracts of *M. oleifera* (con.)

Plant part	Extraction solvent	Targeted biomarker	Cancer type	Ref.
Seeds	Water and 80% ethanol	Inhibit cancer cell proliferation determined by MTS assay.	Human breast cancer MCF7 cells	(49)
Pod/fruit	Hot water	Decreased incidences and multiplicities of tumors when compared to the control group in a dose-dependent manner. Decreased in iNOS and COX-2 protein expression.	<i>In vivo</i> AOM/DSS-induced colorectal carcinogenesis mice	(93)
	Hydro-ethanolic extract	Pretreatment with the MO reversed the DMBA-induced alterations (xenobiotic enzyme, cytochrome P450, and b5, GSH, GST, AST, ALT) in the liver tissue and offered almost complete protection.	<i>In vivo</i> DMBA-induced hepatic carcinogenesis mice	(94)
	70% ethanol	Inhibited the cell viability and promoted apoptosis in a dose-dependent manner by increasing cleaved caspase-9 and caspase-3. Enhancement of iNOS and ROS production.	Human melanoma A2058 cells	(95)

Table 4 Anti-cancer activities of different extracts of *M. oleifera* (con.)

Plant part	Extraction solvent	Targeted biomarker	Cancer type	Ref.
Pod/fruit	Hydro-ethanolic extract	Pretreatment with the MO reversed the DMBA-induced alterations (xenobiotic enzyme, cytochrome P450, and b5, GSH, GST, AST, ALT) in the liver tissue and offered almost complete protection.	<i>In vivo</i> DMBA-induced hepatic carcinogenesis mice	(94)
Bark	Ethanol	Reduction (about 70–90%) in colony formation. Induced cell apoptosis. Arrest the cell cycle at the G2/M phase.	Human breast cancer (MDA-MB-231) cells and colorectal cancer (HCT-8) cells	(85)
Root	PLGA-CSPEG nanocomposites	Induced cell apoptosis of various cell lines	Human hep-2, breast MCF7, and colorectal HCT 116/ Caco-2 cells	(48)

#### 4.5. Immunomodulatory Effects of MO

The medicinal plants can modulate the host immune function which in turn exerts positive health benefits and maintain the resistance of the host body against a wide range of infections (96). Also, all aspects such as immune modulation and differentiation are equally important to regulate the normal immune system of the host (96). Inflammation is a biological reaction and defensive indigenous reaction against injury to cells, tissues, and microbial invasion (96). Controlling inflammatory responses aids to clear hazardous stimuli and recalling normal functioning. Certain immunomodulators can regulate inflammatory stimuli through a complex process that includes numerous cells, tissue, and pro- and anti-inflammatory responses which help to control cell migration, proliferation, and chemotaxis in a highly coordinated manner (96).

Following treatment, MO extract can considerably moderate the development of paw edema paralleled to the control group (97). MO butanol seed extract has inhibitory effects on airway inflammation by modulating the relationship between Th1/Th2 cytokines in pigs (98). Also, the seed powder noticeably improves peak expiratory flow, forced vital capacity, and forced expiratory volume with no adverse effects (98).

The MO root exhibits varied pharmacological activity and is used in traditional medicine to cure inflammation and cancer (99). Recently reported that a differentiation of polysaccharide MRP-1 derived from MO root consists of rhamnose, arabinose, fructose, xylose, mannose, and galactose as a repeating subunit. The MRP-1 shows excellent anti-inflammatory activity via suppressing the production of nitric oxide and TNF- $\alpha$  (100).

MO leaves are an important source of flavonoids, such as kaempferol and quercetin (96). Three MO samples (PKM1, PKM2, and Z-11) were screened for anti-inflammatory activity and PKM1 and PKM2 exhibited excellent anti-inflammatory activity via inhibition of NO production in the RAW 264.7 macrophage cell line (101). MO leaves and associated chemical compounds such as quercetin can be used as alternative medicines against

inflammation and oxidative stress. A recent study concluded that MO leaf extract and associated compounds such as quercetin successfully prevented the development of inflammatory responses in animals fed a high-fat diet feed via quenching of  $H_2O_2$ , superoxide, and reactive oxygen species (ROS) (102).

Various parts of MO have been found to reveal immunosuppressive and immunostimulatory activity. For example, MO leaf extract (1–10  $\mu\text{g/mL}$ ) acts as an immunostimulant for T and B cells. Following treatment, there is a substantial enhancement in the numbers of CD4+, CD8+, and B220+ cells in male BALB/c mice (43). Similarly, the leaf extract encourages both cellular and humoral immunity via the reduction in cyclophosphamide-mediated isothiocyanates and glycoside cyanide-like compounds (96).

Recently it was suggested that oral gastric small intestine digestion influences the bioaccessibility of the phenolic compounds of MO leaves (96). The results show that the release of a total phenolic compound is higher in a digested sample as compared to an un-digested sample. Also, the stimulated colonic fermentation enhances the production of SCFAs which in turn changes the composition of gut microbiota and has helped the host immunity (103). The changes in gut microbiota composition have been regarded as one of the main factors related to the health status of the host.

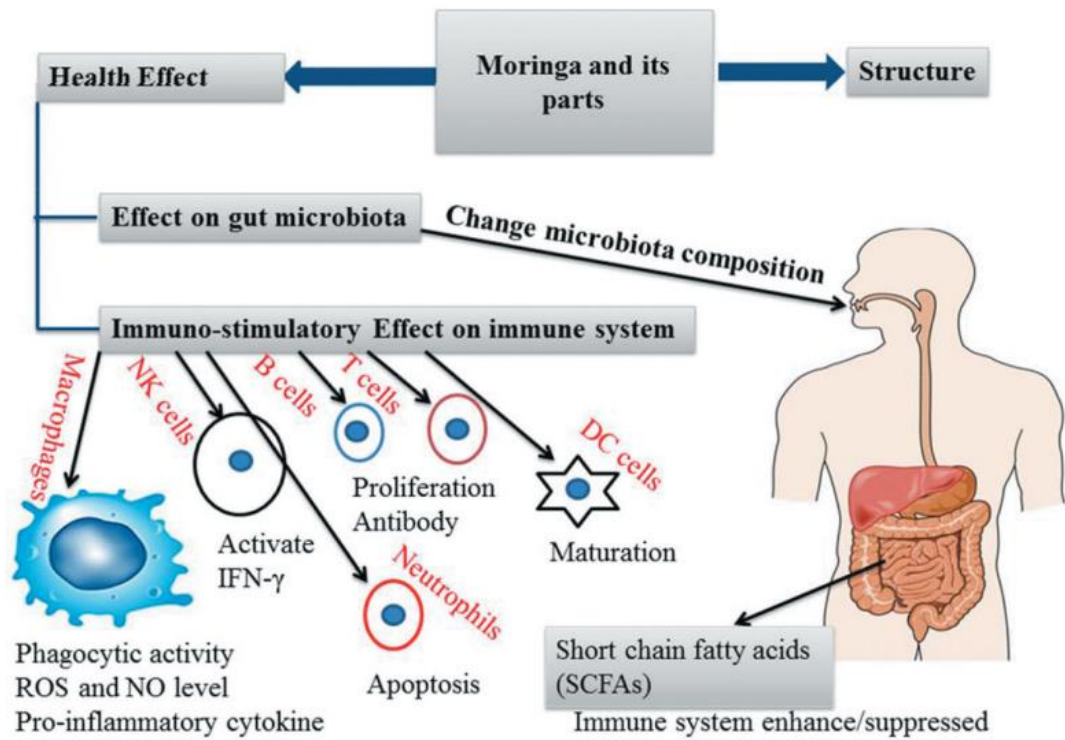


Figure 7 Illustration of immunomodulatory potential of *M. oleifera* after interaction/trigger of several molecular and cellular events.

In some cases, the microbiota may convert the extract compounds into short-chain fatty acids (SCFAs), which may exert an anti-inflammatory effect on hos (96).

## 5. Methods Used for Extraction, Separation, and Characterization of Bioactive Compounds from Plant Extracts

### 5.1. Extractions

Extraction is the first step in the analysis of medicinal plants because it is necessary to extract the desired chemical components from the plant materials for further separation and characterization (104). The basic operation included steps, such as pre-washing, drying of plant materials or freeze-drying, grinding to obtain a homogenous sample, and often improving the kinetics of analytic extraction and also increasing the contact of the sample surface with the solvent system (104). Proper actions must be taken to assure that potential active constituents are not lost, distorted, or destroyed during the preparation of the extract from plant samples (104).

#### 5.1.1. Maceration

In this process, the whole or coarsely powdered material is placed in a stoppered container with the solvent and allowed to stand at room temperature for at least 3 days with frequent agitation. At the end of the process, the solvent is drained off and the remaining miscellany is removed from the plant material through pressing or centrifuging. Maceration is not an advanced technique since active ingredients cannot be completely extracted (105, 106).

#### 5.1.2. Percolation

A percolator that has a narrow cone-shaped vessel open at both ends is used for this technique. The plant material is moistened with the solvent and allowed to place in a percolation chamber. Then the plant material is rinsed with the solvent several times until the active ingredient is extracted. The solvent can be used until its point of saturation (105, 106).

### 5.1.3. Serial exhaustive extraction

It is another common method of extraction that involves successive extraction with solvents of increasing polarity from a non-polar (hexane) to a more polar solvent (methanol or ethanol) to ensure that a wide polarity range of compounds could be extracted. Some researchers employ different extraction of dried plant material using an organic solvent. This method cannot be used for thermolabile compounds as prolonged heating may lead to the degradation of compounds (68, 69).

### 5.1.4. Supercritical fluid extraction (SFE).

SFE involves the use of gases, usually CO<sub>2</sub>, and compressing them into a dense liquid. This liquid is then pumped through a cylinder containing the material to be extracted. From there, the extract-laden liquid is pumped into a separate chamber where the extract is separated from the gas, and the gas is recovered for re-use. Solvent properties of CO<sub>2</sub> can be manipulated and adjusted by varying the pressure and temperature. The advantages of SFE are no solvent residues left in it as CO<sub>2</sub> evaporates completely (68, 69).

### 5.1.5. Microwave-assisted extraction.

Microwave energy facilitates the separation of active ingredients from the plant material into the solvent. Microwaves possess electric and magnetic fields which are perpendicular to each other. The electric field generates heat via dipolar rotation and ionic conduction. As high as the dielectric constant of the solvent, the resulting heating is fast. Unlike the classical methods, microwave-assisted extraction heats the whole sample simultaneously. During the extraction, heat disrupts weak hydrogen bonds due to dipole rotation of molecules and the migration of dissolved ions increases the penetration of solvent into the sample or matrix (68, 69).

#### 5.1.6. Ultrasound-assisted extraction.

This is an advanced technique that has the capability of extracting a large number of bioactive compounds within a shorter extraction time. The main advantage of this technique is the increasing penetration of solvent into the matrix due to the disruption of cell walls produced by acoustical cavitations. And also, this achieves at low temperatures and hence this is more suitable for the extraction of thermally unstable compounds (105, 106).

### 5.2. Separation methods

The components in the extract from the above methods are complex and contain a variety of natural products that require further separation and purification to obtain the active fraction or purely natural products (107). The separation depends on the physical or chemical difference of the individual natural product. Chromatography, especially column chromatography, is the main method used to obtain pure natural products from a complex mixture (107).

#### 5.2.1. Thin-layer chromatography (TLC).

TLC is a simple, quick, inexpensive procedure, and used to support the identity of a compound in a mixture. TLC separation depends on the relative affinity of compounds towards stationary and the mobile phase. The compounds under the influence of the mobile phase (driven by capillary action) travel over the surface of the stationary phase. During this movement, the compounds with higher affinity to the stationary phase travel slowly while the others travel faster. Additional tests involve the spraying of phytochemical screening reagents, which cause color changes according to the phytochemicals existing in plant extract; or by viewing the plate under UV light as shown in Figure 8. This has also been used to confirm of purity and identity of isolated compounds (108, 109).

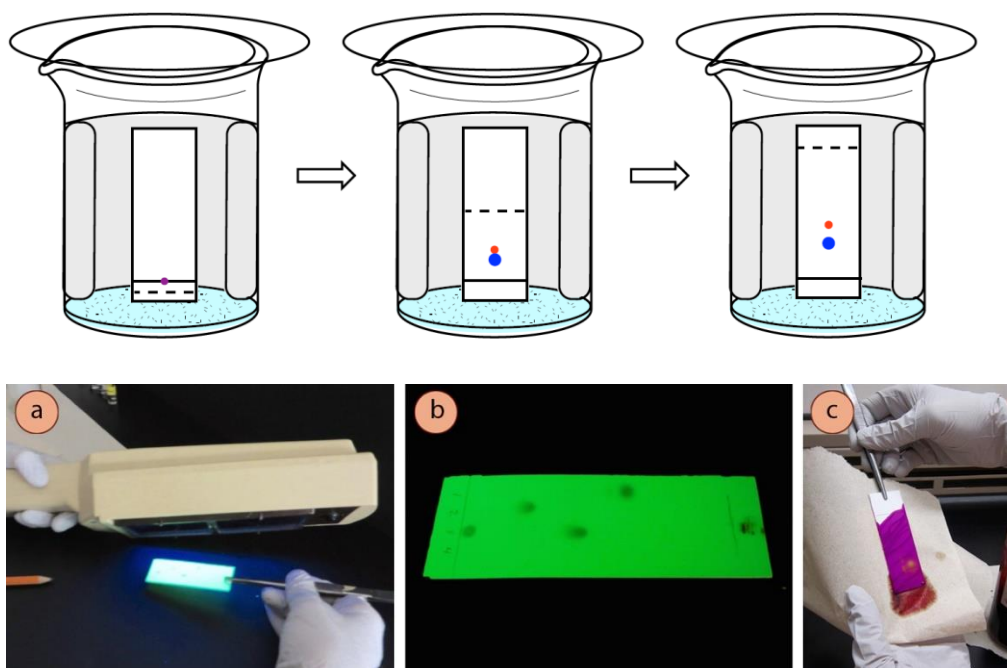


**Figure 8 Thin-layer chromatography (TLC) and Visualization of a TLC plate.**

A) Visualization by using UV light, b) Compounds appear dark against a fluorescent green background, c) Use of a chemical stain to visualize a plate (110).

#### 5.2.2. Column chromatography (CC).

Column chromatography involves ion exchange, molecular sieves, and adsorption phenomena. The flushing in conventional chromatography greatly dilutes the material, and the fractions usually require another step for concentration. A newer method called displacement chromatography elutes with some compounds that have a great affinity for the adsorbent. Fractions of eluting materials can be more concentrated than the original solution applied to the column (109).

### 5.3. Identification and characterization

Since plant extracts usually occur as a combination of various types of bioactive compounds or phytochemicals with different polarities, their separation remains a big challenge for the process of identification and characterization of bioactive compounds. It is a common practice in isolation of these bioactive compounds that several different separation techniques such as TLC, column chromatography, flash chromatography, Sephadex chromatography, and HPLC, should be used to obtain pure compounds. The pure compounds are then used for the determination of structure and biological activity. Besides that, non-chromatographic techniques such as immunoassay, which uses monoclonal antibodies (MAbs), phytochemical screening assay, and Fourier-transform infrared spectroscopy (FTIR), can also be used to obtain and facilitate the identification of the bioactive compounds (104).

#### 5.3.1. High-performance liquid chromatography (HPLC).

HPLC is an analytical technique for the separation and determination of organic and inorganic solutes in any sample. HPLC separates compounds based on their interactions with solid particles of a tightly packed column and the solvent of the mobile phase. Modern HPLC uses a non-polar solid phase, like C18, and a polar liquid phase, generally a mixture of water and another solvent. High pressure of up to 400 bars is required to elute the analyte through the column before they pass through a diode array detector (DAD). The DAD measures the absorption spectra of the analytes to aid in their identification. HPLC is useful for compounds that cannot be vaporized or that decompose under high temperatures, and it provides a good complement to gas chromatography for the detection of compounds (108).

#### 5.3.2. UV-Visible Spectroscopy.

UV-visible spectroscopy can be performed for qualitative analysis and identification of certain classes of compounds in both pure and

biological mixtures. Preferentially, UV-visible spectroscopy can be used for quantitative analysis because aromatic molecules are powerful chromophores in the UV range. Phenolic compounds including anthocyanins, tannins, polymer dyes, and phenols form complexes with iron that have been detected by ultraviolet/visible (UV-Vis) spectroscopy. Moreover, spectroscopic UV-Vis techniques were found to be less selective and give information on the composition of the total polyphenol content. The UV-Vis spectroscopy was used to determine the total phenolic extract (280 nm), flavones (320 nm), phenolic acids (360 nm), and the total anthocyanins (520 nm) (108).

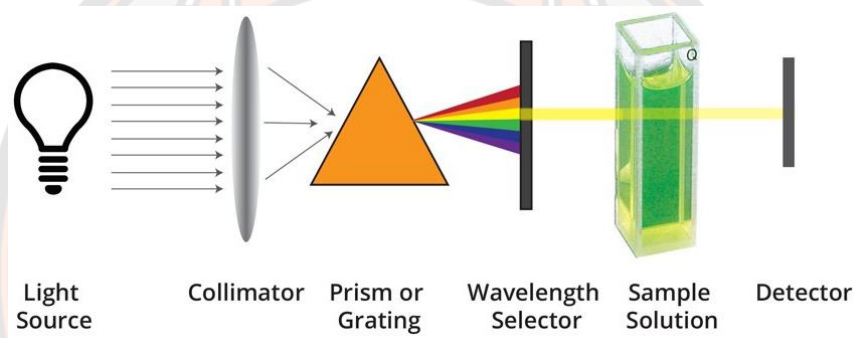


**Figure 9** The principle of UV/Visible spectroscopy.

The basic parts of a spectrophotometer are a light source, a holder for the sample, a diffraction grating in a monochromator or a prism to separate the different wavelengths of light, and a detector (111).

### 5.3.3. Infrared Spectroscopy (IR).

The principle of Infrared Spectroscopy (IR) is based on vibrational changes that happen inside a molecule when it is exposed to infrared radiation. Some of the frequencies will be absorbed when infrared light passes through a sample of an organic compound; however, some frequencies will be transmitted through the sample without any absorption occurring. Therefore, infrared spectroscopy can essentially be described as vibrational spectroscopy. Different bonds (C–C, C=C, C≡C, C–O, C=O, O–H, and N–H) have diverse vibrational

frequencies. If these kinds of bonds are present in an organic molecule, they can be identified by detecting the characteristic frequency absorption band in the infrared spectrum (108).

#### 5.3.4. Nuclear Magnetic Resonance Spectroscopy (NMR).

NMR is primarily related to the magnetic properties of certain atomic nuclei, notably the nucleus of the hydrogen atom, the proton, the carbon, and an isotope of carbon. NMR spectroscopy has enabled many researchers to study molecules by recording the differences between the various magnetic nuclei and thereby giving a clear picture of what the positions of these nuclei are in the molecule. Moreover, it will demonstrate which atoms are present in neighboring groups. Ultimately, it can conclude how many atoms are present in each of these environments (108).

#### 5.3.5. Mass Spectrometry for chemical compounds identification.

Organic molecules are bombarded with either electrons or lasers in mass spectrometry and thereby converted to charged ions, which are highly energetic. A mass spectrum is a plot of the relative abundance of a fragmented ion against the ratio of mass/charge of these ions. Using mass spectrometry, relative molecular mass (molecular weight) can be determined with high accuracy and an exact molecular formula can be determined with a knowledge of places where the molecule has been fragmented. The techniques of UV-visible, IR, NMR, and mass spectrometry were employed to characterize the structure of the bioactive molecule. Furthermore, molecules may be hydrolyzed and their derivatives characterized. Mass spectrometry provides abundant information for the structural elucidation of the compounds when tandem mass spectrometry (MS) is applied. Therefore, the combination of HPLC and MS facilitates rapid and accurate identification of chemical compounds in medicinal herbs, especially when a pure standard is unavailable (108).

## 6. Oleamide

Oleamide (cis-9-octadecenamide) is the prototype long-chain primary fatty acid amide lipid messenger (112). The natural occurrence of oleamide was first reported in human serum in 1989 (112). Subsequently, oleamide was shown to accumulate in the cerebrospinal fluid of sleep-deprived cats and to induce sleep when administered to experimental animals (113). Accordingly, oleamide first became known for its potential role in the mechanisms that mediate the drive to sleep.

### 6.1. Structure

Oleamide (cis-9,10-octadecenoamide) is a long chain fatty acid amides (114). This group is characterized by an alkyl chain of 16 or more carbons and a terminal primary amide, R1-CO-NH<sub>2</sub>. Long-chain secondary amides, represented by anandamide, are characterized by the structure R1-CO-NH-R<sub>2</sub>, where R<sub>1</sub> is a fatty acyl group and -NH-R<sub>2</sub> is a defining moiety such as ethanolamine, an amino acid, dopamine, serotonin, etc (114, 115).

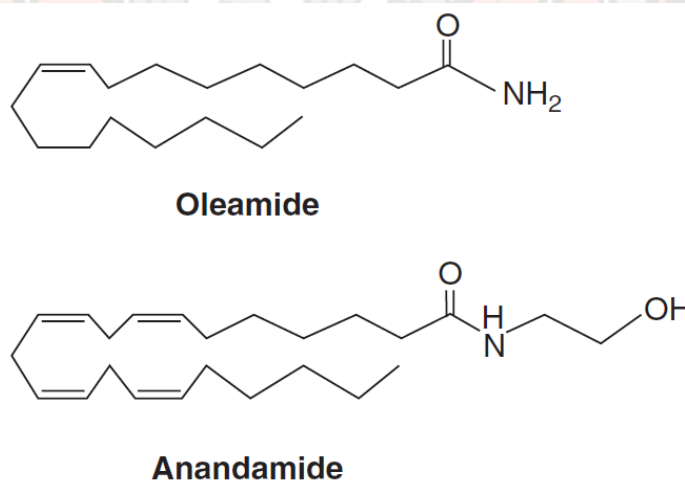


**Figure 10 Structures of the prototype long-chain primary and secondary fatty acid amide classes of lipid messengers.**

Oleamide represents the long-chain primary fatty acid amides. This group is characterized by an alkyl chain of 16 or more carbons and a terminal primary amide, R<sub>1</sub>-CO-NH<sub>2</sub>. Long-chain secondary amides are represented by anandamide (116).

## 6.2. Biosynthesis of oleamide

Oleamide has been noted to be synthesized in brain slices incubated with both oleic acid and ammonia which is mediated by enzymes as boiling the brain slices (denaturing enzymes) abolished the synthesis (114, 116). Oleamide can be degraded into Oleic acid via the membrane enzyme Fatty acid amide hydrolase (FAAH), the same enzyme that metabolites anandamide (arachidonoyl ethanolamide) and bioactive in marijuana (117). Interestingly, inhibiting this enzyme has been noted to inhibit the synthesis of oleamide (mouse N18TG2 cells[14]) although the exact biosynthesis route is not yet determined (117). What appears to be known is that oleic acid is converted into Oleoyl-CoA and then N-Oleoylglycine where oxidative cleavage of N-Oleoylglycine by the enzyme peptidylglycine  $\alpha$ -amidating monooxygenase (PAM) creates oleamide (117). It should be noted that the intermediate N-Oleoylglycine appears to be biologically active as well (117).



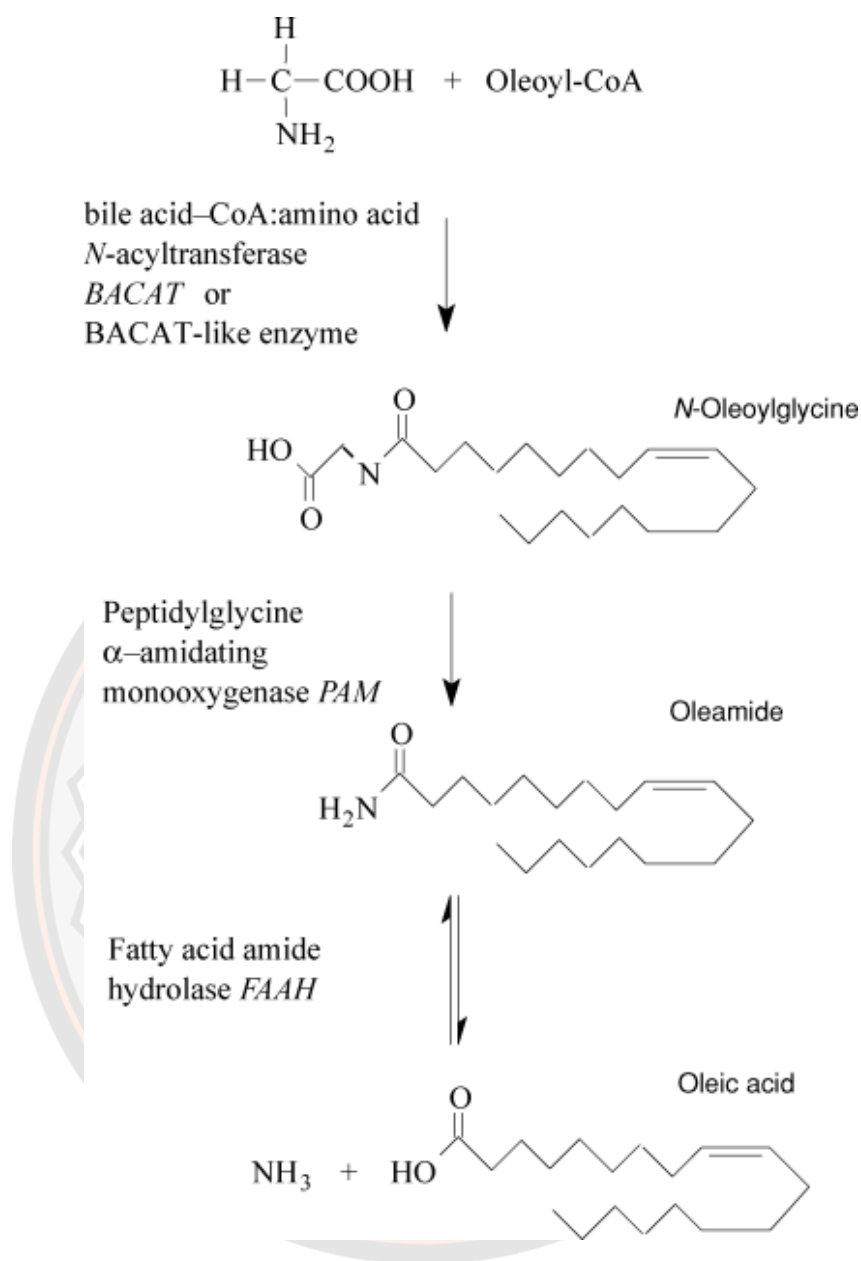


**Figure 11** The synthetic pathway for oleamide.

Which is usually proposed involves the production of *N*-oleoylglycine, possibly simply from oleoyl-CoA and glycine, and then the production of oleamide by PAM. The enzyme producing the oleoylglycine has yet to be identified, but *BACAT*, or a related enzyme, has been suggested as a possible candidate. Oleamide is inactivated by hydrolysis with *FAAH*, but this enzyme can also synthesize oleamide from oleic acid and ammonia and this might also provide a synthetic route to oleamide, although high concentrations of ammonia are required *in vitro* (117).

### 6.3. Biological activity of oleamide

Oleamide was first found to exist in the cerebrospinal fluid of sleep-deprived animals and act as an endogenous sleep-inducing substance (113). Besides inducing sleep, systemic administration of exogenous oleamide has been shown to produce a variety of central nervous system (CNS) effects, including elicitation of hypothermia, analgesia, memory, food intake, hypo-locomotion, and reduction of pentylenetetrazole-induced epileptic behavior (112, 118-122). Furthermore, it was recently reported that oleamide reduces amyloid- $\beta$  ( $A\beta$ ) accumulation via enhanced microglial phagocytosis and suppresses inflammation after amyloid  $A\beta$  deposition (123). Oleamide was found to suppress LPS-induced nitrite production of pro-inflammatory cytokines, NO, and PGE2 secretion in pre-treatment of RAW264.7 cells (97). Oleamide also suppressed the phosphorylation of mitogen-activated protein kinases such as ERK1/2 and JNK (97).

## 7. Introduction to the Immune System

The immune system is a network of cells, tissues, and organs that work together to defend the body from “foreign antigens”, which are live organisms that can cause infections such as bacteria, viruses, parasites, and fungi. (124). The most important physiologic function of the immune system is to prevent or eradicate these infections (**Table 5**) (125).

Table 5 Importance of the immune system in health and disease (125).

<b>Role of the immune system</b>	<b>Implications</b>
<b>Defense against infections</b>	Deficient immunity results in increased susceptibility to infections; vaccination boosts immune defenses and protects against infections
<b>Defense against tumors</b>	Potential for immunotherapy of cancer
<b>The immune system can injure cells and induce pathologic inflammation</b>	Immune responses are the cause of allergic, autoimmune, and other inflammatory diseases
<b>The immune system recognizes and responds to tissue grafts and newly introduced proteins</b>	Immune responses are barriers to transplantation and gene therapy

### 7.1. Innate and adaptive immunity

The immune system has been divided into two general types of reactions: the reactions of innate immunity and the reactions of adaptive immunity (124). Innate immunity, also called natural immunity or native immunity, which provides immediate protection against microbial invasion and rapidly eliminates microbes (125). Adaptive immunity develops more slowly and provides a more specialized defense against infections (125).

Innate immunity is the first line of defense provided by epithelial barriers of the skin and mucosal tissues and by cells and natural antibiotics present in epithelia, all of which function to block the entry of microbes (125). If microbes can pass through the skin barriers and enter the tissues or circulation, they are attacked by tissue-resident immune cells such as phagocytes, natural killer cells, and several plasma proteins as well as proteins of the complement system) (124, 125). All these mechanisms of innate immunity specifically recognize and react against microbes (125). In addition to providing early defense against infections, innate immune

responses enhance adaptive immune responses against the infectious agents (Figure 12) (124, 125).

Adaptive immunity consists of lymphocytes and their products, such as antibodies (125). Whereas the mechanisms of innate immunity recognize structures shared by classes of microbes, the lymphocyte cells of adaptive immunity express receptors that specifically recognize a much wider variety of molecules produced by microbes as well as noninfectious substances. Any substance that is specifically recognized by lymphocytes or antibodies is called an antigen (125). Therefore, adaptive immunity can refer to antigen-specific immune responses. Adaptive immune responses often use the cells and molecules of the innate immune system to eliminate microbes, and adaptive immunity functions to greatly enhance these antimicrobial mechanisms of innate immunity (125).

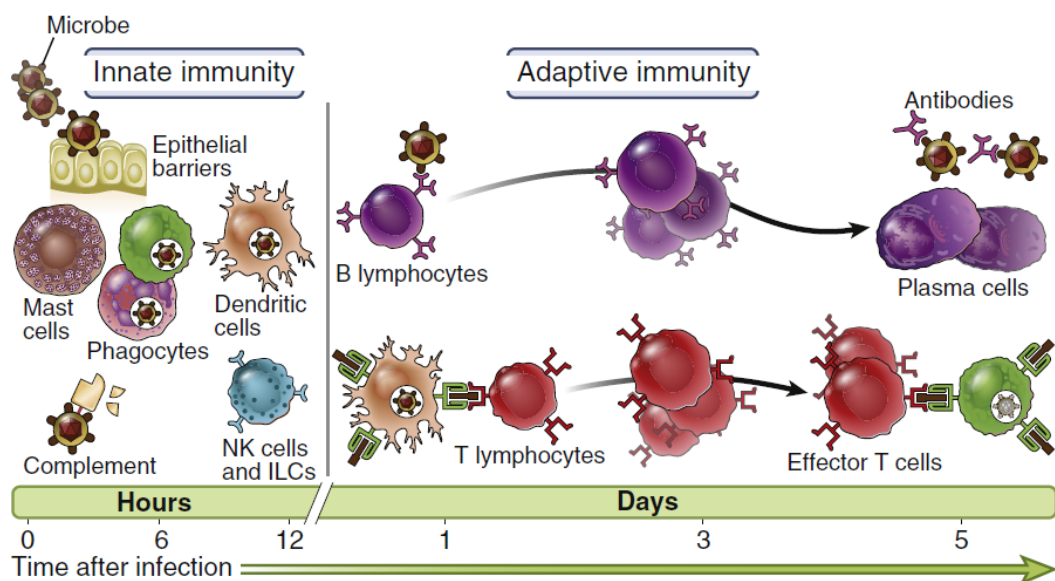


**Figure 12** Principal mechanisms of innate and adaptive immunity.

The mechanisms of innate immunity provide the initial defense against infections. Some mechanisms prevent infections, and other mechanisms eliminate microbes. Adaptive immune responses develop later and are mediated by lymphocytes and their products. Antibodies block infections and eliminate microbes, and T lymphocytes eradicate intracellular microbes. The kinetics of the innate and adaptive immune responses are approximations and may vary in different infections (125).

## 7.2. Components of innate immunity

The components of the innate immune system include epithelial cells; sentinel cells in tissues (macrophages, dendritic cells, mast cells, and others); innate lymphoid cells, including NK cells; and several plasma proteins (125). The properties of these cells and soluble proteins and their roles in the innate immune response are discussed in the following paragraphs (125).

### 7.2.1. Epithelial barriers

The major interfaces between the body and the external environment, include the skin, gastrointestinal tract, respiratory tract, and genitourinary tract. These barriers are protected by continuous epithelia that provide physical and chemical barriers against infection (125).

### 7.2.2. Phagocytes: Neutrophils and monocytes/macrophages

There are two types of circulating phagocytes, neutrophils and monocytes, which are blood cells that are recruited to sites of infection, where they recognize and ingest microbes for intracellular killing (125).

### 7.2.3. Neutrophils

Also called polymorphonuclear leukocytes (PMNs), are the most abundant leukocytes in the blood (125). Neutrophils are the first cell type to respond to most infections, particularly bacterial and fungal infections, and thus are the dominant cells of acute inflammation (125).

### 7.2.4. Monocytes/Macrophages

During inflammatory reactions, monocytes enter extravascular tissues and differentiate into cells called macrophages, which survive in these sites for long periods (125). Macrophages serve several important roles in host defense: they produce cytokines that induce and regulate inflammation, they ingest and destroy microbes, and they clear dead tissues and initiate the process of tissue repair (125).

#### 7.2.5.Dendritic cells

Dendritic cells respond to microbes by producing numerous cytokines that serve two main functions: they initiate inflammation and stimulate adaptive immune responses (125). By sensing microbes and interacting with lymphocytes, especially T cells, dendritic cells constitute an important bridge between innate and adaptive immunity (125).

#### 7.2.6.Mast cells

Mast cells are bone marrow-derived cells with abundant cytoplasmic granules that are present in the skin and mucosal epithelium (125). Mast cell granules contain vasoactive amines such as histamine that cause vasodilation and increased capillary permeability, as well as proteolytic enzymes that can kill bacteria or inactivate microbial toxins (125).

#### 7.2.7.Innate lymphoid cells

Innate lymphoid cells (ILCs) are lymphocyte-like cells that secrete cytokines and perform functions like those of T lymphocytes (125). The difference is that ILCs do not express T cell antigen receptors (TCRs) (125).

#### 7.2.8.Natural killer cells

Natural killer (NK) cells recognize infected and foreign particles and then activate the intracellular process to kill these cells/particles (125).

#### 7.2.9.Complement system

The complement system is a collection of circulating protein and membrane-associated proteins that are important in defense against microbes (125). Many complement proteins are proteolytic enzymes that can opsonize to the pathogens and attack the pathogen's cell by triggering the proteolytic cascades and lysis of the pathogen (125, 126).

#### 7.2.10. Cytokines of innate immunity

Cytokines are soluble proteins that active or suppress immune function and inflammatory reactions as well as responsible for cell-cell communications (125).

### 7.3. Components of adaptive immunity

The adaptive immune system consists of lymphocytes and their secreted products (125). There are two types of adaptive immunity, called humoral immunity and cell-mediated immunity, which are regulated by different cell types and molecules (125).

#### 7.3.1. Humoral immunity

This is mediated by proteins called antibodies, which are produced by B lymphocytes (125). Secreted antibodies enter the blood circulation and mucosal fluids, which functions to clearance microbes and neutralize the extracellular toxin or foreign particle (125).

#### 7.3.2. Cell-mediated immunity

This is mediated by T lymphocytes. T lymphocytes are composed of two major types: cytotoxic T lymphocytes (CD8+ T cells) and helper T lymphocytes (CD4+ T cells) (125). Cytotoxic T lymphocytes kill the infected cells with microbe in the cytoplasm by triggering apoptosis. Whereas helper T lymphocytes recognize microbial (125).

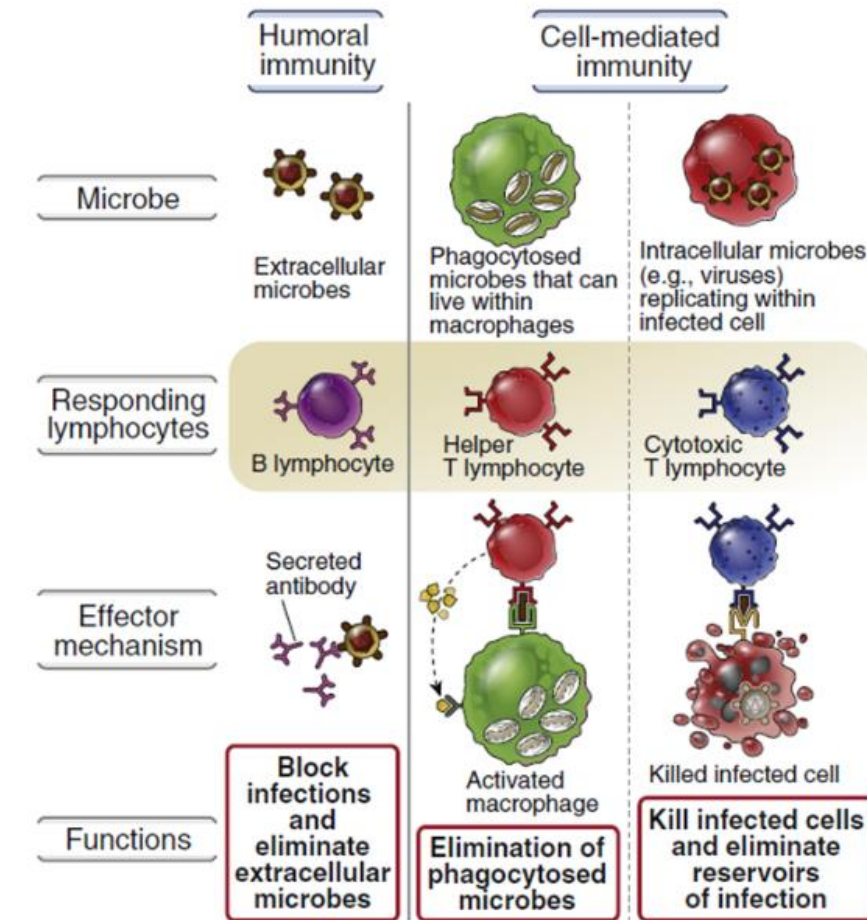


Figure 13 Types of adaptive immunity. In humoral immunity, B lymphocytes secrete antibodies that eliminate extracellular microbes.

In cell-mediated immunity, different types of T lymphocytes recruit and activate phagocytes to destroy ingested microbes and kill infected cells (125).

## 8. Macrophages

Macrophages are tissue-resident innate immune cells that originate from blood circulating monocytes and distribute into specific tissues, where they differentiate into macrophages and contribute to both homeostasis and disease (127). Macrophages were first identified in the late 19<sup>th</sup> century by Elie Metchnikoff, who discovered the phagocytosis process (128). Macrophages are highly effective to sense and respond to tissue invasion by infectious microorganisms and tissue injury through phagocytic receptors on the cell surface

(129). They are strategically placed in many tissues of the body for the protection of the host body. Macrophages can *recognize and phagocytose* pathogens and also play a role in an inflammatory process by secreting cytokines and other mediators into tissues to recruit other immune cells (130). The function of macrophages is a summary of their ontogeny, the local environment in which they reside, and the type of injuries or pathogen to which they are exposed.

### 8.1. Development of monocytes and macrophages

The mononuclear phagocyte system includes circulating cells called monocytes, which become macrophages when they migrate into tissues, and tissue-resident macrophages, which are derived mostly from hematopoietic precursors during fetal life (**Figure 14**) (131). Macrophages are widely distributed in all organs and connective tissue (131). In adults, cells of the monocyte/macrophage lineage arise from committed precursor cells in the bone marrow, driven by a cytokine called monocyte (or macrophage) colony-stimulating factor (M-CSF) (131). These precursors mature into monocytes, which enter and circulate in the blood, and then migrate into tissues, especially during inflammatory reactions, where they further mature into macrophages (131). Many tissues are populated with long-lived resident macrophages derived from the yolk sac or fetal liver precursors during fetal development, and they assume specialized phenotypes depending on the organ (**Figure 14**). Examples are Kupffer cells lining the sinusoids in the liver, alveolar macrophages in the lung, and microglial cells in the brain (131).

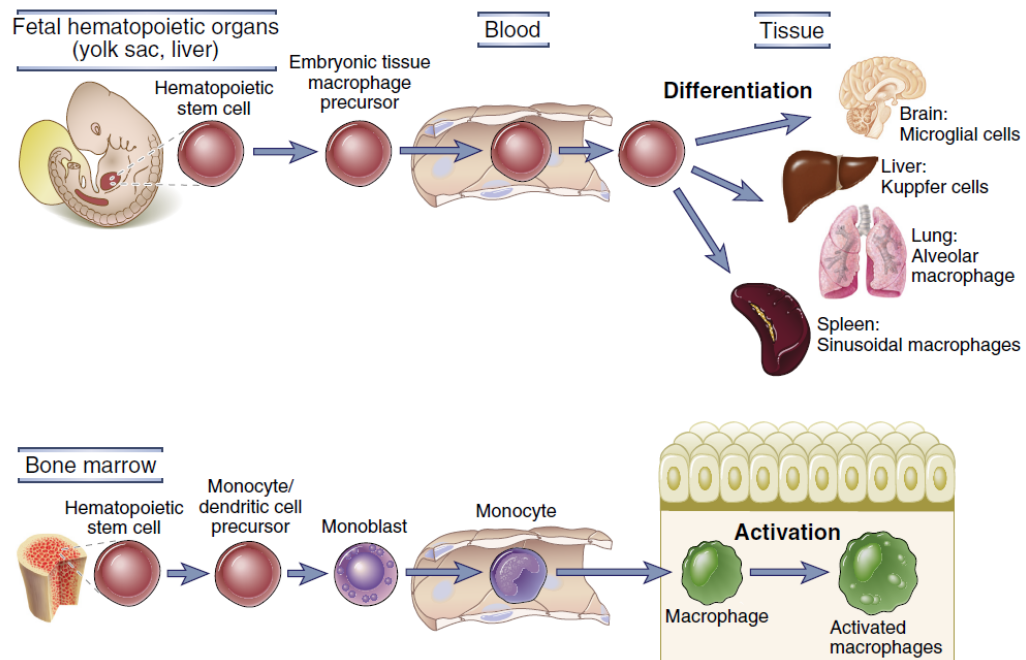


**Figure 14** Maturation of mononuclear phagocytes.

Tissue-resident macrophages are derived from precursors in the yolk sac and fetal liver during fetal life. Monocytes arise from a precursor cell of the myeloid lineage in the bone marrow, circulate in the blood, and are recruited into tissues in inflammatory reactions, where they further mature into macrophages (131).

## 8.2. Macrophage polarization

Macrophage polarization is a process whereby macrophages adopt different functional phenotypes in response to specific microenvironmental stimuli and signals (13). This process is crucial for inflammation, tissue repair, and homeostasis maintenance (132). Macrophage polarization is conventionally divided into three groups as naïve macrophages ( $M\emptyset$ ; also called  $M0$ ), which readily differentiate into two major phenotypes as classically activated macrophages ( $M1$ ) and alternatively activated macrophages ( $M2$ ) (12-14).  $M1$  macrophages, also known as pro-inflammatory macrophages which characterized by high levels of reactive oxygen species (ROS) and nitric oxide (NO) and the production of pro-inflammatory cytokines (1, 5). Whereas  $M2$  macrophages, commonly known as anti-inflammatory macrophages which responsible for immunosuppression, wound healing, and tumor progression mechanisms (3).

### 8.2.1.M1 macrophage

M1 macrophage phenotype, also known as classically activated macrophages which characterized by the production of high levels of pro-inflammatory cytokines, an ability to mediate resistance to pathogens, strong microbicidal properties, high production of cytotoxic mediators, and promotion of T-helper 1 (Th1) responses (14, 133). M1 macrophages produce pro-inflammatory molecules including, interleukin (IL)-1, IL-6, IL-12, IL-23, and tumor necrotic factor-alpha (TNF- $\alpha$ ) (14, 133). These cytokines can induce activation and secretion of inflammatory mediators by other cells. M1 macrophages also play an important role in host defense against microbe (14, 133). During infection, M1 macrophages produce microbicidal and tumoricidal substances, such as reactive oxygen intermediates (ROI) and nitric oxide (NO), leading death of bacteria or tumor cells (14, 133). M1 polarization typically involves IFN- $\gamma$  with a toll-like receptor (TLR) agonist, such as lipopolysaccharide (LPS) (14). Th1 lymphocytes are the main source of IFN- $\gamma$  production that induced M1 macrophage polarization by activating the STAT-1 signalling pathway. whereas LPS promotes M1 macrophage via the toll-like receptor-4 (TLR-4) (14, 133). However, M1 macrophages are sometimes implicated in sustained inflammation and can be harmful to host health (14, 133).

### 8.2.2.M2 macrophage

M2 macrophages, also known as alternatively activated macrophages, play an important role in tissue repair, immunoregulation, and tumor progression (14, 133). M2 macrophages were further divided into M2a, M2b, M2c, and M2d subtypes based on the transcriptional change and stimulation signal (14, 133). M2 macrophages are commonly characterized by high production of IL-10 and arginase-1 (Arg-1), CD206, CD163 expression, and low levels of IL-12 (14, 133). The high level of Arg-1 leads to depletion of L-arginine resulting in T cell proliferation and

IFN-g production (14, 133). Moreover, the increase of Arg-1 further competes with iNOS for L-arginine and reduces NO production (14, 133). In M2 subtypes, M2a polarization is stimulated by IL-4, IL-13, or fungal and helminth infections, and is related to Th2 immune response (14, 133). Th2 cells, eosinophils, basophils, and macrophages produce IL-4 and are important for parasite encapsulation (14, 133). M2b macrophages are activated by immune complex plus TLR or IL-1 receptor ligands, which thereafter regulate immune responses (14, 133). IL-10 production and antigen presentation are up-regulated (MHC II, CD86), whereas IL-12 production is down-regulated (14, 133). M2c macrophages are stimulated by IL-10 and transforming growth factor (TGF)-beta and contribute to tissue remodeling and extracellular matrix production (14, 133). Glucocorticoids also influence adherence, dissemination, apoptosis, and phagocytosis of M2c macrophages (14, 133). Polarization into M2d is activated by IL6 and adenosine (14, 133).

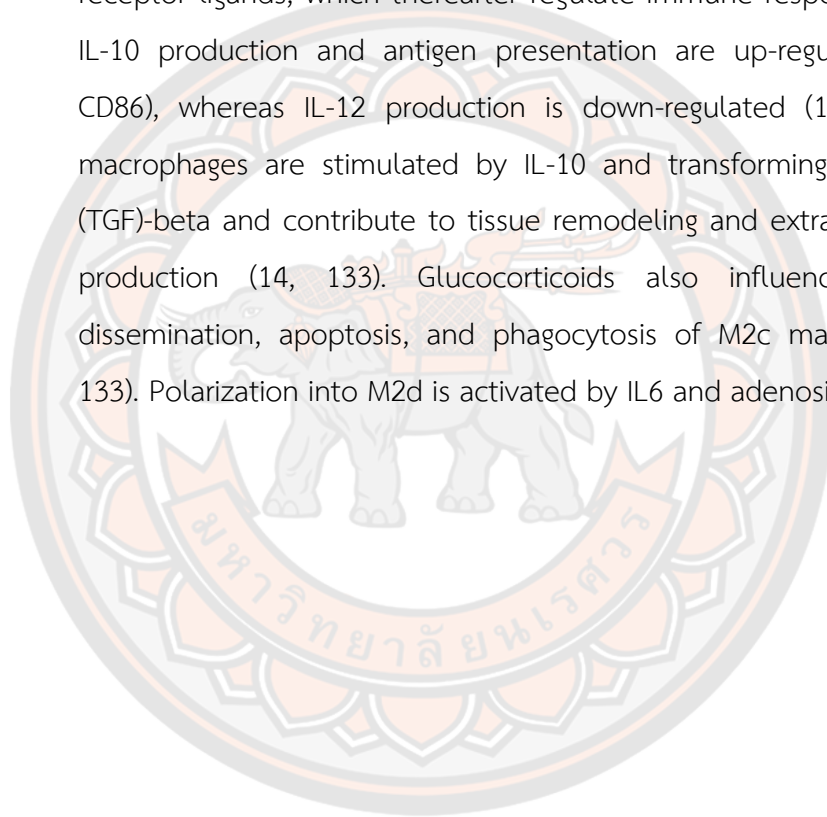


**Table 6 Macrophage differentiation, characteristics, and functions (134, 135)**

Phenotype	Stimulated by	Expressed marker	Secreted factors	Functions
M1	IFN- $\gamma$ , LPS, TLR ligands	IL-1 $\beta$ , TNF- $\alpha$ , IL-6, IL-12, CXCL10, CD80, CD68, CD86, HLA-DR	iNOS, ROI, IL-12 <sup>high</sup> , IL-10 <sup>low</sup> , IL-6, TNF- $\alpha$	Pro-inflammatory, anti-bacterial, anti-tumor
M2a	IL-4 and IL-13	Arg-1, Ym1, CD163, CD206, FIZZ1	IL-10, TGF- $\beta$ , CCL22, CCL17	Tissue remodelling, endocytosis
M2b	TLR ligands, IL-1R ligands	IL-10 <sup>high</sup> , IL-12 <sup>low</sup> , IL-23 <sup>low</sup>	IL-10, TNF- $\alpha$ , IL-6	Immunoregulation
M2c	IL-10, TGF- $\beta$ , glucocorticoids	CD163, CD206, IL-10, MERTK, ECM	IL-10, TGF- $\beta$	Phagocytosis, Efferocytosis
M2d	TLR agonists, IL-6	VEGF-A, IL-10	VEGF-A, IL-10, IL-12, iNOS	Pro-angiogenic, tumor promotion

Arg, arginase; IFN, interferon; IL, interleukin; iNOS, inducible nitric oxide synthase; LPS, lipopolysaccharide; ROI, reactive oxygen intermediates; TGF, transforming growth factor; TNF, tumor necrosis factor; VEGF, vascular endothelial growth factor; TLR, toll-like receptor; MERTK, MER Proto-Oncogene Tyrosine Kinase; ECM, extracellular matrix.

### 8.3. Macrophage-NLRP3 inflammasome

The NOD-, LRR- and pyrin domain-containing protein 3 (NLRP3) inflammasome is a critical component of the innate immune system that mediates caspase-1 activation and the secretion of proinflammatory cytokines IL-1 $\beta$ /IL-18 in response to microbial infection and cellular damage (136, 137). Activation of macrophage NLRP3 inflammasome required two signals, a first signal that is provided by microbial components or

endogenous cytokines primes the NLRP3 inflammasome; a second signal from extracellular ATP, pore-forming toxins, or particulate matter activates the NLRP3 inflammasome (136). Furthermore, multiple post-translational modifications and interacting partners of NLRP3 have been identified for regulating NLRP3 inflammasome activation (136).

#### 8.3.1. Priming the NLRP3 inflammasome (Signal 1).

Macrophages must first be exposed to priming stimuli, such as ligands for toll-like receptors (TLRs), NLRs (e.g. NOD1 and NOD2), or cytokine receptors, which activate the transcription factor NF-**KB** (136, 137). NF-**KB** upregulates the expression of NLRP3, which is thought to exist at concentrations that are inadequate for initiating inflammasome activation under resting conditions, and pro-IL-1 $\beta$ , which is not constitutively expressed in resting macrophages (136, 137). In contrast, priming signals do not appear to affect the expression levels of ASC, pro-caspase-1, and pro-IL-18 (136, 137). Moreover, both signalling molecules MyD88 and TRIF of the NF-**KB** signalling pathway regulate the induction of NLRP3 and pro-IL-1 $\beta$  in response to TLR ligands (136, 137).

#### 8.3.2. Activating the NLRP3 inflammasome (Signal 2)

NLRP3 can be activated by a wide range of stimuli following this priming step, including ATP, K<sup>+</sup> ionophores, heme, particulate matter, pathogen-associated RNA, and bacterial and fungal toxins and components (136, 137). NLRP3 has not been observed to directly interact with any of these agonists and, due to their biochemical dissimilarity, it is suspected that they induce a common cellular signal (136, 137). Currently, multiple molecular and cellular signalling events that are induced by NLRP3 stimuli, including ionic flux, mitochondrial dysfunction and the production of reactive oxygen species (ROS), and

lysosomal damage, have been shown to activate the NLRP3 inflammasome (136, 137).

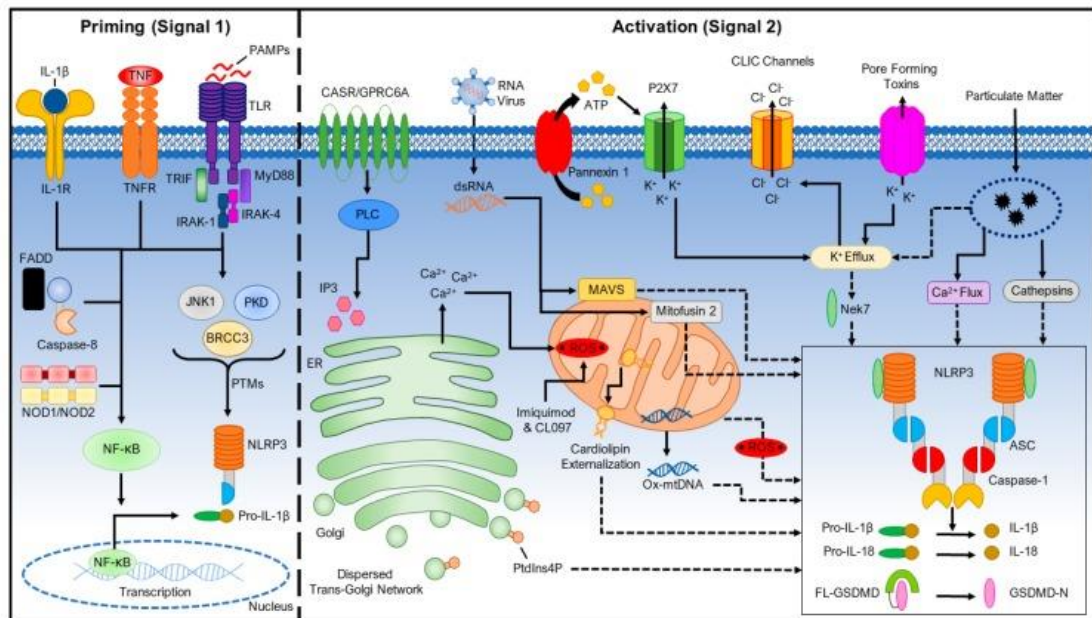


**Figure 15 A Two-Signal Model for NLRP3 Inflammasome Activation.**

The priming signal (signal 1, left) is provided by microbial components or endogenous cytokines, leading to the activation of the transcription factor NF- $\kappa$ B and subsequent upregulation of NLRP3 and pro-interleukin-1 $\beta$  (pro-IL-1 $\beta$ ). Caspase-8 and FAS-mediated death domain protein (FADD), and NOD1/2 are involved in the priming step by regulating the NF- $\kappa$ B pathway. NLRP3 undergoes post-translational modifications that license its activation. The activation signal (signal 2, right) is provided by a variety of stimuli including extracellular ATP, to activate the NLRP3 inflammasome. BRCC3, BRCA1/BRCA2-containing complex subunit 3; IL-1R, IL-1 $\beta$  receptor; JNK1, JUN N-terminal kinase 1; PKD, protein kinase D; TLR, toll-like receptor; TNFR, tumor necrosis factor receptor (136).

## 9. Tumor-associated macrophages (TAMs)

Tumor-associated macrophages (TAMs) are macrophages that participate in the formation of the tumor microenvironment. TAMs are widely present in various tumors (16). TAMs can promote tumor growth, invasion, metastasis, and drug

resistance (16). It has been proposed that the functional difference of macrophages is closely related to the plasticity of macrophages, and its functional phenotype is regulated by molecules in tumor microenvironments (16, 17).

### 9.1. Origins of TAMs

M-MDSCs (monocyte-related myeloid-derived suppressor cells) are currently known as another main circulating precursor of TAMs (16). MDSCs are a type of myeloid leukocytes that is related to immunosuppression (16). Based on surface markers Ly6C+/Ly6C- and Ly6C-/Ly6G+, MDSCs can be divided into monocyte (M)-related and granulocyte (G)-related MDSCs. Among them, M-MDSCs are induced into TAMs by various chemokines (16).

It is known that macrophages derive from bone marrow-derived monocytes (16). In tumors, TAMs mainly originate from bone marrow monocytes, but recent evidence suggests that recruitment of circulating monocytes is essential for TAMs accumulation (16). Circulating inflammatory monocytes could be recruited by multiple chemokines (CCL2 and CCL5) and cytokines (CSF-1 and members of the VEGF family) to the tumor (16, 17). Tumor growth can also induce the differentiation of CCR2+ monocytes into TAMs (16, 17).

### 9.2. Types of TAMs

Macrophages undergo specific differentiation in different tissue environments and can be divided into two different polarization states: M1 type macrophages (M1) and M2 type macrophages (M2) (16, 17).

#### 9.2.1.M1-like TAMs

M1 can respond to dangerous signals transmitted by bacterial products or IFN- $\gamma$ , which attract and activate cells of the adaptive immune system; an important feature of M1 is that it can express nitric oxide synthase (iNOS) and reactive oxygen species (ROS) and cytokine IL-12 (16, 17). M1 also has the function of engulfing and killing target cells (16, 17).

M1-type macrophages have anti-tumor effects, which can distinguish tumor cells from normal cells (16). By identifying tumor cells and ultimately killing tumor cells, studies have found that M1-type macrophages have two different effects on the killing tumor cells mechanism (16, 17). M1-type macrophages directly mediate cytotoxicity to kill tumor cells: macrophage-mediated cytotoxicity is a slow process (generally requires 1 to 3 days) and involves multiple mechanisms (16, 17). For example, macrophages release tumor-killing molecules such as ROS and NO, which have cytotoxic effects on tumor cells (23). The other is antibody-dependent cell-mediated cytotoxicity (ADCC) killing tumor cells: ADCC requires less time to kill tumor cells (generally within a few hours) and requires the participation of anti-tumor antibodies (16, 17).

#### 9.2.2.M2-like TAMs

M2 expresses a large number of scavenger receptors, which is related to the high-intensity expression of IL-10, IL-1 $\beta$ , VEGF, and matrix metalloprotein (MMP) (16, 17). M2 has the function of removing debris, promoting angiogenesis, tissue reconstruction, and injury repairments, as well as promoting tumorigenesis and development (16, 17).

TAM is commonly referred to as M2, which is closely related to tumor cell proliferation (16, 17). Many studies have shown that TAMs can express a variety of cytokines that stimulate tumor cell proliferation and survival, including epithelial growth factor (EGF), platelet-derived growth factor (PDGF), TGF- $\beta$ 1, hepatocyte growth factor (HGF), and epithelial growth ligands of the factor receptor (EGFR) family and basic fibroblast growth factor (BFGF) (16, 17). The ligands of the EGFR family play an important role in tumorigenesis, especially in breast and lung cancers. Members of this family can form homo- or heterodimers on the cell surface, mediating the transduction of cell proliferation signals (16, 17).

### 9.3. Targeting TAMs for Cancer Treatment

TAMs are one of the most important components of the tumor immunosuppression microenvironment with a high degree of plasticity (16). TAMs have both M1 and M2 types and have the potential ability of repolarization to M1-type macrophages. Therefore, targeting TAMs is a new cancer treatment strategy (Figure 16) (16).

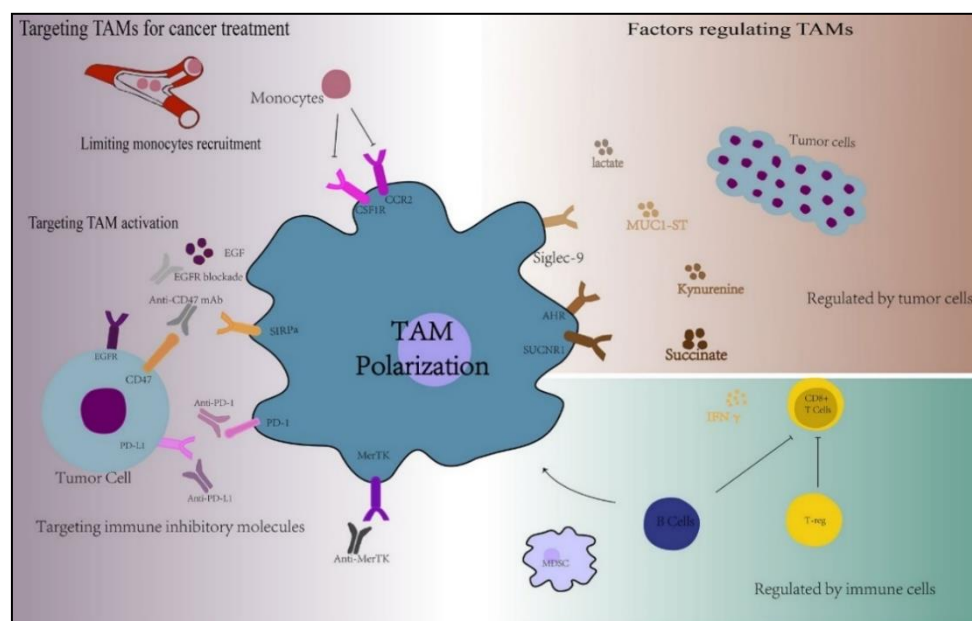


Figure 16 Overview of the factors regulating TAMs functions and the targets of TAMs for cancer treatment (16).

#### 9.3.1. Limiting monocyte recruitment

One of the strategies for targeting TAMs is to block monocyte recruitment to tumor tissue (16). Tumor cells recruit CCR2-expressing monocytes from the peripheral blood to the tumor site by releasing CCL2 and these recruited CCR2-expressing monocytes will finally mature into TAMs, which accelerate the tumor progress (16). Thus, targeting the CCL2-CCR2 axis is a very effective method of cancer therapy (16). Blocking the CCL2-CCR2 axis could greatly reduce the incidence of tumors by preventing TAMs recruitment and enhancing the anti-tumor efficacy of CD8+ T cells in the tumor microenvironment (138).

### 9.3.2.Targeting TAMs activation

Targeted activation of TAMs is an effective tumor treatment method. One of them is inhibiting TAMs from promoting tumor cell activation (16). Epidermal cell growth factor (EGF) secreted by TAM activates EGFR on tumor cells, which in turn upregulates VEGF (vascular endothelial growth factor)/VEGFR signalling in surrounding tumor cells, thereby promoting the proliferation and migration of tumor cells (16). EGFR blockade or ICAM-1 (intercellular adhesion molecule) antibody neutralization in TAM reduced the occurrence of ovarian cancer in mice (139).

### 9.3.3.Reprogramming TAMs into anti-tumor activity

One of the key characteristics of macrophages is their plasticity, which allows them to change their phenotype according to the tumor microenvironment (16). Therefore, reprogramming TAMs into an anti-tumor phenotype is a very promising tumor treatment strategy (16). Anti-tumor macrophages (M1 type) have abilities to clear and destroy tumor cells (16). RP-182 can selectively induce conformational switching of the mannose receptor CD206 expressed on TAM expressing the M2 phenotype, reprogramming M2-like TAM into anti-tumor M1-like TAM phenotype (140).

### 9.3.4.Targeting immune inhibitory molecules on TAMs

Targeting immune inhibitory molecules on TAMs is also an effective method (16). PD-1-PD-L1 therapy can also work by direct action on macrophages. Both mouse and human TAM express PD-1 (16). The expression of TAM PD-1 is negatively correlated with the phagocytic ability against tumor cells, and blocking PD-1-PD-L1 *in vivo* will increase the phagocytosis of macrophages, reduce tumor growth, and rely on macrophage-dependent ways to prolong the survival of mice in cancer models (141).

## 10. Basic methods in cellular and molecular biology

### 10.1. Cell culture

Cell culture refers to laboratory methods that enable the growth of eukaryotic or prokaryotic cells in physiological conditions. Its origin can be found in the early 20th century when it was introduced to study tissue growth and maturation, virus biology and vaccine development, the role of genes in disease and health, and the use of large-scale hybrid cell lines to generate biopharmaceuticals. The experimental applications of cultured cells are as diverse as the cell types that can be grown *in vitro* (134).

### 10.2. Trypan blue exclusion test

It is based on the principle that living cells possess intact cell membranes that exclude trypan blue to enter inside the cells, whereas dead cells do not. In this test, a cell suspension is simply mixed with trypan blue dye and then visually examined to determine whether cells take up or exclude dye. A viable cell will have a clear cytoplasm whereas a nonviable cell will have a blue cytoplasm (142).

### 10.3. MTT assay

The MTT assay is a colorimetric assay that is used to measure the mitochondrial cellular metabolic activity as an indicator of cell viability, proliferation, and cytotoxicity (143). This assay is based on the reduction of a yellow tetrazolium salt (3-(4,5-dimethylthiazol-2-yl)-2,5-diphenyltetrazolium bromide or MTT) to purple formazan crystals by metabolically active cells (**Figure 17**). The viable cells contain NAD(P)H-dependent oxidoreductase enzymes which reduce the MTT to formazan (143). The insoluble formazan crystals are dissolved into clear purple color by using solubilization solutions such as dimethyl sulfoxide (DMSO), isopropanol, and ethanol. This purple solution is quantified by measuring absorbance at 500-600 nm using a spectrophotometer (143). Therefore, the darker solution indicates the greater the number of viable, metabolically active cells. Whereas the clear solution indicates a lower number of viable, low metabolically active cells (143).

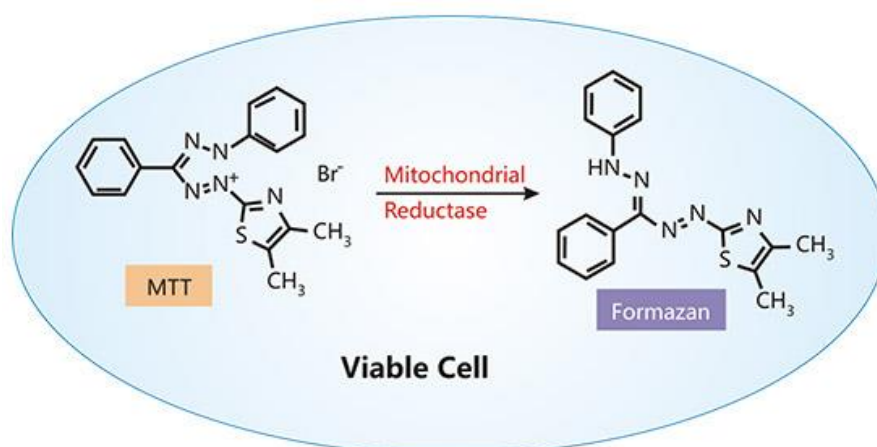


**Figure 17** The principle of MTT assay.

The yellow tetrazolium salt (3-(4,5-dimethylthiazol-2-yl)-2,5-diphenyltetrazolium bromide or MTT) is reduced to purple formazan crystals by mitochondrial reductase, NAD(P)H-dependent oxidoreductase (143).

#### 10.4. Density gradient centrifugation technique

Density gradient centrifugation is a common technique used to isolate and purify any biomolecules and cellular components (144). This technique uses high-speed centrifugate to separate cellular components in a density gradient (144). In suspension, particles that are denser than the solvent will sediment, while those that are less dense will float (144). The high-speed centrifuge is used to accelerate this process to separate cellular components within a density gradient, which can be established by layering liquids of decreasing density in a centrifuge tube (144).

#### 10.5. Colony formation/clonogenic assay

Clonogenic assay or colony formation assay is an *in vitro* cell survival assay based on the ability of a single cell to grow into a colony (145). The colony is defined to consist of at least 50 cells (145). The assay essentially tests every cell in the population for its ability to undergo “unlimited” division (145). Clonogenic assays are widely used in the field of cancer research as the formation of clones is interpreted as a trait of cancer cells

with tumor-initiating capabilities. This technique has become a standard tool in cancer research to evaluate cellular growth and the cytotoxic or genotoxic effects of various agents with a potential clinical application (146). Before or after treatment, cells are seeded out in appropriate dilutions to form colonies in 1–3 weeks (145). Colonies are fixed with glutaraldehyde (6.0% v/v), stained with crystal violet (0.5% w/v), and counted using a stereomicroscope (Figure 18) (145).

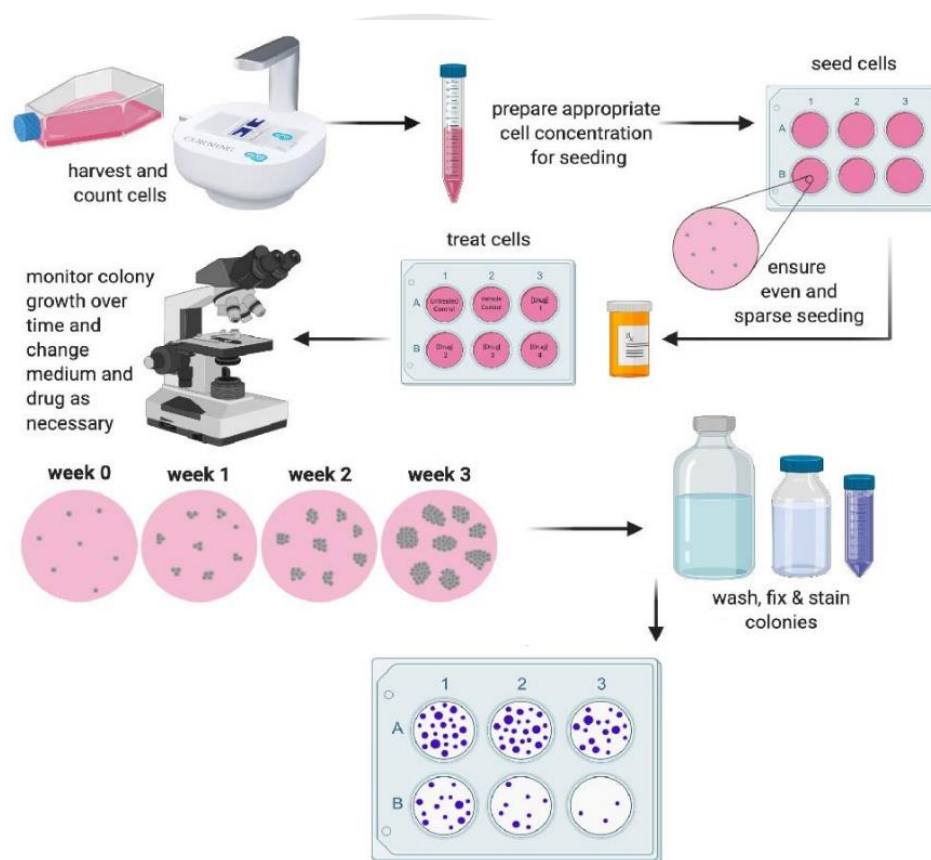


**Figure 18** A summary process of the *clonogenic assay*.

Cells are seeded into a cell culture plate, treated with a target agent, and cells are fixed and stained for visualizing the colony (146).

#### 10.6. Apoptosis analysis

Apoptosis is one of the programmed cell deaths, involving the activation, expression, and regulation of various molecules (147). When apoptosis occurs, a series of apoptotic processes are programmed, such as

phosphatidylserines valgus outside of the cell membrane, mitochondrial membrane potential ( $\Delta\Psi_m$ ) changes, caspase activation, and DNA fragmentation (147). This mechanism can determine by multiple techniques (e.g., Annexin V Detection assay, TUNEL Assay, caspase activation assay) based on the most used principles (147).

I. Apoptosis by Annexin V/ 7-AAD staining

The Annexin V/PI staining is used to determine the population of cells that undergo apoptosis by flow cytometry analysis (148, 149). The annexin V is specifically bound to phosphatidylserine, which is located in the cell membrane (148, 149). Whereas 7-aminoactinomycin D (7-AAD) specifically binds to DNA in the nucleus (148, 149). The normal cells are hydrophobic as they express phosphatidyl serine in the inner membrane (side facing the cytoplasm) but when the cells undergo apoptosis, the inner membrane flips to become the outer membrane, thus exposing phosphatidyl serine (148, 149). The exposed phosphatidyl serine is detected by Annexin V(148, 149). During the latter stages of apoptosis both PS is exposed and 7-AAD can enter the cell and stain the DNA due to the loss of membrane integrin, whereas necrotic cells are leaky DNA content, which is stained by 7-AAD only (**Figure 19**) (148, 149). This assay helps to differentiate and distinguish apoptotic and necrotic cells (148, 149).

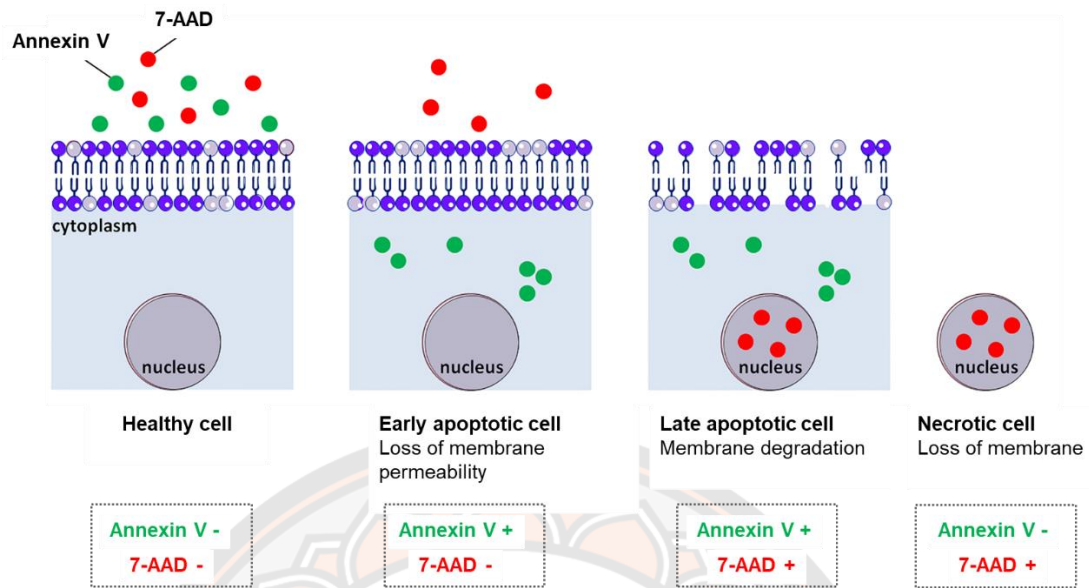


Figure 19 Summary model of Annexin V/7-AAD staining apoptosis assay.

Viable cells (V-/7AAD-), Early apoptosis (V+/7AAD-), late apoptosis (annexinV+/7AAD+), and necrosis (V-/7AAD+) (149).

## II. Cell apoptosis by TUNEL assay

Terminal deoxynucleotidyl transferase (TdT) dUTP Nick-End Labeling (TUNEL) assay has been designed to detect apoptotic cells that undergo extensive DNA degradation during the late stages of apoptosis (150). The method is based on the ability of the enzyme TdT, which attaches to the blunt ends of double-stranded DNA breaks independent of a template (150). In TUNEL staining, the nucleotides attached by TdT are tagged either directly with a fluorescent label or with a chemical label that can be indirectly linked to either a fluorescent label or an enzyme (150). This assay can be visualized by fluorescence/bright-field microscopy and flow cytometer (Figure 20)(150).

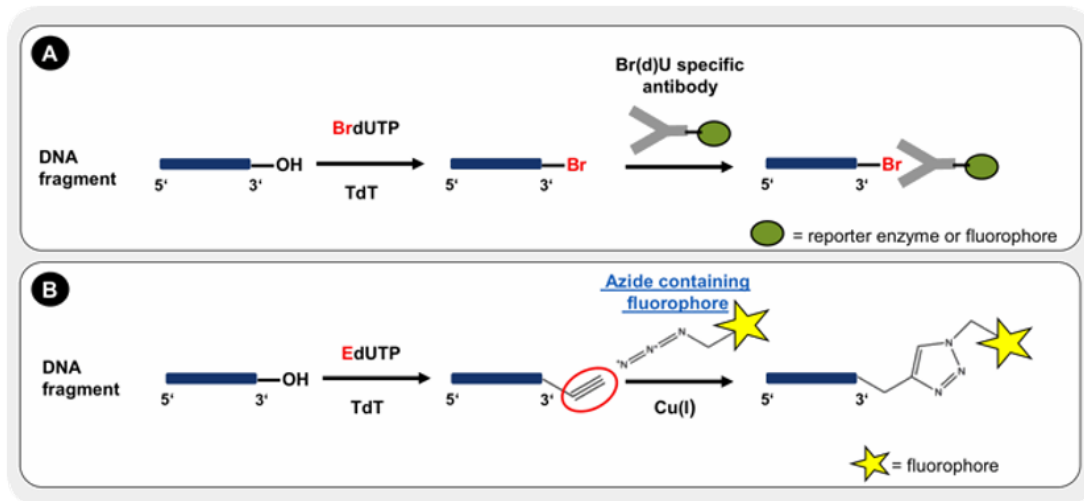


Figure 20 The principle of TUNEL assay.

Incorporated BrdUTP is detected by specific antibody conjugates with a reporter enzyme or fluorescent dye (A). The incorporation of EdUTP is visualized by Cu-catalyzed alkyne-azide click chemistry with an azide containing fluorophore (B) (151).

### III. Cell apoptosis by mitochondrial membrane potential assay

Decreasing the mitochondrial membrane potential ( $\Delta\psi_m$ ) is known to precede apoptosis.  $\Delta\psi_m$  is commonly detected using cationic (positively charged) fluorescent dyes that accumulate in the negatively charged mitochondrial matrix. The dye accumulates in inverse proportion to  $\Delta\psi_m$  i.e., the more negative the  $\Delta\psi_m$ , the more dye accumulates. This means that a healthy cell will contain more dye while an apoptotic cell will contain less. These dyes can be used qualitatively in fluorescence microscopy or quantitatively in flow cytometry or microplate spectrophotometry (Figure 21) (152, 153).

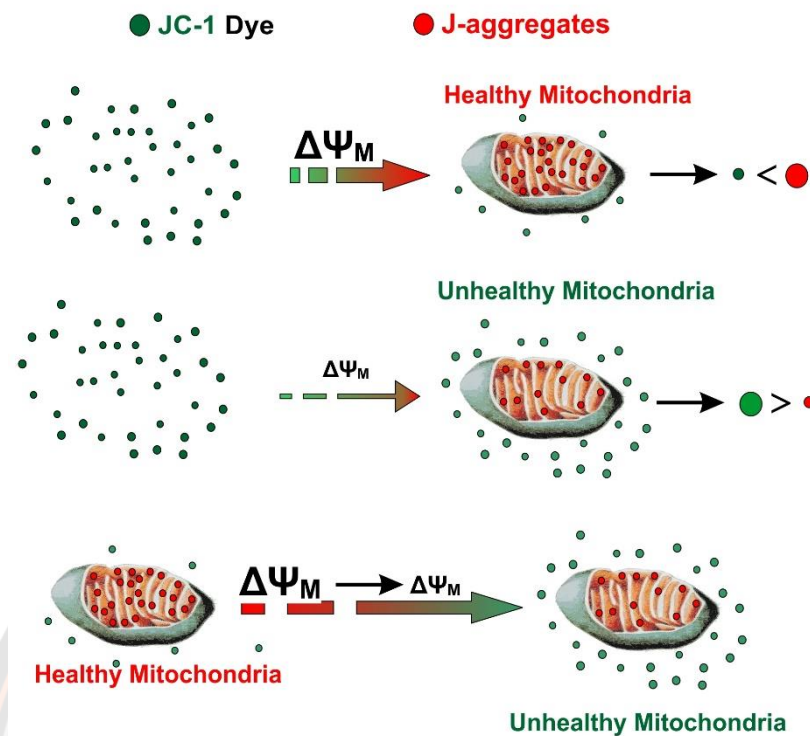


Figure 21 The JC-1 Mitochondrial Membrane Potential Assay.

JC-1 is a cationic dye that accumulates in energized mitochondria. In apoptotic cells with low MMP, JC-1 remains in a monomeric form, which exhibits green fluorescence. While in healthy cells with high MMP concentrations, JC-1 forms complexes known as J-aggregates with intense red fluorescence. The higher the ratio of red to green fluorescence, the higher the polarization of the mitochondrial membrane (152, 153).

#### IV. Apoptosis-associated caspase activation assays

Caspases are aspartate-directed cysteine proteases that cleave a diverse group of intracellular substrates to contribute to various manifestations of apoptosis. These proteases are synthesized as inactive precursors and are activated as a consequence of signalling induced by a wide range of physiological and pathological stimuli. Caspase activation can be detected by measurement of catalytic activity, immunoblotting for cleavage of their substrates, immunolabeling using conformation-sensitive antibodies or affinity labelling followed by flow cytometry or ligand blotting (154).

### 10.7. Cell cycle analysis

The cell cycle is the process by which eukaryotic cells duplicate and divide. The cell cycle consists of two specific and distinct phases: interphase, consisting of G<sub>1</sub> (Gap 1), S (synthesis), and G<sub>2</sub> (Gap 2), and the mitotic phase; M (mitosis) (**Figure 22**) (155). The most common method to determine the cell cycle profile is to use fluorescent dye to stain the cellular DNA content (155). During this process, a fluorescent dye that binds to DNA is incubated with a single cell suspension of permeabilized or fixed cells. Since the dye binds to DNA stoichiometrically, the amount of fluorescent signal is directly proportional to the amount of DNA (155, 156). Because of the alterations that occur during the cell cycle, analysis of DNA content allows discrimination between the G<sub>1</sub>, S, G<sub>2</sub>, and M phases (**Figure 22**) (155, 156).

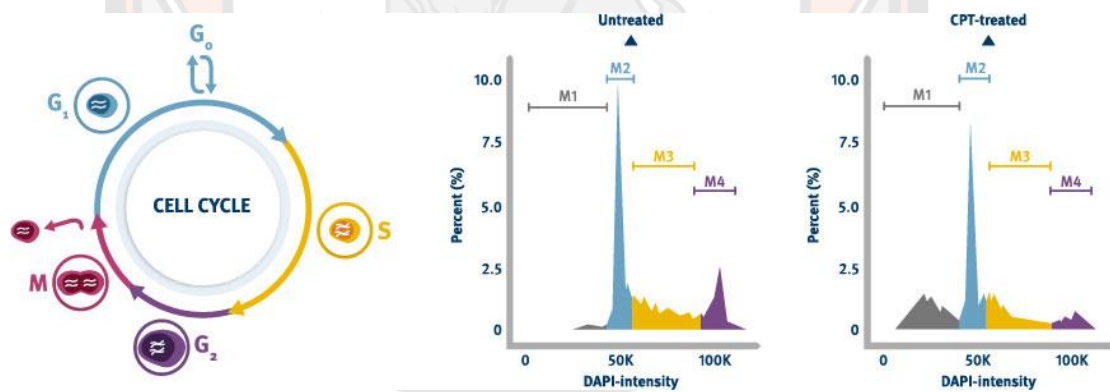


**Figure 22** The cell cycle assay uses the nuclear stain DAPI to measure DNA content. DAPI binds specifically to double-stranded DNA. Consequently, there is no requirement to remove RNA before DNA content measurements. This is a prerequisite for other dyes commonly used for the measurement of cell cycle phases, such as propidium iodide (PI) (157).

### 10.8. *In vitro* scratch assay

The *in vitro* scratch assay is a basic and economical method to study cell migration. This method is based on the observation that, upon the creation of a new artificial gap, called “scratch” on a confluent cell monolayer (158, 159). The cells on the edge of the newly created gap will move toward the opening to close the “scratch” until new cell-cell contacts are established again (158, 159). The basic steps involve the creation of a “scratch” on monolayer cells, capture of images at the beginning and regular intervals during cell migration to close the scratch, and comparison of the images to determine the rate of cell migration (**Figure 23**) (158, 159).

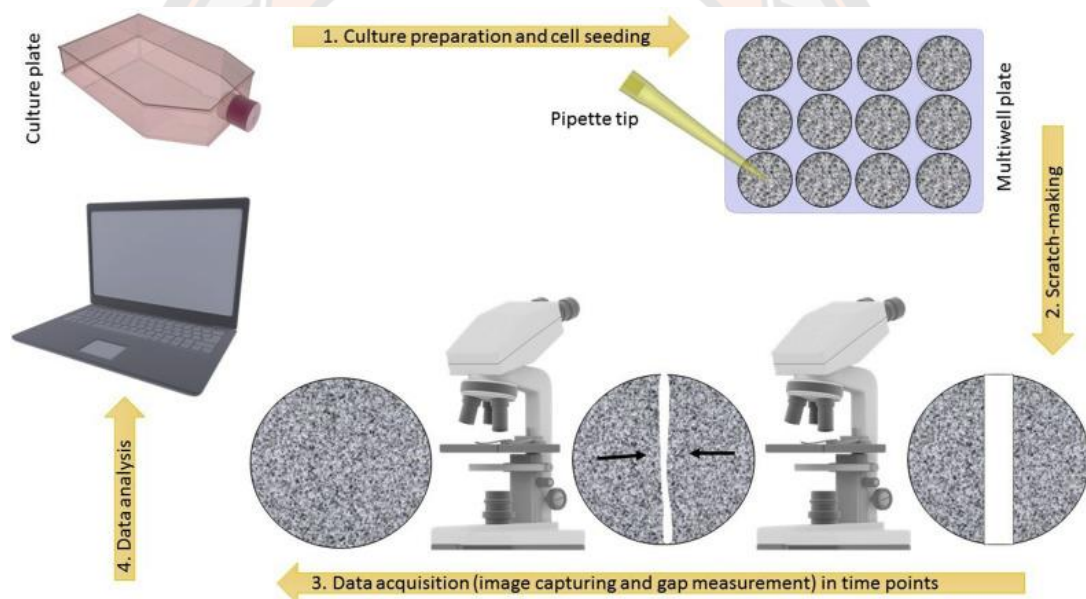


**Figure 23** Graphical summarizing the workflow of the *in vitro* wound-healing assay. The technique involves basic steps applicable to almost all cell types: 1) cell seeding and preparation; 2) making a linear thin scratch “wound” (creating a gap) in a confluent cell monolayer; 3) data acquisition through microscopic image capturing and gap measurement at each time point, and 4) data analysis (160).

#### 10.9. Hoechst 33342 nuclear staining dye

Hoechst 33342 (2'-[4-ethoxyphenyl]-5-[4-methyl-1-piperazinyl]-2,5'-bi-1H-benzimidazole trihydrochloride trihydrate) is a cell-permeable DNA staining dye that is excited by ultraviolet light and emits blue fluorescence at 460 to 490 nm (161). Hoechst 33342 binds preferentially to adenine-thymine (A-T) regions of DNA (161). This stain binds to the adenine-thymine (A-T) regions of DNA and exhibits blue fluorescence emission spectra that are dependent on dye: base pair ratios. This stain is commonly used in combination with 5-bromo-2'-deoxyuridine (BrdU) labeling to distinguish the compact chromatin of apoptotic nuclei, to identify replicating cells and to sort cells based on their DNA content (161). The method can be visualized by both flow cytometric and fluorescence imaging analysis (161).

#### 10.10. Reverse transcription quantitative real-time PCR (RT-qPCR)

Real-Time Quantitative Reverse Transcription PCR (RT-qPCR) has become the standard for the detection and quantification of RNA targets (162). In this technique, the RNA target is first transcribed into complementary DNA (cDNA) by reverse transcriptase (162). The cDNA is then used as the template for the qPCR reaction by three steps of PCR cycles, which are denaturation, annealing, and extension (162). SYBR green is fluorescence that can bind only dsDNA. Therefore, the increasing amount of dsDNA present in the reaction tube led to the increasing amount of DNA binding and the fluorescent signal from SYBR green (162). Thus the amount of the cycle of DNA amplification is measured owing to these properties (**Figure 24**) (162).

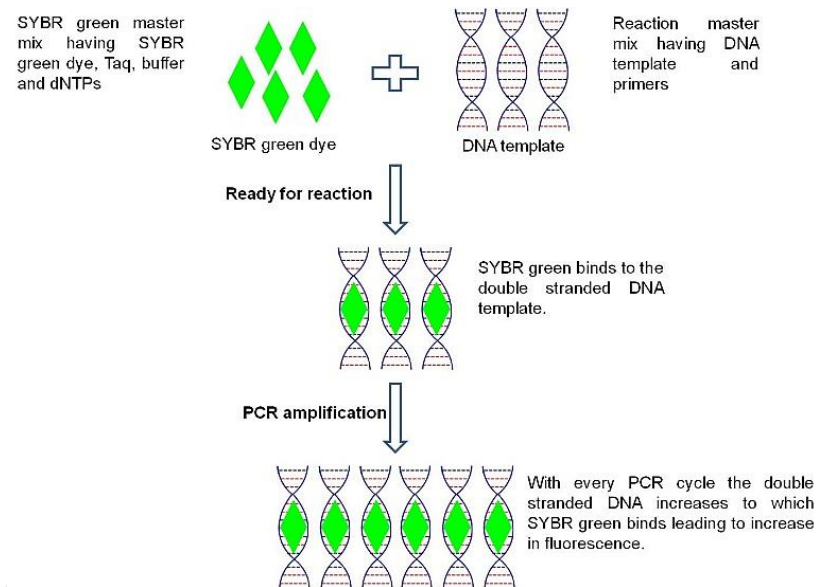


**Figure 24** A real-time PCR assay using SYBR Green dye.

As the amount of DNA increases with every cycle more SG is bound to it corresponding to an increase in fluorescence (163).

#### 10.11. Western blot analysis

Western blotting (protein blotting or immunoblotting) is a sensitive assay for the detection and characterization of proteins (164). It is based on the principle of immunochromatography where proteins are separated into polyacrylamide gel according to their molecular weight (164). The protein thus separated are then transferred onto nitrocellulose membrane and are detected using a specific primary antibody and secondary enzyme-labeled antibody and substrate (**Figure 25**) (164).

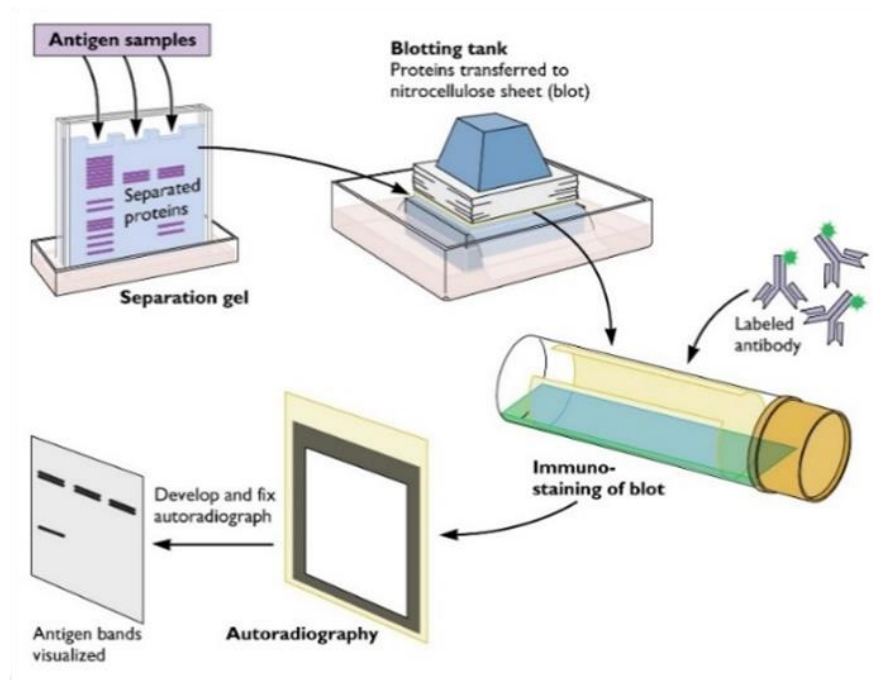


Figure 25 General process of western blot analysis.

Western blot consist of four major steps; 1) separation of proteins 2) transfer of protein into the membrane, 3) detection of protein by specific antibody, 4) measure the reaction by the detector (164).

#### 10.12. Flow cytometry

The basic principle of flow cytometry is the passage of cells in a single file in front of a laser so they can be detected, counted, and sorted (165). Flow cytometry measures multiple physical characteristics of cells such as size, which is detected by forward angle light scatter (FCS), and internal complexity or granularity, which is measured by side-angle scatter (SCS). This light scatter may be derived from fluorescent dyes or antibodies conjugated to fluorescent dyes that can bind specific proteins on cell membranes or inside cells (165). When labeled cells are passed by a light source, the fluorescent molecules are excited to a higher energy state (165). Upon returning to their resting states, the fluorochromes emit light energy at higher wavelengths (165). The emission of light, which is specific to each type of cell, thus this level used to identify cells (165).

### 10.13. Enzyme-linked immunosorbent assay (ELISA)

Enzyme-linked immunosorbent assay (ELISA) is an immunological assay commonly used to detect and quantify soluble substances such as peptides, proteins, antibodies, and hormones (166). The detection of these products is accomplished by complexing antibodies and antigens to produce a measurable result (166). An antibody is a type of protein produced by an individual's immune system. This protein type has specific regions that bind to antigens. An antigen is a protein that can come from some foreign source and, when bound to an antibody, induces a cascade of events through the body's immune system (**Figure 26**) (166). This interaction is utilized in ELISA testing and allows for identifying specific protein antibodies and antigens, with only small amounts of a test sample (166).

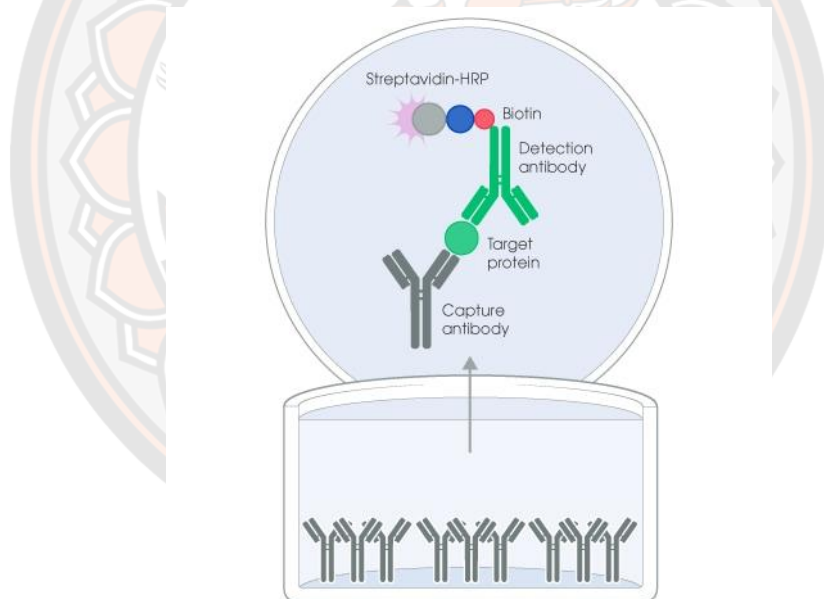


**Figure 26** The basic setup of an ELISA assay.

A capture antibody on a multi-well plate will immobilize the antigen of interest. This antigen will be recognized and bound by a detection antibody conjugated to biotin and streptavidin-HRP (167).

#### 10.14. LDH assay

Lactate dehydrogenase (LDH) is a cytosolic enzyme that presents in a wide variety of organisms (168). Since LDH is a stable enzyme, it can be used as an indicator of cytotoxicity of tissue and cells (168). The LDH assay is based on an enzymatic coupling reaction, which results in the conversion of a tetrazolium salt (iodonitrotetrazolium; INT) into a red formazan product (168). The reaction involves conversion of lactate to pyruvate by LDH and reduction of  $\text{NAD}^+$  to NADH. The diaphorase in presence of NADH reduces INT (a tetrazolium salt) and generates a red color formazan (**Figure 27**) (168). The amount of formazan formed is proportional to the amount of LDH released in the medium and the absorbance can be measured at 490nm, using a spectrophotometer or a 96-well plate reader (168).

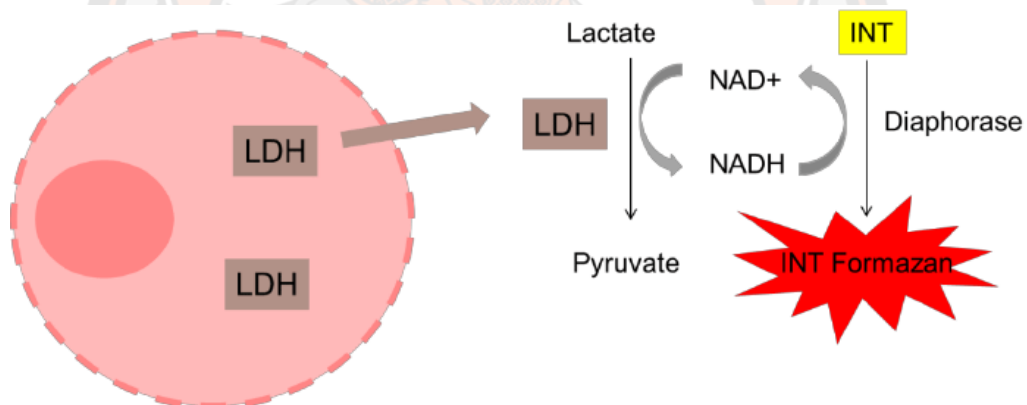


Figure 27 Schematic representation of the principle of the LDH release assay (169).

#### 10.15. Scanning electron microscope (SEM)

Scanning electron microscopes (SEMs) use an electron beam to image samples with a resolution down to the nanometer scale (170, 171). The electrons are emitted from a filament and collimated into a beam in the electron source (170, 171). The beam is then focused on the sample surface by a set of lenses in the electron column. The sample is exposed in SEM to the high-energy electron beam and gives information about the topography, morphology, composition, chemistry, the orientation of grains,

crystallographic information, etc. material, and therefore SEM is a useful tool to be used for the characterization of materials (170, 171). Morphology indicates the shape and size, while topography indicates the surface features of an object, its texture, smoothness, or roughness. The SEM has allowed researchers to examine a much bigger variety of specimens (170, 171).



## CHAPTER 3

### RESEARCH METHODOLOGY

#### Population and sample

Human blood buffy coats were kindly provided from the Blood bank unit of Naresuan University Hospital. The human breast cancer cell line, MDA-MB-231 was authenticated from American type culture collection (ATCC). *Moringa oleifera* leaves (MOL) powder was obtained from the Khaolaor laboratories Co. Ltd, Samutprakan city, Thailand

#### Research Instruments

##### Equipment's

1. Biosafety cabinet (NuAire Laboratory Equipment, USA)
2. Centrifuge (Scanspeed mini)
3. Rotofix 32A Bench Top Centrifuge (Hettich, Germany)
4. Freezer MIRAGE (Panasonic, Thailand)
5. Hematocytometer (Thermo Fisher Scientific Inc., USA)
6. Incubator (SHELLAB CSL)
7. Microcentrifuge (Heraeus Corporation, Germany)
8. Microscope OLYMPUS (Olympus Life Science)
9. Vortex-Genie 2 (Scientific industries Co., Ltd.)
10. Water bath (Julabo sw23)
11. Blotting and Staining System (Thermo Fisher Scientific Inc., USA)
12. Electrophoresis System (Thermo Fisher Scientific Inc., USA)
13. ELISA Plate Reader (PerkinElmer, Inc., USA)
14. Flow Cytometer (Beckman Coulter Life Sciences, USA)
15. Fluorescence Microscope (Zeiss Microscopy, Germany)
16. Gel Imaging System (Bio-Rad Laboratories, Inc., USA)
17. Inverted Microscope (Olympus Corporation, Japan)
18. Real-time PCR (Bio-Rad Laboratories, Inc., USA)

19. Rotary evaporator (Heidolph Instruments, Inc., Germany)
20. LC-ESI-QTOF-MS/MS (Agilent Technologies Inc., Germany)

#### Materials

1. Autopipette (PZ HTL S.A., Poland)
2. Cover glass (Gerhard Menzel GmbH, Germany)
3. Erlenmeyer flask (Corning Incorporated, USA)
4. Filter (Sartorius AG, Germany)
5. Microcentrifuge tube (Labcon North America, USA)
6. PCR tube (Labcon North America, USA)
7. Microscope slide (Yancheng Foreign Trade, China)
8. Plastic Pasteur pipet (Copan Diagnostics Inc., USA)
9. Tissue culture flask (SPL Life Science, Korea)
10. Microtiter plate (Cayman Chemical company, USA)
11. Conical tube (SPL Life Science, Korea)
12. 6-well tissue culture plate (SPL Life Science, Korea)
13. 12-well tissue culture plate (SPL Life Science, Korea)
14. 24-well tissue culture plate (SPL Life Science, Korea)
15. 96-well tissue culture plate (SPL Life Science, Korea)
16. tissue culture dish (100 mm) (SPL Life Science, Korea)
17. Transwell co-culture (SPL Life Science, Korea)

#### Chemical reagents

1. Chloroform (Fisher Scientific, USA)
2. Ethanol (Fisher Scientific, USA)
3. HEPES Sodium Salt (Bio Basic Inc., Canada)
4. Isopropanol (Fisher Scientific, USA)
5. Lymphoprep (Axis-Shield PoC, Norway)
6. Penicillin-Streptomycin Antibiotic (Life Technologies, USA)
7. Percoll (GE Healthcare, Sweden)
8. RPMI-1640 Powder (Life Technologies, USA)

9. DMEM/F12 (Gibco, Carlsbad, CA, USA)
10. 1% penicillin/streptomycin (Gibco, Carlsbad, CA, USA).
11. TRIzol Reagent (Life Technologies, USA)
12. Trypan Blue (Bio Basic Inc., Canada)
13. Bolt® Bis-Tris Plus Gels (Thermo Fisher Scientific Inc., USA)
14. Fetal Bovine Serum (Thermo Fisher Scientific Inc., USA)
15. PCR Primer (Bio Basic Inc., Canada)
16. qPC RT Master Mix (Toyobo Co., LTD., Japan)
17. Thunderbird® SYBR® (Toyobo Co., LTD., Japan)
18. MTT reagent (Thermo Fisher Scientific Inc., USA)
19. Oleamide (Sigma Aldrich, USA).
20. 7-octenoic acid (Sigma Aldrich, USA).
21. 1-phenyl-2-pentanol (Sigma Aldrich, USA).
22. Interleukin-4 (ImmunoTools, Germany)
23. Interferon-gamma (ImmunoTools, Germany)
24. LPS (*E. coli* O55:B5) (Sigma Aldrich, MO, USA)
25. M-CSF (ImmunoTools, Germany)
26. GM-CSF (ImmunoTools, Germany)
27. CyQUANT LDH (Thermo Fisher Scientific Inc., USA)
28. Protease/Phosphatase Inhibitor (Thermo Fisher Scientific Inc., USA)

## Research methodology

The present study is divided into the 3 major parts: 1) *in vitro* bioassay-guided identification of bioactive compound from MOL against the MDA-MB-231 breast cancer cells line, 2) the regulatory effect of the bioactive compound, oleamide that was identified, on the polarization of primary human monocyte-derived macrophages (MDMs), and 3) reprogramming of tumor-associated macrophages (TAMs) using the bioactive compound, oleamide. The research methodology, illustrated in **Figure 28**, is described separately in each part.

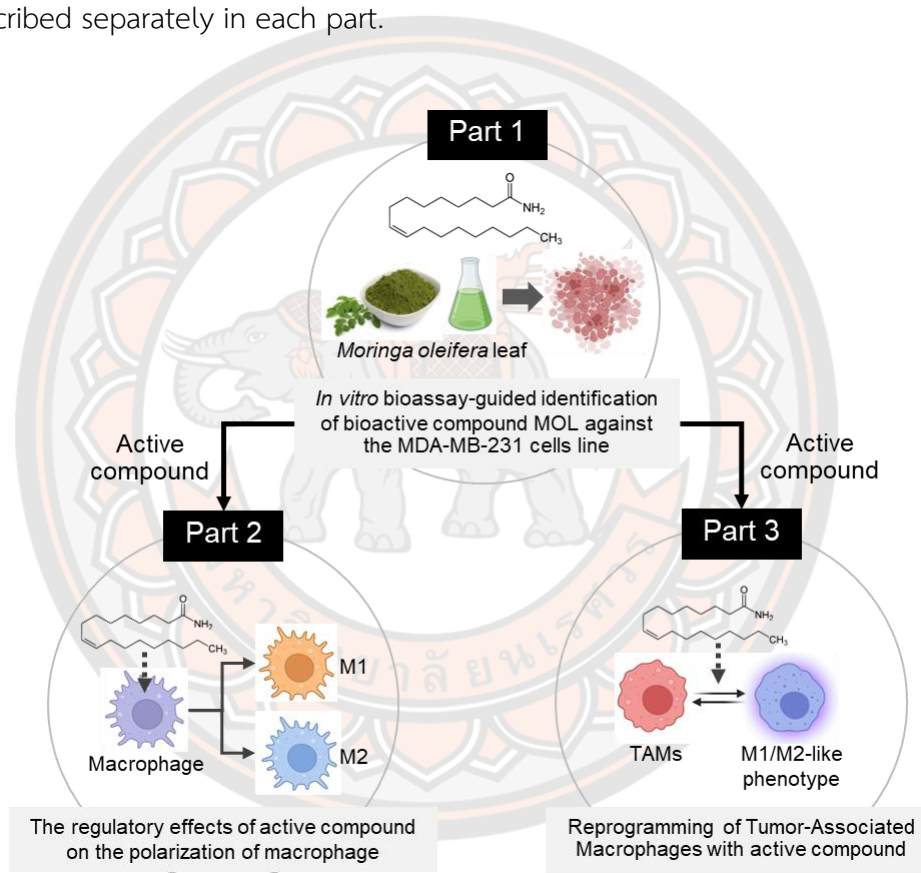


**Figure 28** Overview of the research methodology.

The study consisted of 3 main parts: the Identification of bioactive compounds against MDA-MB-231 cells (part 1), the regulatory effect of the bioactive compounds on the polarization of M1/M2 macrophage (part 2), and the effect on the reprogramming of TAMs (part 3).

**Part 1: *In vitro* bioassay-guided identification of bioactive compound from *Moringa oleifera* Lam. Leaf against the MDA-MB-231 breast cancer cells line.**

MOL powder was sequentially extracted with different organic solvents in increasing polarity, including hexane, ethyl acetate (EtOAc), and ethanol (EtOH). The crude extract obtained from each organic solvent was screened for anti-cancer activity against MDA-MB-231 cells using an MTT assay. The most effective extract was subjected to fractionation to separate the crude extract into various fractions by silica gel column chromatography. All fractions that were collected were determined as being potent fractions for anti-cancer activity, by using multiple *in vitro* bioassays. The strongest fraction was selected for re-fractionation and identification of its bioactive compounds using the liquid chromatography-electrospray ionization-quadrupole time-of-flight-mass spectrometry (LC-ESI-QTOF-MS/MS). To verify the anti-cancer activity of the fraction, the pure identified compounds were re-tested against MDA-MB-231 cells by using MTT assay, *in vitro* scratch assay, Hoechst 33258 staining, RT-qPCR, Western blotting, and cell apoptosis and cell cycle analysis (Figure 29).

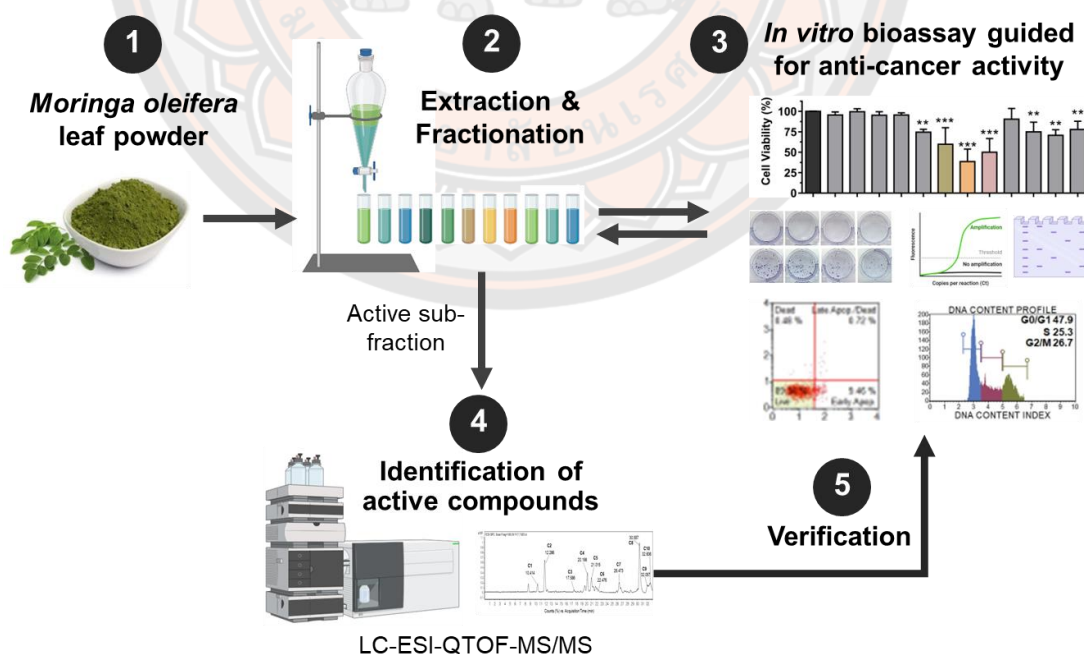


Figure 29 Schematic models of the *in vitro* bioassay-guided identification of bioactive compound from MOL against the MDA-MB-231 breast cancer cells line.

### 1. Cell culture

MDA-MB-231 cells, SCC-15 cells, and K562 cells line were obtained from the American type cell collection (Manassas, VA, USA). The MDA-MB-231 cells were cultured in Dulbecco's modified eagle medium (Gibco, Carlsbad, CA, USA). The SCC-15 were cultured in DMEM/F12 (Gibco, Carlsbad, CA, USA), and K562 cells were cultured in RPMI 1640 (Gibco, Carlsbad, CA, USA), respectively. All culture mediums were supplemented with 10% fetal bovine serum (FBS) (Gibco, Carlsbad, CA, USA) and 1% penicillin/streptomycin (Gibco, Carlsbad, CA, USA). The primary human monocyte-derived macrophages (MDMs) were isolated from the blood buffy coat of a healthy donor. MDMs were cultured in RPMI 1640 with 10% FBS and 1% penicillin/streptomycin for 6 days before experiments. All cells were cultured in a humidified atmosphere with 5% CO<sub>2</sub> at 37°C.

### 2. Collection of plant materials

MOL dried powder (COA Lot. No.5534) was obtained from Khaolaor Laboratories Co. Ltd, Samutprakan city, Thailand. Plant materials were approved for the certificate of analysis (COA) that includes physical control, chemical control, and biological control, by Khaolaor Laboratories Co. Ltd.

### 3. Preparation of MOL extract

MOL extraction was performed using sequential extraction with different organic solvents in an increasing polarity, including hexane, ethyl acetate (EtOAc), and 95% ethanol (EtOH). MOL powder (1 kg) was macerated in 1 L of hexane solvent for 3 days at room temperature. The supernatant was filtered through Whatman filter paper no. 3 and the filtrate were concentrated using a rotary evaporator (Heidolph Hei-VAP Value HB/G3B) at 40°C under reduced pressure to obtain semi-solid masses or crude hexane extract. The residue leaf powder was continually macerated in 1 L of EtOAc solvent for 3 days at room temperature. The supernatant was filtered and evaporated to obtain crude EtOAc extract.

The residue leaf powder was continually macerated in 1 L of 95% EtOH in the same protocol as described above to obtain crude EtOH extract. The extraction process was repeated three times for each solvent. Each crude extract was collected and stored at -20°C until further use. In the experiments, crude extracts were dissolved in dimethyl sulfoxide (DMSO) and diluted in Deionized (DI) water up to a final concentration of 10 mg/ml (5% DMSO residual). All diluted extracts were filtered through a 0.2 µm filter (Millipore), aliquots into microcentrifuge tubes, and stored at -20°C until used.

#### 4. Fractionation of crude MOL extract and active fraction

The crude EtOAc extract (10 g) was dissolved in hexane-EtOAc (70-30%) and separated by chromatography on a silica gel column; a gradient sequentially formed of hexane-EtOAc (90%-10%, 80%-20%, 70%-30%, 60%-40%, 50%-50%, 40%-60%, 30%-70%, 20%-80%, 10%-90%, and 100% EtOAc), and EtOAc-methanol (MeOH) (90%-10%, 80%-20%, and 100% MeOH) were used as the mobile phase for elution. All collected fractions were monitored and combined based on the thin layer chromatography (TLC) pattern.

The active fraction (fraction no. 7; 135 mg) was dissolved in hexane-EtOAc (30-70%) and re-fractionated by silica gel column chromatography; a gradient sequentially formed of hexane-EtOAc (90%-10%, 80%-20%, 70%-30%, 50%-50%, and 100% EtOAc), and EtOAc-MeOH (90%-10%) were used as the mobile phase for elution. All sub-fractions (no. 7.1- 7.8) were tested for anticancer activity using the MTT assay. The strongest active sub-fraction (sub-fraction no. 7.7) was then subjected to the identification of its bioactive compounds using the LC-ESI-QTOF-MS/MS analysis. All extracts were stored at -20°C until used.

5. At-line- Liquid chromatography-electrospray ionization-quadrupole time-of-flight-mass spectrometry (LC-ESI-QTOF-MS/MS) analysis

The active subfraction of MOL extract (20 mg/mL) was prepared and injected into an Agilent 1260 Infinity Series HPLC system (Agilent Technologies Inc., Waldbronn, Germany) coupled with an Agilent 6540 QTOF-MS spectrometer (Agilent Technologies, Inc., Singapore) with an electrospray ionization (ESI) source. For HPLC separation, a mobile phase of 0.1% formic acid in water (v/v) (A) and 0.1% formic acid in acetonitrile (v/v) (B) was used with gradient elution from 20% B to 90% B in 30 min, held for 3 min and a post-run for 5 min. The sample separation was performed on a Luna C18 (2) 100Å, 4.6 × 150 mm, 5 µm column (serial no. 728946-40; Phenomenex, CA, USA) at a flow rate of 0.5 mL/min, with the column temperature set at 35°C. The eluent was split into two flows using a 9:1 ratio. The major part was collected in a 96-well plate with 30 s per well, while the minor part flowed to an ESI-QTOF-MS system. The operating parameters for MS detection were as follows: drying gas (N<sub>2</sub>) flow rate 10.0 L/min; drying gas temperature 350°C; nebulizer pressure 30 psig; capillary 3500 V; skimmer 65 V; octapole RFV 750 V; and fragmentor voltage 100 V in positive mode. The mass range was set at m/z 100–1200 amu with a 250 ms/spectrum. The mass fragmentation was operated on auto ms/ms mode with three collision energies of 10, 20, and 40 eV. All acquisition and analysis of data were controlled by Agilent MassHunter Data Acquisition Software B.05.01 and Agilent MassHunter Qualitative Analysis Software B.06.0. The micro-fractions in a 96-well plate were dried using a sample concentrator (Techne, Staffordshire, UK) and kept at –20°C before being tested.

6. Identification of active compounds

The samples from the 96-well plate that showed bioactivity were linked to the LC-ESI-QTOF-MS/MS chromatogram by time. The active compounds with MS and MS/MS data were tentatively identified: the

mass data were compared with previous reports and using public databases (the Human Metabolomics Database; <http://www.hmdb.ca>; accessed on 30 December 2019), Chemspider (<http://www.chemspider.com>; accessed on 30 December 2019), and Metlin database (<https://metlin.scripps.edu>; accessed on 30 December 2019).

#### 7. Cell viability assay

The cytotoxicity of the MOL extract and its derived fractions was determined using the methyl thiazol tetrazolium (MTT) assay. MDA-MB-231 cells or primary human MDMs were seeded into 96-well plates at a density of  $1 \times 10^4$  cells/well and incubated with serial concentrations of crude MOL extracts (0 – 10 mg/ml), fractions no. 1-11 (50, 75, 100, and 150  $\mu\text{g/ml}$ ), and sub-fraction (75  $\mu\text{g/ml}$ ) for 24 hr at 37 °C with 5%  $\text{CO}_2$ . Following incubation, the supernatant was removed and the MTT salt solution was added and incubated for 3 hr at 37°C. The formazan crystals were dissolved in 100  $\mu\text{l}$  of DMSO. The absorbance was measured at 570 nm using an ELISA plate reader (PerkinElmer, Inc., USA).

#### 8. Colony formation assay

MDA-MB-231 cells were seeded into 6-well plates at a density of 500 cells/well overnight. The cells were treated with crude EtOAc extract of MOL or its derived fractions at concentrations of 50, 75, 100, and 150  $\mu\text{g/ml}$  for 24 hr at 37°C with 5%  $\text{CO}_2$ . After 24 hr, the medium was replaced with 4 ml of fresh complete medium and cultured for 14 days at 37°C with 5%  $\text{CO}_2$ . After 14 days, the cells were fixed with 10% neutral formalin and stained with 0.5% crystal violet to visualize colonies and photographed.

#### 9. Apoptosis and cell cycle analysis

Cell apoptosis and cell cycle analysis were examined on the Muse Cell Analyzer (EMD Millipore, USA). MDA-MB-231 cells were plated into 24-

well plates at the density of  $5 \times 10^4$  cells/well and incubated with crude EtOAc extract of MOL (150  $\mu\text{g/ml}$ ) or its derived fractions no. 1-11 (150  $\mu\text{g/ml}$ ), 7-octenoic acid (2.5 and 4  $\text{mg/ml}$ ), oleamide (70 and 100  $\mu\text{g/ml}$ ), 1-phenyl-2-pentanol (600 and 700  $\mu\text{g/ml}$ ), doxorubicin (1.5  $\mu\text{M}$ ; positive control), or complete medium (negative control) for 24 hr at  $37^\circ\text{C}$  with 5%  $\text{CO}_2$ . The cells were harvested into microcentrifuge tubes and resuspended in 100  $\mu\text{l}$  of fresh medium with 10% FBS. The 100  $\mu\text{L}$  of the Muse™ Annexin V & Dead Cell (EMD Millipore, USA cat. no. MCH100105) was added to each tube and incubated for 20 min at room temperature in the dark. Apoptotic cells were then measured by Muse™ Cell Analyzer.

For cell cycle analysis, MDA-MB-231 cells were incubated in the same conditions as described above. The cells were harvested into microcentrifuge tubes, washed once with 1X PBS, and fixed with ice-cold 75% EtOH at  $-20^\circ\text{C}$  for 3 hr. The ethanol-fixed cells were washed two times in 500  $\mu\text{l}$  of ice-cold PBS. The supernatant was then removed, and the cells pellet was re-suspended in 200  $\mu\text{L}$  of Muse™ Cell Cycle Reagent (Millipore, USA, cat. No# MCH100106) for 30 min at room temperature in dark. After incubation, the cell cycle was analyzed on Muse™ Cell Analyzer.

#### 10. Cell migration assay

The migration of MDA-MB-231 cells was examined by using the *in vitro* scratch assay. The cells were plated into 6-well plates at the density of  $1 \times 10^6$  cells/well and cultured for 24 hr to form monolayers. The wound area was created by scratching with a SPLScar™ Scratcher (SPL Life Sciences, Pocheon, South Korea). The cells were immediately incubated with 7-octenoic acid (1.5  $\text{mg/ml}$ ), oleamide (40  $\mu\text{g/ml}$ ), 1-Phenyl-2-pentanol (250  $\mu\text{g/ml}$ ), doxorubicin (1.5  $\mu\text{M}$ ; positive control), or complete medium (negative control) for 24 hr at  $37^\circ\text{C}$  with 5%  $\text{CO}_2$ . The images were captured at 0, 6, 12, and 24 hr using a right-field inverted microscope (Zeiss

Microscopy, Germany). The percentage of wound closure was calculated using ImageJ software version 1.53.

#### 11. Hoechst staining

To assess the effects of the identified compounds on nuclear material, MDA-MB-231 cells were seeded at a density of  $7 \times 10^5$  cells/well in a 6-well plate containing glass coverslips. The cells were incubated with 7-octenoic acid (2.5 mg/ml), oleamide (70  $\mu\text{g/ml}$ ), and 1-phenyl-2-pentanol (600  $\mu\text{g/ml}$ ) for 24 hr at 37°C with 5% CO<sub>2</sub>. After incubation, cells were washed with PBS, fixed with 4% formaldehyde, and stained with Hoechst 33342 (4  $\mu\text{g/ml}$ ) for 10 min in dark. Cover slides were then mounted with 70% glycerol and images were captured with an inverted microscope using 350 nm excitation and 450 nm emission filters (Zeiss Microscopy, Germany). A total of 3 images per treatment were captured at 40 X magnification.

#### 12. Real-Time Quantitative Reverse Transcription PCR (RT-qPCR)

MDA-MB-231 cells were plated into a 12-well culture plate at the density of  $1 \times 10^5$  cells/well. The cells were incubated with fraction no. 7 (75 and 100  $\mu\text{g/ml}$ ) that was derived from crude EtOAc extract for 24 hr at 37°C with 5% CO<sub>2</sub>. For control, cells were incubated with a complete medium alone. The total RNA was isolated by using Trizol reagent (Invitrogen, Carlsbad, CA) according to the manufacturer's instructions. First-strand cDNA was synthesized using Tetro cDNA Synthesis Kit (BIOLINE USA Inc, Taunton, MA). The resulting cDNAs were amplified with different primers (**Table 7**) using the SensiFAST™ SYBR® No-ROX Kit (BIOLINE USA Inc, Taunton, MA). Relative differences in gene expression among groups were determined from the quantification cycle (Ct) values. These values were first normalized to a housekeeping gene ( $\beta$ -actin) in the same sample ( $\Delta\text{Ct}$ ) and are expressed as the fold-change over control ( $2^{-\Delta\Delta\text{Ct}}$ ). Real-time fluorescence detection was performed using a CFX96 Touch Real-Time PCR Detection System (Bio-Rad).

Table 7 Primer sequences for RT-qPCR assay of the first part

Gene name	Forward primer (5'-3')	Reverse primer (5'-3')
<i>Bcl-2</i>	GATGTGATGCCTCTGCGAAG	CTAGCTGATGTCTCTGGAATCT
<i>Bax</i>	GGTTGTCGCCCTTTTCTA	CGGAGGAAGTCCAATGTC
<i>p53</i>	GTTCCGAGAGCTGAATGAGG	TCTGAGTCAGGCCCTTCTGT
<i>ACTB</i>	AGAAAATCTGGCACCACACC	CCATCTCTTGCTCGAAGTCC

### 13. Western blot analysis

MDA-MB-231 cells were plated into 6-well culture plates at the density of  $7 \times 10^5$  cells/well. The cells were incubated with fraction no. 7 (75 and 100  $\mu\text{g/ml}$ ), 7-octenoic acid (2.5 and 4 mg/ml), oleamide (70 and 100  $\mu\text{g/ml}$ ), 1-phenyl-2-pentanol (600 and 700  $\mu\text{g/ml}$ ), or doxorubicin (1.5  $\mu\text{M}$ ) for 2-4 hr. Cells were lysed in RIPA buffer (Bio Basic Inc.) supplemented with Protease/Phosphatase inhibitor cocktail (Sigma Aldrich, St. Louis, MO, USA) for 30 min and then centrifuged at  $14,000 \times g$  for 15 min at  $4^\circ\text{C}$ . The protein concentration was determined by the Bradford assay. Equal amounts of protein samples were heated, separated in 12% SDS-PAGE (150 V, 1 hr), and transferred onto nitrocellulose membranes (100 V, 1.30 hr). The membranes were washed and blocked with 2% BSA in Tris-buffered saline containing 0.5% Tween 20 (TBST) for 1 hr at room temperature. The membranes were probed with primary antibodies against  $\beta$ -actin, Bax, Bcl-2, caspase-3, or cleaved caspase-3 by incubating overnight at  $4^\circ\text{C}$  and then washed three times with TBST and incubated with secondary antibodies for 1 hr at room temperature. Protein detection was performed by adding a horseradish peroxidase chemiluminescence substrate. The intensity of each band was analyzed using Image lab software.

#### 14. Isolation of human MDMs

MDMs were isolated from a blood buffy coat of healthy donors as previously described (172). Briefly, the buffy coat was transferred into two 50 ml tubes and centrifuged at 3,000 rpm for 30 min. The White blood cells (WBCs) layer was transferred into a new tube and resuspended in PBS-EDTA (1 mM) for up to 20 ml. Diluted WBC was gently overlaid on top of Ficoll-paque solution (density 1.077 g/ml, GE Healthcare, Chicago, USA) at a 1:1 ratio and then centrifuged at 3,000 rpm for 30 min. The peripheral blood mononuclear cell (PBMC) layer at the interface was then collected in a new 50 ml tube and washed once in 40 ml PBS-EDTA. The supernatant was removed and the PBMC pellet was resuspended in 15 ml of PBS-EDTA. Diluted PBMC was gently overlaid on top of 46% Percoll-solution (density 1.131 g/ml, GE Healthcare, Chicago, USA) at a 1:1 ratio followed by centrifugation at 3,000 rpm for 30 min. The monocyte layer at the interface was then collected to a new 50 ml tube and washed 3-5 times in 40 ml PBS-EDTA to remove the residual platelet. The monocyte was then cultured in RPMI with 10% FBS and 1% penicillin/streptomycin at 37°C with 5% CO<sub>2</sub> for 6 days. The cell culture medium was replaced every 3 days.

#### 15. Statistical analysis

Data are shown as mean  $\pm$  standard error (SEM) of three independent experiments. For comparisons of more than two groups, one-way ANOVA was performed with multiple comparison correction (Dunnnett test) using GraphPad Prism 6.0 software. P-values < 0.05 were considered statistically significant.

## Part 2: The regulatory effect of the bioactive compound on the polarization of primary Human Monocyte-Derived Macrophages (MDMs).

The bioactive compound that had been identified in the first part was subjected to further investigation that focused on how oleamide influences human macrophage polarization and NLRP3-inflammasome activation. The *in vitro* culture of primary human MDMs was used as a model for this study. The effect of oleamide on the progression of M1/M2 macrophage polarization was examined by monitoring the morphological change, cell-surface markers, gene expressions, and cytokine productions. The underlying mechanism of oleamide-regulated MDMs polarization and NLRP3-inflammasome activation was also explored by western blot analysis (Figure 30).

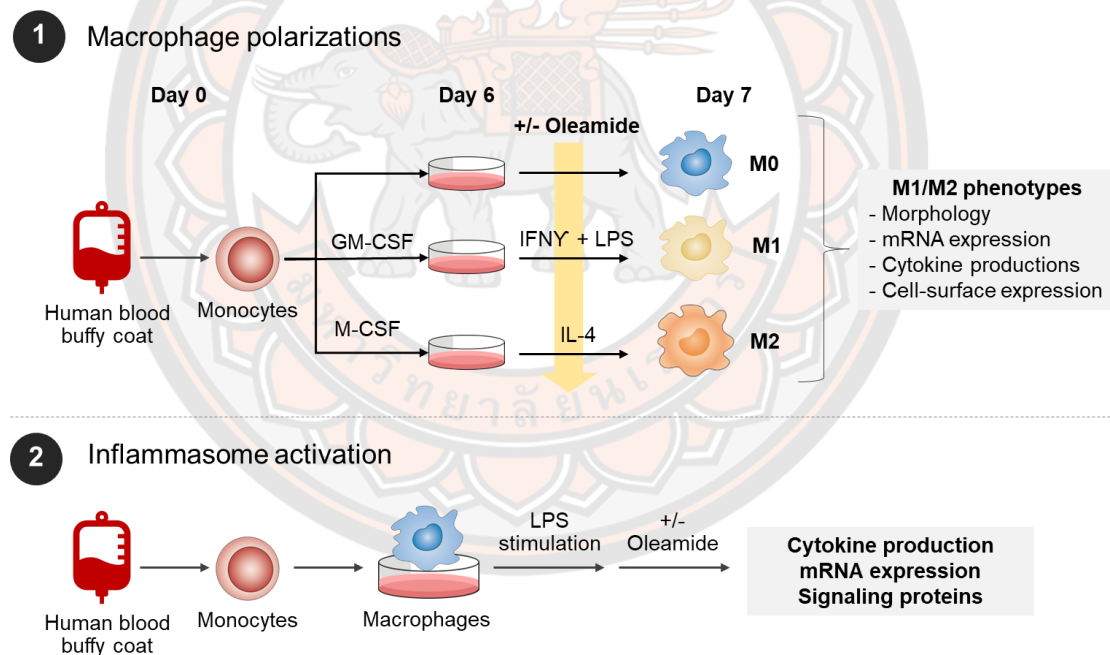


Figure 30 Schematic model of the regulator effect of the oleamide on macrophage polarization and inflammasome activation.

(1) human MDMs were isolated and stimulated in the presence or absence of oleamide. The M1/M2 phenotypes were investigated with multi-bioassay (2) Inflammasome activation was generated using the LPS-primed MDMs model, followed by oleamide stimulation.

1. Isolation of human MDMs

MDMs were isolated from a blood buffy coat of healthy donors as previously described (172). Briefly, the buffy coat was transferred into two 50 ml tubes and centrifuged at 3,000 rpm for 30 min. The serum was collected for preparation of single donor human serum, whereas the WBC layer was transferred into a new tube and resuspended in PBS-EDTA (1 mM) up to 20 ml. Diluted WBC was gently overlaid on top of Ficoll-paque solution (density 1.077 g/ml, GE Healthcare, Chicago, USA) at a 1:1 ratio and then centrifuged at 3,000 rpm for 30 min. The peripheral blood mononuclear cell (PBMC) layer at the interface was then collected in a new 50 ml tube and washed once in 40 ml PBS-EDTA. The supernatant was removed and the PMBC pellet was resuspended in 15 ml of PBS-EDTA. Diluted PMBC was gently overlaid on top of 46% Percoll-solution (density 1.131 g/ml, GE Healthcare, Chicago, USA) at a 1:1 ratio followed by centrifugation at 3,000 rpm for 30 min. The monocyte layer at the interface was collected into a new 50 ml tube and washed 3-5 times in 40 ml PBS-EDTA to remove the residual platelet. Monocyte was then cultured in desired conditions.

2. Preparation of heat-inactivated single donor human serum

Human serum was collected from a blood buffy coat of healthy donors. Buffy coat was transferred to two 50 ml tubes and centrifuged at 3,000 rpm for 30 min. The serum was then transferred to a new 50 ml tube and incubated for 30 min at 56°C in a water bath to inactivate the complements and remove fibrin. The serum was then centrifuged at 3,000 rpm for 15 min to remove precipitates and residual platelets. All supernatants were collected in 15 ml tubes and stored at -20°C until used.

3. MDMs culture and polarization

MDMs were cultured in RPMI 1640 supplemented with 10% human serum from buffy coats of healthy donors and 1% antibiotic-antimycotic

(Gibco™, USA #15240062) at 37°C with 5% CO<sub>2</sub>. In the M0 macrophages condition, monocytes were cultured in a complete medium only, for 6 days. In the M1 macrophages, the monocytes were cultured in the presence of 50 ng/ml of GM-CSF (ImmunoTools GmbH, Germany) for 6 days, called M1-liked cells. In the M2 macrophages, the monocytes were cultured in the presence of 50 ng/ml M-CSF (ImmunoTools GmbH, Germany) for 6 days, called M2-liked cells. Cell culture mediums were replaced every 3 days in all conditions. For the polarization steps, M1-liked cells were incubated with 20 ng/ml IFN- $\gamma$  (ImmunoTools GmbH, Germany) plus 10 ng/ml LPS of *Escherichia coli* O55:B5 (Sigma Aldrich, MO, USA) for 24 hr to obtain M1 macrophage. M2-like cells were incubated with 20 ng/ml IL-4 (ImmunoTools GmbH, Germany) for 24 hr to obtain M2 macrophage. While M0 macrophages were incubated in a complete medium alone for 24 hr to serve as naïve macrophage or negative control cells (Figure 31). For the experimental groups, macrophages (day 6) were cultured in desired conditions (M0; complete media only, M1; LPS + IFN- $\gamma$ , and M2; IL-4) in the presence or absence of oleamide (15  $\mu$ g/ml) for 24 hr.

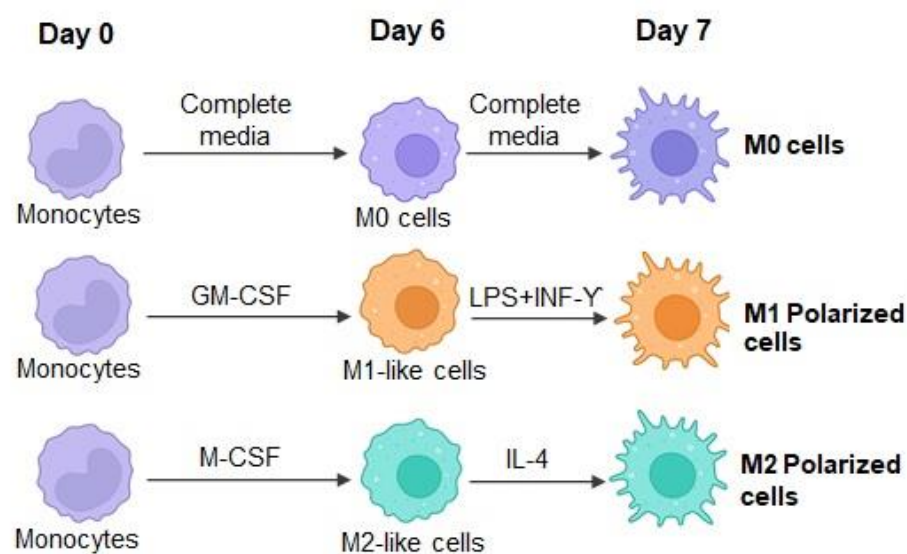


Figure 31 Scheme of primary human monocyte-derived macrophages (MDMs) culture and polarization.

#### 4. THP-1 cell culture and differentiation

THP-1 cells that were obtained from ATCC were maintained in RPMI-1640 supplemented with 10% FBS and 1% Antibiotic-Antimycotic (Gibco™, USA #15240062) at 37°C with 5% CO<sub>2</sub>. THP-1 cells were differentiated into macrophages by incubating with 100 nM phorbol-12-myristate-13-acetate (PMA) (Sigma-Aldrich, St. Louis, MO, USA) for 24 hr and then replaced with PMA-free complete medium for 72 hr. Following differentiation, the cells were polarized into M1 macrophages by incubation with 20 ng/ml IFN- $\gamma$  (ImmunoTools GmbH, Germany) and 10 ng/ml LPS (Sigma Aldrich, MO, USA) for 24 hr. M2 macrophages were obtained by incubation with 20 ng/ml IL-4 (ImmunoTools GmbH, Germany) for 24 hr. M0 macrophages were incubated with a complete medium only for 24 hr. For experimental groups, M0, M1, and M2 macrophages were cultured in desired conditions in the presence or absence of oleamide (15  $\mu$ g/ml) for 24 hr.

#### 5. Inflammasome activation

Isolated monocytes (Day 0) were seeded at a density of  $4 \times 10^5$  cells/well in 12-well plates and differentiated for 6 days in a complete medium. The cell culture medium was replaced every 3 days. On day 6, the MDMs were stimulated with 100 ng/ml LPS for 3 hr and the cells were stimulated with oleamide (10-40  $\mu$ g/ml) (Sigma Aldrich, St. Louis, MO, USA) or adenosine triphosphate (ATP) (Sigma-Aldrich, St. Louis, MO, USA) as the positive control for 1 hr and 3 hr. After stimulation, the supernatants were collected, and cytokine levels were measured using an ELISA. The cells were collected, and RT-qPCR was used to examine mRNA expression.

#### 6. Cell viability assay

Cell viability was determined using the Methyl Thiazol Tetrazolium (MTT) assay. MDMs (Day 6) were seeded at a density of  $2.0 \times 10^4$  cells/well in a 96-well plate and incubated with the serial concentration

of oleamide for 48 hr. The MTT salt solution (Thermo Fisher Scientific, Waltham, MA, USA) was then added and incubated for 3 hr at 37°C. To dissolve the formazan crystal, 100 µl of dimethyl sulfoxide (DMSO) (VWR International, West Chester, PA, USA) was added to each well. Plates were gently shaken at 70 rpm for 5-10 min. The absorbance was measured at 570 nm using a microplate reader (PerkinElmer, Inc., USA).

#### 7. Flow cytometry

Human monocytes were plated and cultured in the cell culture dishes (100 mm) at the density of  $5 \times 10^6$  cells/dish. The cells were cultured and polarized in desired conditions with the presence or absence of oleamide (15 µg/ml) as described above. After treatment, the MDMs were harvested using Trypsin-EDTA for 15 min and then scraped with a cell scraper. The cells were washed once with ice-cold PBS and resuspended in ice-cold FACS buffer (0.5% BSA and 0.05% sodium azide in PBS). Cells ( $1 \times 10^6$  cells) were stained with the fluorochrome-conjugated anti-human antibodies, including CD80-FITC, CD163-PE, and CD206-FITC (BioLegend, San Diego, CA, USA), CD14-PE, CD16-FITC, and isotype control (ImmunoTools GmbH, Germany) for 30 min at 4°C in FACS buffer. The cells were then washed three times in ice-cold PBS and fixed with 2% formaldehyde (Sigma Aldrich, MO, USA) at 4°C for 10 min. After fixation, cells were washed once in PBS, resuspended in FACS buffer, and stored at 4°C in the dark until used. Cell surface expressions were detected using CytoFlex S (Beckman Coulter Life Sciences, Indiana, USA) and analyzed with CytoExpert software.

#### 8. Real-Time Quantitative Reverse Transcription PCR (RT-qPCR)

Total RNA was extracted using Trizol reagent according to the manufacturer's instructions. cDNA was synthesized using Tetro cDNA Synthesis Kit (Bioline, Tennessee, USA). The resulting cDNAs were amplified with different primers (**Table 8**) using the SensiFAST™ SYBR® No-ROX Kit. Results were analyzed using the relative gene expression

method. Briefly, the relative expression of the target genes was calculated by relating the Ct-value of the target gene to unstimulated M0 macrophage. The quantitative cycle (Ct) values were used to calculate relative variations in gene expression between groups. These values were normalized to a housekeeping gene ( $\beta$ -actin) in the same sample ( $\Delta$ Ct) and expressed as the fold-change over control ( $2^{-\Delta\Delta Ct}$ ). Real-time fluorescence detection was performed using a CFX96 Touch real-time PCR detection system (Bio-Rad).

**Table 8 Primer sequences for RT-qPCR assay of the second part**

Gene name	Forward primer (5'-3')	Reverse primer (5'-3')
<i>IL-1<math>\beta</math></i>	AGCTACGAATCTCCGACCAC	CGTTATCCCATGTGTCTGAAGAA
<i>TNF</i>	CCTCTCTAATCAGCCCTCTG	GAGGACCTGGGAGTAGATGAG
<i>IL6</i>	ACTCACCTCTTCAGAACGAATTG	CCATCTTTGGAAGGTTTCAGGTTG
<i>CXCL10</i>	GTGGCATTCAAGGAGTACCTC	TGATGGCCTTCGATTCTGGATT
<i>CCL22</i>	CGAGGAAGAGGTTTCGGTTCACC	CATCTTCACCCAGGGCACTCT
<i>CD206</i>	TCCGGGTGCTGTTCTCCTA	CCAGTCTGTTTTTGATGGCACT
<i>iNOS</i>	CAGGGTGTGCCCAAACCTG	GGCTGCGTTCTTCTTTGCT
<i>Arg1</i>	GTGGAAACTTGCATGGACAAC	AATCCTGGCACATCGGGAATC
<i>NLRP3</i>	ACAAACTCATGGTGGCTTCC	CGTGCATTATCTGAACCCAC
<i>IL-18</i>	GAAGATGCCAGGGGTAATGA	TACCTGCCCAAACCTGAAAC
<i>PYCARD</i>	TGACGGATGAGCAGTACCAG	AGGATGATTTGGTGGGATTG
<i>ACTB</i>	AGAAAATCTGGCACCACACC	CCATCTCTTGCTCGAAGTCC

#### 9. Scanning electron microscope (SEM)

MDM cells were plated into 12-cell well plate containing sterile coverslips. After differentiation, the samples were fixed with 4% paraformaldehyde and 2.5% glutaraldehyde in 0.1 M phosphate buffer (1.14 g NaH<sub>2</sub>PO<sub>4</sub>, 1.69 g Na<sub>2</sub>HPO<sub>4</sub> in a 100-ml final volume of ddH<sub>2</sub>O, pH 7.4) for 30 min at 4°C. The samples were washed three times for 5 min each in 0.1 M phosphate buffer and then dehydrated with graded ethanol

(EtOH) series beginning with 25%, 50%, 75%, 95%, and 100% EtOH (5 min for each). The cells were further dehydrated with 1:1 (Hexamethyldisilazane (HMDS): ETOH) for 5 min and 100% HMDS twice for 5 min at room temperature and then coated with gold particles and imaged with an Apreo 2 SEM (Thermo Fisher Scientific) using a 5 kV incident beam.

#### 10. Enzyme-linked immunosorbent assay (ELISA)

The cell culture supernatants of the macrophages in each condition were used to measure the levels of TNF- $\alpha$ , IL-6, IL-1 $\beta$ , and IL-18 cytokines by a sandwich ELISA kit according to the manufacturer's instructions (Sino Biological Inc., China). The capture antibody was diluted to the working concentration in PBS and immediately coated in a 96-well microplate at 100  $\mu$ l/well. The plate was sealed and incubated overnight at 4°C then washed three times with 200  $\mu$ l of wash buffer (phosphate-buffered saline solution with 0.05% Tween 20 - PBST). The 300  $\mu$ l of blocking buffer (2% BSA in wash buffer) was added to each well and incubated at room temperature for 2 hr. The plate was washed three times with 200  $\mu$ l of wash buffer. The 100  $\mu$ l of sample or standards were added to each well and incubated for 2 hr at room temperature. The plate was washed three times and 100  $\mu$ l of detection antibody was added to each well and incubated for 1 hr at room temperature. The plate was washed three times with wash buffer. The 200  $\mu$ l of substrate solution was added to each well and incubated for 20 min at room temperature in the dark. The 50  $\mu$ l of stop solution was added to each well and the plate was gently tapped to ensure a thorough mix. The absorbance of the reaction was measured at 450 nm using an EnSpire® Multimode microplate reader (PerkinElmer, Inc., MA, USA).

#### 11. Lactate dehydrogenase (LDH) assay

The release of lactate dehydrogenase (LDH) was measured using the CyQUANT LDH cytotoxicity assay (Thermo Fisher, Waltham, USA). MDMs were plated into a 96-well plate at a density of  $2.0 \times 10^4$  cells/well overnight, and then incubated with LPS for 3 hr followed by oleamide (10 - 40  $\mu\text{g/ml}$ ) or ATP (30 mM) for 3 hr. After incubation, 50  $\mu\text{l}$  of culture medium was transferred to a new 96-well plate and 50  $\mu\text{l}$  of LDH reaction mixture was added, mixed, and incubated for 30 min at room temperature. Then, 50  $\mu\text{l}$  of stop solution was added to terminate the reactions and the absorbances of the reaction mixtures were measured at 490 nm and 680 nm.

#### 12. Western blot analysis

Human monocytes were plated and cultured in the cell culture dishes (100 mm) at the density of  $5 \times 10^6$  cells/dish. Monocytes were cultured for 6 days to differentiate into macrophages. The inflammasome activation was then performed as described above. Total proteins were extracted by washing cells with ice-cold PBS and lysed with RIPA buffer containing 1X Protease/Phosphatase Inhibitor Cocktail (Sigma Aldrich, St. Louis, MO, USA) for 30 min on ice. The lysate was transferred into microcentrifuge tubes and centrifuged at 12,000 rpm for 10 min at 4°C. The supernatant containing whole protein was collected and measured for protein concentration by the Bradford assay. Equal amounts of each sample were loaded and separated in 8%-12% of SDS-PAGE at 100 V for 1.30 hr. Protein was then transferred onto PVDF membrane at 100 V for 1.30 hr in an icebox. The membranes were blocked with TBST containing 5% BSA for 1 hr and subsequently incubated with the appropriate primary antibodies; Rabbit mAb against IL-1 $\beta$ , cleaved- IL-1 $\beta$ , caspase-1, cleaved caspase-1, NLRP3, ASC/TMS1, P2X7 receptor (Cell Signalling Technology, MA, USA) at 4°C overnight. The membranes were washed 3-5 times in TBST for 5 min each and then incubated with Anti-rabbit IgG with HRP-

linked Antibody (Cell Signalling Technology, MA, USA) for 1 hr at room temperature. After incubation, the membranes were washed in TBST 3-5 times for 5 min each and the blots were developed by chemiluminescence solution for 1 min. The protein was detected using ChemiDoc™ Touch Imaging System (Bio-Rad, Hercules, CA, USA).

### 13. Statistical analysis

All data were expressed as mean  $\pm$  standard deviation ( $n = 3$ ). For comparisons of more than two groups, one-way ANOVA was performed with multiple comparison corrections (Dunnett test) using GraphPad Prism 6.0 software (GraphPad Software Inc., San Diego, CA, USA).  $p$ -values  $< 0.05$  were considered statistically significant.

### **Part 3: The reprogramming of TAMs with a bioactive compound (oleamide).**

This study aims to explore the regulatory effect of oleamide on human TAMs polarization and how it influences cancer cell progression. The primary human monocyte-derived TAMs were *in vitro* generated using transwell co-culture of human MDMs with an MDA-MB-231 cell line as a model. The effect of oleamide on the reprogramming of TAMs was investigated by studying gene expressions by RT-qPCR, measuring cytokine productions by ELISA, and monitoring cell morphology by a bright-field microscope. Moreover, the conditioned medium of oleamide-treated TAMs was determined for the anti-cancer activity against the MDA-MB-231 cell line using cell viability assay and cell apoptosis analysis (**Figure 32**).

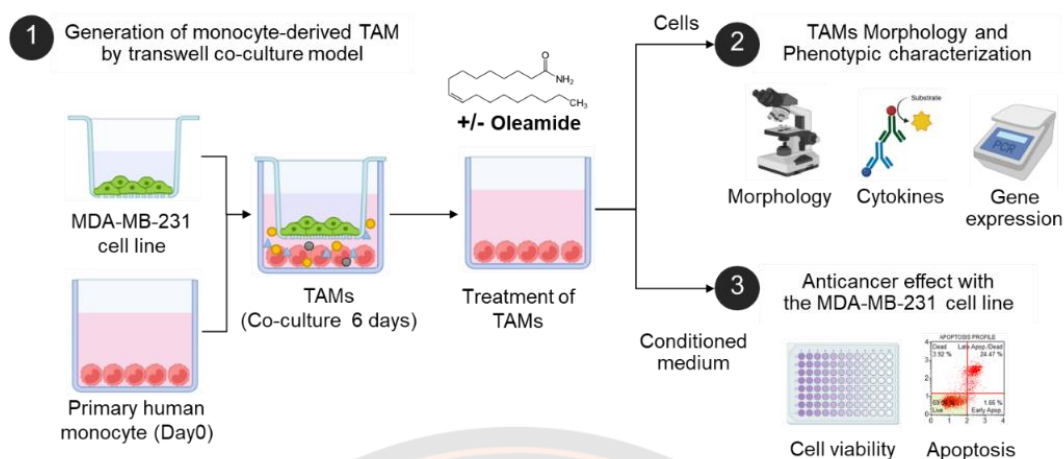


**Figure 32** Schematic models of the oleamide-induced reprogramming of TAMs and its anticancer effect against MDA-MB-231 cells.

(1) TAMs were generated by co-culturing of primary monocyte and MDA-MB-231 cells for 6 days. (2) Morphology and phenotypic characterization of the TAMs after treatment with oleamide. (3) Anticancer effect of the TAMs-conditioned medium after treatment with oleamide.

### 1. Cell Culture

Primary MDMs were isolated from a blood buffy coat of a healthy donor at Blood bank, Naresuan University Hospital. MDMs were cultured in RPMI 1640 (Gibco, Carlsbad, CA, USA) supplemented with 10% single donor human serum and 1% penicillin/streptomycin (Gibco, Carlsbad, CA, USA). The MDA-MB-231 cell line was obtained from the ATCC (Manassas, VA, USA). Cells were cultured in DMEM (Gibco, Carlsbad, CA, USA) supplemented with 10% fetal bovine serum (Gibco, Carlsbad, CA, USA) and 1% penicillin/streptomycin (Gibco, Carlsbad, CA, USA). All cells were maintained in a humidified atmosphere at 37°C with 5% CO<sub>2</sub>.

### 2. Harvesting tumor-conditioned media

To obtain culture supernatants for the generation of tumor-conditioned media (TCM), MDA-MB-231 cells at  $2 \times 10^5$  cells were grown in a T-75 flask until reached 80% confluence in a complete medium.

Then culture medium was replaced with a 0.2% fetal bovine serum medium for 24 hr. After incubation, the TCM was harvested and centrifuged at 3,000 rpm for 5 min to remove suspended cells. The supernatant was collected, and 10% single donor human serum was added to reconstitute the medium.

### 3. Isolation of human MDMs

MDMs were isolated from a blood buffy coat of healthy donors as described above. Briefly, the buffy coat was transferred into two 50 ml tubes and centrifuged at 3,000 rpm for 30 min. The WBCs layer was collected and resuspended in PBS. Diluted WBC was gently overlaid on top of Ficoll-paque solution (density 1.077 g/ml, GE Healthcare, Chicago, USA) at a 1:1 ratio and then centrifuged at 3,000 rpm for 30 min. Then, the PBMC layer was collected, resuspended in PBS, and overlaid on top of 46% Percoll solution (density 1.131 g/ml, GE Healthcare, Chicago, USA) at a 1:1 ratio followed by centrifugation at 3,000 rpm for 30 min. The monocyte layer was collected, washed 4-5 times in PBS, and cultured in complete RPMI 1640 with 10% human serum and 1% penicillin/streptomycin.

### 4. Preparation of heat-inactivated single donor human serum

Human serum was collected from a blood buffy coat of healthy donors. Buffy coat was transferred to two 50 ml tubes and centrifuged at 3,000 rpm for 30 min. The serum was then transferred to a new 50 ml tube and then incubated for 30 min at 56°C in a water bath to inactivate complement and remove fibrin. The serum was then centrifuged at 3,000 rpm for 15 min to get rid of precipitates and residual platelets. All supernatants were collected in 15 ml tubes and stored at -20°C until used.

## 5. Generation of TAMs

TAMs were generated by co-culturing of human MDMs and MDM-MB-231 breast cancer cells using Transwell co-culture systems (Polycarbonate, pore size 0.4  $\mu\text{m}$ ) (SPL Life Sciences, Pocheon, Korea). MDM-MB-231 cells were plated in an upper chamber at a density of  $6 \times 10^3$  cells/well in complete DMEM overnight before co-culture. Freshly isolated human monocytes were plated in a lower chamber at a density of  $1 \times 10^5$  cells/well. Monocytes were cultured in different conditions including, 1) complete medium alone (Neg control); 2) complete medium plus IL-4 (50 ng/mL), IL-10 (50 ng/mL), and M-CSF (50 ng/mL); 3) a 1:1 ratio of complete medium and TCM plus the addition of IL-10 (50 ng/mL), and M-CSF (50 ng/mL). Then, the upper chamber containing MDM-MB-231 cells was inserted into the lower chamber (MDMs) and the co-culture systems were maintained for 7 days. For negative control, MDMs were cultured in a complete medium alone without co-culture systems. Medium and cytokines were replaced every 3 days and cells were harvested on day 7.

## 6. RT-qPCR analysis

Total RNA extraction and cDNA synthesis were performed by using Trizol reagent (Invitrogen, Carlsbad, CA, USA) and Tetro cDNA Synthesis Kit (Bioline, Tennessee, USA), respectively as mentioned above. Briefly, the resulting cDNAs were amplified with specific primers (**Table 9**) using the SensiFAST™ SYBR® No-ROX Kit (Bioline USA Inc., Taunton, MA, USA). Real-time fluorescence detection was performed using a CFX96 Touch Real-Time PCR Detection System (Bio-Rad). Results are expressed as relative mRNA expression (normalized to beta-actin mRNA expression of untreated control cells: MØ macrophage), which is calculated by using the  $2^{-\Delta\Delta\text{CT}}$  method.

Table 9 Primer sequences for RT-qPCR assay of the third part

Gene name	Forward primer (5'-3')	Reverse primer (5'-3')
<i>c-Myc</i>	ATGGCCATTACAAAGCCG	TTTCTGGAGTAGCAGCTCCTAA
<i>MMP-9</i>	TGTACCGCTATGGTTACTCTCG	GGCAGGGACAGTTGCTTCT
<i>VEGFA</i>	AGGGCAGAATCATCACGAAGT	AGGGTCTCGATTGGATGGCA
<i>HLA-DR</i>	ATACTCCGATCACCAATGTACCT	GACTGTCTCTGACTCCTGT
<i>CD163</i>	TTTGTCAACTTGAGTCCCTTAC	TCCCGCTACACTTGTTTTAC
<i>CD206</i>	CTACAAGGGATCGGGTTTATGGA	CTACAAGGGATCGGGTTTATGGA
<i>iNOS</i>	TTCAGTATCACAACCTCAGCAAG	TGGACCTGCAAGTTAAAATCCC
<i>IL-10</i>	GGAGAACCTGAAGACCCTCA	GATGTCAAACCTCACTCATGGC
<i>ACTB</i>	AGAAAATCTGGCACACACC	CCATCTCTTGCTCGAAGTCC

#### 7. Cell viability assay

Cell viability was determined using the MTT assay. MDA-MB-231 cells were plated into a 96-well plate at a density of  $1.0 \times 10^4$  cells/well in a 100  $\mu$ l complete medium. The cells were incubated with conditioned mediums from untreated TAMs (TAMs), oleamide-treated TAMs (TAMs + OLA), or M0 macrophages (MØ Ctr). For the control groups, cells complete medium (neg control) or complete medium plus 20  $\mu$ g/ml OLA (OLA only). All cells were incubated for 24, 48, and 72 hr.

For cytotoxicity of oleamide, MDA-MB-231 cells were incubated with a serial concentration of oleamide ranging between 0 - 240  $\mu$ g/ml for 24 hr. The cells were then washed once in PBS and incubated with MTT salt solution (Thermo Fisher Scientific, Waltham, MA, USA) for 3 hr at 37°C. The media were then removed and the 100  $\mu$ l of dimethyl sulfoxide (DMSO) (VWR International, West Chester, PA, USA) was added to dissolve the formazan crystal. The plates were gently shaken at 70 rpm for 5-10 min. The absorbance was measured at 570 nm using a microplate reader (PerkinElmer, Inc., USA).

#### 8. Apoptosis analysis

Cell apoptosis was examined by using Muse Cell Analyzer (EMD Millipore, USA). MDA-MB-231 cells were plated into 24-well plates at the density of  $5 \times 10^4$  cells/well. Cells were incubated with conditioned mediums of untreated TAMs (TAMs), oleamide-treated TAMs (TAMs + OLA), or M0 macrophages (MØ Ctr), or incubated in complete medium alone (control), or complete medium plus 20 µg/ml OLA (OLA only) for 24 hr at 37°C with 5% CO<sub>2</sub>. The cells were harvested and diluted with 5% FBS in a complete medium up to 100 µl. The 100 µl of Muse™ Annexin V and dead cell reagent (EMD Millipore, USA cat. no. MCH100105) were then added to stained cells by incubating for 20 min at room temperature. The Cells were then read within 10 min.

#### 9. ELISA assay

Levels of TNF- $\alpha$ , IL-6, IL-1 $\beta$ , and IL-10 cytokines were measured by a sandwich ELISA kit according to the manufacturer's instructions (Sino Biological Inc., China) as described above. The absorbance of the reaction was measured at 450 nm using an EnSpire® Multimode microplate reader (PerkinElmer, Inc., MA, USA).

#### 10. Statistical analysis

All data were expressed as mean  $\pm$  standard deviation (n = 3). For comparisons of more than two groups, one-way ANOVA was performed with multiple comparison corrections (Dunnett test) using GraphPad Prism 6.0 software (GraphPad Software Inc., San Diego, CA, USA). p-values < 0.05 were considered statistically significant.

## CHAPTER 4

### RESULTS

In this chapter, the results are described, based on *in vitro* bioassay-guided identification of bioactive compounds from *Moringa oleifera* lam. leaves (MOL) against the MDA-MB-231 breast cancer cells line (part 1), the regulatory effect of bioactive compound (oleamide) on the polarization of primary human monocyte-derived macrophages (MDMs) (part 2), and the reprogramming of tumor-associated macrophages (TAMs) with active compound (oleamide) (part 3).

#### **Part 1: *In vitro* bioassay-guided identification of bioactive compound from MOL against the MDA-MB-231 breast cancer cells line.**

##### 1.1 Certification of analysis (COA) MOL dried powder

MOL dried powder was obtained from the Khaolaor Laboratories Co. Ltd, Samutprakan city, Thailand. Plants material was approved for a certificate of analysis (COA) that includes physical control, chemical control, and biological control by Khaolaor Laboratories Co. Ltd. (**Table 10**).

##### 1.2 The yield of crude MOL by sequential extraction

MOL was sequentially extracted with a defined series of organic solvents with an increasing polarity (hexane < Ethyl acetate; EtOAc < Ethanol; EtOH). The results revealed that higher polarity produced the highest extraction yield compared to the others (**Table 11**).

Table 10 Certification of analysis of *Moringa oleifera* leaf dried powder from Khaolaor Laboratories Co. Ltd

Item	Specification	Results
<b>Physical Control</b>		
Appearance	Greenish powder	Greenish powder
Odor & Taste	Characteristic	Characteristic
Loss on Drying	10% Max	4.84%
Bulk Density	0.400 – 0.600 g./ml.	0.400 – 0.600 g./ml.
<b>Chemical Control</b>		
Arsenic (As)	< 2 ppm	< 2 ppm
Lead (Pb)	< 1 ppm	< 1 ppm
Cadmium (Cd)	< 0.3 ppm	< 0.3 ppm
<b>Microbiological Control</b>		
Total plate count	< 10,00 CFU/g	< 10,00 CFU/g
Yeast & Mold	< 500 CFU/g	< 500 CFU/g
<i>Staphylococcus aureus</i>	Absent/1 g	Absent/1 g
<i>Clostridium</i> spp.	Absent/10 g	Absent/10 g
<i>Salmonella</i> spp.	Absent/10 g	Absent/10 g

Table 11 The yield of crude MOL extract by sequential extraction

Organic solvents	Polarity index*	Yield (g.)
Hexane	0.1	35.37
Ethyl acetate (EtOAc)	4.4	44.78
95% Ethanol (EtOH)	5.1	66.63

\*The polarity index is a relative measure of the degree of interaction of the solvent with various polar test solutes. (Source: Snyder Polarity Index. Date retrieved 20 May 2011)

1.3 Screening for cytotoxic effects of crude hexane, EtOAc, and EtOH extracts of MOL on breast cancer cells and normal cells.

To compare the cytotoxic effects of crude MOL extracts against MDA-MB-231 cells, sample cells were plated into 96-well plates and incubated with serial concentrations of crude hexane, crude EtOAc, and crude EtOH extracts of MOL for 24 hr. Cell viability was assessed using the MTT assay. Crude EtOAc extract showed the lowest  $IC_{50}$  value (233.5  $\mu\text{g/ml}$ ) followed by crude EtOH extract (241.1  $\mu\text{g/ml}$ ), and crude hexane extract (342.6  $\mu\text{g/ml}$ ) (**Figure 33A**). This result indicated that the crude EtOAc extract exhibited higher anti-cancer activity compared to the others. To study the cytotoxicity of MOL extract on normal cells, primary human MDMs were used as a model of normal cells and incubated with a serial concentration of crude MOL extracts. The results showed that the crude hexane extract exhibited lowest cytotoxicity against normal cells ( $IC_{50} = 387.1 \mu\text{g/ml}$ ) followed by crude EtOAc extract ( $IC_{50} = 350.2 \mu\text{g/ml}$ ), and crude EtOH extract ( $IC_{50} = 254.6 \mu\text{g/ml}$ ) (**Figure 33B**). Taken together, crude EtOAc extract of MOL represented a more adequate subject for future fractionation with the highest cytotoxicity against MDA-MB-231 cells with low cytotoxicity to normal human MDMs.

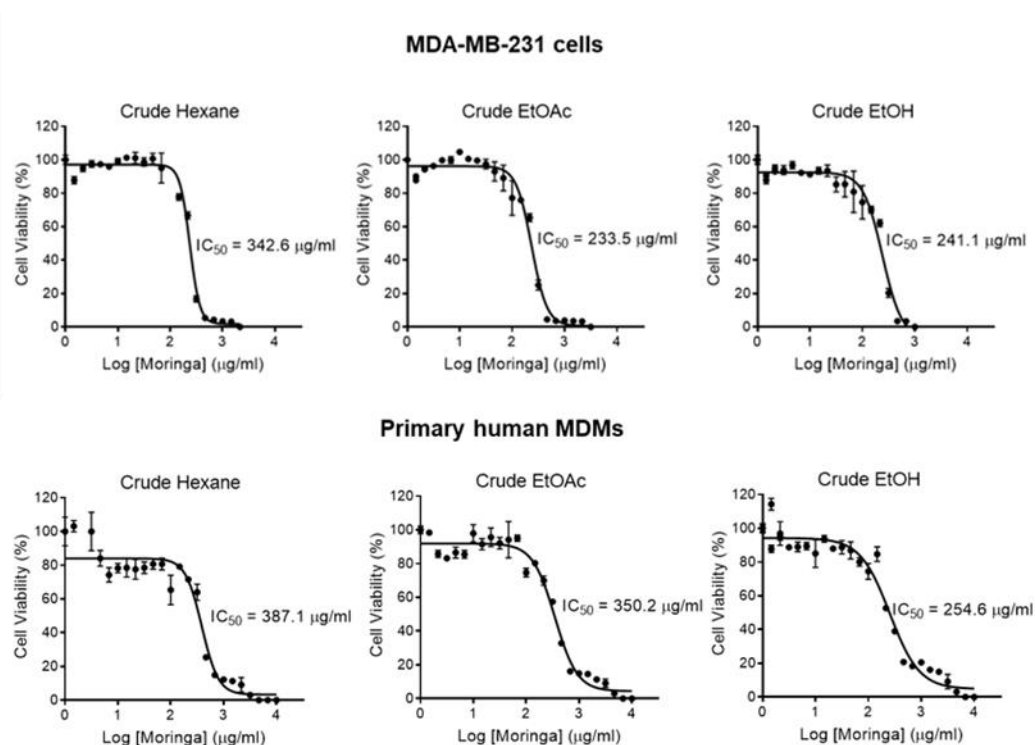


Figure 33 Cytotoxicity of Crude hexane, EtOAc, and EtOH extracts of MOL on the viability of MDA-MB-231 cells and primary human MDMs. (A) MDA-MB-231 cells. (B) normal human MDMs. (A-B) The IC<sub>50</sub> values of MDA-MB-231 cells and primary human MDMs after treatment with a serial concentration of each extract (0-10 mg/ml) for 24 hr. The IC<sub>50</sub> values were calculated using GraphPad Prism 6.0 software. Each dot represents the mean + SEM of three independent experiments. IC<sub>50</sub>, the half-maximal inhibitory concentration; EtOAc, ethyl acetate; EtOH, ethanol.

#### 1.4 Anti-cancer activity of EtOAc extract of MOL and its derived fractions on MDA-MB-231 cells.

To screen the anti-cancer activity of EtOAc extract and its derived fractions, MDA-MB-231 cells were incubated with crude EtOAc extract and fractions no. 1-11 for 24 hr. The results showed that crude EtOAc extract and fractions no. 5-8 and 10-11 exhibited a significantly decreased MDA-MB-231 cell viability. This result was a noticeable difference with fractions no. 6-8 shows a significant decrease in a dose-

dependent manner (Figure 34A). As fraction no. 7 showed the strongest cytotoxicity, it was investigated further at different time points. Cell viability was significantly decreased in a time-dependent manner after treatment with 100  $\mu\text{g/ml}$  of fraction no.7 (Figure 34B). To confirm the anti-cancer activity of EtOAc extract and its derived fractions, the MDA-MB-231 cells were further investigated in the clonogenic assay (Figure 35). Fractions no. 6-8 exhibited complete absence in the number of colonies at concentrations of 50, 100, and 150  $\mu\text{g/ml}$ . Fractions no. 4,5, and 9-11 also showed a reduction of colonies number but not a complete absence. The other fraction was not altered in the number of colonies when compared to the control. Taken together, these results suggested that fraction no. 7 exhibited a more potent fraction for further fractionation and identification of bioactive compounds.

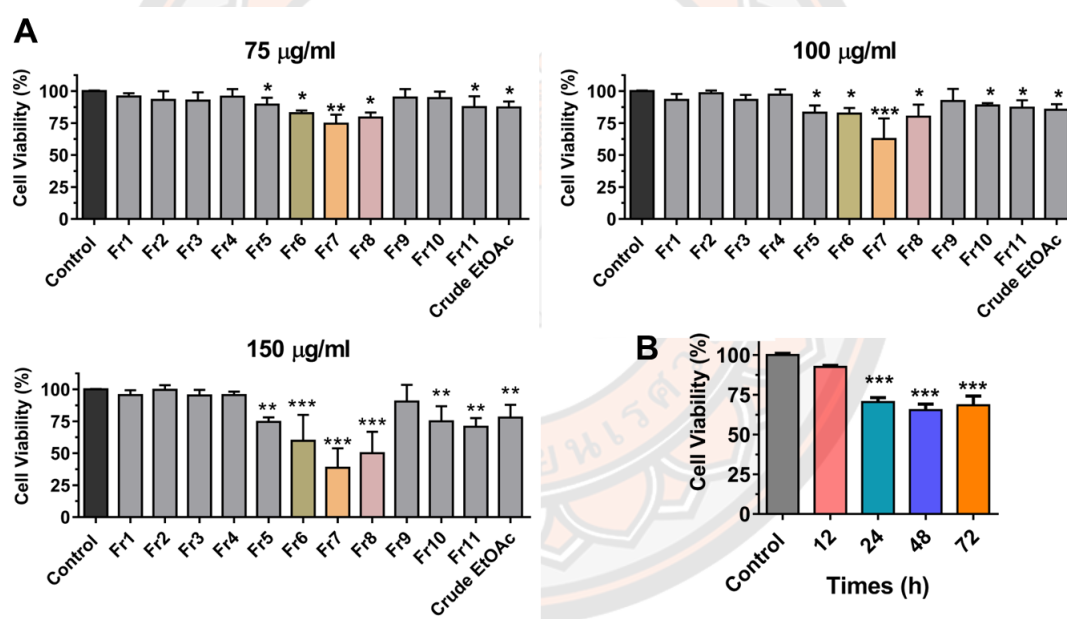
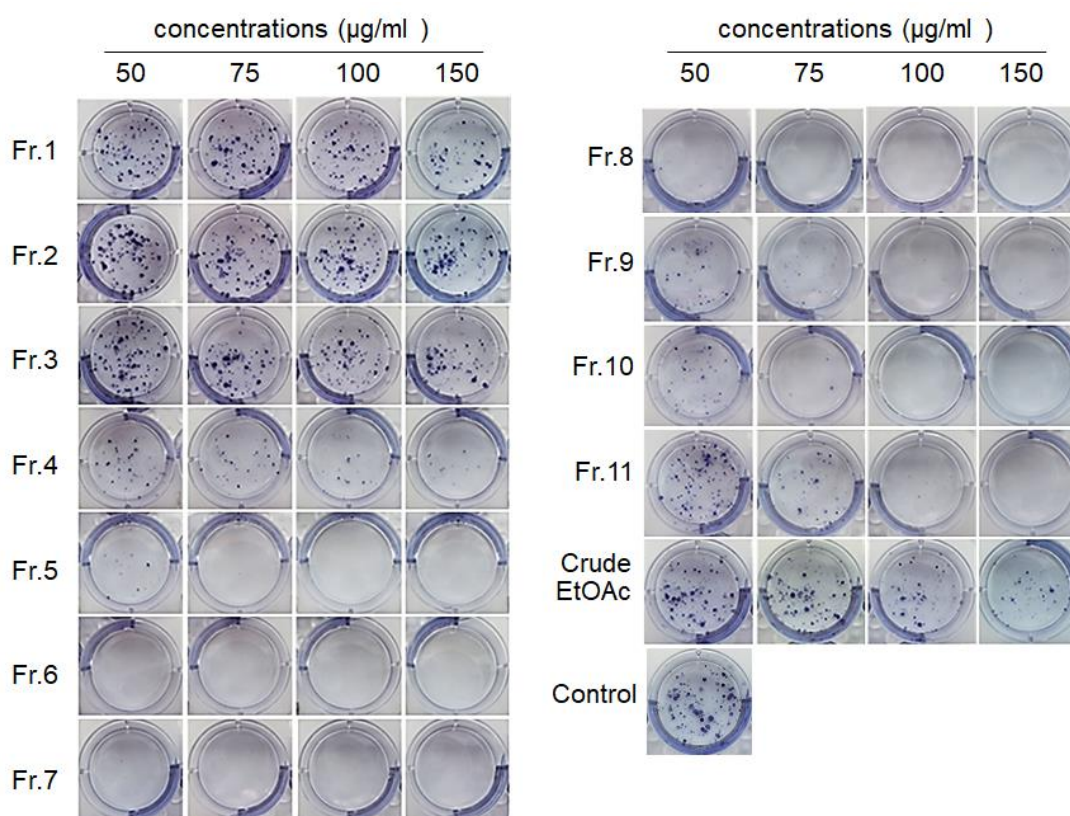


Figure 34 Cell viability of MDA-MB-231 cells after treatments with EtOAc extract and its derived fractions.

(A) Cells were treated with crude EtOAc extract and fractions no.1-11 at concentrations 70, 100, and 150  $\mu\text{g/ml}$  for 24 hr. (B) Cells were incubated with fraction no. 7 (100  $\mu\text{g/ml}$ ) at different time points. One-way ANOVA was performed with multiple comparison corrections (Dunnnett test). Data represent the mean  $\pm$  SEM of three independent experiments. (\* $p < 0.05$ , \*\* $p < 0.01$ , \*\*\* $p < 0.001$ ). EtOAc, ethyl acetate; Fr, fraction.



**Figure 35** Effect of EtOAc extract and its derived fractions on the clonogenic growth of MDA-MB-231 cells.

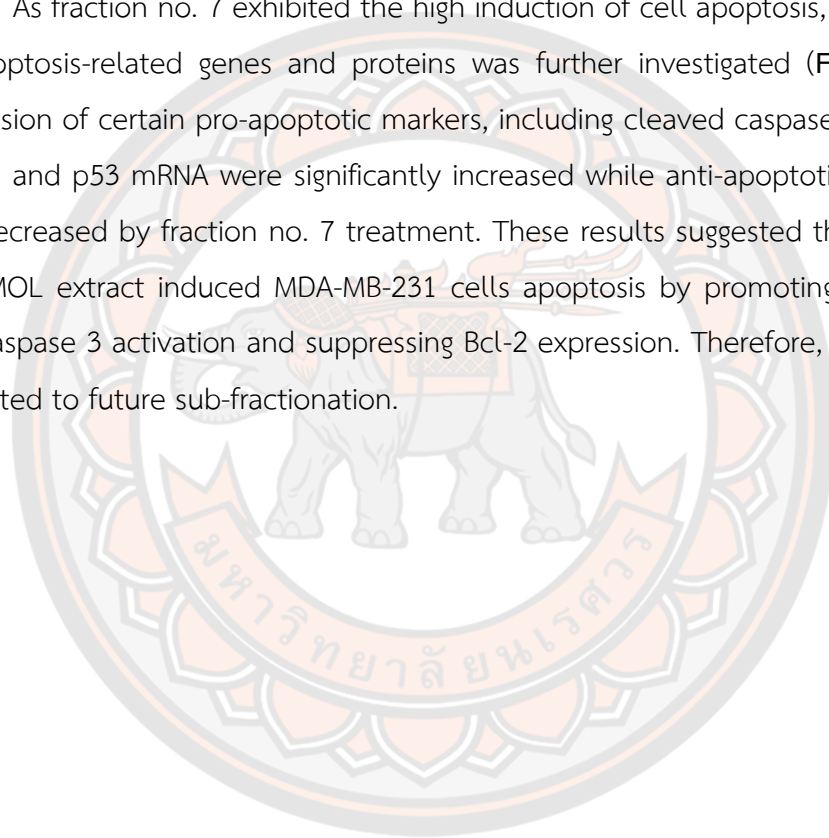
The cells were incubated with crude EtOAc extract and its fractions at a concentration of 50 – 150 µg/ml for 24 hr. After incubation, cells were cultured for 14 days in a complete medium and then stained with crystal violet to visualize the colonies. EtOAc, ethyl acetate; Fr, fraction.

1.5 The fractions on. 6-7 induced apoptosis and cell cycle arrest on the MDA-MB-231 cells line.

To evaluate the role of crude EtOAc extract and its derived fractions on cell apoptosis and cell-cycle regulation, MDA-MB-231 cells were incubated with crude EtOAc extract and its derived fractions, for 24 hr. Cell apoptosis was analyzed by Muse cell analyzer using Annexin V/7-AAD staining (**Figure 36**). The results showed that crude EtOAc and fractions no. 6-8 significantly increased the proportion of late apoptotic cells from 1.46% (untreated control) up to 16.0%, 23.90%, 44.20%, and 39.80%, respectively. The proportion of dead cells also increased to 43.6%, 75.8%,

54.2%, and 60.10%, respectively. In addition, the alteration of the cell-cycle distribution was analyzed (**Figure 37**). Treatment with fractions no. 6 and 8 resulted in the accumulation of cells at the G0/G1 phase. This varied from 53.5% (untreated control) to 61.8% and 63.4%. Fraction no. 7 resulted in the accumulation of cells at the G2/M phase (from 26.2% to 38.4%). These results indicated that fractions no.6-8 can promote cell cycle arrest and apoptosis of MDA-MB-231 cells, and fraction no. 7 represented the most effective fraction compared to others.

As fraction no. 7 exhibited the high induction of cell apoptosis, the expression of apoptosis-related genes and proteins was further investigated (**Figure 38**). The expression of certain pro-apoptotic markers, including cleaved caspase 3 protein, Bax mRNA, and p53 mRNA were significantly increased while anti-apoptotic Bcl-2 protein was decreased by fraction no. 7 treatment. These results suggested that fraction no. 7 of MOL extract induced MDA-MB-231 cells apoptosis by promoting the p53, Bax, and caspase 3 activation and suppressing Bcl-2 expression. Therefore, fraction no.7 is subjected to future sub-fractionation.



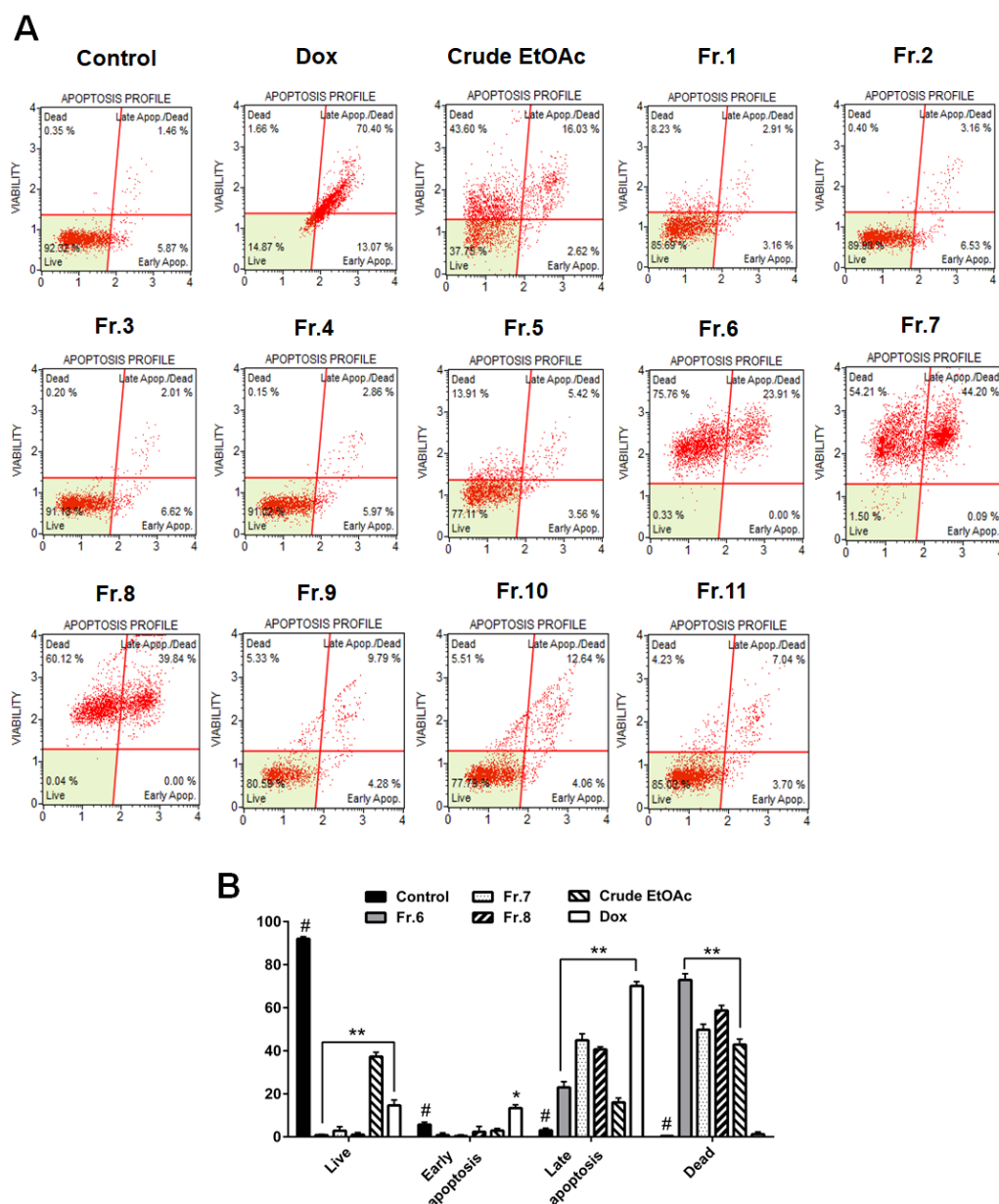


Figure 36 Effect of crude EtOAc extract and its derived fractions on the MDA-MB-231 cell apoptosis.

(A) Cells apoptosis by Muse cell analyzer. (B) The corresponding linear diagram of (%) cell apoptosis. Cells were incubated with crude EtOAc extract, 11 fractions (150  $\mu\text{g}/\text{ml}$ ), (1.5  $\mu\text{M}$ , positive control), or complete medium (untreated control) for 24 hr. The upper-left quadrant (annexin V $^-$ , 7-AAD  $^+$ ) represents dead cells. The lower left quadrant (annexin V $^-$ , 7-AAD  $^-$ ) represents live cells. Data represents mean  $\pm$  SEM of three independent experiments (\* $p < 0.05$ , \*\* $p < 0.01$ , \*\*\* $p < 0.001$ ). EtOAc, ethyl acetate; Fr, fraction; Dox, doxorubicin.

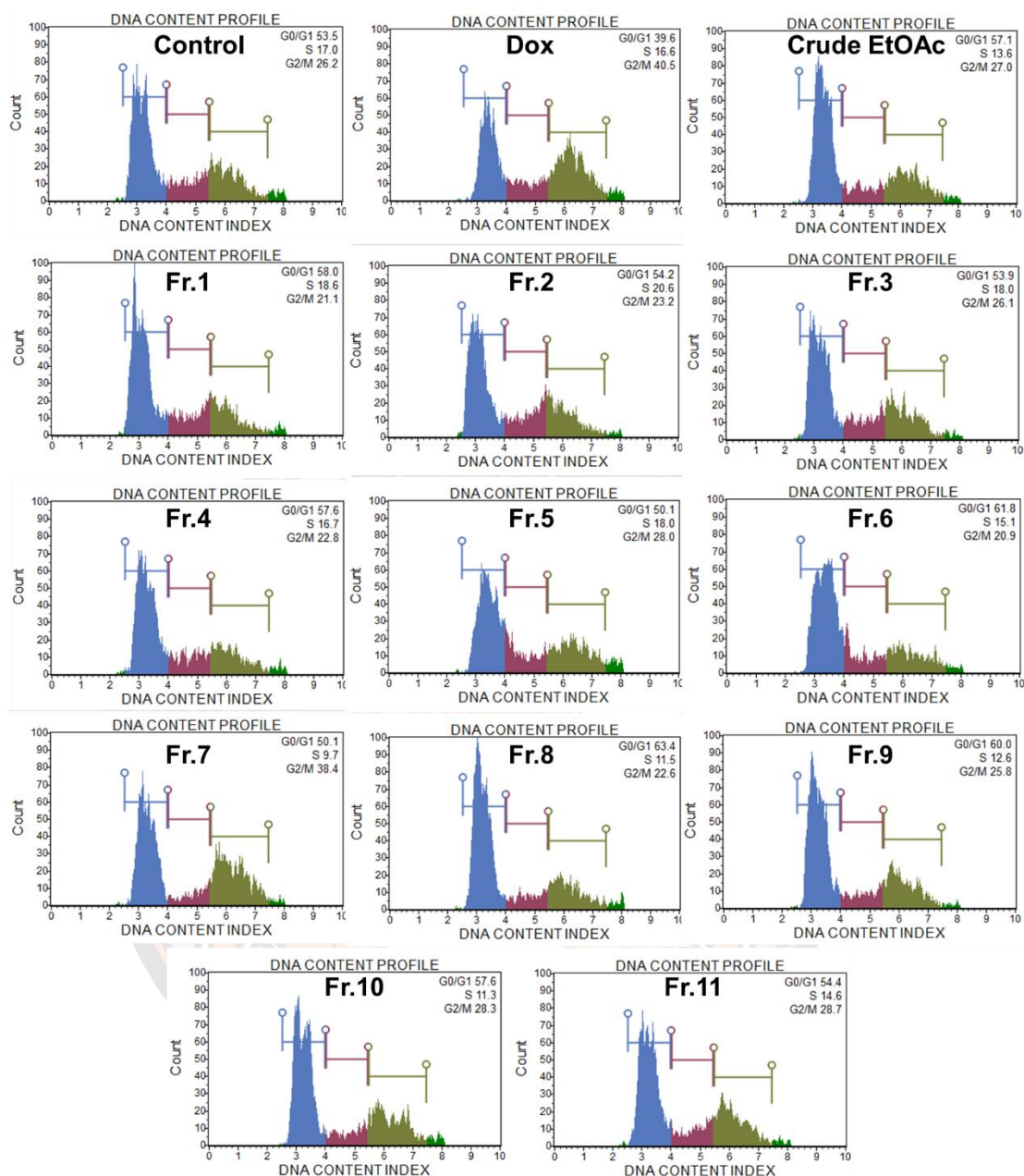


Figure 37 Effect of MOL extract and its derived fractions on the distribution of MDA-MB-231 cells in the cell cycle.

Cells were incubated with crude EtOAc extract, 11 fractions (150  $\mu\text{g/ml}$ ), or doxorubicin (1.5  $\mu\text{M}$ ) for 24 hr. For control, cells were incubated with a complete medium alone. EtOAc, ethyl acetate; Fr, fraction; Dox, doxorubicin.

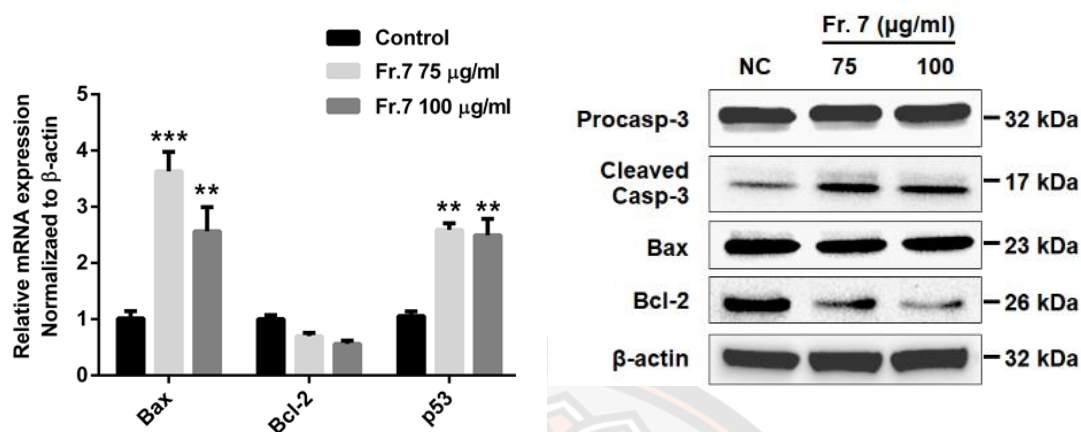


Figure 38 Expression of apoptosis-related genes and proteins in MDA-MB-231 cells after treatment with fraction no.7 of MOL extract.

(A) mRNA expression by RT-qPCR. (B) Western blot analysis. The cells were incubated with fraction no.7 (75 and 100  $\mu$ g/ml) for 24 hr. For the untreated control, cells were incubated with a complete medium alone. For the positive control, cells were incubated with doxorubicin (1.5  $\mu$ M). Data represent the mean  $\pm$  SEM of three independent experiments. (\* $p < 0.05$ , \*\* $p < 0.01$ , \*\*\* $p < 0.001$ ). One-way ANOVA was performed with multiple comparison corrections (Dunnnett test). EtOAc, ethyl acetate; Fr, fraction; Dox, doxorubicin; NC, negative control; Fr, fraction;  $\beta$ -actin, beta-actin.

1.6 Sub-fractionation of fraction no. 7 and identification of compounds using the Liquid chromatography-electrospray ionization-quadrupole time-of-flight-mass spectrometry (LC-ESI-QTOF-MS/MS)

To separate the chemical components in active fraction no. 7, it was next re-fractionated using silica gel column chromatography. Eight sub-fractions (no. 7.1-7.8) were obtained (**Table 12**) and their cytotoxicity against MDA-MB-231 cells was assessed using an MTT assay (**Figure 39**). Sub-fraction no. 7.7 strongly reduced the viability of MDA-MB-231 cells compared to the other sub-fractions. Thus, sub-fraction no 7.7 was attempted to tentatively identify the bioactive compounds using LC-ESI-QTOF-MS/MS. This sub-fraction was injected into an Agilent 1260 infinity series HPLC system, and the constituents were collected in a 96-well plate with 30 s per well

until 33 min. In total, ten candidate compounds (C1 - C10) were identified. All collected samples were screened for cytotoxicity using the MTT assay and the acquisition times represented active compounds between 10.414 (C1), 12.286 (C2), 17.586 (C3), 20.198 (C4), 21.015 (C5), 22.476 (C6), 26.473 (C7), 30.557 (C8), 32.057 (C9), and 32.606 (C10) min (**Figure 40**). The full tentative identification is listed in **Table 13**.

**Table 12** The yield of sub-fractions no.7.1 – 7.8 from active fraction no.7 of MOL extract

Sub-fractions No.	Yield (mg)
Fr 7.1	1.70
Fr 7.2	1.40
Fr 7.3	11.60
Fr 7.4	2.50
Fr 7.5	6.10
Fr 7.6	12.70
Fr 7.7	40.00
Fr 7.8	10.20

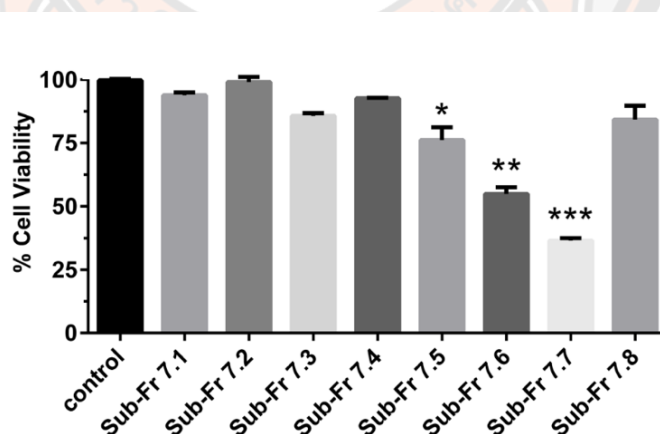


**Figure 39** Cell viability of MDA-MB-231 cells after treatment with sub-fractions no.7.1-7.8.

The cells were incubated with sub-fractions (75 µg/ml) for 24 hr. Data represent mean ± SEM of three independent experiments. (\* $p < 0.05$ , \*\* $p < 0.01$ , \*\*\* $p < 0.001$ ). Fr, fraction

Table 13: Tentative identification of bioactive compounds identified in sub-fraction 7.7 of MOL extract by LC-ESI-QTOF-MS.

No.	RT (min)	m/z [M+H] <sup>+</sup>	MS/MS	Tentative identification	Formula	Error (ppm)
C1	10.414	197.1166	179.1015,161.091 1,135.1127,107.08 22	2 -(benzyloxy) butane- 1,4-diol	C <sub>11</sub> H <sub>16</sub> O <sub>3</sub>	3.15
C2	12.286	143.1057	128.0550,101.091 2,83.0814,62.9783, 59.0458,55.0513	7-octenoic acid	C <sub>8</sub> H <sub>14</sub> O <sub>2</sub>	6.68
C3	17.586	165.1272	147.1157,95.0482	1-Phenyl-2-pentanol	C <sub>11</sub> H <sub>16</sub> O	1.16
C4	20.198	291.1955	273.1828	8-oxo-9,11- octadecadiynoic acid	C <sub>18</sub> H <sub>26</sub> O <sub>3</sub>	-0.79
C5	21.015	291.1958	273.1806,171.101 9	4-oxo-octadeca- 9Z,11E,13E,15Z-tetraenoic acid, Chrysobalanic acid	C <sub>18</sub> H <sub>26</sub> O <sub>3</sub>	-1.13
C6	22.476	325.2013	291.1925,233.151 8,137.0949	12-oxo-14,18-dihydroxy- 9Z,13E,15Z- octadecatrienoic acid	C <sub>18</sub> H <sub>28</sub> O <sub>5</sub>	-1.08
C7	26.473	277.2148	135.1125,93.0669, 79.0517	3E,9Z,12Z,15Z- Octadecatetraenoic acid	C <sub>18</sub> H <sub>28</sub> O <sub>2</sub>	5.09
C8	30.557	372.3457	354.3303,337.305 2,319.2933,97.099 3,83.0840	13,14- dihydroxydocosanamide	C <sub>22</sub> H <sub>45</sub> NO <sub>3</sub>	2.75
C9	32.057	354.3379	337.3075,319.296 5,301.2865	N-(11Z-eicosaenoyl)- ethanolamine	C <sub>22</sub> H <sub>43</sub> NO <sub>2</sub>	-3.51
C10	32.606	282.2784	*	9Z-octadecenamide	C <sub>18</sub> H <sub>35</sub> NO	2.63

\*Data not determined

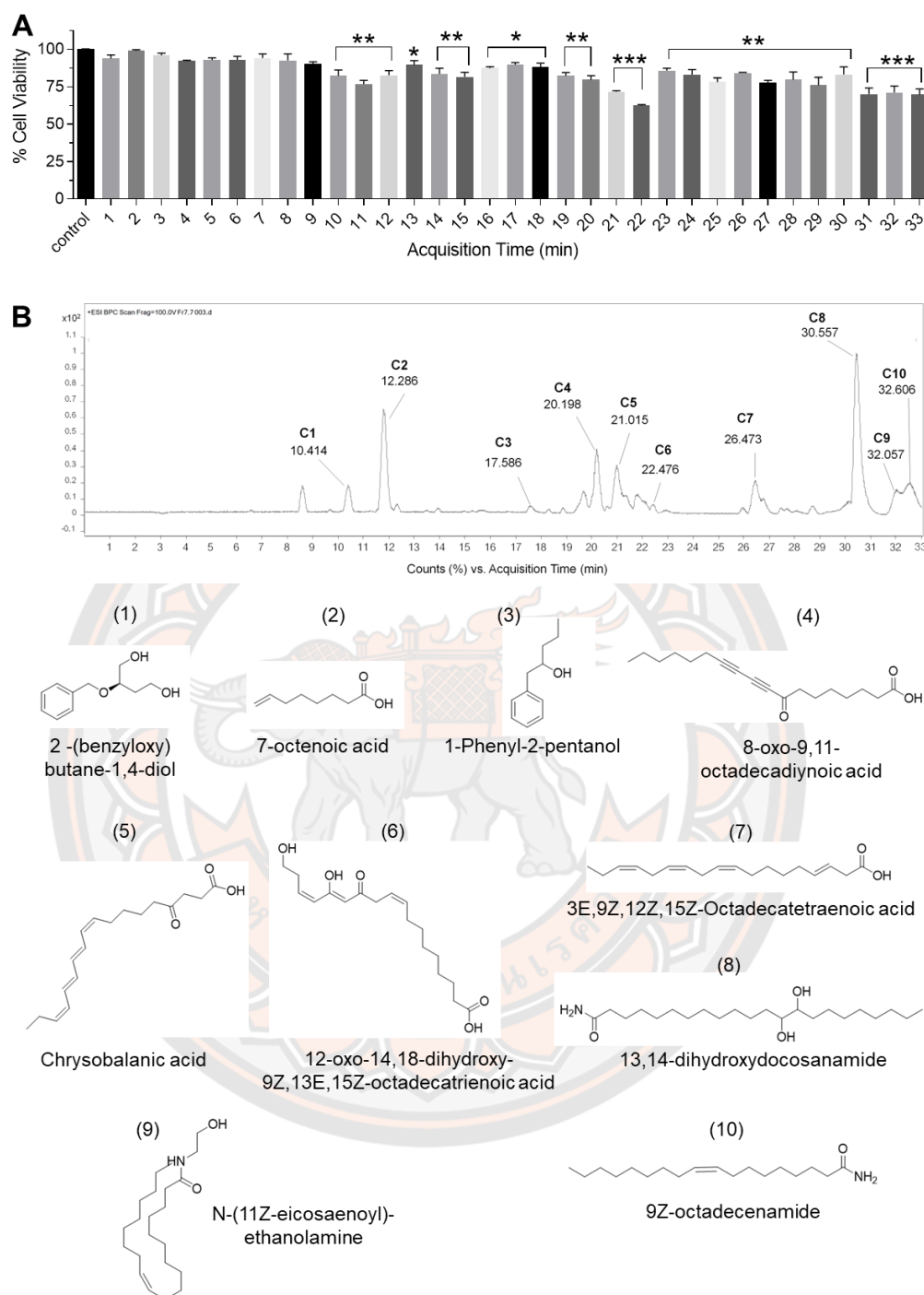


**Figure 40** Cytotoxic effect and LC-ESI-QTOF-MS/MS analysis of eluted compounds from sub-fraction no. 7.7.

(A) Cell viability of MDA-MB-231 cells after treatment with each eluted compound for 24 hr. (B) LC-ESI-QTOF-MS/MS chromatogram and the identified compounds (C1-C10). Data represent the mean  $\pm$  SEM of three independent experiments. (\* $p < 0.05$ , \*\* $p < 0.01$ , \*\*\* $p < 0.001$ ).

### 1.7 The role of three-identified compounds, 7-octenoic acid, oleamide, and 1-Phenyl-2-pentanol on MDA-MB-231 cells apoptosis and cell cycle progression

Based on commercially available compounds, three pure compounds were selected as candidates to verify the anti-cancer activity against MDA-MB-231 cells. Cells were incubated with serial concentrations of 7-octenoic acid (7-Oct), cis-9-octadeceneamide, or oleamide (OLA), and 1-phenyl-2-pentanol (1-Phe) for 24 hr. The result of the cytotoxicity assay showed that oleamide exhibits the strongest cytotoxicity with lowest  $IC_{50}$  (61.81  $\mu\text{g/ml}$ ) followed by 1-phenyl-2-pentanol ( $IC_{50}$  = 536.4  $\mu\text{g/ml}$ ), and 7-octenoic acid ( $IC_{50}$  = 2,250  $\mu\text{g/ml}$ ) (Figure 41).

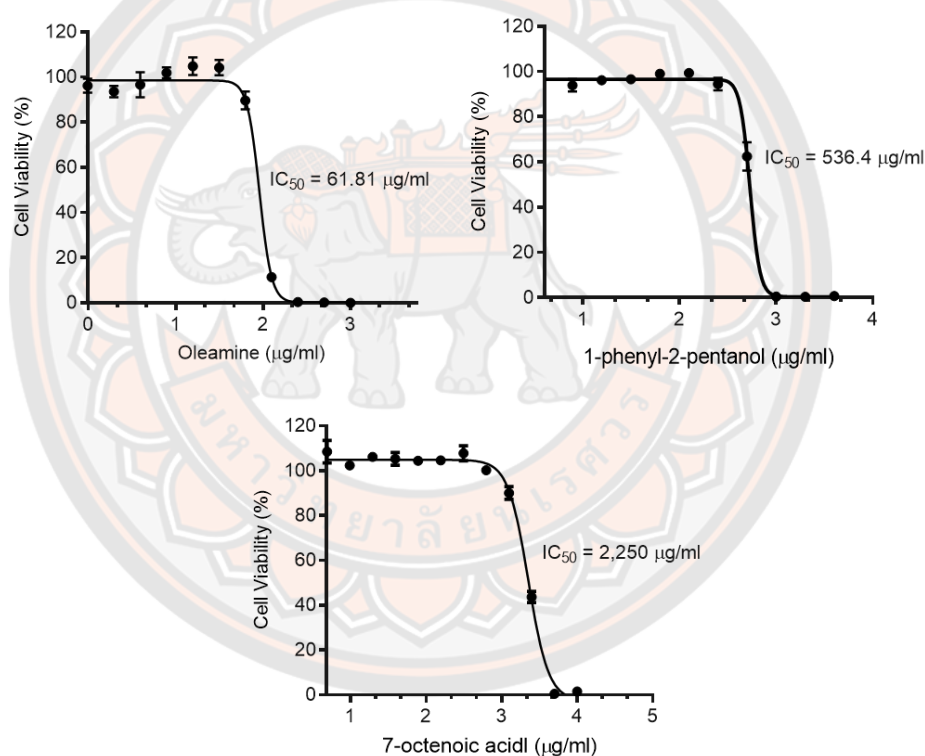


**Figure 41** Cytotoxicity of oleamide, 1-phenyl-2-pentanol, and 7-octenoic acid on MDA-MB-231 cells.

Cells were plated into 96-well plates and incubated with increasing concentrations of compounds for 24 hr. The viability was measured by using an MTT assay. Each bar graph represents mean + SEM. Data represent the mean  $\pm$  SEM of three independent experiments. (\* $p < 0.05$ , \*\* $p < 0.01$ , \*\*\* $p < 0.001$ ).

To confirm the anti-cancer activity, the effect of these compounds on MDA-MB-231 cells apoptosis was tested. An apoptotic morphology was observed after treatments with oleamide, 1-phenyl-2-pentanol, and 7-octenoic acid for 24 hr, whereas the control cells were round and homogeneously stained (**Figure 42A**). The proportion of apoptotic cells was assessed by AnnexinV/7-AAD staining with a Muse cell analyzer. Treatment with oleamide and 1-phenyl-2-pentanol significantly increased the proportion of both early and late apoptotic cells, while 7-octenoic acid significantly increased the proportion of late apoptotic cells (**Figure 42B-C**). Moreover, the expression of apoptotic-associated proteins; Bcl-2, Bax, pro-caspase 3, and cleaved caspase-3 were determined by Western blot. The increase of cleaved caspase-3 with the decrease of Bcl-2 was observed in MDA-MB-231 cells after treatment with each compound (**Figure 42D**). Additionally, the Muse cell analyzer indicated cell cycle arrest (**Figure 43**). The accumulation of cells in the G<sub>0</sub>/G<sub>1</sub> phase was significantly increased in oleamide-treated cells, while 7-octenoic acid and 1-phenyl-2-pentanol resulted in the accumulation of cells at the G<sub>2</sub>/M phase. Taken together, these suggested that a low concentration of oleamide was potent to induce apoptosis and cell cycle arrest of MDA-MB-231 cells, whereas other compounds required a high concentration. Therefore, oleamide represented more potential as an anti-cancer agent.

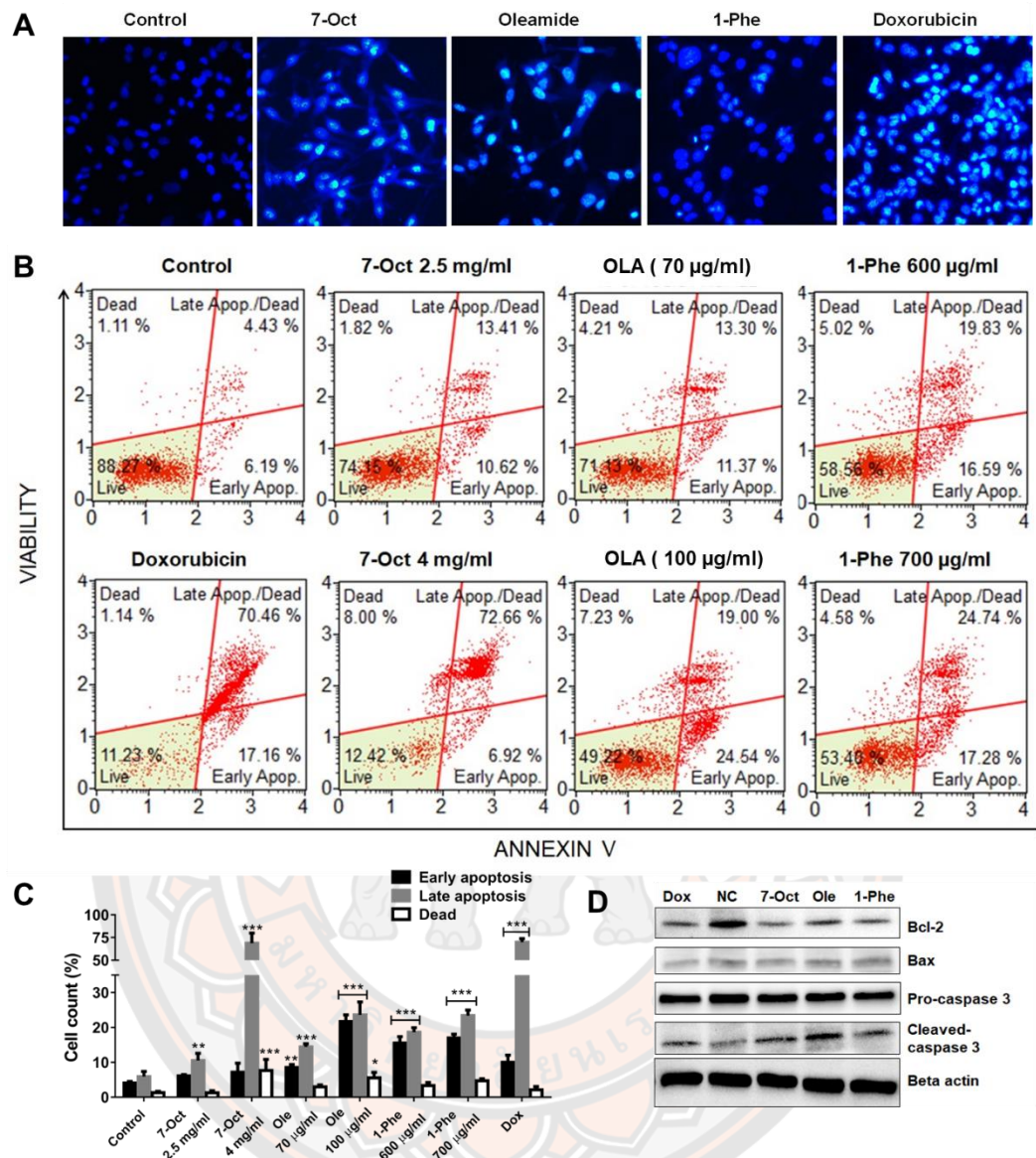


Figure 42 Effect of oleamide, 1-phenyl-2-pentanol, and 7-octenoic acid on MDA-MB-231 cells apoptosis.

(A) Hoechst 33258 staining. (B-C) Apoptosis analysis using AnnexinV/7-AAD staining. (D) Western blot analysis. Cells were incubated with 7-octenoic acid (2.5 mg/ml), oleamide (70 µg/ml), 1-phenyl-2-pentanol (600 µg/ml), or doxorubicin (Dox; 1.5 µM) for 24 hr in all experiments. Data represent the mean ± SEM of three independent experiments. (\* $p < 0.05$ , \*\* $p < 0.01$ , \*\*\* $p < 0.001$ ). 7-Oct, 7-octenoic acid; 1-Phe, 1-Phenyl-2-pentanol; OLA, oleamide; dox, doxorubicin; NC, negative control.

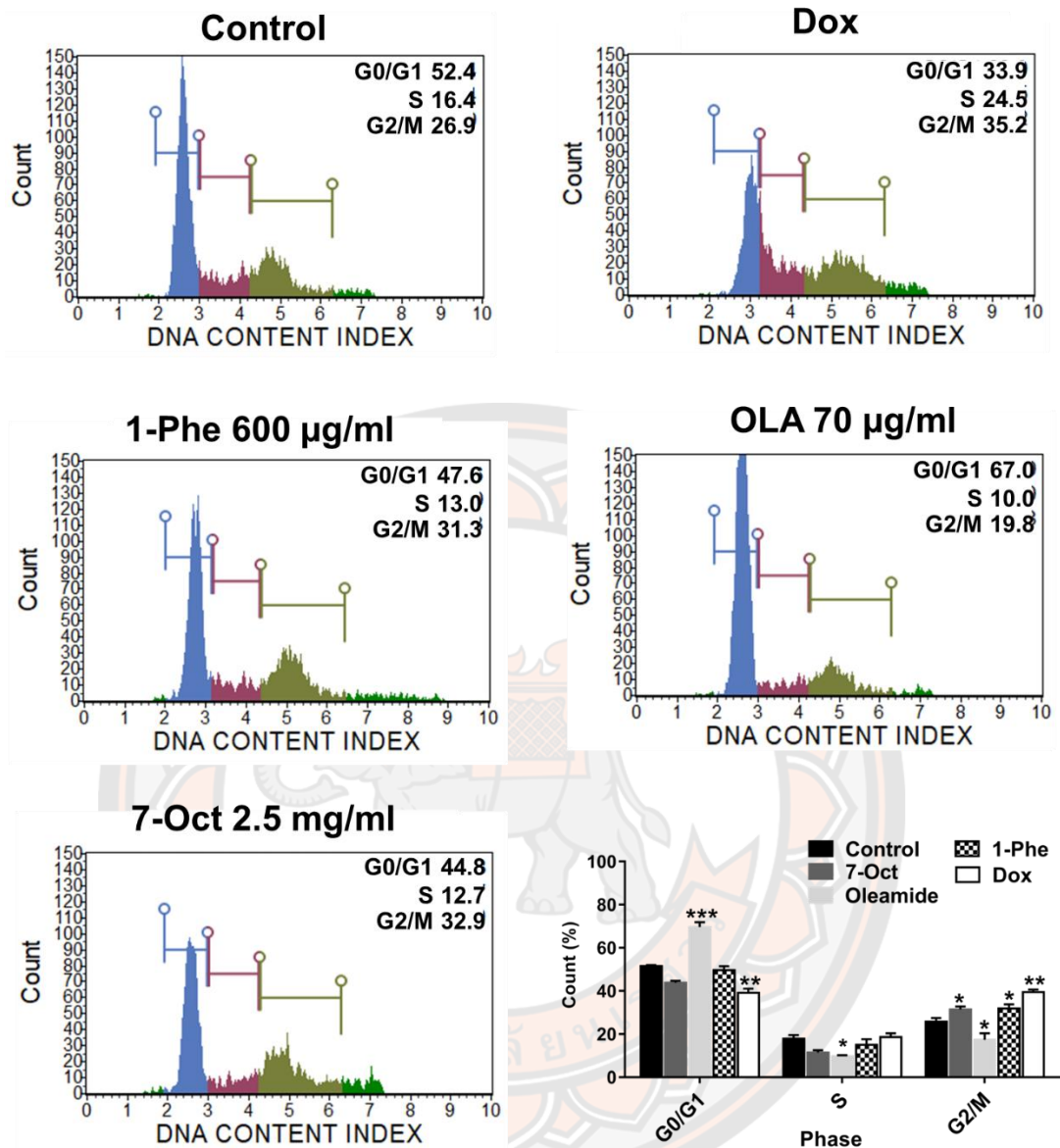


Figure 43 Effect of oleamide, 1-phenyl-2-pentanol, and 7-octenoic acid on cell cycle progression of MDA-MB-231 cells.

Cells were incubated with 7-octenoic acid (2.5 mg/ml), oleamide (70 µg/ml), 1-phenyl-2-pentanol (600 µg/ml), or doxorubicin (Dox; 1.5 µM) for 24 hr in all experiments. Data represent the mean ± SEM of three independent experiments. (\*p < 0.05, \*\*p < 0.01, \*\*\*p < 0.001). 7-Oct, 7-octenoic acid; 1-Phe, 1-Phenyl-2-pentanol; OLA, oleamide; dox, doxorubicin; NC, negative control.

### 1.8 Bioactive compounds suppressed MDA-MB-231 cell migration and induced apoptosis in different cancer cell lines

As the MDA-MB-231 cell line is an aggressive and invasive breast cancer cell line, the effects of the compounds on MDA-MB-231 cell migration were determined using the *in vitro* scratch assay (**Figure 44A**). The number of migratory cells across the wound regions was significantly decreased after treatment with 7-octenoic acid, oleamide, and 1-phenyl-2-pentanol. This result indicated that 7-octenoic acid, oleamide, and 1-Phenyl-2-pentanol may have the ability to inhibit MDA-MB-231 cell migration.

As oleamide exhibited notable anti-cancer effects against MDA-MB-231, further investigation with different types of cancer cell lines, including K562 (human myelogenous leukemia cell) and SCC-15 (human squamous cell carcinoma lines) was performed. Results revealed that treatment with 70 and 100  $\mu\text{g/ml}$  of oleamide increased late apoptosis in both K562 (13.76% and 87.11%) and SCC-15 (11.37% and 24.47%) when compared to the control (**Figure 45A**). Besides, cell cycle analysis indicated that oleamide induced cell cycle arrest at G<sub>0</sub>/G<sub>1</sub> phase in both K562 (36.8% to 54.7%) and SCC-15 (47.9% to 51.5%) when compared to the control (**Figure 45B**). The results suggested that oleamide has potential as an anticancer treatment for MDA-MB-231 TNBC and other cell lines.

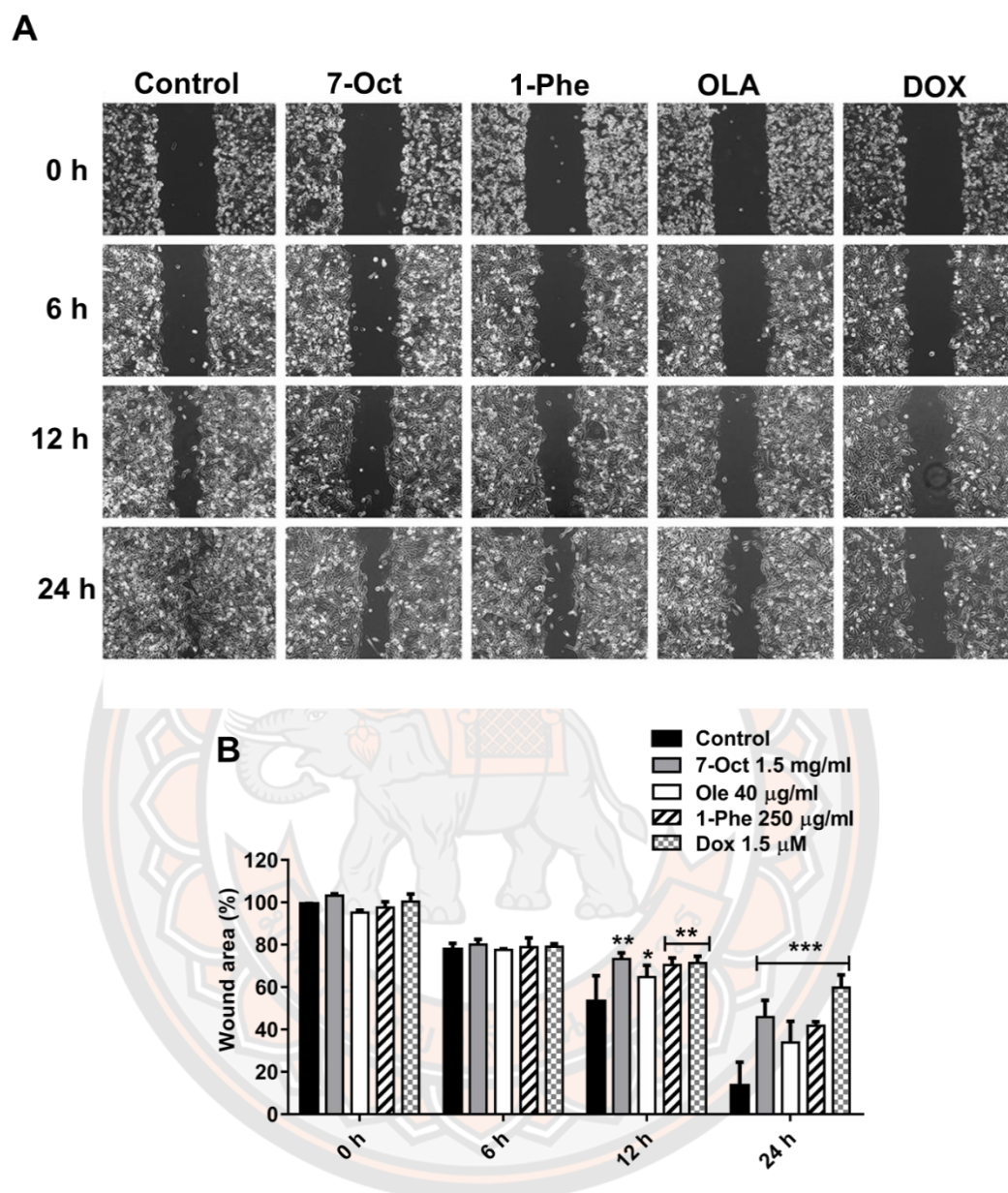


Figure 44 Effect of 7-octenoic acid, oleamide, and 1-phenyl-2-pentanol on the migration of MDA-MB-231 cells.

(A) *in vitro* scratch assay. (B) Wound area (%) summarized from triplicate data. Cells were scratched and incubated with compounds, doxorubicin, or complete medium (control). The wound areas were imaged at 0 hr, 6 hr, 12 hr, and 24 hr post-scratching. Data represent the mean  $\pm$  SEM of three independent experiments. (\* $p < 0.05$ , \*\* $p < 0.01$ , \*\*\* $p < 0.001$ ). 7-Oct, 7-octenoic acid; 1-Phe, 1-Phenyl-2-pentanol; OLA, oleamide; dox, doxorubicin.

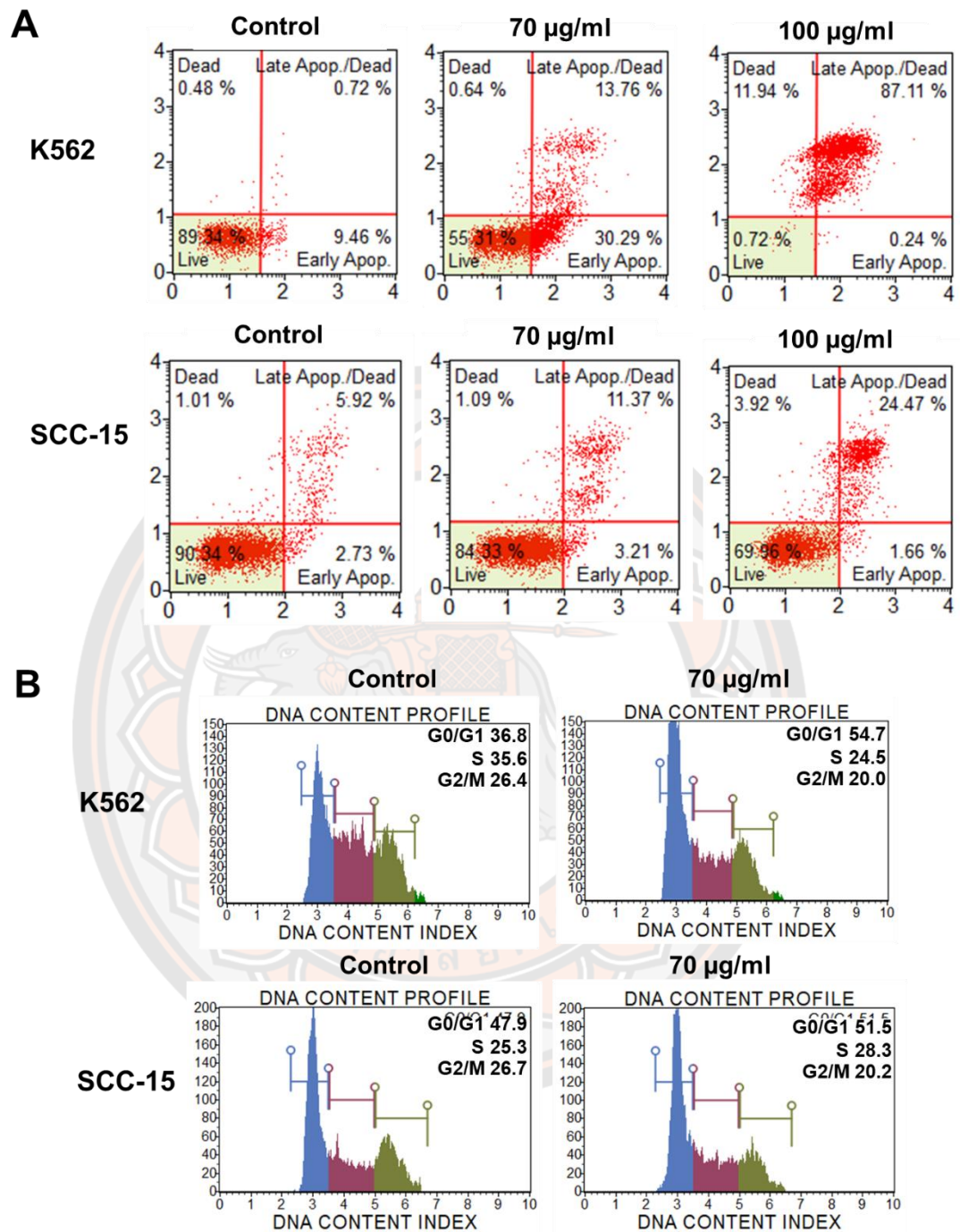


Figure 45 Effect of oleamide on the apoptosis and cell cycle regulation of other cancer cell lines.

(A) Apoptosis analysis. (B) Cell cycle analysis. K562 and SCC-15 cell lines were incubated with oleamide for 24 hr. Cell apoptosis and cell cycle were analyzed by a Muse cell analyzer.

## Part 2: The regulatory effect of oleamide on the polarization of primary human MDMs.

### 2.1 Culture, purity, and differentiation of primary human MDMs at days 0-6.

The human monocytes were isolated from the blood buffy coat of healthy donors using the density gradient centrifugation technique. Monocytes and macrophages are typical high CD14 expression on cells surface, thus CD14<sup>+</sup> was used to monitor cell purity. The purity of human MDAMs was 80.16% (day 0), 98.68% (day 3), and up 98.71% (day 6) (**Figure 46**). This demonstrated the success of the isolation technique and represented that cell purity was improved during the *in vitro* culture. The differentiation of monocyte into macrophages was monitored on days 0-6 of cell culture by flow cytometry analysis based on CD14 and CD16 surface expression (**Figure 47**). The classical monocyte CD14<sup>+</sup> CD16<sup>+</sup> was found at about 80.51% on day 0. The increase of CD14<sup>+</sup> CD16<sup>+</sup> was observed during days 3 and 6 of culture, which indicated the differentiation of monocytes into macrophages.

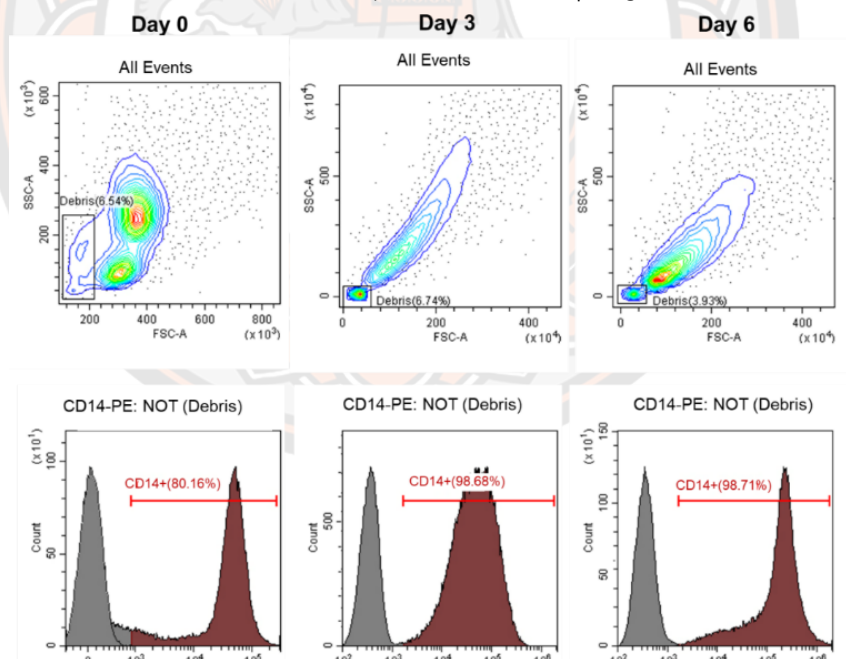


**Figure 46** Purity of human MDMs at days 0, 3, and 6 by flow cytometry.

Human monocytes were cultured and differentiated in a complete medium only for 6 days. The cell culture medium was replaced every 3 days. Percentage of CD14<sup>+</sup> cells were analyzed on days 0, 3, and 6 as shown in the right diagram, which is the result of cell grading from all events except debris cells.

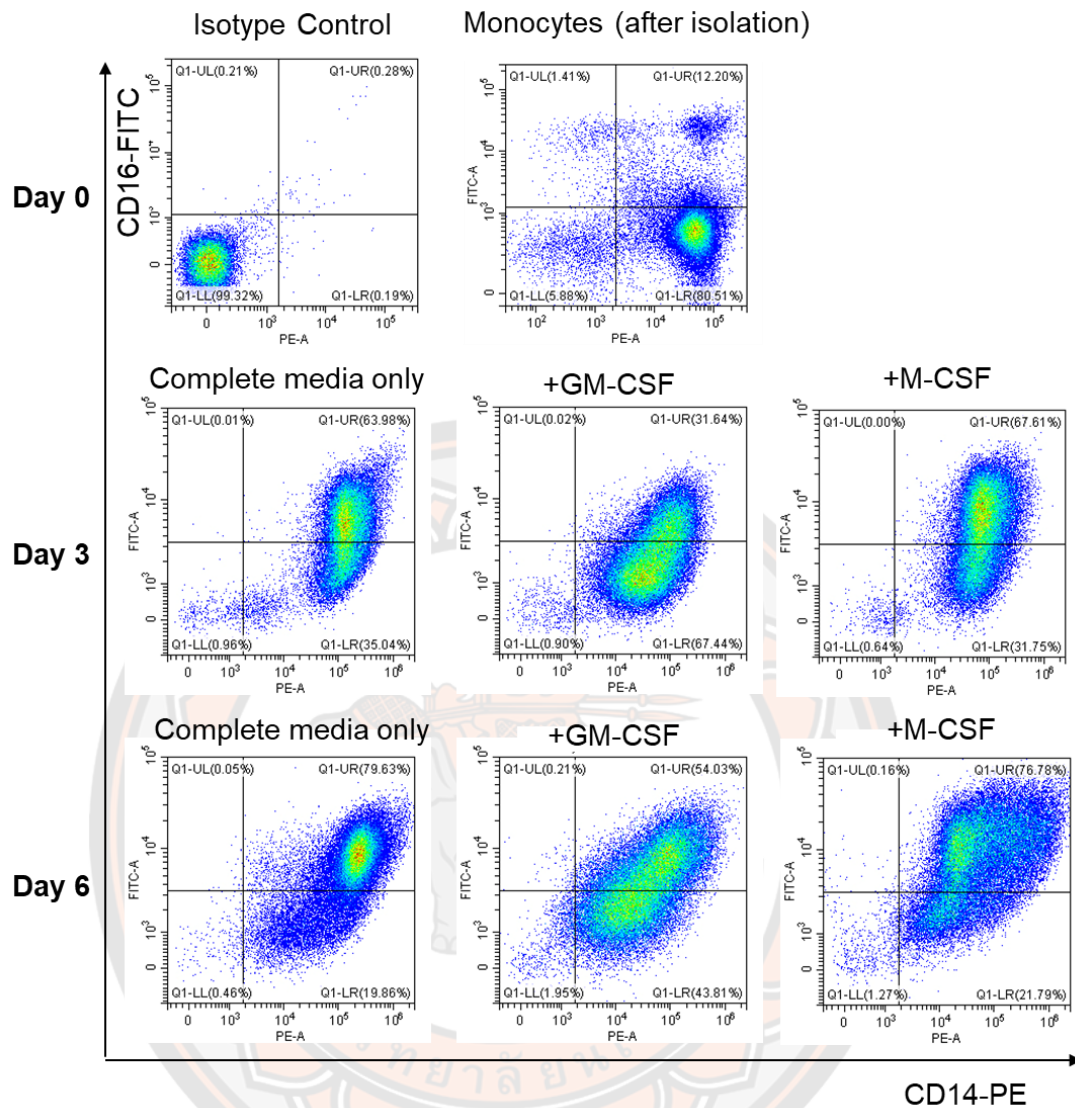


**Figure 47** Flow cytometry analysis of CD14 and CD16 expression on human MDMs. Flow cytometry dot plot showing the gating of the CD14-PE and CD-16-FITC of MDMs at days 0, 3, and 6. M0 cells were cultured in a complete medium only. M1-like cells were cultured in 50  $\mu\text{g}/\text{ml}$  of GM-CSF. M2-like cells were cultured in 50  $\mu\text{g}/\text{ml}$  of M-CSF. Cell culture mediums were replaced every 3 days.

## 2.2 Generation of *in vitro* culture and polarization of MDMs

To imitate naturally occurring macrophages, monocytes were freshly isolated from the blood buffy coat of healthy donors. MDMs were cultured in a complete medium containing human serum alone (M0 cells), or a complete medium containing GM-CSF (M1-like cells) or M-CSF (M2-like cells) for 6 days. MDMs were further cultivated for 24 hr in the same medium (M0 macrophage) or in the presence of LPS plus IFN- $\gamma$  (M1 macrophage) or IL-4 (M2 macrophage). The presence of GM-CSF led to a majority of round adhered with short-elongated shapes, whereas the presence of M-CSF enhanced elongation. MDMs cultured in a complete medium containing human serum alone exhibited dual morphology (round adherend and elongated shape), indicating the mixed phenotypes in the M0 macrophages (**Figure 48A**). Differentiation of MDMs on days 0-6 was analyzed by flow cytometry using CD80 as a marker of M1 macrophage, and CD163 as a marker of M2 macrophage (**Figure 48B**). Results revealed that M1-like cells or the presence of GM-CSF upregulated CD80 expression, correlating with downregulation of CD163 at days 0-6. By contrast, M2-like cells displayed upregulation of CD163 expression with downregulation of CD80. MDMs cultured in a medium containing human serum alone displayed increased expression of CD163 rather than CD80 on the cell surface.

For fully polarized macrophages, LPS plus IFN- $\gamma$  treated cells displayed strong induction of CD80 and downregulation of CD163 compared to unpolarized M0 cells. Conversely, IL-4-treated cells displayed high expression of CD163 and low levels of CD80 expression (**Figure 49**). Collectively, these data confirmed the M1 and M2 polarization state of LPS plus IFN- $\gamma$  and IL-4-treated MDMs.

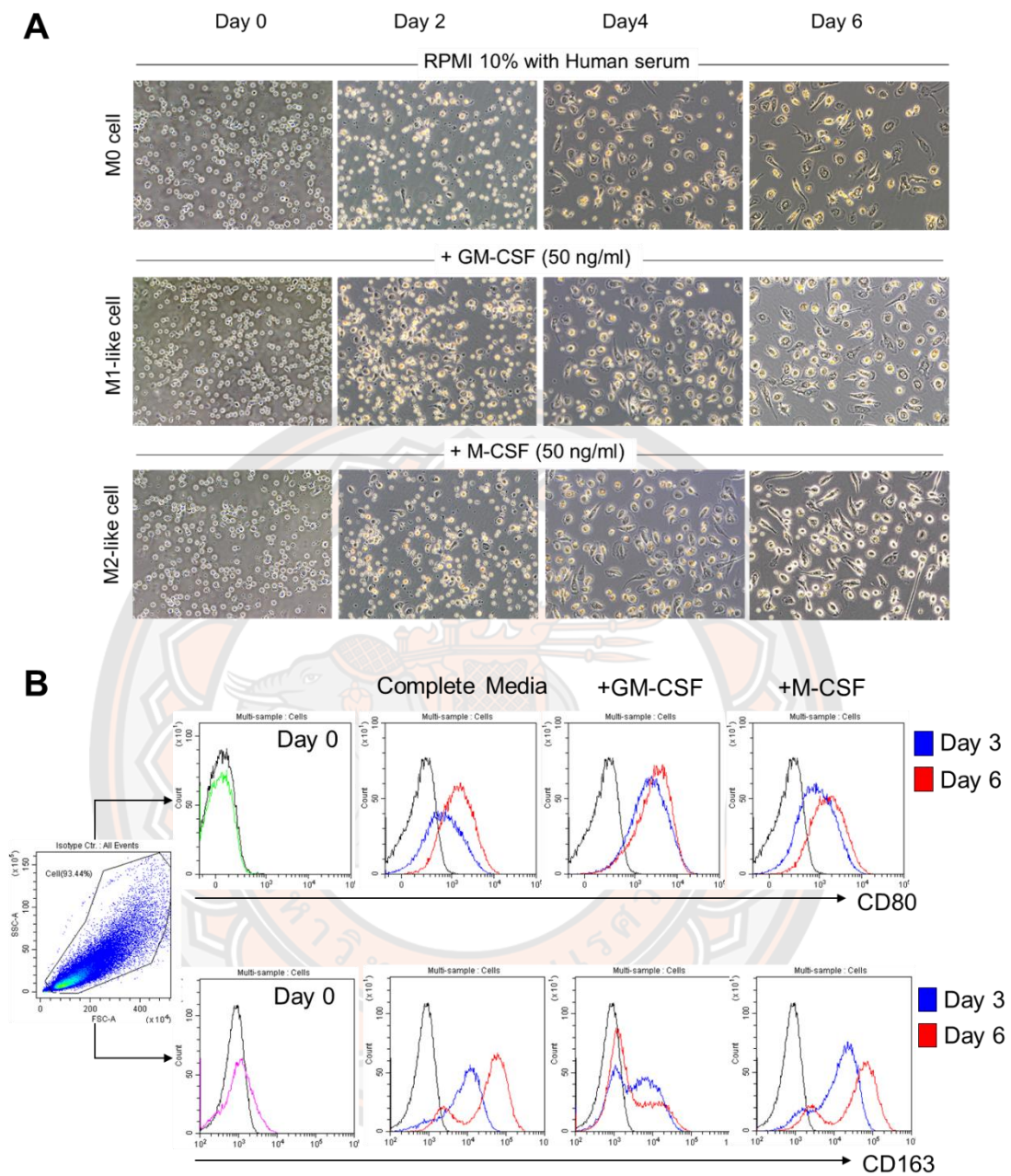


**Figure 48 Morphology and phenotypical characterization of human MDMs (Days 0-6).** (A) Morphological changes by bright-field microscopy (Magnification = 10X). (B) Flow cytometry analysis of CD80 and CD163 expression. M0 cells were cultured in a complete medium only. M1-like cells were cultured in the presence of 50  $\mu\text{g/ml}$  of GM-CSF. M2-like cells were cultured in the presence of 50 ng/ml of M-CSF.

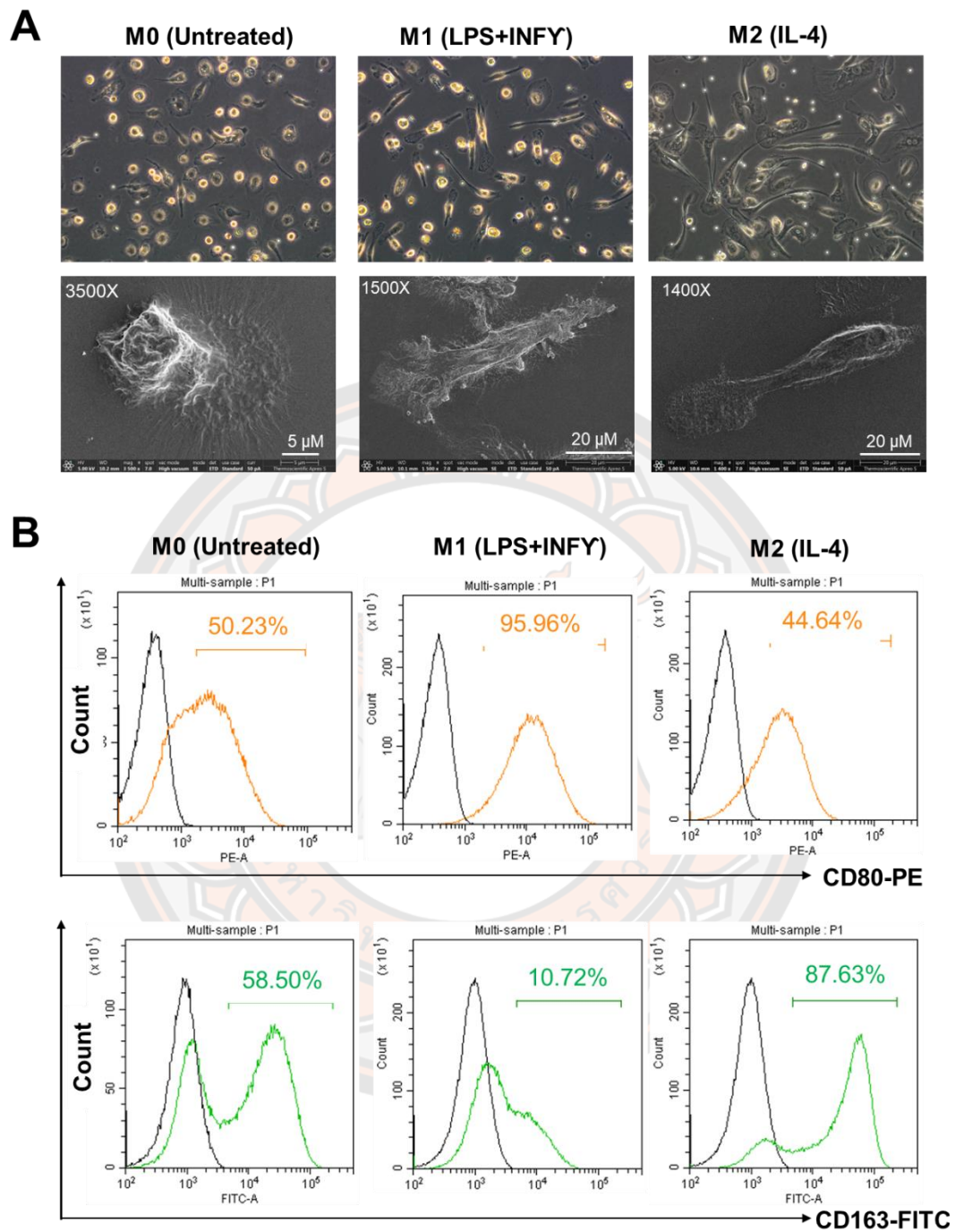


**Figure 49 Morphology and phenotypical analysis of macrophage polarization.**

(A) Morphological changes observed by bright-field microscope and SEM. (B) Flow cytometry analysis of CD80 and CD163 expression. Human MDMs (day 6) were polarized in desired conditions: M1 (LPS plus IFN- $\gamma$ ), M2 (IL-4), and M0 (complete medium only) for 24 hr.

### 2.3 Oleamide mediated M1 macrophage polarization and IL-1 $\beta$ production.

To investigate the effect of oleamide on macrophage polarization, MDMs were cultured in conditioned media for M1 (LPS + IFN- $\gamma$ ), M2 (IL-4), and M0 (untreated) in the presence or absence of oleamide. These cells were characterized in different techniques based on surface markers, gene expression, and cytokine production. The presence of oleamide enhanced elongation as spindle-like shapes of the M0 and M1 macrophages (**Figure 50**).

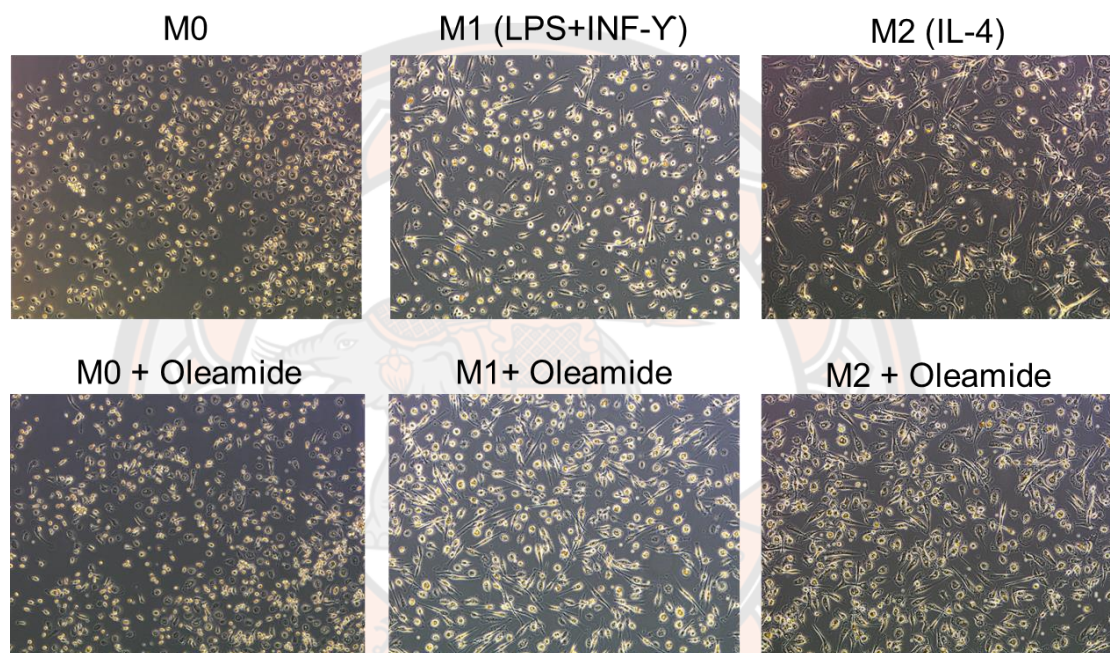


**Figure 50** Morphology of polarized M0, M1, and M2 macrophages plus oleamide.

On day 6, MDMs were cultured in complete medium only (M0), LPS + IFN- $\gamma$  (M1), or IL-4 (M2) in the presence or absence of oleamide (15  $\mu\text{g/ml}$ ) for 24h. (Magnification = 10X).

Surface expressions were analyzed by flow cytometry using polarization markers including CD80 for the M1 phenotype and CD163 and CD206 for the M2 phenotype. Flow cytometry assay revealed that CD80 expression was upregulated in M0 phenotypes treated with oleamide (from 53.09% to 62.17%), whereas CD163 and CD206 were downregulated in M0 phenotypes treated with oleamide compared to the untreated control (from 58.50% to 42.10% and 63.85% to 56.24%, respectively).

For the M1 phenotype, CD163 and CD206 expression levels were downregulated (from 10.72% to 5.36% and 74.14% to 54.20%, respectively), whereas CD80 was not differenced in M1 treated with oleamide compared to M1 untreated control. For the M2 phenotype, CD163 and CD206 expression levels were downregulated (from 85.32% to 59.67% and 86.04% to 71.03%, respectively), whereas CD80 was upregulated in M2 treated with oleamide compared to the control (58.21% to 64.60%) (Figure 51).

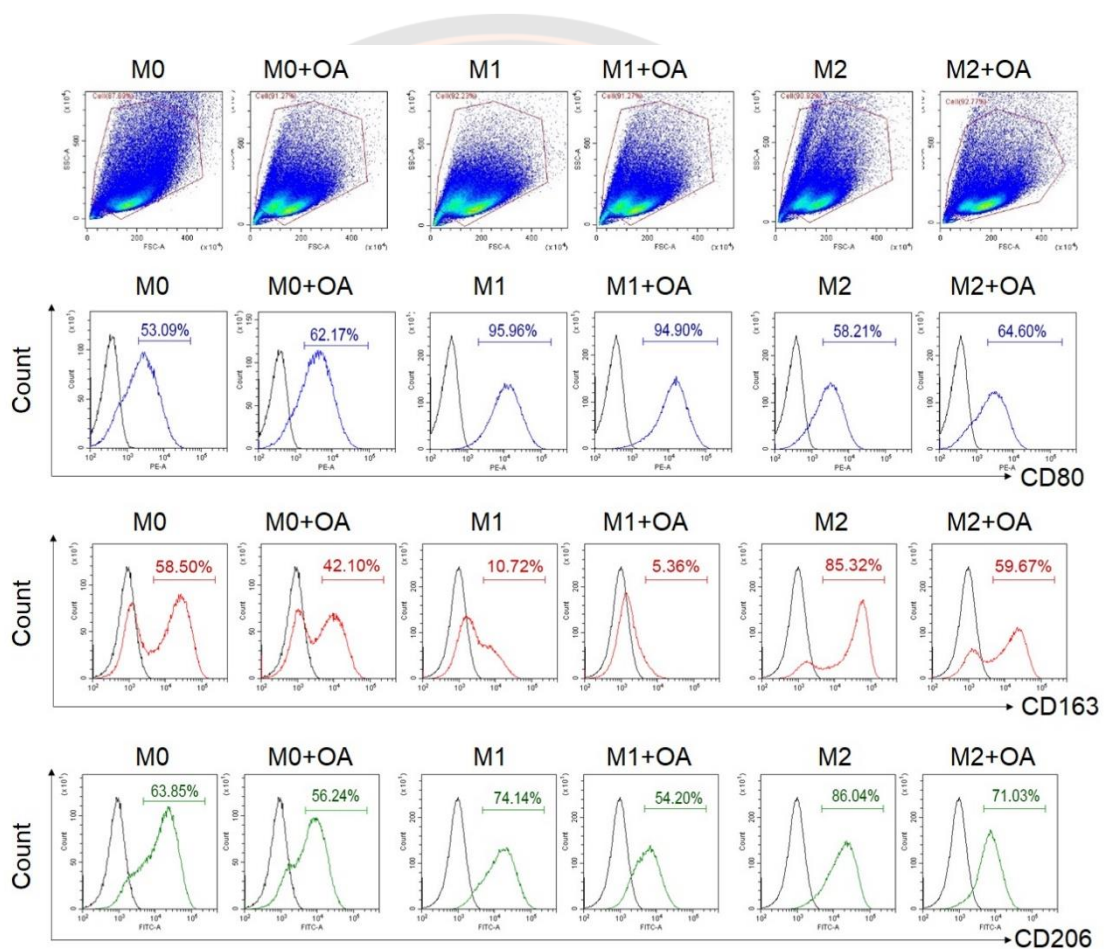


**Figure 51** Flow cytometry analysis of surface expressions.

MDMs on day 6 were cultured in complete medium only (M0), LPS +  $\text{INF-}\gamma$  (M1), or IL-4 (M2) in the presence or absence of oleamide (15  $\mu\text{g/ml}$ ) for 24h. LPS, lipopolysaccharides; OA, oleamide.

M1/M2 phenotypes were further confirmed by studying the expression of M1-associated genes (TNF- $\alpha$ , IL-1 $\beta$ , IL-6, iNOS, CXCL10), along with the expression of M2-associated genes (*Arg-1*, *CD206*, and *CCL22*) using RT-qPCR. Results showed that M0 macrophages treated with oleamide displayed increased expression of TNF- $\alpha$ , IL-1 $\beta$ , IL-6, and iNOS genes, while M2 macrophages treated with oleamide displayed defective expression of M2-associated genes (*Arg-1*, *CD206*, and *CCL22*) along with increased expression of the IL-1 $\beta$  gene. For M1 macrophages, treatment with oleamide displayed a minor change in both M1 and M2-associated genes (**Figure 52A**). To support these results, pro-inflammatory cytokines IL-1 $\beta$ , IL-6, and TNF- $\alpha$  were determined by ELISA. Interestingly, augmented releasing of IL-1 $\beta$  was observed in all macrophage phenotypes after treatment with oleamide, whereas TNF- $\alpha$  and IL-6 increased in M0 macrophages but not significantly (**Figure 52B**). To confirm these results, cytokine production was further investigated using the THP-1-derived macrophage model. Surprisingly, increasing IL-1 $\beta$  production was also observed in M0 macrophages treated with oleamide, similar to the MDM model (**Figure 52C**). Therefore, this suggested that oleamide induced IL-1 $\beta$  production in both MDMs and THP-1 cells. Taken together, these results indicated that oleamide mediated naïve macrophages (M0) toward the M1 phenotype and promoted IL-1 $\beta$  production while hindering the polarization of M2 phenotypes.

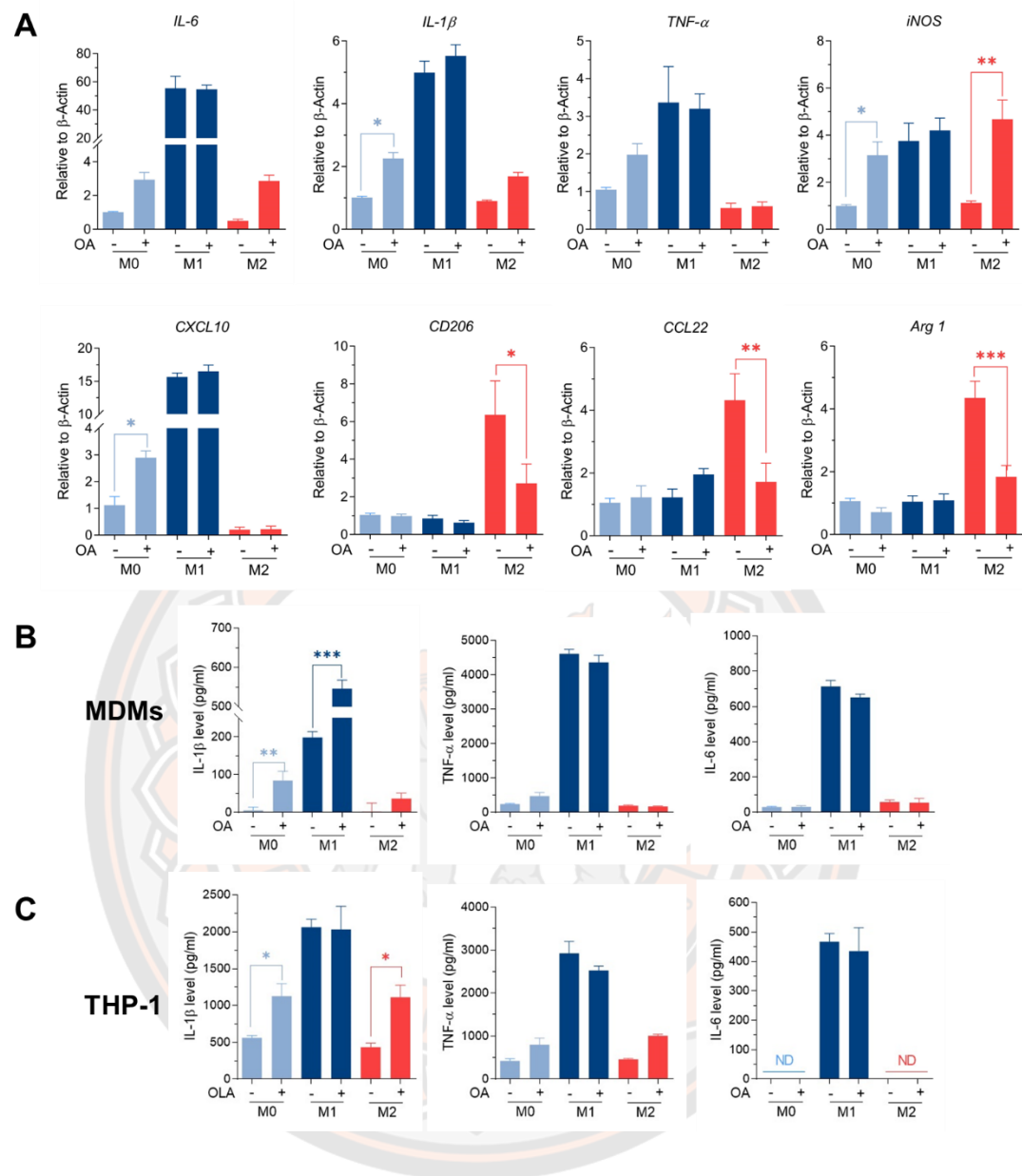


**Figure 52** Oleamide mediated M1 macrophage polarization.

(A) M1/M2 gene expression by RT-qPCR. (B, C) Cytokine levels by ELISA. MDMs (Day 6) or differentiated THP-1 were cultured in complete medium only (M0), LPS + INF-g (M1), or IL-4 (M2) in the presence or absence of oleamide (15  $\mu$ g/ml) for 24 hr in all experiments. One-way ANOVA was performed with multiple comparison corrections (Dunnett test). Data represent the mean  $\pm$  SEM of three independent experiments. (\* $p < 0.05$ , \*\* $p < 0.01$ , \*\*\* $p < 0.001$ ).

#### 2.4 Oleamide-induced IL-1 $\beta$ production in LPS-primed MDMs involves activation of the NLRP3-inflammasome pathway

An increase in IL-1 $\beta$  production was observed in both MDMs and THP-1 treated with oleamide, suggesting that oleamide functioned as a secondary signal to trigger NLRP3 inflammasome activation and leading to the production of IL-1 $\beta$ . To explore this hypothesis, naïve macrophages (M0) were primed with LPS (signal 1) followed by oleamide treatment for 1-3 hr (**Figure 53A**). Cell morphology was observed using a bright-field microscope (**Figure 53B**). Cell-free supernatant was detected for IL-1 $\beta$  and IL-18 secretion and inflammasome-related genes (*IL-1 $\beta$* , *IL-18*, *ASC*, *NLRP3*) were analyzed by RT-qPCR. As predicted, IL-1 $\beta$  and IL-18 were readily produced in LPS-primed MDMs exposed to oleamide in a dose- and time-dependent manner (**Figure 53 C-D**). Furthermore, a high concentration of oleamide (30-40  $\mu\text{g/ml}$ ) induced IL-1 $\beta$  and IL-18 production equivalent to ATP, which is known as the NLRP3 inflammasome activation molecule. Consistent with results obtained using cell-free supernatant, oleamide induced upregulation of NLRP3, IL-1 $\beta$ , and IL-18 mRNA expression compared to the control cells. Therefore, results suggested that oleamide mediated IL-1 $\beta$  and IL-18 production by triggering the NLRP3 inflammasome pathway.

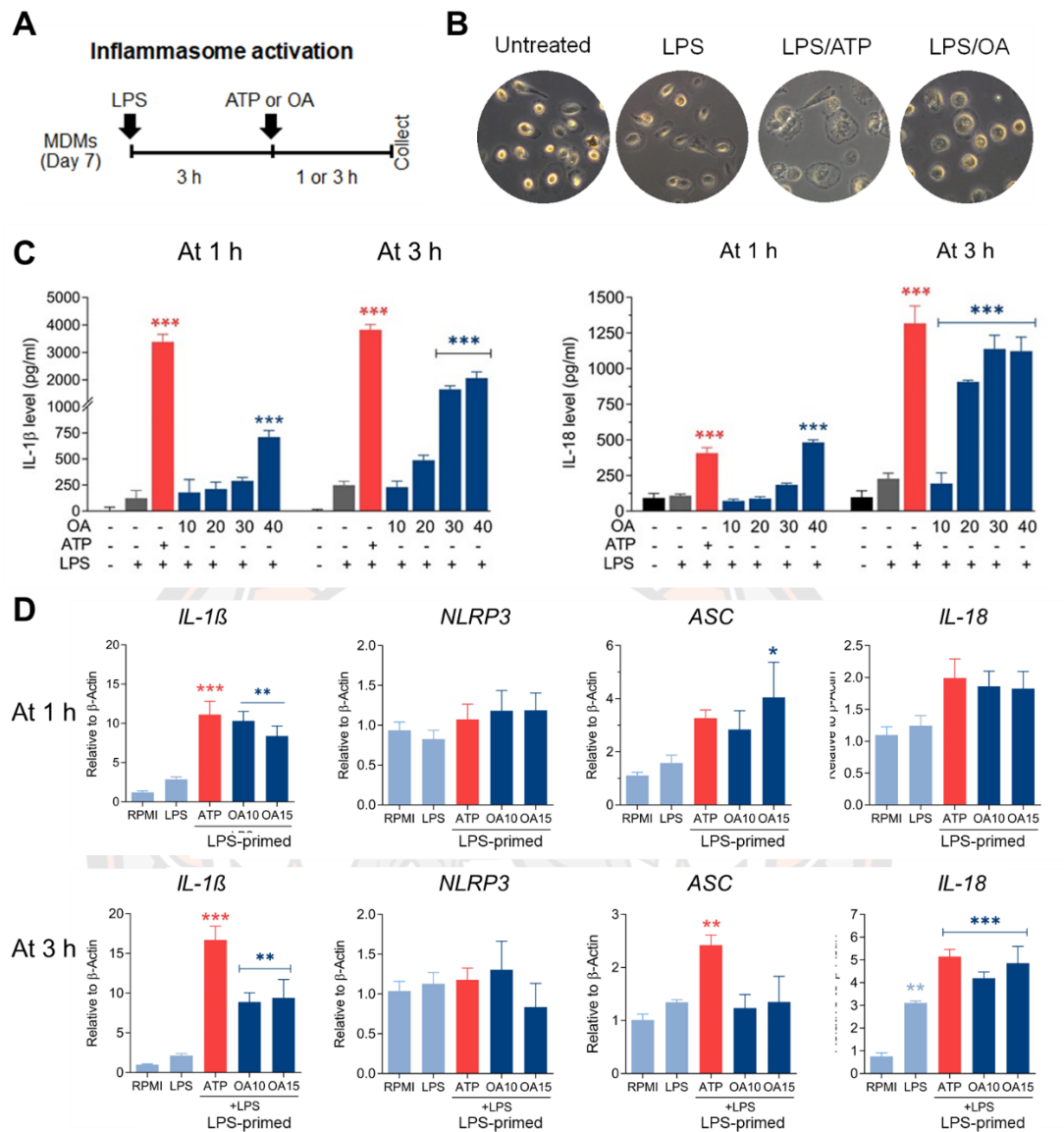


**Figure 53** Oleamide mediated inflammasome activation, and IL-1 $\beta$  and IL-18 production in LPS-primed MDMs.

(A) Scheme of inflammasome activation. (B) Cell morphology by inverted microscope. (C) IL-1 $\beta$  and IL-18 levels by ELISA. (D) mRNA expressions by RT-qPCR. MDMs were primed with LPS (100 ng/ml) for 3 hr followed by oleamide (OA) (15  $\mu$ g/ml) or ATP (30 mM) for 1-3 hr in all experiments. Data represents the mean  $\pm$  SEM of three independent experiments (\* $p$  < 0.05, \*\* $p$  < 0.01, \*\*\* $p$  < 0.001). NC, negative control; LPS, lipopolysaccharides; ATP; adenosine triphosphate, OA; oleamide, ASC; apoptosis-associated speck-like protein containing a C-terminal caspase recruitment domain; NLRP3, NOD-, LRR- and pyrin domain-containing protein 3.

#### 2.4 Oleamide mediated IL-1 $\beta$ production by regulating NLRP3-inflammasome in LPS-primed MDMs.

To further investigate how oleamide impacted NLRP3 inflammasome activation and IL-1 $\beta$  production, LPS-primed MDMs were treated with oleamide for 3 hr. The results showed that oleamide-induced activation of NLRP3 and ASC speck formation is similar to induction by ATP, which activated the NLRP3 inflammasome via the purinergic P2X7 receptor. Both IL-1 $\beta$  and IL-18 are initially produced as biologically inactive pro-forms that require cleavage into mature cytokines. Typically, this processing is mediated by caspase-1, which is activated following the formation of an inflammasome (173). Our results showed that oleamide induced upregulation of cleaved caspase 1 and cleaved IL-1 $\beta$  in the supernatant, correlating to the downregulation of these proteins in cell lysate (**Figure 54A**). The release of lactate dehydrogenase (LDH) induced by oleamide in LPS-primed MDMs significantly increased in a dose-dependent manner (**Figure 54B**), suggesting that oleamide increased caspase-1-mediated pyroptosis. Similar to LDH, an increase in cell death was observed in a dose-dependent manner (**Figure 54C**). These findings suggested that oleamide induced activation of the NLRP3 inflammasome pathway and mediated IL-1 $\beta$  production in LPS-primed MDMs.

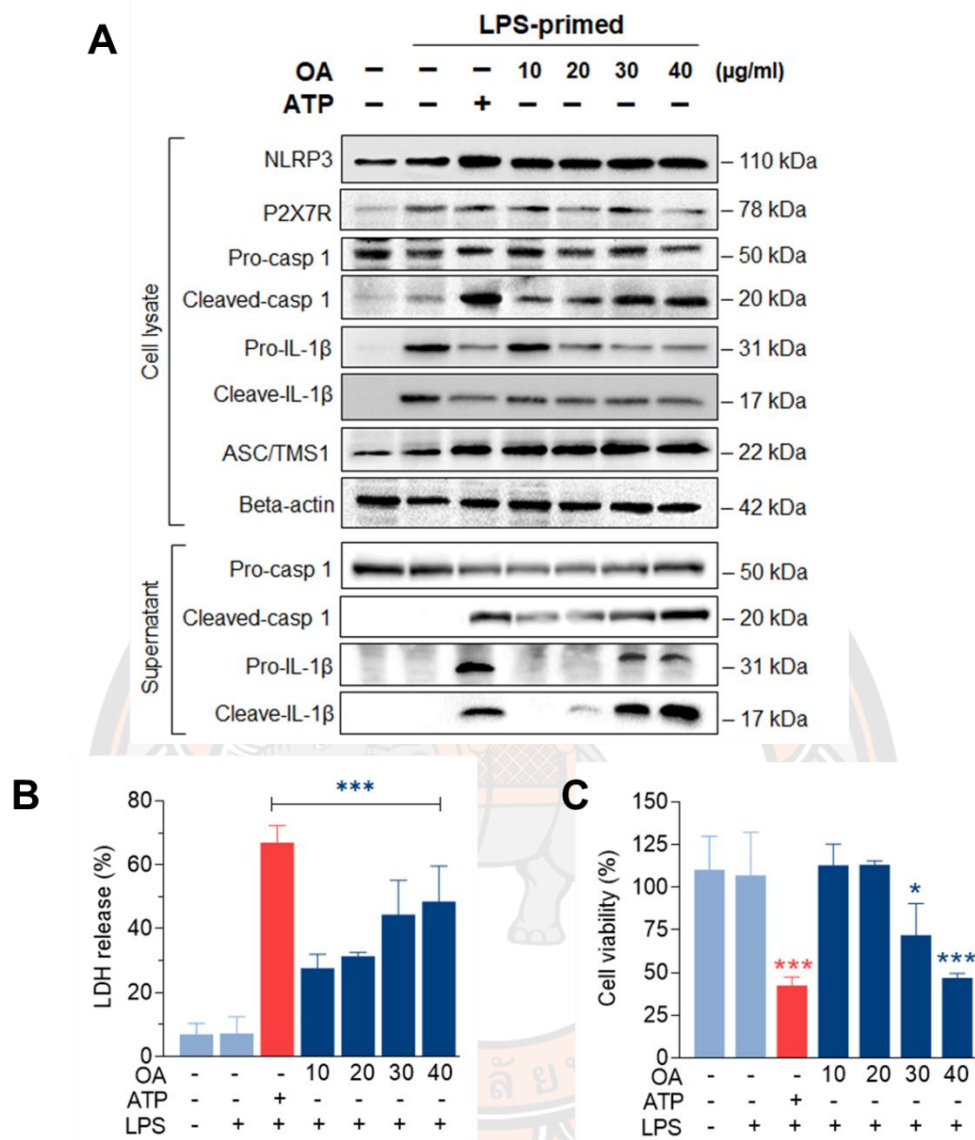


**Figure 54** Oleamide promoted NLRP3 inflammasome activation in LPS-primed MDMs. (A) Western blot of whole cell lysate and supernatant from LPS-primed MDMs treated with oleamide (OA) (10 - 40  $\mu\text{g/ml}$ ) or ATP (30 mM) for 3 hr. (B) Release of LDH and (C) Cell viability (%) in LPS-primed MDMs treated with OA (10-40  $\mu\text{g/ml}$ ) or ATP (30 mM) for 3 hr. Data represent the mean  $\pm$  SEM of three independent experiments (\* $p < 0.05$ , \*\* $p < 0.01$ , \*\*\* $p < 0.001$ ). LPS, lipopolysaccharides; ATP, adenosine triphosphate; OA, oleamide; LDH, lactate dehydrogenase; ASC, apoptosis-associated speck-like protein containing a C-terminal caspase recruitment domain; NLRP3, NOD-, LRR- and pyrin domain-containing protein 3; P2X7R, purinergic P2X7 receptor.

### Part 3: The reprogramming of TAMs with a bioactive compound (oleamide)

#### 3.1 *In vitro* generation of primary monocyte-derived TAMs by transwell co-culture model

To determine the optimal condition for the generation of TAMs, primary human monocyte-derived macrophages (MDMs) were co-cultured with human breast cancer MDA-MB-231 cells using the transwell co-culture model. MDMs were cultured in the lower chamber of the transwell plate in different conditions including complete medium only, complete medium with the addition of IL-4, IL-10, and M-CSF, or complete medium: tumor-conditioned medium (1:1 ratio) with the addition of IL-4, IL-10, and M-CSF. MDMs were co-cultured with MDA-MB-231 cells for 6 days to induce differentiation of naïve monocytes into TAMs (Figure 55).

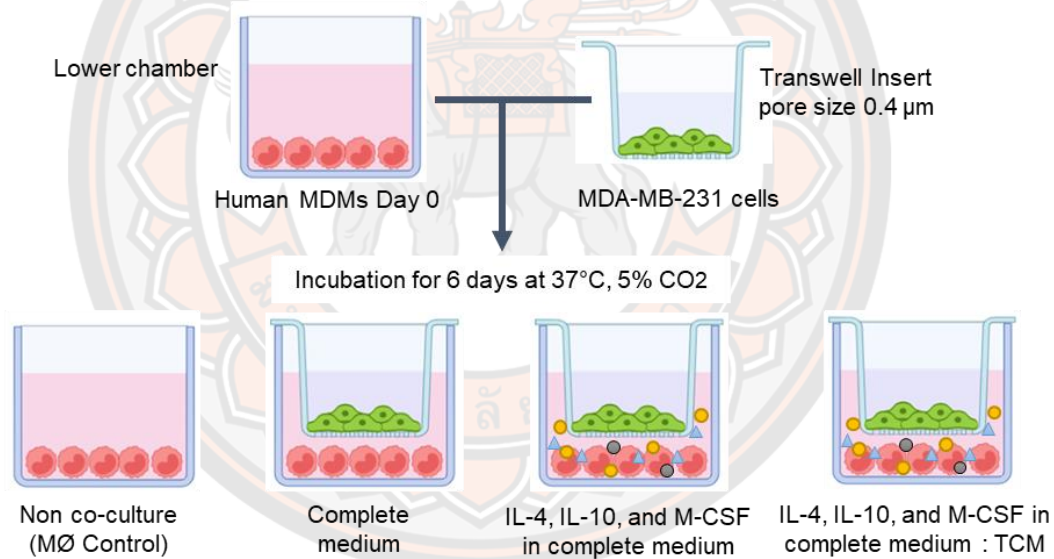


**Figure 55** Schematic diagram of *in vitro* generation of human monocyte-derived TAMs using the transwell co-culture model.

Primary human monocytes were co-cultured with MDA-MB-231 cells for 6 days under different conditions. Non-co-cultured represented as control cells. MDMs (monocyte-derived macrophages), MØ (naïve macrophages or M0 macrophages), IL-4 (interleukin-4), IL-10 (interleukin-10), M-CSF (macrophage colony-stimulating factor), TCM (tumor-conditioned medium).

The morphology of the co-cultured macrophages was observed on day 6 using bright-field microscopy (**Figure 56A**). The results showed that macrophages in each condition exhibited a similar pattern of cell alignment by aggregating and lining up across the well. Macrophages in complete medium alone were small round and elongated in shapes. However, macrophages cultured in the presence of cytokines or tumor-conditioned medium-plus cytokines exhibited greater cell elongation as spindle-like shapes. The phenotypic characteristics of TAMs were determined based on the expression of signature genes for M2-like TAM phenotypes including *c-Myc* (pro-tumor oncogene), *MMP9* (enzyme-mediated extracellular matrix degradation), *VEGFA* (angiogenesis growth factor) and *CD206* (mannose receptor) along with expression of the M1-like TAM phenotype gene *HLA-DR*, the molecules are expressed on antigen-presenting cells (APC).

Interestingly, regarding tumor-associated gene expression, the results showed that MDMs co-cultured with MDA-MB-231 cells without cytokine stimulation was sufficient to induce *VEGFA* and *MMP-9* gene expression but did not alter *c-Myc* gene expression (**Figure 56B**). However, MDMs cultured in complete medium plus the addition of cytokines or complete medium: tumor-conditioned medium-plus addition of cytokines significantly induced all TAM gene expressions. Moreover, MDMs cultured in a complete medium with the addition of cytokines exhibited greater *c-Myc* and *MMP-9* expression compared to those in the tumor-conditioned medium (**Figure 56B**). These results suggested that transwell co-culturing of macrophages and MDA-MB-231 cells with the addition of IL-4, IL-10, and M-CSF represented a more adequate model for *in vitro* generation of M2-like TAMs.

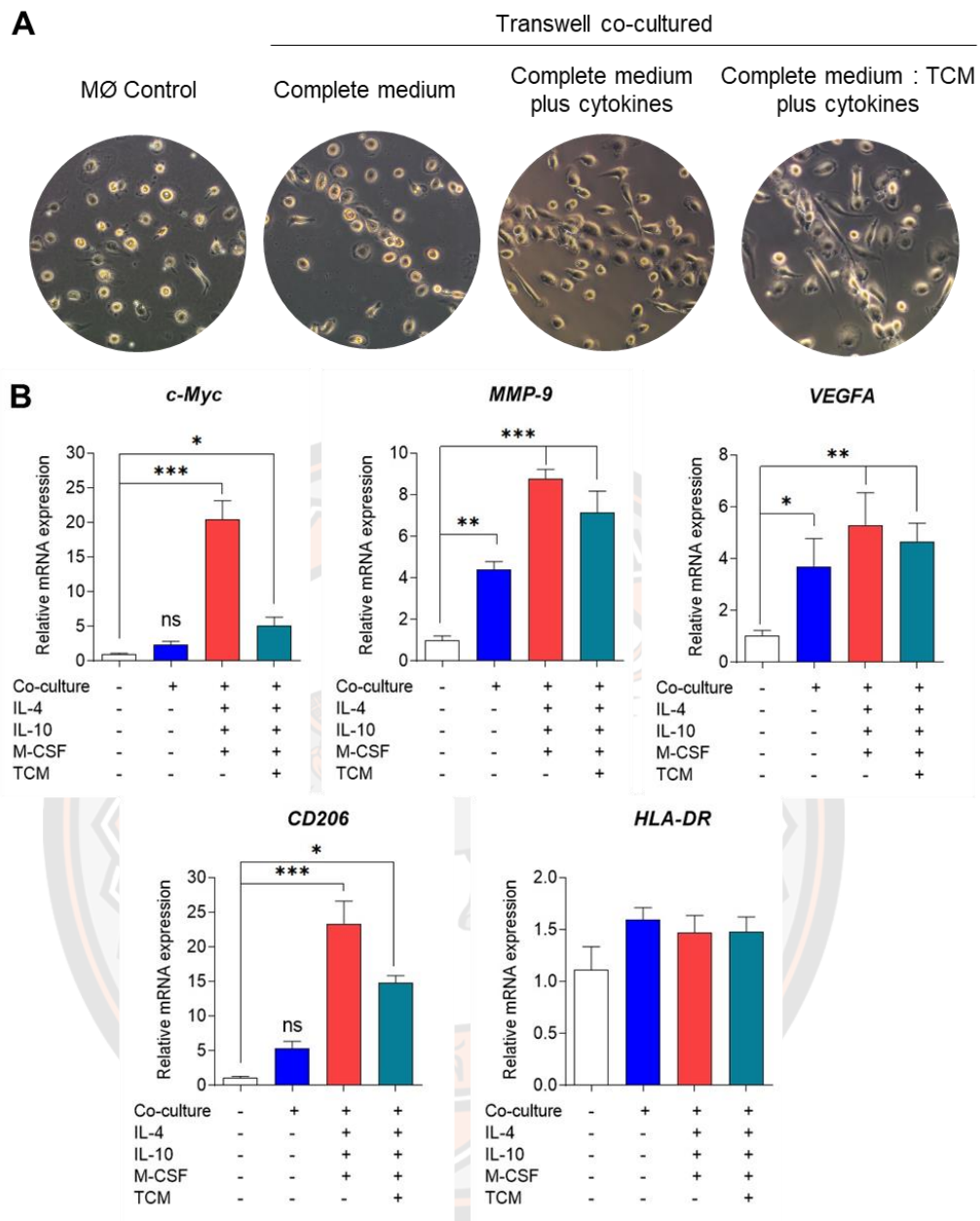


**Figure 56 Morphological and Phenotypical characterization of human monocyte-derived TAMs using transwell co-culture model.**

(A) Cell morphology (at day 6) by bright-field microscope (10X magnification). (B) Gene expression by RT-qPCR. Data represent the mean  $\pm$  SEM of three independent experiments (\* $p < 0.05$ , \*\* $p < 0.01$ , \*\*\* $p < 0.001$ ), ns (not significant), TCM (tumor-conditioned medium), c-Myc (pro-tumor oncogene), MMP9 (matrix metalloproteinase 9), VEGFA (vascular endothelial growth factor A), CD206 (mannose receptor), HLA-DR (major histocompatibility complex class II), M-CSF (macrophage colony-stimulating factor), IL (interleukin).

### 3.2 Oleamide induced reprogramming of M2-like TAMs toward M1-like TAM phenotypes.

Recently, oleamide has been reported to have an immunomodulatory effect by promoting naïve M1 macrophage polarization and inflammasome activation (174). They hypothesized that oleamide might have a similar effect on TAM polarization. To investigate this, monocyte-derived TAMs were generated using transwell co-culture as described. On day 6, TAMs were cultured in the presence or absence of oleamide (20 µg/ml) for 24 hr. The TAM phenotypes were analyzed by studying the expression of TAM-associated genes (*VEGFA*, *c-Myc*, and *MMP-9*) along with M1-like TAM genes (*iNOS* and *HLA-DR*) and M2-like TAM genes (*CD206*, *IL-10*, and *CD163*). The results showed that TAMs incubated with oleamide significantly decreased the expression of *c-Myc*, *VEGFA*, *CD206*, and *IL-10* genes compared to untreated TAMs (**Figure 57A**). This indicated that oleamide suppressed the differentiation of M2-like TAM phenotypes. Furthermore, oleamide upregulated the expression of *HLA-DR* and slightly increased the expression of *iNOS* genes, which were associated with M1-like TAMs (**Figure 57A**).

To support these results, pro-inflammatory cytokines (IL-1 $\beta$ , IL-6, and TNF- $\alpha$ ) and the anti-inflammatory cytokine (IL-10) were determined by ELISA (**Figure 57B**). Interestingly, increasing IL-1 $\beta$  was observed in TAMs after treatment with oleamide, while TNF- $\alpha$  and IL-6 were not significantly different to untreated TAMs. Moreover, a decrease in IL-10 was observed in TAMs treated with oleamide, correlating with the downregulation of IL-10 gene expression. Taken together, these data suggested that treating TAMs with oleamide reduced protumor M2-like TAMs while preserving antitumor M1-like TAMs in a transwell co-culture model with MAD-MB-231 cells.

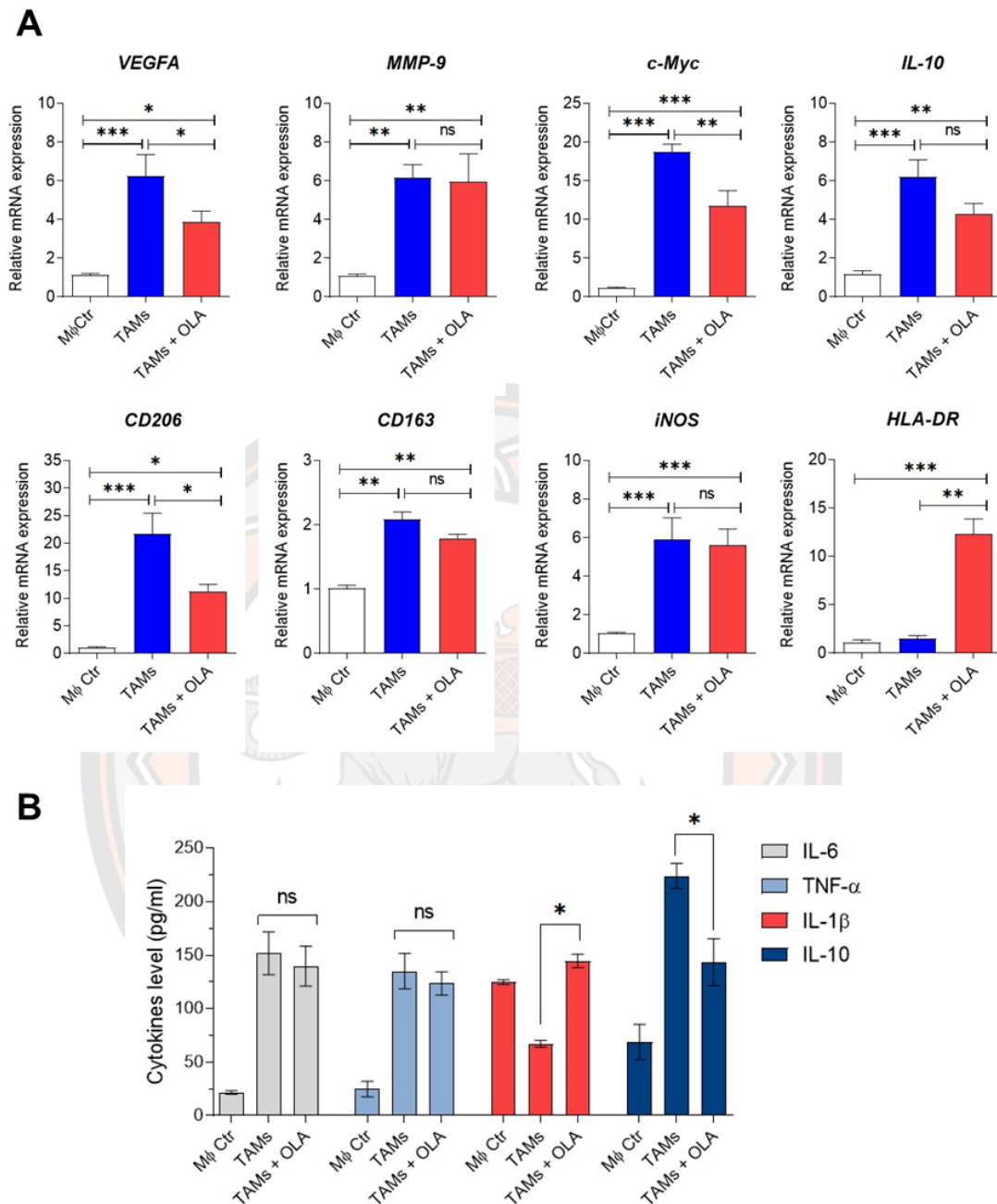


**Figure 57 Effect of oleamide on human TAM polarization.**

(A) Gene expression by RT-qPCR. (B) Cytokine levels by ELISA. TAMs (day 6) were incubated in the presence or absence of oleamide (20  $\mu\text{g/ml}$ ) for 24 hr. The MØ control represented M0 macrophages. Data are represented as mean  $\pm$  SEM of three independent experiments (\*p < 0.05, \*\*p < 0.01, \*\*\*p < 0.001), ns (not significant), TAMs (tumor-associated macrophages), OLA (oleamide)

### 3.3 Conditioned medium of oleamide-treated TAMs inhibited cell viability and induced apoptosis in MDA-MB-231 cells

Since reprogramming of protumor M2-like TAMs toward antitumor M1-like TAM phenotypes was observed in oleamide-treated TAMs, we next hypothesized that oleamide may show anti-tumor activity by enhancing M1-like TAM-mediated cytotoxicity to kill tumor cells. To prove this, different types of conditioned medium from co-cultured TAMs in the presence or absence of oleamide were collected to study anticancer activity. The MDA-MB-231 cells were incubated with the different types of conditioned medium for 72 hr and cell viability was assessed using the MTT assay. The results showed that the conditioned medium of untreated TAMs enhanced cancer cell proliferation at 48 hr and 72 hr. By contrast, the conditioned medium of oleamide-treated TAMs significantly suppressed cancer cell proliferation at 24 and 48 hr (**Figure 58A**). To confirm these results, MDA-MB-231 cells were incubated with the different types of conditioned medium for 24 hr. The cells were then stained with Annexin V/7-AAD to determine cell apoptosis. The results revealed that the conditioned medium of oleamide-treated TAMs increased the proportion of late apoptotic cells from 3.39% up to 13.63% while the conditioned medium of untreated TAMs did not alter the apoptosis profile (**Figure 58B**). Moreover, the direct effect of oleamide on the MDA-MB-231 cell line was determined by incubating cells with 20  $\mu\text{g/ml}$  of oleamide in a complete medium for 24 hr. Oleamide displayed a slightly insignificant increase in late apoptotic cells from 3.39% (untreated cells) to 4.0%, but not significant (**Figure 58B**).

To further clarify the direct effect of oleamide, MDA-MB-231 cells were incubated with a serial concentration of oleamide in a complete medium for 24 hr. The results showed that low doses of oleamide ( $\leq 30 \mu\text{g/ml}$ ) did not alter the viability of the MDA-MB-231 cells. By contrast, oleamide at 60 and 120  $\mu\text{g/ml}$  exhibited a more potent anticancer effect by reducing cancer cell viability to 89.60% and 11.41%, respectively, while cell viability was completely inhibited at 240  $\mu\text{g/ml}$  of oleamide treatment (**Figure 58C**). This result suggested that low doses of oleamide did not alter the viability of the MDA-MB-231 cells. Taken together, these results indicated that anticancer activity was an indirect consequence of oleamide-

promoted TAM toward M1-like TAM phenotypes associated with cytotoxicity against cancer cells.

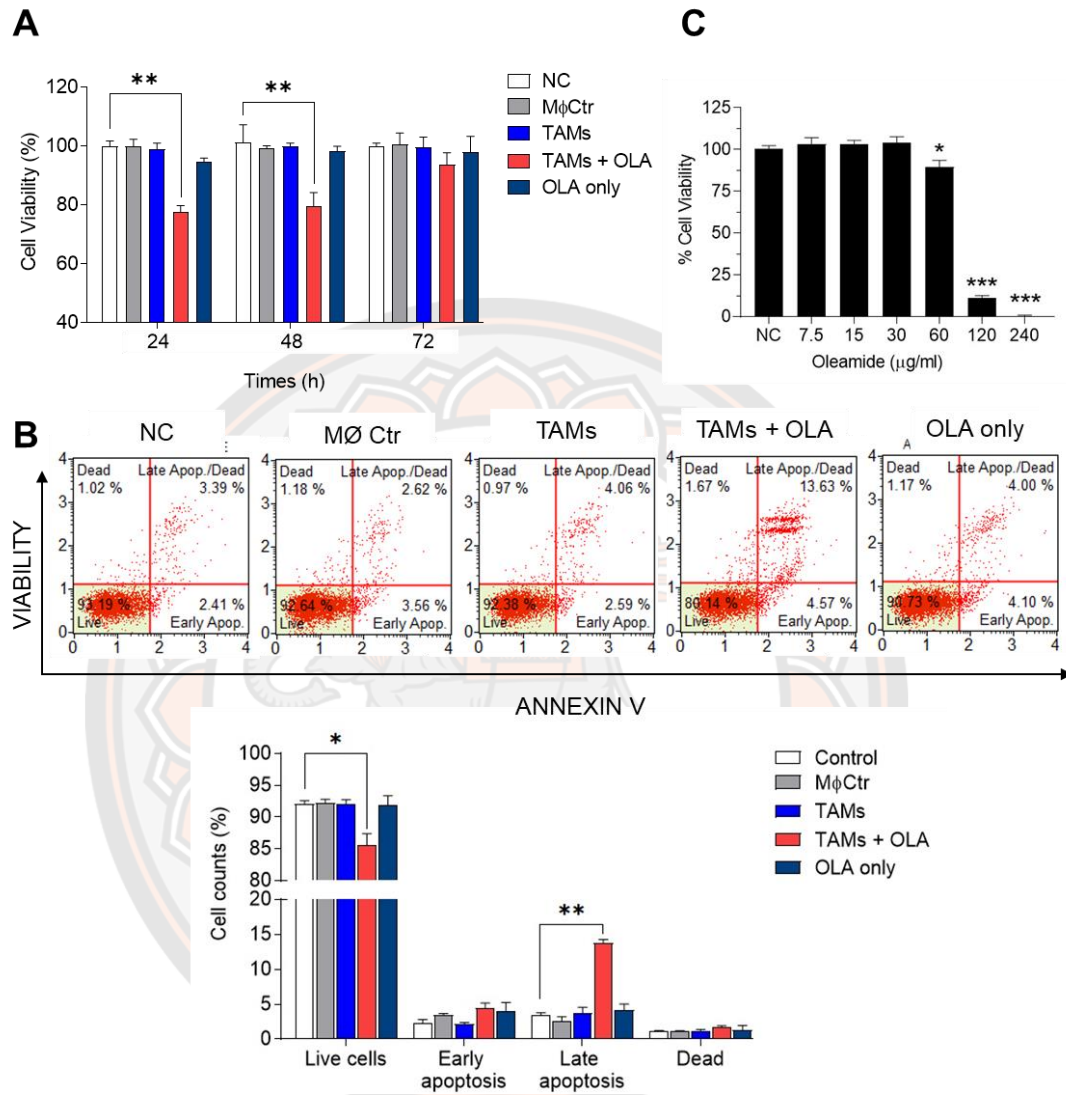


**Figure 58** Effect of oleamide-treated TAM-conditioned medium on the viability and apoptosis of MDA-MB-231 cells.

(A, C) Cell viability by MTT assay. (B) Analysis of MDA-MB-231 cell apoptosis at 24 hr. (A-B) Cells were incubated with TAM-conditioned mediums (TAMs, TAMs + OLA), Mφ Ctr-conditioned medium, complete medium only (NC), or complete medium plus 20 μg/ml oleamide (OLA only) for 24 hr, 48 hr, and 72 hr. (C) Cells were incubated with oleamide at concentrations of 0-240 μg/ml for 24 hr. Data represent the mean ± SEM of three independent experiments (\* $p < 0.05$ , \*\* $p < 0.01$ , \*\*\* $p < 0.001$ ). TAMs (tumor-associated macrophages), OLA (oleamide) and NC (negative control).

## CHAPTER 5

### CONCLUSIONS AND DISCUSSIONS

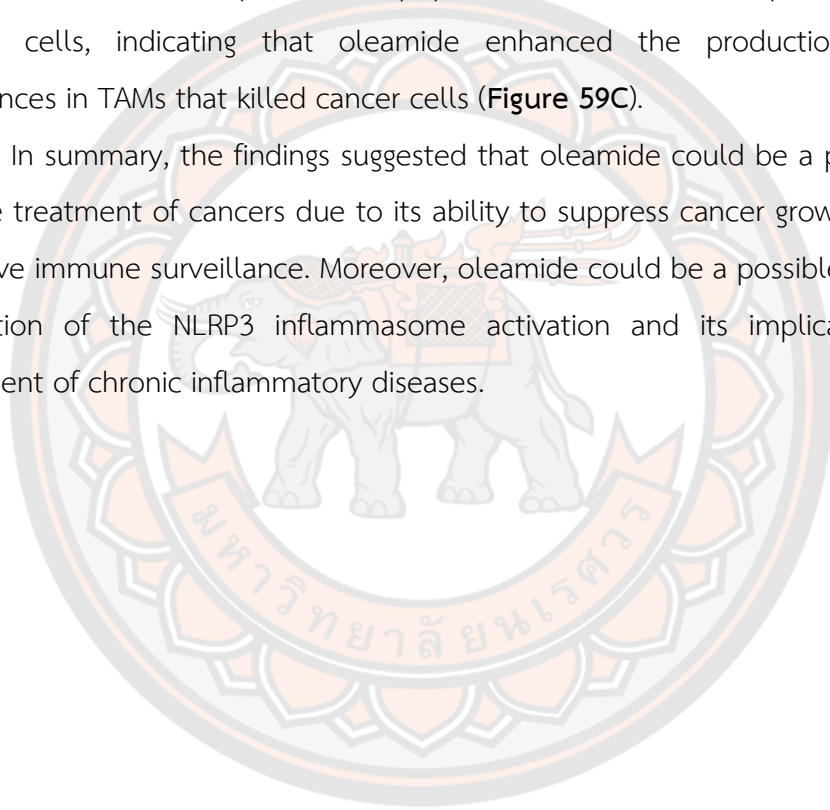
#### Conclusions

The present study demonstrated the *in vitro* bioassay-guided fractionations and identifications of the potential anti-cancer compounds in *Moringa oleifera* leaf (MOL) extract against tumor negative breast cancer (TNBC) cell lines, MDA-MB-231. The crude Ethyl acetate (EtOAc) extract and their fractions (no.1 -11) were screened for anti-cancer activity using multi-bioassay-guided fractionation to select the most effective fraction, which proved to be fraction no. 7. This active fraction was further separated into eight sub-fractions (no.7.1-7.8) and screened for anti-cancer activity. Ten compounds were tentatively identified from sub-fraction no.7.7 using at-line- Liquid chromatography-electrospray ionization-quadrupole time-of-flight-mass spectrometry (LC-ESI-QTOF-MS/MS) analysis. Three compounds were identified, including 7-octenoic acid, oleamide, and 1-phenyl-2-pentanol, and these were used to verify the anti-cancer activity against MDA-MB-231 cells and other types of cancer cell lines. The findings suggested that oleamide exerts the strongest potential as an anti-cancer agent by inducing apoptosis through Bcl-2 suppression and subsequent activation of caspase 3 (Figure 59A).

Oleamide identified from MOL was subjected to further study focusing on the progression of human M1/M2 macrophage polarization. The findings indicated that oleamide mediates naïve macrophages (M0) toward the M1 phenotype and promoted IL-1 $\beta$  production while hindering the polarization of M2 phenotypes. As secretion of IL-1 $\beta$  requires additional activation of the inflammasome pathway, the effect of oleamide on the activation of NLRP3 inflammasome was next investigated. This study suggested that oleamide induced NLRP3 inflammasome activation and subsequently activated caspase 1, leading to the production of mature IL-1 $\beta$ , which secreted and promoted polarization of naïve macrophages (M0) into M1 phenotypes (Figure 59B).

As oleamide exerts anti-cancer and immunomodulatory activity, the next study focused on the reprogramming of tumor-associated macrophages (TAMs) by oleamide. This study suggested that oleamide induced the reprogramming of protumor M2-like toward anti-tumor M1-like TAMs phenotypes. Oleamide reduced the M2-like TAM phenotypes by suppressing IL-10 production and *VEGFA*, *c-Myc*, and *CD206* gene expression. By contrast, oleamide promoted M2-like switch to M1-like TAMs by upregulating *HLA-DR* gene expression. Moreover, a conditioned medium of oleamide-treated TAMs promoted apoptosis of MDA-MB-231 triple-negative breast cancer cells, indicating that oleamide enhanced the production of harmful substances in TAMs that killed cancer cells (**Figure 59C**).

In summary, the findings suggested that oleamide could be a potential agent for the treatment of cancers due to its ability to suppress cancer growth and restore effective immune surveillance. Moreover, oleamide could be a possible target for the regulation of the NLRP3 inflammasome activation and its implications for the treatment of chronic inflammatory diseases.



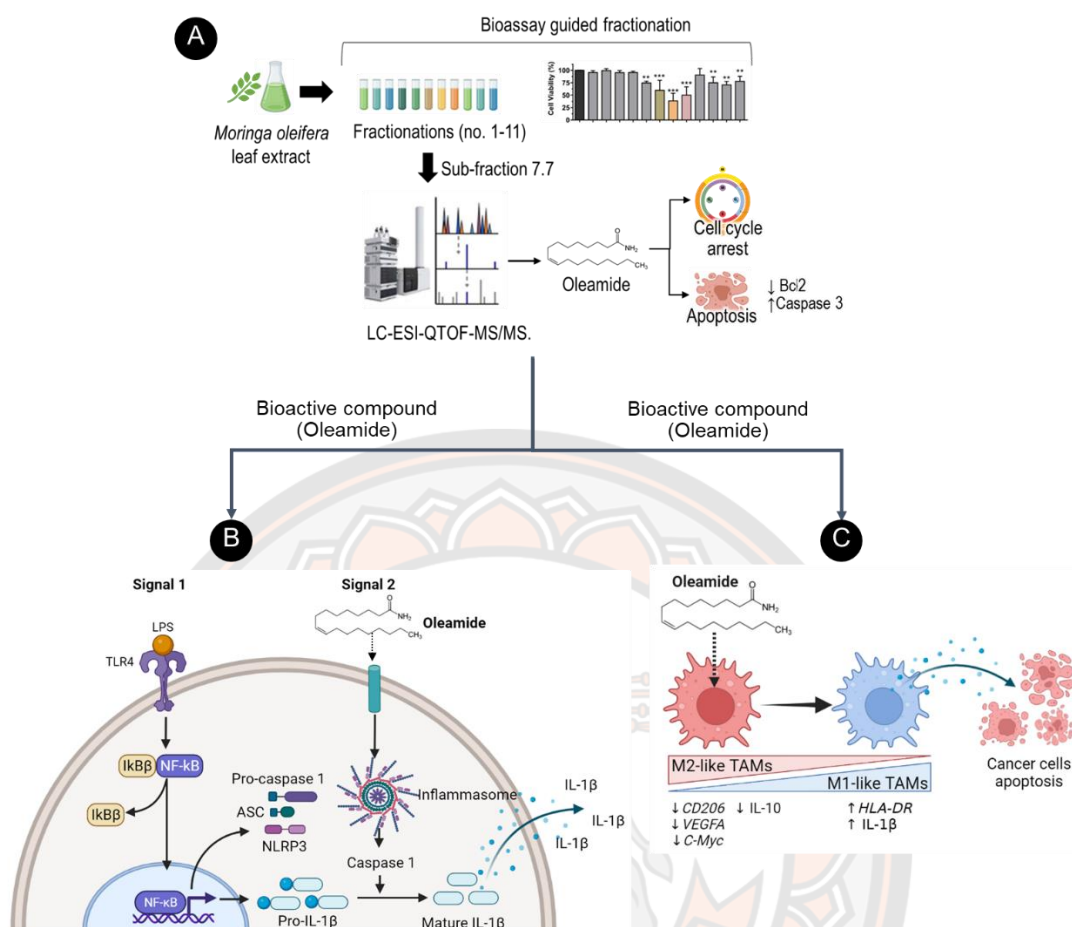


**Figure 59** Summarizes the main research findings of the study.

(A) *In vitro* Bioassay-guided fractionation and identification of potential anticancer compounds from MOL extract against MDA-MB-231 cells. Crude EtOAc extract was fractionated (no.1-11) and screened for anticancer activities with multi-bioassay guidance. Sub-fraction no. 7.7 was selected for the identification of bioactive compounds using LC-ESI-QTOF-MS/MS. Oleamide exhibited the strongest anticancer effects compared to others. (B) Oleamide activation of NLRP3 inflammasome of M1 phenotypes. The priming step (signal 1) by LPS involved an NF- $\kappa$ B-dependent upregulation of cellular NLRP3 and pro-IL-1 $\beta$ , while the second step (signal 2) was induced by oleamide activating inflammasome and cleaving IL-1 $\beta$ . The released IL-1 may help to induce the polarization of naive macrophages (M0) into M1 phenotypes by supporting oleamide. (C) Oleamide targets TAMs by reprogramming the protumor M2-like phenotypes toward antitumor M1-like TAM phenotypes. Oleamide restrained the M2-like TAM phenotypes by suppressing the M2-like genes (*CD206*, *VEGFA*, *C-Myc*) and IL-10 production. Oleamide also promoted M1-like TAM phenotypes by enhancing the HLA-DR gene and IL-1 $\beta$  production. Moreover, oleamide-treated TAM-conditioned medium exerted anticancer property by inducing MDA-MB-231 cell apoptosis.

## Discussion

MO is traditionally consumed in many Asian and Southeast Asian countries, including Thailand (22-24). MOL possesses many bioactive compounds with potential health benefits including being anti-inflammatory and an antioxidant, and also demonstrates anti-cancer properties (25). Although much research supports the anti-cancer effect of MOL, the actual bioactive compounds responsible have not been fully characterized. The first part of this research study demonstrated the *in vitro* bioassay-guided fractionation and identification of the potential anti-cancer compounds from MOL extract against TNBC cell lines MDA-MB-231. The 10 candidate compounds were tentatively identified, and the oleamide exerts the strongest potential as an anticancer agent by inducing apoptosis of MDA-MB-231 cell and other types of cancer cell lines.

Apoptosis is a crucial mechanism to maintain the balance between survival and death in cells to prevent the development of cancer (175, 176). The mechanism of apoptosis is mainly divided into two pathways: extrinsic pathway and intrinsic pathway (175, 176). The extrinsic pathway refers to the death receptors-mediated pathway, while the intrinsic pathway is mitochondrial-mediated (175, 176). Both extrinsic and intrinsic pathways converge at the same point (execution phase), which refers to the final pathway of apoptosis (175, 176). In the execution phase, caspase-8, and 9 are initiator caspases while caspase-3, caspase-6 and caspase-7, caspase-10, CAD (caspase-activated DNase) and PARP (poly (ADP-ribose) polymerase) are classified as effector or executioner caspases (175, 176). In addition to caspases, other proteins also contribute to the apoptotic mechanism. The Bcl-2 family protein is the central gatekeeper of the intrinsic or mitochondrial apoptotic response (177). Bcl-2 is also known as an anti-apoptotic molecule (177). By contrast, Bax (Bcl-2-associated X protein) is a pro-apoptotic molecule that initiates cell apoptosis. In this research study, the expression of caspase-3, cleaved caspase-3, Bcl-2, and Bax were used as a marker to monitor the apoptosis pathway (178). The results revealed that fraction no. 7 and oleamide initiate the MDA-MB-231 cell apoptosis by upregulating the pro-apoptotic Bax and cleaved caspase-3 while downregulating the anti-apoptotic Bcl-2 protein expression.

On the other hand, the Muse cell analyzer with annexin V and 7-AAD staining indicated that MOL fraction no. 7 was able to not only induce apoptosis but also triggered necrotic cell death in MDA-MB-231 cells. This mechanism might be caused by the activation of caspase-3 which triggers crosstalk to necrotic signalling, resulting in secondary necrosis (179, 180). The main features of secondary necrosis are osmotic cell swelling and lysis that lead to leakage of the cell contents; thereby it may cause tissue injury and induction of inflammation and other immune responses if the dying cells are not quickly removed by phagocytes (179, 180). Additionally, MOL fraction no. 7 induced cell cycle arrest at the G2/M phase, which correlated to the study of Al-Asmari *et al.*, that found the increase of MDA-MB-231 cell accumulation in the G2/M phase after treatment with crude EtOAc MOL extract (85).

MOL has been shown to contain many phenolic compounds that exert anti-cancer effects including quercetin, kaempferol, isothiocyanate, and gallic acid (28, 181). Moreover, long-chain fatty acids and their derivatives are also considered anticancer compounds (28, 181). In this study, the 10 compounds were tentatively identified using LC-ESI-QTOF-MS analysis. Two aromatic compounds (C1 and C3), five fatty acids (C2, C5-C8), two fatty amides (C9 and C10), and a lactone compound (C4). The octadecadienoic acid and oleamide have been discovered in MOL as described in the previous studies (182-184). Using commercially available compounds, three candidate compounds (oleamide, 7-octenoic acid, and 1-phenyl-2-pentanol) were selected to verify the anti-cancer activity against MDA-MB-231 cells. Oleamide (9-octadecenamide), is a long-chain fatty acid amide discovered in the cerebrospinal fluid of sleep-deprived cats (185). Oleamide has been reported to have a wide range of effects on the neurotransmitter systems (120, 121, 186, 187). It has also been reported that oleic acid (9-cis-Octadecenoic acid), a precursor of oleamide synthesis was found at about 20.89% in MOL (26). By contrast, 7-octenoic acid and 1-phenyl-2-pentanol have not been reported in MOL as well as biological activity.

Interestingly, the present study firstly demonstrated the effects of oleamide, 7-octenoic acid, and 1-phenyl-2-pentanol against MDA-MB-231 cells. A low concentration of oleamide exerts a remarkable anticancer activity while 1-phenyl-2-pentanol and 7-octadecenoic acid required a high concentration to suppress cancer

cells. However, the anti-cancer effect of each compound was measured individually in all experiments, thus, 1-phenyl-2-pentanol and 7-octadecenoic acid may require a combination of compounds, or synergistic action with other compounds, to enhance their activity. This aspect requires further investigation. The evidence from previous studies indicated that combination therapy can improve the efficacy of the drug on TNBC cell lines (188-190). For example, the combination treatment of selumetinib (MEK1/2 inhibitor) with buparlisib (PI3K inhibitor) is synergistic in MDA-MB-231 cells (188). Therefore, future investigation of the combined effect of natural compounds with other compounds, chemotherapy, radiotherapy, and any anti-cancer agents is still required.

Although oleamide presents as a potential agent for the treatment of cancer, the molecular mechanism underlying the oleamide–target interactions and compound–compound interaction remains unclear. One limitation of this study is that we only performed one model of TNBCs, MDA-MB-231. It is unclear whether these compounds still show the same efficacy as other TNBC cell lines. Therefore, further studies should be performed on other TNBC cell lines such as MDA-MB-175, MDA-MB-435, and MDA-MB-436 (191). However, this study also demonstrated the anti-cancer effect of oleamide with other types of cancer cell lines, including human myelogenous leukemia cell K562 and human squamous cell carcinoma lines SCC-15, which revealed that oleamide has potential as an anticancer agent for other cancer types.

Recently, patient-derived cancer models have been proposed to gradually replace the cancer cell lines for translational research (192-194). For example, lung cancer patients derived samples were studied for their effective drug combination responses (192). T-cell prolymphocytic leukemia-derived models were successfully used for the identification and prediction of drug combination treatment (194). Therefore, further investigation of oleamide on TNBC patient-derived samples and patient-derived xenograft models are a powerful tool for combining effects and overcoming the resistance mechanisms is suggested.

Macrophage polarization is a process whereby macrophages adopt different functional phenotypes in response to specific microenvironmental stimuli and signals

(13). This process is crucial for inflammation, tissue repair, and homeostasis maintenance (132). The second part of this research demonstrated that oleamide mediated naïve macrophages (M0) toward the M1 phenotype and promoted NLRP-3 inflammasome-mediated IL-1 $\beta$  production in primary human MDMs *in vitro*.

Macrophage polarization is conventionally subdivided into three groups as naïve macrophages (M $\emptyset$ ; also called M0), which readily differentiate into the other two major phenotypes as classically activated macrophages (M1) and alternatively activated macrophages (M2) (12-14). Most research on macrophage polarization used simply *in vitro* techniques. Generally, macrophages derived from *in vitro* culture in the presence of specific cytokines stimulate M1 or M2 polarization. Here, M1 polarization was stimulated by LPS and IFN- $\gamma$ , which are toll-like receptor (TLR) agonists. M2 polarization was stimulated by IL-4, designed to mimic what happens when macrophages are exposed to polarized CD4<sup>+</sup> T cells, producing their distinctive cytokine combinations (14). M0 macrophages were cultured in complete media only without polarizing agents and considered naïve macrophages that had not been exposed to any pro- or anti-inflammatory stimuli or environment. This also avoids discrepancies from M-CSF or GM-CSF-dependent cultures (29, 30). All phenotypes (M0, M1, and M2) were cultured in the presence or absence of oleamide. The M0 and M2 macrophages displayed upregulation of CD80 coupled with downregulation of CD163 and CD206 on the cell surface after treatment with oleamide. In M1 macrophages, CD80 expression remained stable but displayed downregulation of CD163 and CD206 on the cell surface after treatment with oleamide (**Figure 51**). CD206 (also known as macrophage mannose receptor; MMR) is primarily expressed on the surface of macrophages and immature dendritic cells, where it acts as a pattern recognition receptor (PRR) (195, 196). The expression of CD206 is generally used as a marker of M2 macrophages (197-199). However, more than half of the M0, M1, and M2 phenotypes exhibited CD206 on the cell surface, indicating that using CD206 as an M2 marker in MDMs should be considered in terms of specificity.

Macrophage polarization is also characterized by the production of cytokines and the expression of M1/M2-associated genes. M1 macrophages are characterized by the production of proinflammatory cytokines like TNF- $\alpha$ , IL-1 $\beta$ , and IL-6. M2

macrophages are characterized by the production of IL-10 and TGF- $\beta$ . Surprisingly, oleamide treatment did not alter the basal levels of IL-6 and TNF- $\alpha$  but specifically stimulated the production of IL-1 $\beta$  in both MDMs and differentiated THP-1 (**Figure 52 B-C**). This indicated that oleamide might have some impact on IL-1 $\beta$  signalling and/or NLRP3 inflammasome.

IL-1 $\beta$  is a master regulator of inflammation by controlling a variety of innate immune cells (200-203). In macrophages, inflammasome activation is required to process pro-IL-1 $\beta$  and pro-IL-18 into their mature forms and secrete active forms (IL-1 $\beta$  and IL-18), resulting in initiating inflammation. Currently, a two-step model is used for initiating inflammasome activation (200-203). The first step or priming step (signal 1) typically involves an NF- $\kappa$ B-dependent upregulation of cellular NLRP3, pro-IL-1 $\beta$ , and pro-IL-18 protein synthesis. The second step (signal 2) is the activation of NLRP3 oligomerization. This step can be induced by numerous PAMP or DAMP such as extracellular ATP and K<sup>+</sup> efflux through the ATP-gated P2X7 channel, nigericin toxin as well as lysosomal destabilization agents (200-202). Upon activation, NLRP3 triggers self-oligomerization and recruitment of apoptosis-associated speck-like protein containing a caspase-recruitment domain (ASC) and pro-caspase-1, leading to the assembly of inflammasome complex (200-202). NLRP3 inflammasome activation results in active caspase-1, which cleaves the pro-IL-1 $\beta$  and pro-IL-18 into their mature forms, which then facilitates robust immune responses and pyroptosis (200-202).

Dysregulation of NLRP3 inflammasome activation is linked with the development of many diseases, especially age-associated ailments such as neurologic disorders and metabolic diseases. Enhanced NLRP3 inflammasome-mediated IL-1 $\beta$  secretion in microglia is associated with the progression of Alzheimer's disease by reducing the phagocytosis of amyloid- $\beta$  (A $\beta$ ) from microglia (204, 205). The previous study by Yasuhisa Ano *et.al* reported that oleamide reduces A $\beta$  accumulation via enhanced microglial phagocytosis, next hypothesized that oleamide could affect human macrophage NLRP3 inflammatory activation. Surprisingly, our research discovered that oleamide has a divisive effect on human macrophages. Results showed that oleamide mediated IL-1 $\beta$  and IL-18 secretion in

LPS-primed MDMs nearly to ATP (**Figure 53C**). Moreover, oleamide induced activation of intracellular inflammasome-associated proteins including NLRP-3, ASC, cleaved casp-1 and cleaved IL-1 $\beta$ , correlating with upregulation of cleaved IL-1 $\beta$  and cleaved casp-1 in the supernatant or secreted proteins (**Figure 54A**). However, no alteration of purinergic P2X7 receptor expression was observed after treatment with oleamide. This result indicated that oleamide-mediated NLRP-3 inflammasome activation was not involved in the activation of the P2X7 receptor. A previous study reported that P2Y-type receptors, a family of G protein-coupled receptors, are potential targets of oleamide in primary murine microglia and human dendritic cells (28). P2Y-type receptors involve the coupling of several intracellular pathways and second messengers but act more slowly than P2X receptors (29). However, the regulatory effect of oleamide via the P2Y receptor in the inflammasome activation has not been studied. Therefore, how oleamide regulates the NLRP-3 inflammasome still requires further investigation. Furthermore, our findings were the first to show that oleamide can cause M1 macrophage polarization and inflammasome activation as well as IL-1 release in MDMs. However, the exact mechanism by which these released IL-1 regulate MDM polarizations is unknown.

Oleamide is an endogenous fatty acid amide that was first reported as a sleep-inducing substance and was later identified as having a wide range of receptors and neurotransmitter systems (120, 121, 186, 187). Nervous and immune systems are often cross-regulated and the potential immunoregulatory activity of oleamide was also studied. Oleamide suppressed the expression of iNOS and COX-2 and secretion of pro-inflammatory cytokines including TNF- $\alpha$ , IL-1 $\beta$ , and IL-6 in LPS-induced RAW264.7 murine macrophages (97). Surprisingly, this study found the opposite effect of oleamide that promoted the production of IL-1 $\beta$  and NLRP3 inflammasome activation in LPS-primed human MDMs. These opposite results were due to different experimental designs (pre-treatment vs. post-treatment), and cell culture models (RAW264.7 cell vs. MDMs).

The present study explored the immunoregulatory effects of oleamide on human macrophage polarization and NLRP3 inflammasome activation using primary human MDMs cultured in a medium containing human serum as a model. Our results

indicated that oleamide promoted naïve macrophages (M0) toward the M1 phenotype and IL-1 $\beta$  production by regulating NLRP3 inflammasome activation in MDMs. This research shows that oleamide has a new effect on human MDMs and could be used as a therapeutic target for NLRP3-related inflammatory diseases, particularly neurodegenerative disorders.

The purpose of the third part of this study was to explore the regulatory effect of oleamide on human TAMs polarization and how it influences cancer progression. TAMs are a major population of tumor-infiltrating immune cells and are involved in tumor formation (16). TAMs are often assumed to have an immunoregulatory M2 phenotype, also called M2-like TAMs associated with more aggressive tumor behavior (invasion, progression, and metastases) (16, 17). However, TAMs not only have the characteristics of M2 but also have an M1-like phenotype (16, 17). M1-like TAMs have antitumor activity. They can distinguish tumor cells from normal cells and induce tumor-killing (16, 17). Several lines of evidence support that higher M2-like TAMs are associated with tumor progression and treatment resistance, whereas higher M1-like TAMs are associated with positive outcomes (18-20). Thus, targeting the TAM polarization state by switching the immunosuppressive M2 into the tumoricidal M1-like TAM phenotype offers a promising strategy to improve cancer treatment.

The *in vitro* generation of TAMs is one of the simplest models for studying TAM functions and TAM-targeted therapies. The three most relevant approaches to obtaining *in vitro* fully differentiated macrophages include peripheral blood monocytes, immortalized cell lines such as THP-1, and human-induced pluripotent stem cells (206). This study presented a modified protocol for the *in vitro* polarization of peripheral blood human monocytes into TAMs using transwell co-culture with MDA-MB-231 breast cancer cells. The results demonstrated that human monocytes co-cultured with MDA-MB-231 cells plus the addition of M-CSF, IL-4, and IL-10 strongly induced *c-Myc*, *VEGFA*, *MMP-9*, and *CD206* gene expression (**Figure 56**). Furthermore, the present study found that co-cultured monocytes and MDA-MB-231 cells in a complete medium promoted monocyte polarization into M2-like TAM phenotypes by upregulating *MMP-9* and *VEGFA* but did not alter *c-Myc* and *CD206*

gene expression. This finding concurred with the previous finding by Hollmén M *et al.* that MDA-MB-231 cells could induce human monocyte differentiation into M2-like macrophages with increased MMR protein expression and CCL2 secretion using a transwell co-culture system (207). However, TAMs are activated by T-helper 2 cytokines IL-4 and IL-13, and immunosuppressive cytokines such as IL-10 and TGF- $\beta$ , hence, additional cytokines are still required for fully differentiated TAMs. As monocyte cultivation in the tumor-conditioned medium is a common and simple process for generating TAM-like cells, which are the next co-cultured monocytes, and MDA-MB-231 cells in a 1:1 ratio of tumor-conditioned medium: complete medium plus the addition of M-CSF, IL-4, and IL-10. The results revealed that co-cultured monocytes with tumor-conditioned medium-plus cytokines significantly increased the expression of *c-Myc*, *VEGFA*, *MMP-9*, and *CD206* genes but not as strongly as those co-cultured in complete medium plus cytokines (**Figure 56B**). This suggested that the addition of a tumor-conditioned medium is not required for TAM generation using the transwell co-culture model. Overall, the findings suggested that the transwell co-culture of human monocytes and MDA-MB-231 cells, along with the addition of M-CSF, IL-4, and IL-10, was an effective paradigm for TAMs production *in vitro*.

Oleamide (cis-9,10-octadecenoamide) is a fatty acid amide belonging to the family of endogenous lipid signalling molecules that act as sleep-inducing substances (113). Oleamide was later determined as a neuromodulator with the ability to interact with a wide range of neurotransmitter receptors such as dopamine acetylcholine, serotonin, gamma-aminobutyric acid (GABA), and cannabinoid (112, 113, 119, 208). Oleamide has also been reported to have anticancer properties by inducing apoptosis in various types of cancer cell lines, for example, MDA-MB-231 breast cancer cells, SSC-15 squamous cell carcinoma, and K-562 myelogenous leukemia cells (209). Moreover, a recent study found that oleamide has immunomodulatory activity by promoting M1 macrophage polarization in the primary human MDMs model (210). In this study, we found that oleamide induced the reprogramming of M2-like TAMs toward M1-like TAM phenotypes by suppressing *c-Myc*, *VEGFA*, and *CD206* gene expression, as well as upregulating the M1-like TAM gene, *HLA-DR*, in oleamide-treated TAMs (**Figure 57A**). In general, M1-like TAMs

largely secreted pro-inflammatory cytokines like IL-6, IL-12, IL-23, and TNF- $\alpha$  (211). In contrast, M2-like TAMs highly expressed immunosuppressive molecules such as IL-10, TGF- $\beta$ , and programmed death-ligand 1 (PD-L1), which are associated with cancer progression. We found that oleamide-treated TAMs suppressed the production of IL-10 in TAMs (**Figure 57B**). These results supported that oleamide mediated M1-like TAM polarization.

M1-like TAMs are known to have an anti-tumorigenic phenotype. There are three major mechanisms, by which macrophages recognize and kill tumor cells: 1) direct killing through the release of a harmful mediator such as tumor necrosis factor (TNF) and nitric oxide (NO), reactive oxygen species (ROS) or actively taking up the cancer cells by phagocytosis, 2) direct cytolysis of cancer cells through antibody-dependent cellular cytotoxicity (ADCC) and 3) indirect killing by activating other immune cells such as NK cells and T cells (16, 17, 212). Interestingly, results showed that conditioned medium collected from oleamide-treated TAMs suppressed MDA-MB-231 cell proliferation at 24 hr and 48 hr (**Figure 58A**). Moreover, flow cytometry analysis indicated that a conditioned medium of oleamide-treated TAMs induced apoptosis of MDA-MB-231 cells after 24 hr of treatment, whereas oleamide alone did not alter cell apoptosis (**Figure 58B**). Taken together, these results suggested that the conditioned medium collected from oleamide-treated TAMs was composed of effective mediators which then triggered tumor cell apoptosis.

This study has some limitations. The major limitation is that monocyte-derived TAM phenotypes are only defined by gene expression profiles, which may or may not be fully complete for the characterization of TAM phenotypes. We suggest that studying gene expressions coupled with surface marker expressions would be more reliable for the characterization of TAM phenotypes. The results suggested that a conditioned medium of oleamide-treated TAMs exhibited cytotoxicity on tumor cells but levels of cell toxic substances such as NO and ROS were not measured. Other mechanisms whereby macrophages kill tumor cells, such as ADCC, and activate other immune cells were also not investigated. Therefore, further experiments are required to assess the underlying mechanisms of oleamide-mediated TAM polarization and tumor progression.

The present study revealed the immunoregulatory effect of oleamide-mediated TAM phenotypes, indicating that oleamide targeting showed potential for cancer treatment. We also demonstrated the modified *in vitro* generation of primary human monocyte-derived TAMs using a transwell co-culture system.



## REFERENCES

(213)



1. American Cancer Society. Breast Cancer Facts & Figures 2017-2018. American cancer society.
2. Society AC. Cancer Facts & Figures 2018. American cancer society.
3. Hwang SY, Park S, Kwon Y. Recent therapeutic trends and promising targets in triple negative breast cancer. *Pharmacol Ther.* 2019;199:30-57.
4. Kumar P, Aggarwal R. An overview of triple-negative breast cancer. *Arch Gynecol Obstet.* 2016;293(2):247-69.
5. Foulkes WD, Smith IE, Reis-Filho JS. Triple-negative breast cancer. *N Engl J Med.* 2010;363(20):1938-48.
6. Yang R, Li Y, Wang H, Qin T, Yin X, Ma X. Therapeutic progress and challenges for triple negative breast cancer: targeted therapy and immunotherapy. *Mol Biomed.* 2022;3(1):8.
7. Li Y, Zhan Z, Yin X, Fu S, Deng X. Targeted therapeutic strategies for triple-negative breast cancer. *Front Oncol.* 2021;11.
8. Anderson NR, Minutolo NG, Gill S, Klichinsky M. Macrophage-based approaches for cancer immunotherapy. *Cancer Research.* 2021;81(5):1201-8.
9. Heimes A-S, Schmidt M. Immuno-oncology in triple-negative breast cancer. *J cancer Metastasis Treat.* 2021;7:9.
10. Standish LJ, Sweet ES, Novack J, Wenner CA, Bridge C, Nelson A, et al. Breast cancer and the immune system. *J Soc Integr Oncol.* 2008;6(4):158-68.
11. Savas P, Salgado R, Denkert C, Sotiriou C, Darcy PK, Smyth MJ, et al. Clinical relevance of host immunity in breast cancer: from TILs to the clinic. *Nat Rev Clin Oncol.* 2016;13(4):228-41.
12. Genin M, Clement F, Fattaccioli A, Raes M, Michiels C. M1 and M2 macrophages derived from THP-1 cells differentially modulate the response of cancer cells to etoposide. *BMC Cancer.* 2015;15(1):577.
13. Orecchioni M, Ghosheh Y, Pramod AB, Ley K. Macrophage polarization: different gene signatures in m1(lps+) vs. Classically and m2(lps-) vs. Alternatively activated macrophages. *Front Immunol.* 2019;10(1084).
14. Murray PJ. Macrophage polarization. *Annu Rev Physiol.* 2017;79(1):541-66.

15. Yao Y, Xu X-H, Jin L. Macrophage polarization in physiological and pathological pregnancy. *Front Immunol.* 2019;10(792).
16. Pan Y, Yu Y, Wang X, Zhang T. Tumor-associated macrophages in tumor immunity. *Front Immunol.* 2020;11.
17. Zhou J, Tang Z, Gao S, Li C, Feng Y, Zhou X. Tumor-associated macrophages: recent insights and therapies. *Front Oncol.* 2020;10.
18. Zhang M, He Y, Sun J, Li Q, Wang W, Zhao A, et al. A high M1/M2 ratio of tumor-associated macrophages is associated with extended survival in ovarian cancer patients. *J Ovarian Res.* 2014;7:19.
19. Oshi M, Tokumaru Y, Asaoka M, Yan L, Satyananda V, Matsuyama R, et al. M1 macrophage and M1/M2 ratio defined by transcriptomic signatures resemble only part of their conventional clinical characteristics in breast cancer. *Sci Rep.* 2020;10(1):16554.
20. Lv C, Li S, Zhao J, Yang P, Yang C. M1 macrophages enhance survival and invasion of oral squamous cell carcinoma by inducing gdf15-mediated erbb2 phosphorylation. *ACS Omega.* 2022;7(13):11405-14.
21. Yuan ZY, Luo RZ, Peng RJ, Wang SS, Xue C. High infiltration of tumor-associated macrophages in triple-negative breast cancer is associated with a higher risk of distant metastasis. *Onco Targets Ther.* 2014;7:1475-80.
22. Thurber MD, Fahey JW. Adoption of *Moringa oleifera* to combat under-nutrition viewed through the lens of the "Diffusion of innovations" theory. *Ecol Food Nutr.* 2009;48(3):212-25.
23. Saini RK, Sivanesan I, Keum YS. Phytochemicals of *Moringa oleifera*: a review of their nutritional, therapeutic and industrial significance. *3 Biotech.* 2016;6(2):203.
24. Dholvitayakhun A, Cushnie TP, Trachoo N. Antibacterial activity of three medicinal Thai plants against *Campylobacter jejuni* and other foodborne pathogens. *Nat Prod Res.* 2012;26(4):356-63.
25. Leone A, Spada A, Battezzati A, Schiraldi A, Aristil J, Bertoli S. Cultivation, genetic, ethnopharmacology, phytochemistry and pharmacology of *Moringa oleifera* Leaves: an overview. *Int J Mol Sci.* 2015;16(6):12791-835.

26. Sodvadiya M, Patel H, Mishra A, Nair S. Emerging insights into anticancer chemopreventive activities of nutraceutical *Moringa oleifera*: molecular mechanisms, signal transduction and *in vivo* efficacy. *Curr Pharmacol Rep.* 2020;6(2):38-51.
27. Baldisserotto A, Buso P, Radice M, Dissette V, Lampronti I. *Moringa oleifera* leaf extracts as multifunctional ingredients for "natural and organic" sunscreens and photoprotective preparations. *Molecules.* 2018;23(3).
28. Paikra BK, Dhongade HKJ, Gidwani B. Phytochemistry and pharmacology of *Moringa oleifera* Lam. *J Pharmacopuncture.* 2017;20(3):194-200.
29. Panda S, Kar A, Sharma P, Sharma A. Cardioprotective potential of N,α-L-rhamnopyranosyl vincosamide, an indole alkaloid, isolated from the leaves of *Moringa oleifera* in isoproterenol induced cardiotoxic rats: *in vivo* and *in vitro* studies. *Med Chem Lett.* 2013;23(4):959-62.
30. Ghasi S, Nwobodo E, Ofili JO. Hypocholesterolemic effects of crude extract of leaf of *Moringa oleifera* Lam in high-fat diet fed wistar rats. *J Ethnopharmacol.* 2000;69(1):21-5.
31. Ganguly R, Guha D. Alteration of brain monoamines & EEG wave pattern in rat model of Alzheimer's disease & protection by *Moringa oleifera*. *Indian J Med Res.* 2008;128(6):744-51.
32. Cheenpracha S, Park EJ, Yoshida WY, Barit C, Wall M, Pezzuto JM, et al. Potential anti-inflammatory phenolic glycosides from the medicinal plant *Moringa oleifera* fruits. *Bioorg Med Chem.* 2010;18(17):6598-602.
33. Siddhuraju P, Becker K. Antioxidant properties of various solvent extracts of total phenolic constituents from three different agroclimatic origins of drumstick tree (*Moringa oleifera* Lam.) leaves. *J. Agric Food Chem J Arg Food Chem.* 2003;51(8):2144-55.
34. Singh BN, Singh BR, Singh RL, et al. Oxidative DNA damage protective activity, antioxidant and anti-quorum sensing potentials of *Moringa oleifera*. *Food Chem Toxicol.* 2009;47(6):1109-1116. doi:10.1016/j.fct.2009.01.034
35. Sreelatha S, Padma PR. Protective mechanisms of *Moringa oleifera* against CCl(4)-induced oxidative stress in precision-cut liver slices. *Forsch Komplementmed.* 2010;17(4):189-194. doi:10.1159/000318606

36. Faizi S, Siddiqui BS, Saleem R, Siddiqui S, Aftab K, Gilani AH. Fully acetylated carbamate and hypotensive thiocarbamate glycosides from *Moringa oleifera*. *Phytochemistry*. 1995;38(4):957-63.
37. Mahajan SG, Mehta AA. Inhibitory action of ethanolic extract of seeds of *Moringa oleifera* Lam. on systemic and local anaphylaxis. *J Immunotoxicol*. 2007;4(4):287-94.
38. Jaiswal D, Kumar Rai P, Kumar A, Mehta S, Watal G. Effect of *Moringa oleifera* Lam. leaves aqueous extract therapy on hyperglycemic rats. *J Ethnopharmacol*. 2009;123(3):392-6.
39. Mbikay M. Therapeutic potential of *Moringa oleifera* Leaves in chronic hyperglycemia and dyslipidemia: a review. *Fron. Pharmacol*. 2012;3:24.
40. Lurling M, Beekman W. Anti-cyanobacterial activity of *Moringa oleifera* seeds. *J Appl Phycol*. 2010;22(4):503-10.
41. Viera GH, Mourao JA, Angelo AM, Costa RA, Vieira RH. Antibacterial effect (*in vitro*) of *Moringa oleifera* and *Annona muricata* against Gram positive and Gram negative bacteria. *Rev Inst Med Trop Sao Paulo*. 2010;52(3):129-32.
42. Sudha P, Asdaq SM, Dhamingi SS, Chandrakala GK. Immunomodulatory activity of methanolic leaf extract of *Moringa oleifera* in animals. *Indian J Physiol Pharmacol*. 2010;54(2):133-40.
43. Gupta A, Gautam MK, Singh RK, Kumar MV, Rao Ch V, Goel RK, et al. Immunomodulatory effect of *Moringa oleifera* Lam. extract on cyclophosphamide induced toxicity in mice. *Indian J Exp Biol*. 2010;48(11):1157-60.
44. Khor KZ, Lim V, Moses EJ, Abdul Samad N. The *in vitro* and *in vivo* anticancer properties of *Moringa oleifera*. *Evid Based Complement Alternat Med*. 2018:1071243.
45. Madi N, Dany M, Abdoun S, Usta J. *Moringa oleifera*'s nutritious aqueous leaf extract has anticancerous effects by compromising mitochondrial viability in an ros-dependent manner. *J Am Coll Nutr*. 2016;35(7):604-13.
46. Gismondi A, Canuti L, Impei S, Di Marco G, Kenzo M, Colizzi V, et al. Antioxidant extracts of African medicinal plants induce cell cycle arrest and differentiation in B16F10 melanoma cells. *Int J Oncol*. 2013;43(3):956-64.

47. Nair S, Varalakshmi K. Anticancer, cytotoxic potential of *Moringa oleifera* extracts on HeLa cell line. *J Nat Pharm*. 2011;2:138.
48. Abd-Rabou AA, Abdalla AM, Ali NA, Zoheir KM. *Moringa oleifera* root induces cancer apoptosis more effectively than leave nanocomposites and its free counterpart. *Asian Pac J Cancer Prev*. 2017;18(8):2141-9.
49. Adebayo IA, Arsad H, Samian MR. Antiproliferative effect on breast cancer (mcf7) of *moringa oleifera* seed extracts. *Afr J Tradit Complement Altern Med*. 2017;14(2):282-7.
50. Badiu DC, Zgura A, Gales L, Iliescu L, Anghel R, Haineala B. Modulation of Immune System - Strategy in the Treatment of Breast Cancer. *In Vivo*. 2021;35(5):2889-94.
51. Fard MT, Arulselvan P, Karthivashan G, Adam SK, Fakurazi S. Bioactive extract from *Moringa oleifera* inhibits the pro-inflammatory mediators in lipopolysaccharide stimulated macrophages. *Pharmacogn Mag*. 2015;11(Suppl 4):S556-63.
52. Luetragoon T, Pankla Sranujit R, Noysang C, Thongsri Y, Potup P, Suphrom N, et al. Bioactive compounds in *Moringa oleifera* lam. Leaves inhibit the pro-inflammatory mediators in lipopolysaccharide-induced human monocyte-derived macrophages. *Molecules*. 2020;25(1):191.
53. Gaikwad SB, Mohan G, Reddy KJ. *Moringa oleifera* leaves: Immunomodulation in Wistar albino rats. *Int J Pharm Pharm Sci*. 2011;3:426-30.
54. Rachmawati I, Rifa'i M. *In vitro* immunomodulatory activity of aqueous extract of *Moringa oleifera* Lam. leaf to the CD4 +, CD8+ and B220+ cells in musculus. *J Exp Life Sci*. 2014;4:15-20.
55. American Cancer Society. *Cancer Facts & Figures 2018*. American Cancer Society. 2018.
56. Ray S. *The Cell: A Molecular Approach*: Yale J Biol Med. 2014 Dec 12;87(4):603-4. eCollection 2014 Dec.
57. Sever R, Brugge JS. Signal transduction in cancer. *Cold Spring Harbor perspectives in medicine*. 5(4):a006098.
58. Types of cancer [Internet]. November 2017. Available from: <https://www.cancerresearchuk.org/what-is-cancer/how-cancer-starts/types-of-cancer>.

59. Virani S, Bilheem S, Chansaard W, Chitapanarux I, Daoprasert K, Khuanchana S, et al. National and subnational population-based incidence of cancer in Thailand: assessing cancers with the highest burdens. *Cancers*. 2017;9(8).
60. The American Cancer Society medical and editorial content team. Types of Breast Cancer September, 2017 [Available from: [https://www.cancer.org/cancer/breast-cancer/understanding-a-breast-cancer-diagnosis/types-of-breast-cancer.html#written\\_by](https://www.cancer.org/cancer/breast-cancer/understanding-a-breast-cancer-diagnosis/types-of-breast-cancer.html#written_by)].
61. National Comprehensive Cancer Network (NCCN), American Cancer Society (ACS). Breast cancer September 2006.
62. Harbeck N, Penault-Llorca F, Cortes J, Gnant M, Houssami N, Poortmans P, et al. Breast cancer. *Nat Rev Dis Primers*. 2019;5(1):66.
63. Almansour NM. Triple-negative breast cancer: a brief review about epidemiology, risk factors, signaling pathways, treatment and role of artificial intelligence. *Front Mol Biosci*. 2022;9.
64. Łukasiewicz S, Czelelewski M, Forma A, Baj J, Sitarz R, Stanisławek A. Breast cancer-epidemiology, risk factors, classification, prognostic markers, and current treatment strategies-an updated review. *Cancers (Basel)*. 2021;13(17).
65. Sex hormones and risk of breast cancer in premenopausal women: a collaborative reanalysis of individual participant data from seven prospective studies. *Lancet Oncol*. 2013;14(10):1009-19.
66. Shiovitz S, Korde LA. Genetics of breast cancer: a topic in evolution. *Ann Oncol*. 2015;26(7):1291-9.
67. Hill DA, Prossnitz ER, Royce M, Nibbe A. Temporal trends in breast cancer survival by race and ethnicity: A population-based cohort study. *PLoS One*. 2019;14(10):e0224064.
68. Hoover RN, Hyer M, Pfeiffer RM, Adam E, Bond B, Chevillat AL, et al. Adverse health outcomes in women exposed in utero to diethylstilbestrol. *N Engl J Med*. 2011;365(14):1304-14.
69. Hilakivi-Clarke L. Maternal exposure to diethylstilbestrol during pregnancy and increased breast cancer risk in daughters. *Breast Cancer Res*. 2014;16(2):208.

70. Palmer JR, Wise LA, Hatch EE, Troisi R, Titus-Ernstoff L, Strohsnitter W, et al. Prenatal diethylstilbestrol exposure and risk of breast cancer. *Cancer Epidemiol Biomarkers Prev.* 2006;15(8):1509-14.
71. Kolb R, Zhang W. Obesity and Breast Cancer: A Case of Inflamed Adipose Tissue. *Cancers (Basel).* 2020;12(6).
72. Rachdaoui N, Sarkar DK. Effects of Alcohol on the Endocrine System. *Endocrinol Metab Clin North Am.* 2013;42(3):593-615.
73. Casey SC, Vaccari M, Al-Mulla F, Al-Temaimi R, Amedei A, Barcellos-Hoff MH, et al. The effect of environmental chemicals on the tumor microenvironment. *Carcinogenesis.* 2015;36 Suppl 1(Suppl 1):S160-83.
74. Ram Makena M, Gatla H, Verlekar D, Sukhavasi S, M KP, K CP. Wnt/ $\beta$ -catenin signaling: the culprit in pancreatic carcinogenesis and therapeutic resistance. *Int J Mol Sci.* 2019;20(17).
75. Zhu Y, Tian Y, Du J, Hu Z, Yang L, Liu J, et al. Dvl2-dependent activation of Daam1 and RhoA regulates Wnt5a-induced breast cancer cell migration. *PLoS One.* 2012;7(5):e37823.
76. Jamdade VS, Sethi N, Mundhe NA, Kumar P, Lahkar M, Sinha N. Therapeutic targets of triple-negative breast cancer: a review. *Br J Pharmacol.* 2015;172(17):4228-37.
77. Wang X, Osada T, Wang Y, Yu L, Sakakura K, Katayama A, et al. CSPG4 Protein as a New Target for the Antibody-Based Immunotherapy of Triple-Negative Breast Cancer. *J Natl Cancer Inst.* 2010;102(19):1496-512.
78. Cooney CA, Jousheghany F, Yao-Borengasser A, Phanavanh B, Gomes T, Kieber-Emmons AM, et al. Chondroitin sulfates play a major role in breast cancer metastasis: a role for CSPG4 and CHST11 gene expression in forming surface P-selectin ligands in aggressive breast cancer cells. *Breast Cancer Res.* 2011;13(3):R58.
79. Ali R, Wendt MK. The paradoxical functions of EGFR during breast cancer progression. *Signal Transduct Target Ther.* 2017;2:16042-.
80. Blanco E, Sangai T, Wu S, Hsiao A, Ruiz-Esparza GU, Gonzalez-Delgado CA, et al. Colocalized delivery of rapamycin and paclitaxel to tumors enhances synergistic targeting of the PI3K/Akt/mTOR pathway. *Mol Ther.* 2014;22(7):1310-9.

81. Wieduwilt MJ, Moasser MM. The epidermal growth factor receptor family: biology driving targeted therapeutics. *Cell Mol Life Sci.* 2008;65(10):1566-84.
82. Nouman W, Basra SMA, Siddiqui MT, Yasmeen A, Tehseen G, Alcayde MAC. Potential of *Moringa oleifera* L. as livestock fodder crop: a review. *Turk J Agric For.* 2014;38:1-14.
83. Falowo AB, Mukumbo FE, Idamokoro EM, Lorenzo JM, Afolayan AJ, Muchenje V. Multi-functional application of *Moringa oleifera* Lam. in nutrition and animal food products: A review. *Int Food Res J.* 2018;106:317-34.
84. Wu Y-Y, Xu Y-M, Lau ATY. Anti-cancer and medicinal potentials of moringa Isothiocyanate. *Molecules.* 2021;26(24):7512.
85. Al-Asmari AK, Albalawi SM, Athar MT, Khan AQ, Al-Shahrani H, Islam M. *Moringa oleifera* as an anti-cancer agent against breast and colorectal cancer cell lines. *PLOS ONE.* 2015;10(8):e0135814.
86. Tiloke C, Phulukdaree A, Chuturgoon AA. The antiproliferative effect of *Moringa oleifera* crude aqueous leaf extract on cancerous human alveolar epithelial cells. *BMC complementary and alternative medicine.* 2013;13:226.
87. Jung IL. Soluble extract from *Moringa oleifera* leaves with a new anticancer activity. *PLoS One.* 2014;9(4):e95492.
88. Madi N, Dany M, Abdoun S, Usta J. *Moringa oleifera*'s nutritious aqueous leaf extract has anticancerous effects by compromising mitochondrial viability in an ROS-dependent manner. *J Am Coll Nutr.* 2016;35(7):604-13.
89. Berkovich L, Earon G, Ron I, Rimmon A, Vexler A, Lev-Ari S. *Moringa Oleifera* aqueous leaf extract down-regulates nuclear factor-kappaB and increases cytotoxic effect of chemotherapy in pancreatic cancer cells. *BMC Complement Altern. Med.* 2013;13:212.
90. Tiloke C, Phulukdaree A, Chuturgoon AA. The antiproliferative effect of *Moringa oleifera* crude aqueous leaf extract on human esophageal cancer cells. *J Med Food.* 2016;19(4):398-403.
91. Sreelatha S, Jeyachitra A, Padma PR. Antiproliferation and induction of apoptosis by *Moringa oleifera* leaf extract on human cancer cells. *Food Chem. Toxicol.* 2011;49(6):1270-5.

92. Cuellar-Nunez ML, Luzardo-Ocampo I, Campos-Vega R, Gallegos-Corona MA, Gonzalez de Mejia E, Loarca-Pina G. Physicochemical and nutraceutical properties of moringa (*Moringa oleifera*) leaves and their effects in an *in vivo* AOM/DSS-induced colorectal carcinogenesis model. *Food Res. Int.* 2018;105:159-68.
93. Budda S, Butryee C, Tuntipopipat S, Rungsipipat A, Wangnaithum S, Lee JS, et al. Suppressive effects of *Moringa oleifera* Lam pod against mouse colon carcinogenesis induced by azoxymethane and dextran sodium sulfate. *Asian Pac J Cancer Prev.* 2011;12(12):3221-8.
94. Sharma V, Paliwal R, Janmeda P, Sharma S. Chemopreventive efficacy of *Moringa oleifera* pods against 7, 12-dimethylbenz[a]anthracene induced hepatic carcinogenesis in mice. *Asian Pac J Cancer Prev.* 2012;13(6):2563-9.
95. Guon TE, Chung HS. *Moringa oleifera* fruit induce apoptosis via reactive oxygen species-dependent activation of mitogen-activated protein kinases in human melanoma A2058 cells. *Oncol Lett.* 2017;14(2):1703-10.
96. Mehwish HM, Riaz Rajoka MS, Xiong Y, Zheng K, Xiao H, Anjin T, et al. *Moringa oleifera* – a functional food and its potential immunomodulatory effects. *Food Rev Int.* 2022;38(7):1533-52.
97. Moon SM, Lee SA, Hong JH, Kim JS, Kim DK, Kim CS. Oleamide suppresses inflammatory responses in LPS-induced RAW264.7 murine macrophages and alleviates paw edema in a carrageenan-induced inflammatory rat model. *Int Immunopharmacol.* 2018;56:179-85.
98. Mahajan SG, Banerjee A, Chauhan BF, Padh H, Nivsarkar M, Mehta AA. Inhibitory Effect of n-butanol Fraction of *Moringa oleifera* Lam. seeds on ovalbumin-induced airway inflammation in a guinea pig model of asthma. *Int J Toxicol.* 2009;28(6):519-27.
99. Abd-Rabou AA, Abdalla AM, Ali NA, Zoheir KMA. *Moringa oleifera* root induces cancer apoptosis more effectively than leave nanocomposites and its free counterpart. *Asian Pac J Cancer Prev.* 2017;18(8):2141-9.
100. Cui C, Chen S, Wang X, Yuan G, Jiang F, Chen X, et al. Characterization of *Moringa oleifera* roots polysaccharide MRP-1 with anti-inflammatory effect. *Int J Biol Macromol.* 2019;132:844-51.

101. Coppin JP, Xu Y, Chen H, Pan M-H, Ho C-T, Juliani R, et al. Determination of flavonoids by LC/MS and anti-inflammatory activity in *Moringa oleifera*. *J Funct Foods*. 2013;5(4):1892-9.
102. Pei Y, Parks JS, Kang HW. Quercetin alleviates high-fat diet-induced inflammation in brown adipose tissue. *J Funct Foods*. 2021;85:104614.
103. Dou Z, Chen C, Fu X. Bioaccessibility, antioxidant activity and modulation effect on gut microbiota of bioactive compounds from *Moringa oleifera* Lam. leaves during digestion and fermentation *in vitro*. *Food & Function*. 2019;10(8):5070-9.
104. Sasidharan S, Chen Y, Saravanan D, Sundram KM, Yoga Latha L. Extraction, isolation and characterization of bioactive compounds from plants' extracts. *Afr J Tradit Complement Altern Med*. 2011;8(1):1-10.
105. Gusthinnadura Oshadie De Silva ATAaMMWA. Extraction methods, qualitative and quantitative techniques for screening of phytochemicals from plants. *Am J Essent Oil*. 2017;5(2):29-32.
106. Amita Pandey and Shalini Tripathi. Concept of standardization, extraction and pre phytochemical screening strategies for herbal drug. *J pharmacogn phytochem*. 2014;5(2):115-9.
107. Zhang Q-W, Lin L-G, Ye W-C. Techniques for extraction and isolation of natural products: a comprehensive review. *Chinese Medicine*. 2018;13(1):20.
108. Altemimi A, Lakhssassi N, Baharlouei A, Watson DG, Lightfoot DA. Phytochemicals: extraction, isolation, and identification of bioactive compounds from plant extracts. *Plants*. 2017;6(4).
109. Krishnananda P Ingle, Amit G Deshmukh, Dipika A Padole, Mahendra S Dudhare, Mangesh P Moharil and Vaibhav C. Khelurkar. Phytochemicals: extraction methods, identification and detection of bioactive compounds from plant extracts. *J pharmacogn phytochem*. 2017;6(1):32-6.
110. College PCaBC. Overview of TLC. Chemistry Libertexts 2017.
111. obpl. Molecular analysis using UV/Visible spectroscopy. Orbit Biotech; April 2018.
112. Mendelson WB, Basile AS. The hypnotic actions of the fatty acid amide, oleamide. *Neuropsychopharmacology*. 2001;25(1):S36-S9.

113. Boger DL, Henriksen SJ, Cravatt BF. Oleamide: an endogenous sleep-inducing lipid and prototypical member of a new class of biological signaling molecules. *Curr Pharm Des.* 1998;4(4):303-14.
114. Mueller GP, Driscoll WJ. Biosynthesis of oleamide. *Vitam Horm.* 2009;81:55-78.
115. Boger DL, Patterson JE, Jin Q. Structural requirements for 5-HT<sub>2A</sub> and 5-HT<sub>1A</sub> serotonin receptor potentiation by the biologically active lipid oleamide. *Proc Natl Acad Sci U S A.* 1998;95(8):4102-7.
116. Otrubova K, Brown M, McCormick MS, Han GW, O'Neal ST, Cravatt BF, et al. Rational design of fatty acid amide hydrolase inhibitors that act by covalently bonding to two active site residues. *J Am Chem Soc.* 2013;135(16):6289-99.
117. Hiley CR, Hoi PM. Oleamide: a fatty acid amide signaling molecule in the cardiovascular system. *Cardiovasc Drug Rev.* 2007;25(1):46-60.
118. Nam HY, Na EJ, Lee E, Kwon Y, Kim HJ. Antiepileptic and neuroprotective effects of oleamide in rat striatum on kainate-induced behavioral seizure and excitotoxic damage via calpain inhibition. *Front Pharmacol.* 2017;8:817.
119. Maya-López M, Rubio-López LC, Rodríguez-Alvarez IV, Orduño-Piceno J, Flores-Valdivia Y, Colonnello A, et al. A cannabinoid receptor-mediated mechanism participates in the neuroprotective effects of oleamide against excitotoxic damage in rat brain synaptosomes and cortical slices. *Neurotox Res.* 2020;37(1):126-35.
120. Akanmu MA, Adeosun SO, Ilesanmi OR. Neuropharmacological effects of oleamide in male and female mice. *Behav Brain Res.* 2007;182(1):88-94.
121. Murillo-Rodríguez E, Giordano M, Cabeza R, Henriksen SJ, Méndez Díaz M, Navarro L, et al. Oleamide modulates memory in rats. *Neurosci Lett.* 2001;313(1-2):61-4.
122. Ano Y, Ozawa M, Kutsukake T, Sugiyama S, Uchida K, Yoshida A, et al. Preventive effects of a fermented dairy product against alzheimer's disease and identification of a novel oleamide with enhanced microglial phagocytosis and anti-inflammatory activity. *PLOS ONE.* 2015;10(3):e0118512.
123. Oh YT, Lee JY, Lee J, Lee JH, Kim JE, Ha J, et al. Oleamide suppresses lipopolysaccharide-induced expression of iNOS and COX-2 through inhibition of NF- $\kappa$ B activation in BV2 murine microglial cells. *Neurosci Lett.* 2010;474(3):148-53.

124. HEALTH USDOHAHSNIO. Understanding the immune system how it works u. NIH Publication2003.
125. Abul K. Abbas, Andrew H. Lichtman SP. Basic immunology: functions and disorders of the immune system. EDITION F, editor. Philadelphia, PA: Elsevier Saunders; 2016.
126. Merle NS, Church SE, Fremeaux-Bacchi V, Roumenina LT. complement system part I – molecular mechanisms of activation and regulation. *Front Immunol.* 2015;6.
127. Gordon S, Plüddemann A. Tissue macrophages: heterogeneity and functions. *BMC Biology.* 2017;15(1):53.
128. Luke C. Davies SJJ, Judith E. Allen, and Philip R. Taylor. Tissue-resident macrophages. *Nat Immunol.* 2013;14(10):986–95.
129. Yonit Lavin AM, Adeeb Rahman and Miriam Merad. Regulation of macrophage development and function in peripheral tissues. *Nat Rev Cancer.* 2015;15:731-44.
130. Chaplin DD. Overview of the Immune Response. *J Allergy Clin Immunol.* 2010;125(2):S3–23.
131. Abbas, A. K., Lichtman, A. H., Pillai S. Cellular and molecular immunology. 6, editor. Philadelphia: Saunders/Elsevier.; 2010.
132. Patel U, Rajasingh S, Samanta S, Cao T, Dawn B, Rajasingh J. Macrophage polarization in response to epigenetic modifiers during infection and inflammation. *Drug Discov.* 2017;22(1):186-93.
133. Lee K. M1 and M2 polarization of macrophages: a mini-review. *Med Biol Sci Eng.* 2019;2:1-5.
134. De Paoli F, Staels B, Chinetti-Gbaguidi G. Macrophage phenotypes and their modulation in atherosclerosis. *Circ J.* 2014;78(8):1775-81.
135. Raymond A. Isidro CBA. Colonic macrophage polarization in homeostasis, inflammation, and cancer. *Am J Physiol* 2016;311(1).
136. Kelley N, Jeltema D, Duan Y, He Y. The NLRP3 Inflammasome: An Overview of Mechanisms of Activation and Regulation. *Int J Mol Sci.* 2019;20(13):3328.
137. Swanson KV, Deng M, Ting JPY. The NLRP3 inflammasome: molecular activation and regulation to therapeutics. *Nat Rev Immunol.* 2019;19(8):477-89.

138. Yang H, Zhang Q, Xu M, Wang L, Chen X, Feng Y, et al. CCL2-CCR2 axis recruits tumor associated macrophages to induce immune evasion through PD-1 signaling in esophageal carcinogenesis. *Mol Cancer*. 2020;19(1):41-.
139. Yin M, Li X, Tan S, Zhou HJ, Ji W, Bellone S, et al. Tumor-associated macrophages drive spheroid formation during early transcoelomic metastasis of ovarian cancer. *J Clin Invest*. 2016;126(11):4157-73.
140. Wang W, Marinis JM, Beal AM, Savadkar S, Wu Y, Khan M, et al. RIP1 Kinase Drives Macrophage-Mediated Adaptive Immune Tolerance in Pancreatic Cancer. *Cancer Cell*. 2018;34(5):757-74.e7.
141. Zou W, Wolchok JD, Chen L. PD-L1 (B7-H1) and PD-1 pathway blockade for cancer therapy: Mechanisms, response biomarkers, and combinations. *Sci Transl Med*. 2016;8(328):328rv4.
142. W S. Trypan blue exclusion test of cell viability. *Curr Protoc Immunol*. 2001;38(3).
143. Kumar P, Nagarajan A, Uchil PD. Analysis of cell viability by the mtt assay. *Cold Spring Harb Protoc*. 2018;2018(6).
144. Chapter 7 - Applications of density gradient centrifugation. In: Work TS, Work E, editors. *Laboratory techniques in biochemistry and molecular biology*. 6: Elsevier; 1978. p. 205-42.
145. Franken NAP, Rodermond HM, Stap J, Haveman J, van Bree C. Clonogenic assay of cells *in vitro*. *Nature Protocols*. 2006;1(5):2315-9.
146. Bleloch J. Clonogenic assay: what, why and how Cyto™ SmartMay, 2020 [Available from: <https://cytosmart.com/resources/clonogenic-assay-what-why-how>].
147. Banfalvi G. Methods to detect apoptotic cell death. *Apoptosis*. 2017;22(2):306-23.
148. Lakshmanan I, Batra SK. Protocol for Apoptosis Assay by Flow Cytometry Using Annexin V Staining Method. *Bio Protoc*. 2013;3(6).
149. Basmacıyan L, Azas N, Casanova M. Calcein+/PI- as an early apoptotic feature in Leishmania. *PLOS ONE*. 2017;12(11):e0187756.

150. Kyrylkova K, Kyryachenko S, Leid M, Kioussi C. Detection of apoptosis by tunel assay. In: Kioussi C, editor. *Odontogenesis: Methods Protoc.* Totowa, NJ: Humana Press; 2012. p. 41-7.
151. Bioarray C. TUNEL Apoptosis Assay (Fluorescent) 2022 [Available from: <https://www.creative-bioarray.com/support/tunel-apoptosis-assay-fluorescent.htm>].
152. Sivandzade F, Bhalerao A, Cucullo L. Analysis of the mitochondrial membrane potential using the cationic jc-1 dye as a sensitive fluorescent probe. *Bio-protocol.* 2019;9(1):e3128.
153. Sakamuru S, Attene-Ramos MS, Xia M. Mitochondrial membrane potential assay. In: Zhu H, Xia M, editors. *High-Throughput Screening Assays in Toxicology.* New York, NY: Springer New York; 2016. p. 17-22.
154. Kaufmann SH, Lee SH, Meng XW, Loegering DA, Kottke TJ, Henzing AJ, et al. Apoptosis-associated caspase activation assays. *Methods.* 2008;44(3):262-72.
155. Laura Cobb, Samayita Das. The cell cycle analysis. *Materials and Methods.* 2013;3:172.
156. Pozarowski P, Darzynkiewicz Z. Analysis of cell cycle by flow cytometry. *Methods Mol Biol.* 2004;281:301-11.
157. Chemometec. Cell cycle assay: analyze fixed or live cells in two simple steps using the cell cycle assay 2022 [Available from: <https://chemometec.com/resources/cell-assays/cell-cycle-assay/>].
158. Bobadilla AVP, Arévalo J, Sarró E, Byrne HM, Maini PK, Carraro T, et al. *In vitro* cell migration quantification method for scratch assays. *J R Soc Interface.* 2019;16(151):20180709.
159. Liang C-C, Park AY, Guan J-L. *In vitro* scratch assay: a convenient and inexpensive method for analysis of cell migration *in vitro*. *Nature Protocols.* 2007;2(2):329-33.
160. Grada A, Otero-Vinas M, Prieto-Castrillo F, Obagi Z, Falanga V. Research techniques made simple: analysis of collective cell migration using the wound healing assay. *J Invest Dermatol.* 2017;137(2):e11-e6.
161. Chazotte B. Labeling nuclear DNA with hoechst 33342. *Cold Spring Harb Protoc.* 2011;2011(1):pdb.prot5557.

162. Morteza Seifi AG, Siamak Heidarzadeh Polymerase Chain Reaction.
163. Ali SAaS. Differential Gene Expression and Its Possible Therapeutic Implications 2011 [Available from: <https://www.intechopen.com/books/gene-therapy-developments-and-future-perspectives/differential-gene-expression-and-its-possible-therapeutic-implications>].
164. Yang TMAP-C. Western Blot: Technique, Theory, and Trouble Shooting. *N Am J Med Sci*. 2012;4(9):429–34.
165. Bakke AC. The Principles of Flow Cytometry. *laboratorymedicine*. 2001;32(4):207-11.
166. Alhadj M, Farhana A. Enzyme Linked Immunosorbent Assay. StatPearls. Treasure Island (FL): StatPearls Publishing  
Copyright © 2022, StatPearls Publishing LLC.; 2022.
167. ELISA principles and types: Abcam; 2022 [Available from: <https://www.abcam.com/kits/elisa-principle>].
168. Kumar P, Nagarajan A, Uchil PD. Analysis of cell viability by the lactate dehydrogenase assay. *Cold Spring Harb Protoc*. 2018;2018(6).
169. Forest V, Figarol A, Boudard D, Cottier M, Grosseau P, Pourchez J. Adsorption of Lactate dehydrogenase enzyme on carbon nanotubes: how to get accurate results for the cytotoxicity of these nanomaterials. *Langmuir : the ACS journal of surfaces and colloids*. 2015;31.
170. Akhtar K, Khan SA, Khan SB, Asiri AM. Scanning Electron Microscopy: Principle and applications in nanomaterials characterization. In: Sharma SK, editor. *Handbook of Materials Characterization*. Cham: Springer International Publishing; 2018. p. 113-45.
171. Fischer ER, Hansen BT, Nair V, Hoyt FH, Dorward DW. Scanning electron microscopy. *Curr Protoc Microbiol*. 2012;Chapter 2:Unit 2B..
172. Menck K, Behme D, Pantke M, Reiling N, Binder C, Pukrop T, et al. Isolation of human monocytes by double gradient centrifugation and their differentiation to macrophages in teflon-coated cell culture bags. *J Vis Exp*. 2014(91):e51554.
173. Lang T, Lee JPW, Elgass K, Pinar AA, Tate MD, Aitken EH, et al. Macrophage migration inhibitory factor is required for NLRP3 inflammasome activation. *Nat Commun*. 2018;9(1):2223.

174. Wisitpongpun P, Potup P, Usuwanthim K. Oleamide-mediated polarization of m1 macrophages and il-1 $\beta$  production by regulating nlrp3-inflammasome activation in primary human monocyte-derived macrophages. *Front Immunol.* 2022;13:856296.
175. Hassan M, Watari H, AbuAlmaaty A, Ohba Y, Sakuragi N. Apoptosis and molecular targeting therapy in cancer. *Biomed Res Int.* 2014;2014:150845.
176. Jan R, Chaudhry GE. Understanding Apoptosis and Apoptotic pathways targeted cancer therapeutics. *Adv Pharm Bull.* 2019;9(2):205-18.
177. Adams CM, Clark-Garvey S, Porcu P, Eischen CM. Targeting the Bcl-2 family in B cell lymphoma. *Frontiers in Oncology.* 2019;8.
178. Berens HM, Tyler KL. The proapoptotic Bcl-2 protein Bax plays an important role in the pathogenesis of reovirus encephalitis. *J Virol.* 2011;85(8):3858-71.
179. Nikolettou V, Markaki M, Palikaras K, Tavernarakis N. Crosstalk between apoptosis, necrosis and autophagy. *Biochim Biophys Acta.* 2013;1833(12):3448-59.
180. Silva MT. Secondary necrosis: the natural outcome of the complete apoptotic program. *FEBS letters.* 2010;584(22):4491-9.
181. Vergara-Jimenez M, Almatrafi MM, Fernandez ML. Bioactive components in *Moringa oleifera* leaves protect against chronic disease. *Antioxidants.* 2017;6(4).
182. Harith Jameel Mahdi, Nurzalina Abdul Karim Khan, Roziahaman Mahmud MZBA, Murugaiyah VAL. LC/MS, GC/MS screening and *in vivo* anti-inflammatory activity of Malaysian *Moringa oleifera* Lam leaf extracts and fractions against carrageenan -induced paw oedema in rats. *JIPBS.* 2017;4(3): 48-54.
183. Govindarajan Karthivashan, Masoumeh Tangestani Fard, Palanisamy Arulselvan, Faridah Abas, Sharida Fakurazi. Identification of bioactive candidate compounds responsible for oxidative challenge from hydro-ethanolic extract of *Moringa oleifera* Leaves. *J Food Sci.* 2013;78(9).
184. Lin H, Zhu H, Tan J, Wang H, Wang Z, Li P, et al. Comparative analysis of chemical constituents of *moringa oleifera* leaves from China and India by ultra-performance liquid chromatography coupled with quadrupole-time-of-flight mass spectrometry. *Molecules.* 2019;24(5).

185. Cravatt BF, Prospero-Garcia O, Siuzdak G, Gilula NB, Henriksen SJ, Boger DL, et al. Chemical characterization of a family of brain lipids that induce sleep. *Science*. 1995;268(5216):1506-9.
186. Boger DL, Patterson JE, Guan X, Cravatt BF, Lerner RA, Gilula NB. Chemical requirements for inhibition of gap junction communication by the biologically active lipid oleamide. *Proc Natl Acad Sci U S A*. 1998;95(9):4810-5.
187. Guan X, Cravatt BF, Ehring GR, Hall JE, Boger DL, Lerner RA, et al. The sleep-inducing lipid oleamide deconvolutes gap junction communication and calcium wave transmission in glial cells. *J Cell Biol*. 1997;139(7):1785-92.
188. Van Swearingen AED, Sambade MJ, Siegel MB, Sud S, McNeill RS, Bevill SM, et al. Combined kinase inhibitors of MEK1/2 and either PI3K or PDGFR are efficacious in intracranial triple-negative breast cancer. *Neuro-Oncology*. 2017;19(11):1481-93.
189. McLaughlin RP, He J, van der Noord VE, Redel J, Foekens JA, Martens JWM, et al. A kinase inhibitor screen identifies a dual cdc7/CDK9 inhibitor to sensitise triple-negative breast cancer to EGFR-targeted therapy. *Breast Cancer Res*. 2019;21(1):77.
190. Tang J, Gautam P, Gupta A, He L, Timonen S, Akimov Y, et al. Network pharmacology modeling identifies synergistic Aurora B and ZAK interaction in triple-negative breast cancer. *NPJ Syst Biol Appl*. 2019;5(1):20.
191. Chavez KJ, Garimella SV, Lipkowitz S. Triple negative breast cancer cell lines: one tool in the search for better treatment of triple negative breast cancer. *Breast Dis*. 2010;32(1-2):35-48.
192. Crystal AS, Shaw AT, Sequist LV, Friboulet L, Niederst MJ, Lockerman EL, et al. Patient-derived models of acquired resistance can identify effective drug combinations for cancer. *Science*. 2014;346(6216):1480-6.
193. Khan MSS, Asif M, Basheer MKA, Kang CW, Al-Suede FS, Ein OC, et al. Treatment of novel IL17A inhibitor in glioblastoma implementing 3rd generation co-culture cell line and patient-derived tumor model. *Eur J Pharmacol*. 2017;803:24-38.
194. He L, Tang J, Andersson EI, Timonen S, Koschmieder S, Wennerberg K, et al. Patient-customized drug combination prediction and testing for t-cell prolymphocytic leukemia patients. *Cancer Res*. 2018;78(9):2407-18.

195. Azad AK, Rajaram MV, Schlesinger LS. Exploitation of the macrophage mannose receptor (cd206) in infectious disease diagnostics and therapeutics. *J Cytol Mol Biol.* 2014;1(1).
196. Jaynes JM, Sable R, Ronzetti M, Bautista W, Knotts Z, Abisoye-Ogunniyan A, et al. Mannose receptor (CD206) activation in tumor-associated macrophages enhances adaptive and innate antitumor immune responses. *Sci Transl Med.* 2020;12(530):eaax6337.
197. Bertani FR, Mozetic P, Fioramonti M, Iuliani M, Ribelli G, Pantano F, et al. Classification of M1/M2-polarized human macrophages by label-free hyperspectral reflectance confocal microscopy and multivariate analysis. *Sci Rep.* 2017;7(1):8965.
198. Zhu Y, Zhang L, Lu Q, Gao Y, Cai Y, Sui A, et al. Identification of different macrophage subpopulations with distinct activities in a mouse model of oxygen-induced retinopathy. *Int J Mol Med.* 2017;40(2):281-92.
199. Smith TD, Tse MJ, Read EL, Liu WF. Regulation of macrophage polarization and plasticity by complex activation signals. *Integrative biology : quantitative biosciences from nano to macro.* 2016;8(9):946-55.
200. Lopez-Castejon G, Brough D. Understanding the mechanism of IL-1 $\beta$  secretion. *Cytokine Growth Factor Rev.* 2011;22(4):189-95.
201. Paik S, Kim JK, Silwal P, Sasakawa C, Jo E-K. An update on the regulatory mechanisms of NLRP3 inflammasome activation. *Cell Mol Immunol.* 2021;18(5):1141-60.
202. Martín-Sánchez F, Diamond C, Zeitler M, Gomez AI, Baroja-Mazo A, Bagnall J, et al. Inflammasome-dependent IL-1 $\beta$  release depends upon membrane permeabilisation. *Cell Death Differ.* 2016;23(7):1219-31.
203. Gritsenko A, Yu S, Martin-Sanchez F, Diaz-del-Olmo I, Nichols E-M, Davis DM, et al. Priming is dispensable for NLRP3 inflammasome activation in human monocytes *in vitro*. *Front Immunol.* 2020;11(2573).
204. Hanslik KL, Ulland TK. The role of microglia and the Nlrp3 inflammasome in Alzheimer's disease. *Front Neurol.* 2020;11:570711.
205. Zhang Y, Dong Z, Song W. NLRP3 inflammasome as a novel therapeutic target for Alzheimer's disease. *Signal Transduct Target Ther.* 2020;5(1):37.

206. Heideveld E, Horcas-Lopez M, Lopez-Yrigoyen M, Forrester LM, Cassetta L, Pollard JW. Chapter Eight - Methods for macrophage differentiation and *in vitro* generation of human tumor associated-like macrophages. In: Galluzzi L, Rudqvist N-P, editors. Meth. Enzymol. 632: Academic Press; 2020. p. 113-31.
207. Hollmén M, Roudnicky F, Karaman S, Detmar M. Characterization of macrophage - cancer cell crosstalk in estrogen receptor positive and triple-negative breast cancer. Sci Rep. 2015;5(1):9188.
208. Verdon B, Zheng J, Nicholson RA, Ganelli CR, Lees G. Stereoselective modulatory actions of oleamide on GABA(A) receptors and voltage-gated Na(+) channels *in vitro*: a putative endogenous ligand for depressant drug sites in CNS. Br J Pharmacol. 2000;129(2):283-90.
209. Wisitpongpun P, Suphrom N, Potup P, Nuengchamnonng N, Calder PC, Usuwanthim K. *In vitro* bioassay-guided identification of anticancer properties from *Moringa oleifera* Lam. Leaf against the MDA-MB-231 cell line. Pharmaceuticals (Basel). 2020;13(12).
210. Wisitpongpun P, Potup P, Usuwanthim K. Oleamide-mediated polarization of m1 macrophages and il-1 $\beta$  production by regulating nlrp3-inflammasome activation in primary human monocyte-derived macrophages. Front Immunol. 2022;13:856296.
211. Zheng X, Turkowski K, Mora J, Brüne B, Seeger W, Weigert A, et al. Redirecting tumor-associated macrophages to become tumoricidal effectors as a novel strategy for cancer therapy. Oncotarget. 2017;8(29):48436-52.
212. Aminin D, Wang Y-M. Macrophages as a “weapon” in anticancer cellular immunotherapy. Kaohsiung J Med Sci. 2021;37(9):749-58.
213. Tang J, Tanoli ZU, Ravikumar B, Alam Z, Rebane A, Vähä-Koskela M, et al. Drug Target Commons: A Community Effort to Build a Consensus Knowledge Base for Drug-Target Interactions. Cell Chem Biol. 2018;25(2):224-9.e2.
214. Sudhahar V, Shaw S, Imig JD. Mechanisms involved in oleamide-induced vasorelaxation in rat mesenteric resistance arteries. Eur J Pharmacol. 2009;607(1-3):143-50.

215. Thomas EA, Carson MJ, Neal MJ, Sutcliffe JG. Unique allosteric regulation of 5-hydroxytryptamine receptor-mediated signal transduction by oleamide. *Proc Natl Acad Sci U S A*. 1997;94(25):14115-9.
216. Kita M, Ano Y, Inoue A, Aoki J. Identification of P2Y receptors involved in oleamide-suppressing inflammatory responses in murine microglia and human dendritic cells. *Scientific Reports*. 2019;9(1):3135.
217. Boger DL, Fecik RA, Patterson JE, Miyauchi H, Patricelli MP, Cravatt BF. Fatty acid amide hydrolase substrate specificity. *Bioorg Med Chem Lett*. 2000;10(23):2613-6.
218. Lambert DM, Fowler CJ. The endocannabinoid system: drug targets, lead compounds, and potential therapeutic applications. *J Med Chem*. 2005;48(16):5059-87.
219. Seierstad M, Breitenbucher JG. Discovery and development of fatty acid amide hydrolase (FAAH) inhibitors. *J Med Chem*. 2008;51(23):7327-43.
220. Xu MZ, Lee WS, Kim MJ, Park DS, Yu H, Tian GR, et al. Acyl-CoA: cholesterol acyltransferase inhibitory activities of fatty acid amides isolated from *Mylabris phalerata* Pallas. *Bioorg Med Chem Lett*. 2004;14(16):4277-80.